THE CHARACTERISTICS OF MARINE FOG OCCURRING OFF THE COAST OF NOVA SCOTIA

CALSPAN CORPORATION

JUNE 1976

Calspan

THE CHARACTERISTICS OF MARINE FOG OCCURRING OFF THE COAST OF NOVA SCOTIA

by
Eugene J. Mack and Ulrich Katz

Calspan Report No. CJ-5756-M-1

Project Sea Fog
Fourth Annual Summary Report

Part 1

Prepared For:
NAVAL AIR SYSTEMS COMMAND
WASHINGTON, D.C. 20360
CODE AIR-370C

CONTRACT NO. N00019-75-C-0508
JUNE 1976

Calspan Corporation
Buffalo, New York 14221

APPROVED FOR PUBLIC RELEASE:
DISTRIBUTION UNLIMITED

ABSTRACT

During early August 1975, Calspan Corporation participated in the Naval Research Laboratory-sponsored cruise aboard the USNS HAYES to investigate marine fog occurring off the coast of Nova Scotia. Measurements of visibility, air and sea surface temperatures, dew point, fog microphysics, and CCN concentration were obtained, and hi-vol samples of the ambient aerosols and discrete samples of fog water were collected for later chemical analysis.

The data show conclusively that areas of cold water were contributing factors in the development of most fogs and that spatial fluctuations in sea surface temperature were directly responsible for spatial fluctuations in the surface-level features of the fogs. Results of the chemical analyses of the aerosol and fog water samples suggest that sulfate aerosols served as the primary nucleants for the marine fogs observed off the coast of Nova Scotia. (In contrast, sea salt aerosols have been found to serve as the primary droplet nuclei in fogs occurring off the California coast.) As a result of the major differences in the aerosol populations existent off the two coasts, fog microphysics also differed markedly in fogs formed in those respective areas. Relative to West Coast marine fogs, fogs occurring off the coast of Nova Scotia were characterized by higher concentrations of smaller droplets. With comparable quantities of liquid water, the Nova Scotia fogs tend, as a result of the droplet spectra, to exhibit lower visibilities.

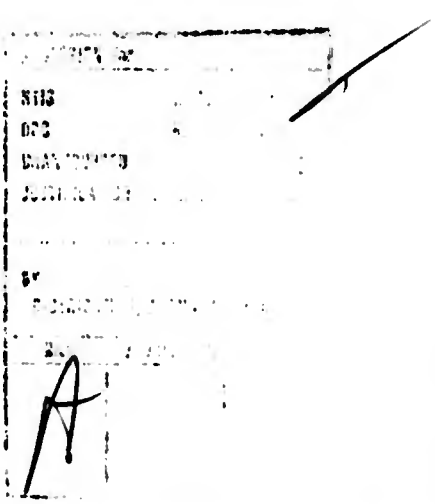

TABLE OF CONTENTS

LIST OF TABLES

LIST OF FIGURES

LIST OF FIGURES (Cont'd)

Section 1

INTRODUCTION AND SUMMARY

For the fourth consecutive year, Calspan Corporation under contract from the Naval Air Systems Command is continuing its investigation of the physics and characteristics of fog forming at sea. During the previous three years of study, attention was focused on marine fog occurring off the coast of California. Results of those years' efforts are summarized in annual summary reports (Mack et al., 1973; 1974; and 1975).

The major portion (Task I) of this year's effort was directed at obtaining detailed observations and providing descriptions of marine fog occurring in the Atlantic off the coast of Nova Scotia. To this end, Calspan participated in the Naval Research Laboratory sponsored cruise aboard the USNS Hayes to investigate marine fog occurring in the area. Calspan's participation was limited to the period 28 July-12 August 1975, and results of that participation are presented within this report.

Task II of this year's program involved a modest effort to modify and exercise the existing Calspan numerical model of advection fog. The objective of this task was to provide a better framework within the model for incorporation of dynamic effects which may contribute to the development of marine fog. Results of this effort are reported in a separate volume (Eadie et al., 1976).

The major objective of Calspan's participation in the Summer 1975 cruise aboard the USNS HAYES was to obtain data describing the micrometeorological, microphysical and chemical characteristics of marine fogs occurring in the area off the southeast coast of Nova Scotia. The cruise track in the vicinity of Nova Scotia is shown in Figure 1. (The numbers 1 through 11 denote ship's position at the 0000 hour (EDT) of those respective days of August 1975.) The cruise was highly successful having encountered approximately

FIGURE 1 PLOT OF THE TRACK OF THE USNS HAYES OFF THE COAST OF NOVA SCOTIA FOR THE PERIOD 1-11 AUGUST 1975.

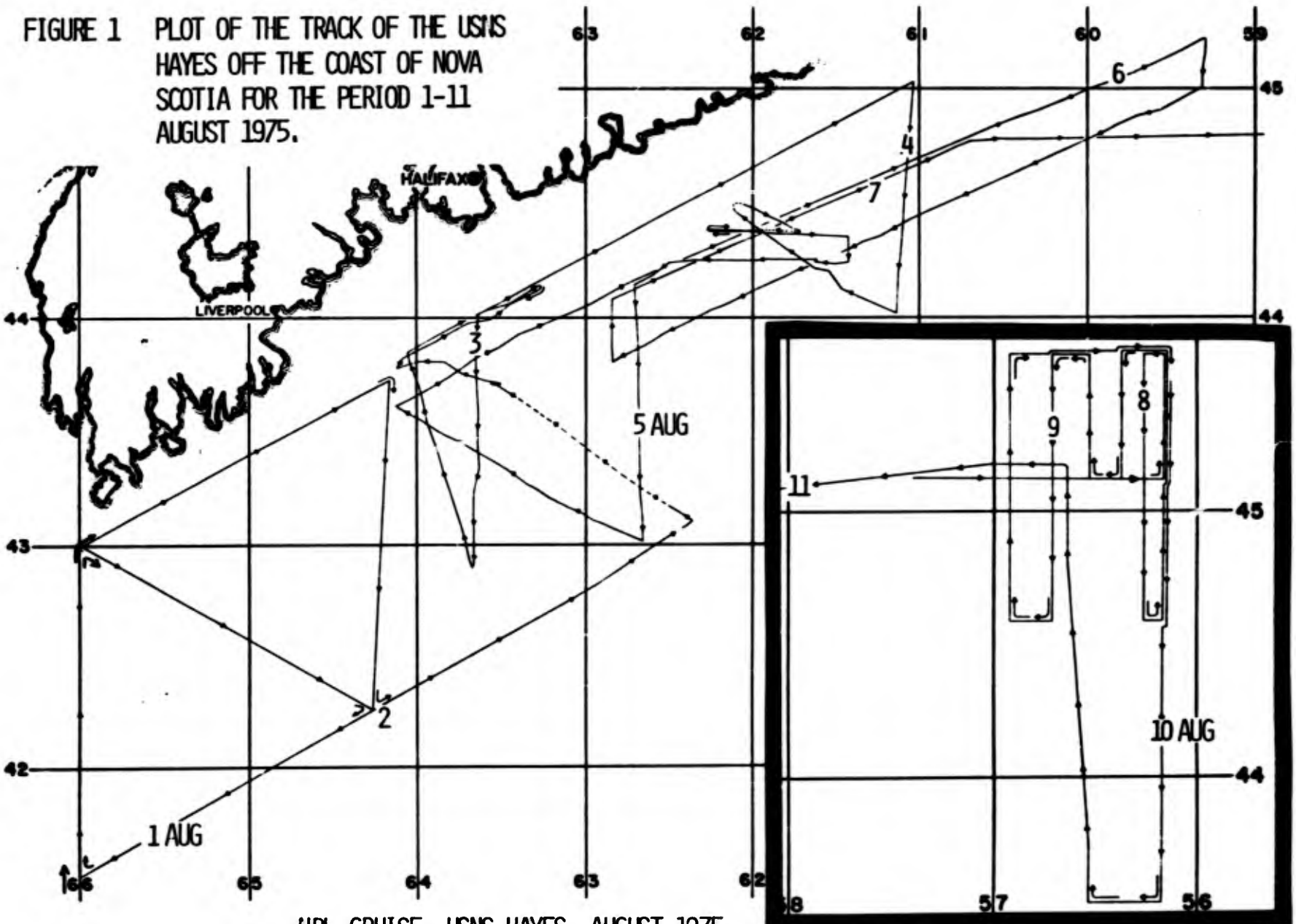

NRL CRUISE, USNS HAYES, AUGUST 1975
(AFTER G. SCHACHER, NPS)

18 fog events over a ten-day period and logging approximately 95 hours of observations in fog with visibility <5000 m, including 65 hours of dense fog (visibility <1000 m). Visibility, air and sea surface temperature and dew point were monitored continuously; in excess of 450 measurements of drop size distribution and over 160 samples of fog water were also obtained for later chemical analysis. Numerous measurements of the cloud nucleus spectrum and hi-vol samples of atmospheric aerosols (for chemical analysis) were also acquired during periods between fog events, providing data on the characteristics of the air masses in which the fogs formed. The complete data set (in reduced form) obtained during the cruise and a brief description of instrumentation set-up are provided in Appendix A.

During the observational study, fogs were observed to develop off the East Coast through at least two mechanisms which have been previously observed by Calspan to operate off the West Coast: by the lowering of a stratus cloud to the surface; and by advection of air over warmer water. In addition, although the data are not conclusive, it appears that several fogs may have formed as a direct result of advection of air over cold water--a mechanism not yet observed off the West Coast. The data further suggest that areas of cold water were contributing factors in the development of most of the fogs (at the surface) and that spatial variations in sea surface temperature were directly responsible for spatial fluctuations in the surface-level characteristics of the fogs. Discussion of these mechanisms and evidence supporting the findings are presented in Section 2.

Analyses of aerosol and air chemistry data obtained off the Nova Scotia coast by Calspan established that the aerosol constituents of the air masses in this offshore area downwind of the continent were comprised (during the observation period) primarily of relatively high concentrations of continental soil particulates and sulfate aerosols; only trace concentrations of sea salt aerosols were observed. Chemical analysis of samples of fog water from fogs formed in those air masses revealed almost quantitative capture of the ambient sulfate aerosol by the fog droplets. Only negligible amounts of sea salt and no soil particulates were found in the fog water, indicating that

the sulfate aerosols served as the primary nucleants of the marine fogs occurring off the coast of Nova Scotia. (Sea salt aerosols have been found to serve as the primary fog droplet nuclei in the clean marine air off the West Coast.) The data supporting these conclusions are discussed in detail in Section 3.

Although the processes of fog development and persistence off the East Coast appear to differ (with respect to the contribution of the cold water) from those operative off the West Coast, the strengths of the driving mechanisms are of comparable magnitude (as evidenced by the quantities of liquid water produced). However, differences in the nucleus populations apparently give rise to differences in the resultant droplet populations. Off the East Coast, with many more smaller nuclei competing for the same quantities of condensable water, the resultant droplet spectrum is comprised of greater numbers of droplets and is shifted to smaller sizes than has been typically observed in fogs off the West Coast. As a result, visibilities tend to be somewhat lower in fogs off the Nova Scotia coast than in fogs off the northern California coast. These data are also discussed in Section 3.

A brief outline of the principal conclusions derived from this year's investigation of marine fog is provided in Section 4.

Section 2

THE PROCESSES OF MARINE FOG FORMATION OFF THE COAST OF NOVA SCOTIA

During the August 1975 study, approximately 18 separate fogs events were encountered off the southeast coast of Nova Scotia (N.S.). The individual fog events are documented in detail in Appendix A, and regions of reduced visibility (i.e., where visibility was <1000 m) observed along ship's track are depicted by the shaded areas in Figure 2. Also shown on Figure 2 are mean sea surface isotherms based on Calspan data for the entire cruise and numbers initially assigned to individual fog events. (See Appendix A for details.) For convenience the fog "numbers" are used throughout the discussion to identify individual fog events. Data not presented within the text may be reviewed in Appendix A.

The highly variable sea surface temperature pattern existent along the southern coast of N.S. during early August is immediately evident from Figure 2. In general, the sea surface was coldest closer to the coast and warmer with distance offshore. Observed sea surface temperatures ranged from minima of ~8°C off the western end of N.S. and ~10°C at several locations within ~50 km of the entire southern coast to maxima of 18-20 C ~100 km offshore.

Casual inspection of the data presented in Figure 2 suggests an apparent correlation of fog occurrence with areas of relatively cold water. The figure, however, reveals that many of the fog events were widespread with horizontal dimensions at the surface of the order of 100 km and that surface features of the fogs in some instances persisted across substantial gradients in sea surface temperature. Detailed analyses of visibility, sea surface temperature and wind records of the individual fog events suggests the following: that the growth and persistence of at least one fog was due to air advecting to warmer water, that several fogs formed at the surface probably due to direct cooling of the air by the cold sea surface, and that

FIGURE 2 ISOPLETHS OF SEA SURFACE TEMPERATURE (°C) AND REGIONS OF REDUCED VISIBILITY (<1000 M DUE TO FOG) ALONG SHIP'S TRACK

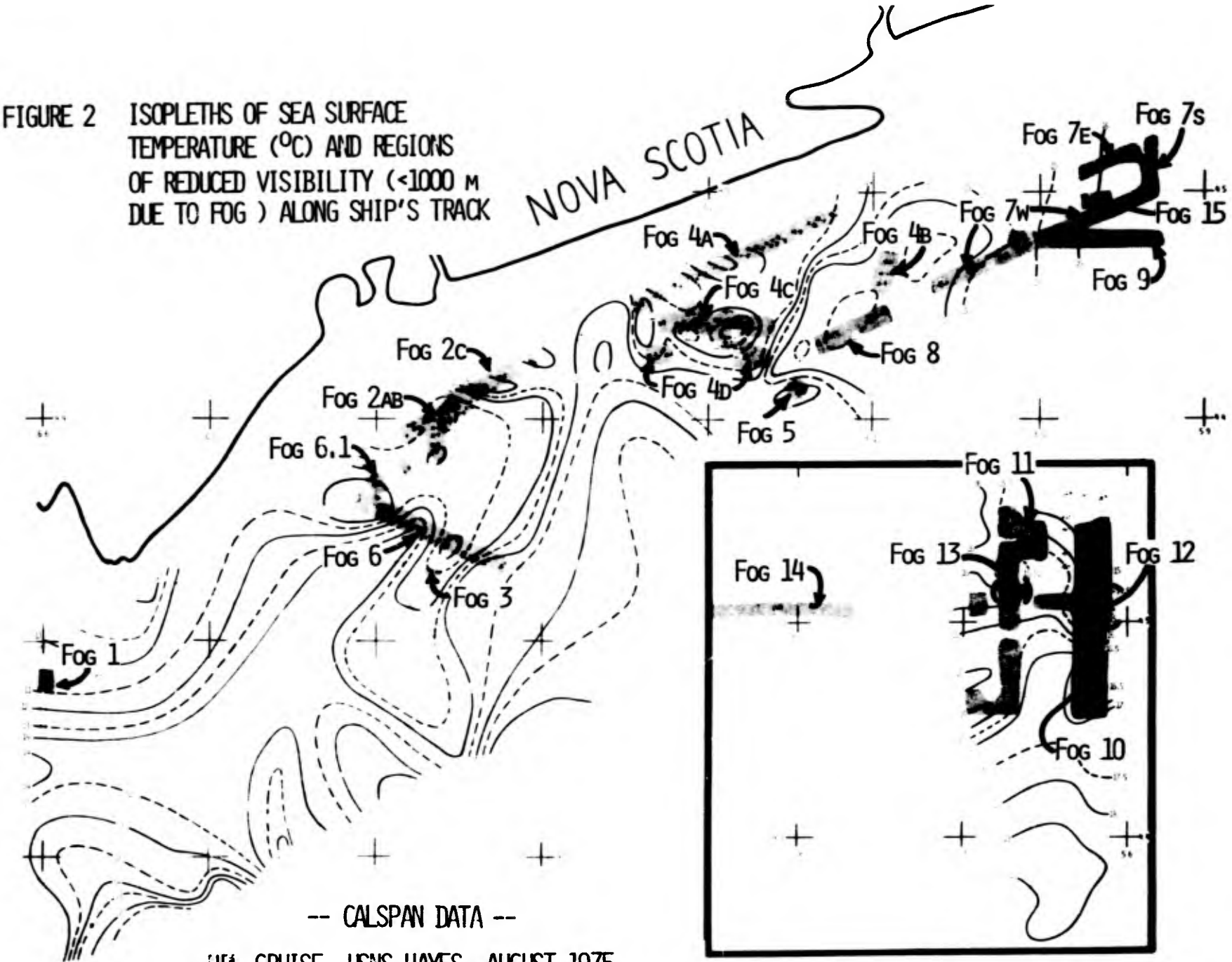

many fogs formed through a stratus-lowering mechanism (Mack et al., 1973). There is no doubt that in some instances the cold underlying sea surface contributed substantially, augmenting the stratus-lowering mechanism to produce fog at the surface.

It is not possible to establish without some doubt the mechanisms responsible for formation of all fogs encountered during the cruise. Problems in coordinating necessarily-instantaneous maneuvers with pre-planned cruise patterns completely prevented data acquisition in the exact upwind direction for every fog. Thus, many of the conclusions concerning formation mechanisms are based on deduction and on assumption of true upwind conditions.

It became apparent during analyses that the 18 fog episodes encountered off Nova Scotia were not isolated events; but rather, in many instances, four or five sequential events were related within a larger scale meteorological condition. Within the context of the larger scale system, surface features of the fogs were apparently controlled by the distribution of cold water along the coast. In this section, an effort has been made to interpret the data from this viewpoint, in a large-scale sense, tying together apparently-related fog events and establishing the contribution of cold sea surface to surface-level fluctuations in fog density.

2.1 The Fog Event of 2-3 August 1975

The fog labeled 2A and 2B was encountered during the late evening of 2 August 1975. The ship cruised through the fog twice, and detailed data for those two tracks are given in Figures A-5 through A-12 in Appendix A. A correlation of visibility data with sea surface and air temperature data suggests that this fog formed over, and as a direct result of, an area of very cold water.

In Figures 3 and 4, the ship's track has been reproduced and an attempt has been made to draw isotherm contours for the sea surface (Figure 3)

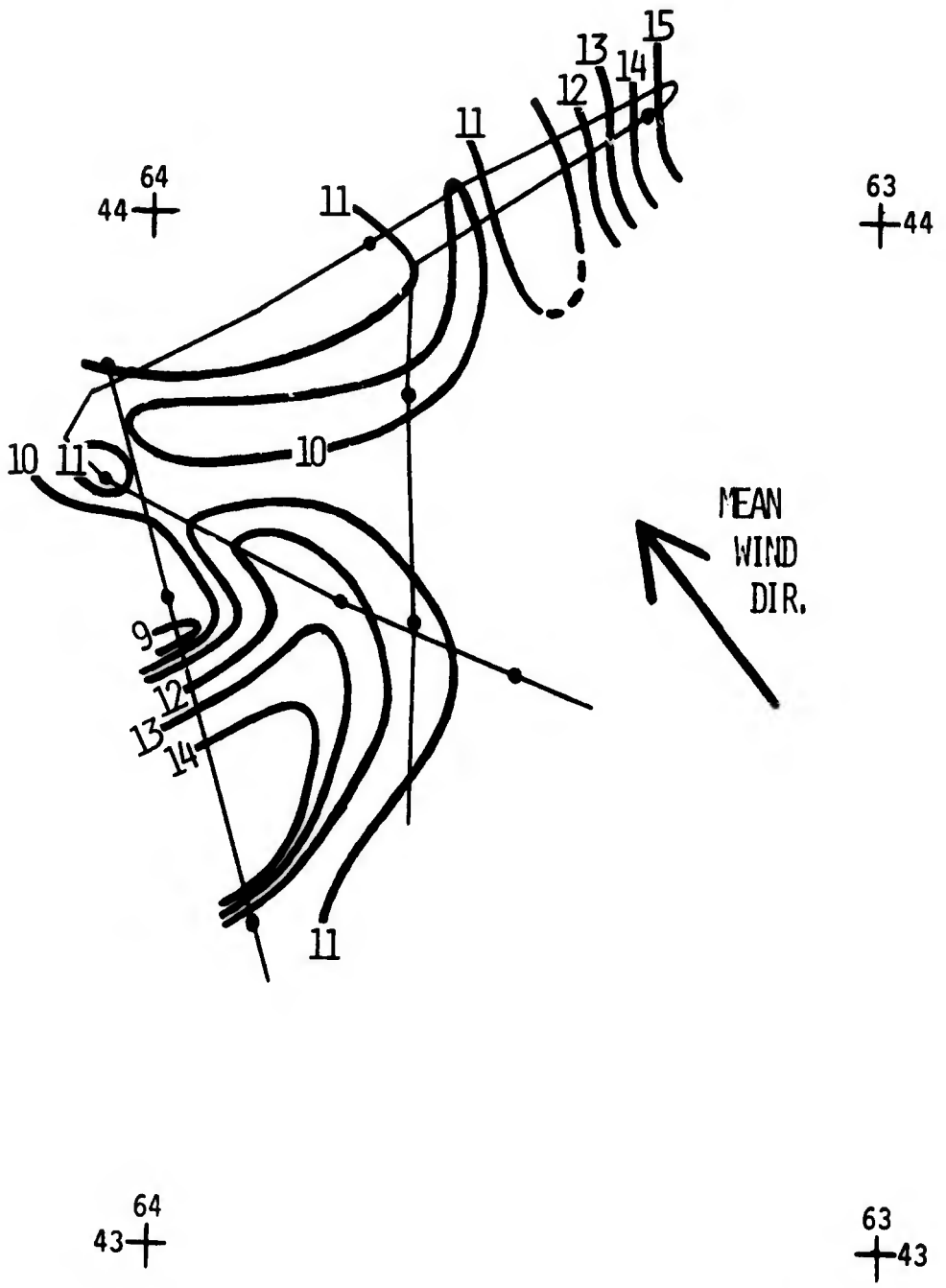

FIGURE 3: SEA SURFACE ISOTHERM (C) CHART FOR THE FOG OF 1915-0040, 2-3 AUGUST 1975.

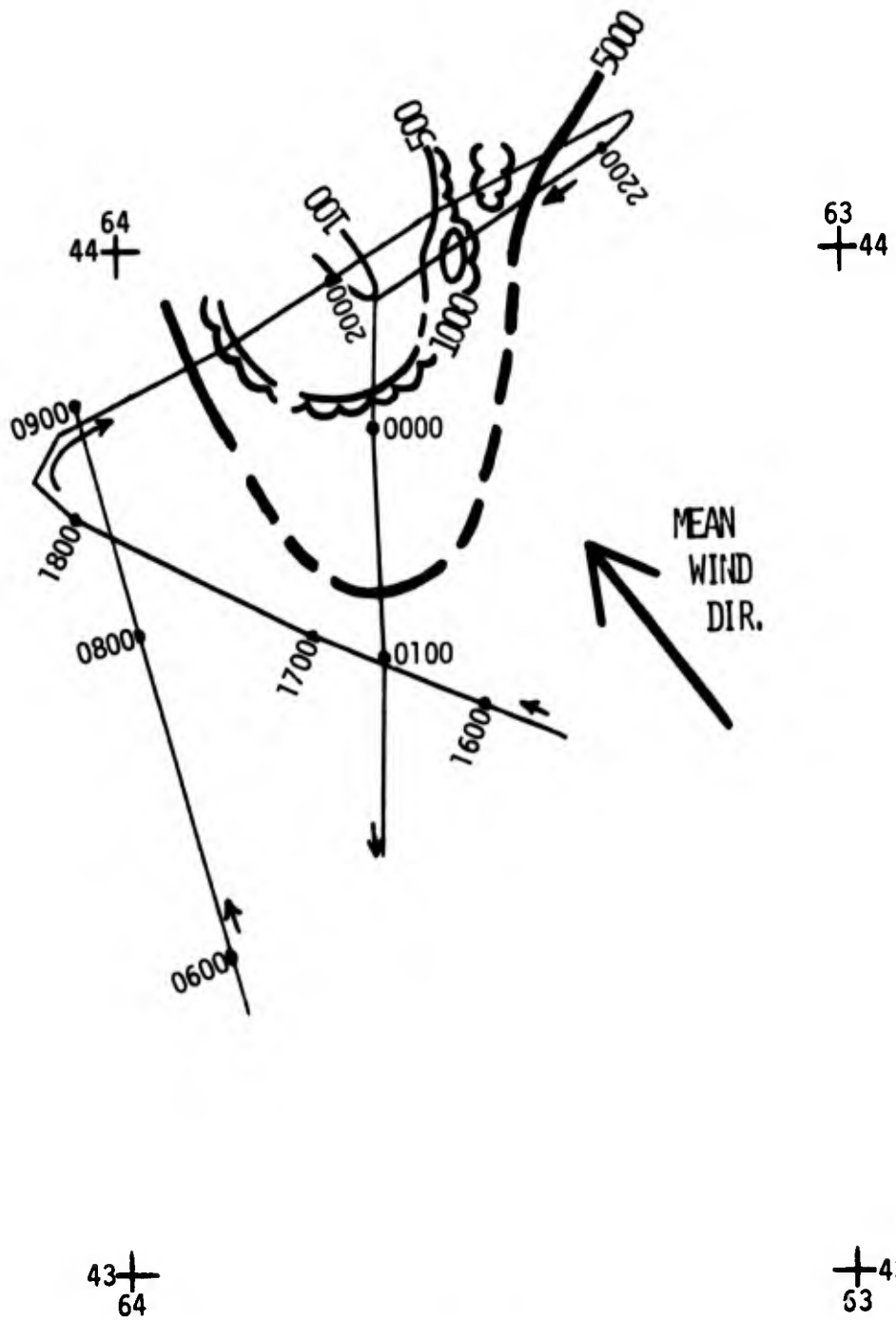

FIGURE 4: CONTOURS OF VISIBILITY (M) FOR THE FOG OF 1915-0040 EDT, 2-3 AUGUST 1975.

and to delineate boundaries of the fog by isopleths of visibility (Figure 4). Visibility isopleths are labeled in meters, and the 1000 m visibility level is represented by the scalloped line. Note that the contours of visibility follow the general pattern of the sea surface isotherms and that the fog was located over and just downwind of the coldest water in the vicinity.

The fog of 2-3 August was quite shallow, and fog top was generally at or below the 20 m height. Only in the centermost portion of the fog did fog top reach above the 27 m level, and there only momentarily. Visually, the fog appeared (from the 20 m vantage point) as sketched in Figure 5. Fog depth increased gradually from the edges toward the center of the fog, and fog top was very ragged--not like the smooth, regular appearance of fogs formed beneath and capped by inversion layers. Fog 3 (Figures A-14 to A-17), observed later in the early morning of 3 August, exhibited similar features but was of much smaller dimension in both the horizontal and the vertical.

The bulk microphysical features of Fog 2 are difficult to assess because sampling instrumentation was located at a height of 20 m (i.e., near fog top). Thus, the measurements of fog microphysics for Fog 2 may be representative of fog top only. These data may be found in Figures A-9 and A-13. Briefly summarizing, mean drop radii of about 5 μm and maximum drop sizes of ~ 17 μm were characteristic of the fog. Droplet concentration varied from about 30 to 110 cm^{-3}, and liquid water content ranged from ~0.03 to ~0.20 g m^{-3}. Minimum observed visibility was <100 m.

The best wind information indicates that during the period of observation of the fog, winds shifted gradually from southerly at 1800 EDT to SE (~140°) by 2200 EDT. Unfortunately, sea surface temperature data are not available from the upwind quadrant, and thus it is not possible to demonstrate conclusively that this fog formed as a direct result of cooling from below.

Some insight into the mechanism responsible for this fog may be deduced from analyses of the vertical temperature profiles and surface-level

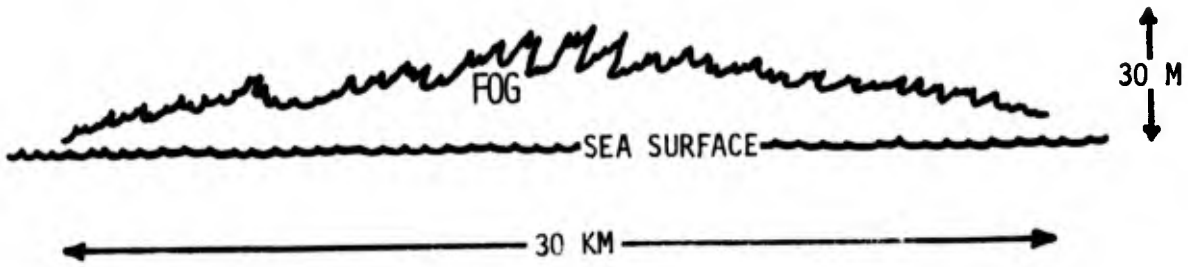

FIGURE 5: SKETCH OF THE VERTICAL PROFILE OF THE FOG OF 1915-0040, 2-3 AUGUST 1975.

humidity data obtained in the vicinity. In Figure 6 selected vertical temperature profiles (surface to 27.5 m) are shown for the areas outside the western, eastern, and southern boundaries (5000 m visibility isopleth) of the fog and for the center region of the fog. Approximate upwind conditions may be represented by the two profiles (shown dashed) obtained outside the southern boundary of the fog before and after (1630 and 0050 EDT) encountering the fog. These two profiles indicate that upwind conditions remained relatively unchanged through the period. Note that all profiles exhibited an inverted lapse down to the surface and that the absolute values of air temperature were similar at all points outside the fog except for the near-surface level at the eastern edge of the fog. (Vertical soundings obtained at 1730 and 2030 EDT by Gathman (1976) show that the inverted lapse extended up to ~200 m.) From Figure 3, it can be seen that advection of air nearly parallel to sea surface isotherms accounts for the small change (from upwind conditions) in air temperature along the western edge of the fog and that advection from substantially warmer water can account for the warmer air temperatures along the eastern edge of the fog.

The sea surface temperature immediately upwind of the fog was the coldest (i.e., ~9.5°C) observed along ship's track in the area and may have been even colder in the area farther upwind (not traversed). It can be seen

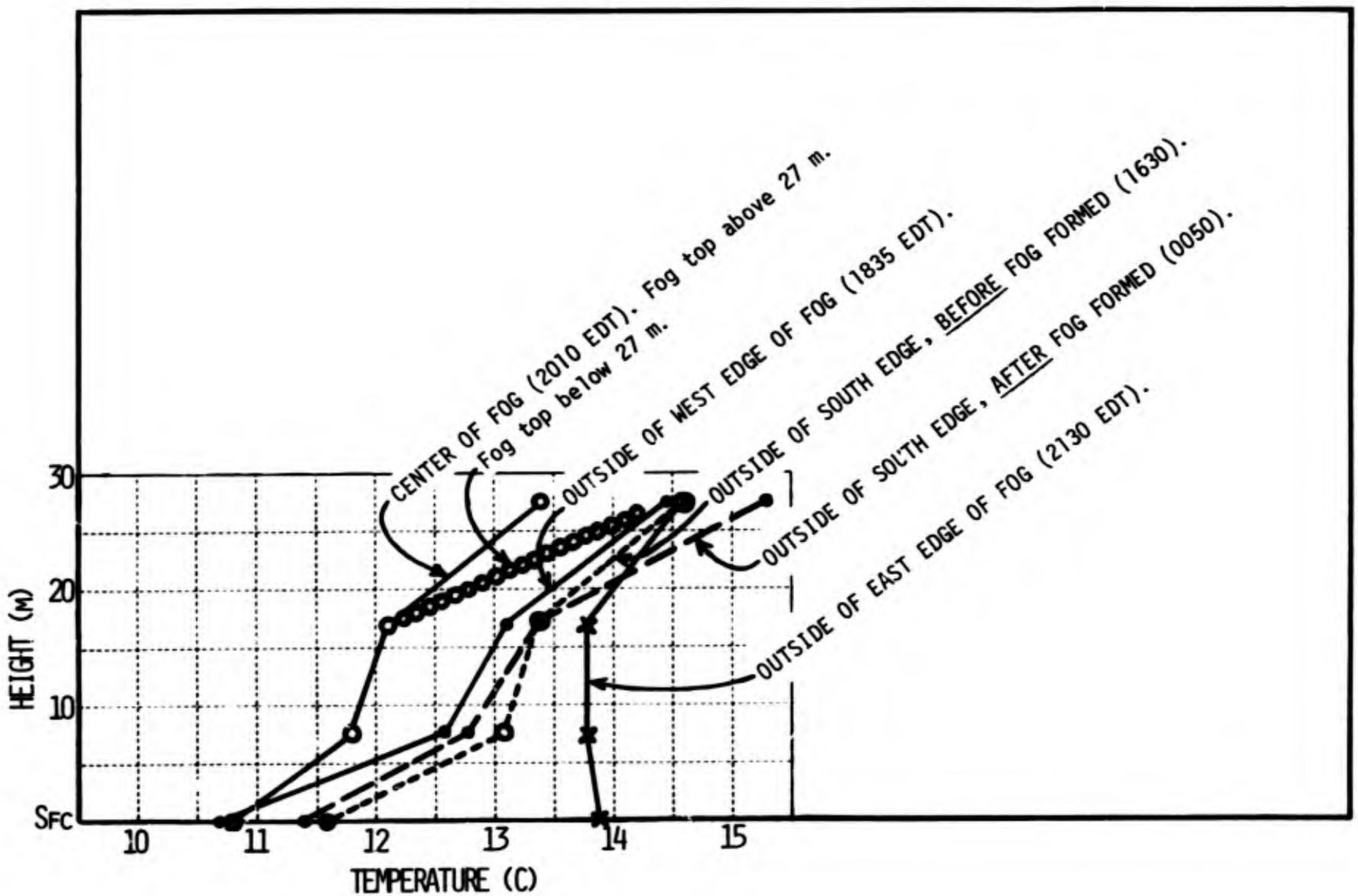

FIGURE 6: SELECTED VERTICAL TEMPERATURE PROFILES IN AND AROUND THE FOG OF 2-3 AUGUST 1975.

from Figure 6 that within the fog the inverted lapse was maintained; but that after advection over the cold water, lower level air temperatures were colder by ~1.5°C than upwind conditions. At levels above fog top, air temperatures were nearly the same as those measured at upwind locations--indicating a cooling mechanism confined to the lowest tens of meters.

It appears that a sea surface temperature gradient--from ~11.5°C in the general upwind area to ~9.5°C under the leading edge of the fog--was responsible for cooling the boundary layer (below ~25 m) by ~1.5°C. Upwind of the fog, measured relative humidity was approximately 90% (89-94% depending on the instrumentation one wishes to believe). At these relative humidities, cooling of the air by 1.5°C is more than sufficient to produce saturation (assuming no water vapor losses to the cold sea surface) and account for the fog. The ragged structure of the fog top and the shallow depth of the fog are, in themselves, indicative of boundary exchange processes, driven by surface-level influences. It is interesting to note that the condition of this fog nearly duplicate those predicted by numerical models of fog (Rogers et al., 1975; Eadie et al., 1976) formed by advective cooling at the surface.

That radiative processes do not appear to contribute measurably to the observed situation may be readily explained by the low optical density of the fog. Previous measurements of radiative transmissivity in shallow radiation fogs on land (Mack and Pilié, 1973) suggest that for a fog to be optically opaque to long wave radiation (and, hence, to radiate as a black body), it must have an optical density equivalent to an integrated liquid water (per square meter over the entire fog depth) in excess of ~3.0 grams. The liquid water content values shown in Figures A-9 and A-13, if taken as average values over the depth of Fog 2, give values of integrated liquid water between 0.3 and 2.0 g. Thus, with such a low optical density and considering the relatively short advection time from fog edge to the centermost point of observation (i.e., ~15 km @ ~5 m sec^{-1} or 50 min), radiative processes could not be an effective mechanism for cooling this fog.

2.2 The Fog Situation of 3-4 August 1975

Analysis of the fog episode of 3-4 August 1975 has led to the conclusion that fog events labeled 2C, 4A, 4B, 5, 4C and 4D all occurred within and were a part of a large-scale meteorological situation. Detailed data obtained during the numerous encounters of this fog may be found in Figures A-18 through A-40 in Appendix A.

An attempt was made to delineate the areal extent of this fog episode by contouring visibilities measured along ship's track during the period. The results of this effort, along with mean wind directions at various locations along ship's track, are presented in Figure 7. This interpretation suggests that the fog of 3-4 August was of mesoscale dimensions and was broken into two segments: the easternmost one with an areal extent of approximately 10,000 km^2; and the other located to the west and downwind of the first fog with a horizontal dimension of approximately 70 km. At all locations beyond the 5000 m visibility boundary of the fog (both upwind and downwind), low stratus was present aloft. Considerable liberty was taken in estimating fog characteristics in the area enclosed by ship's track, particularly in view of the 28-hour period required to complete the track. However, wind direction remained relatively constant throughout the period, and diurnal influences were not apparent. Thus, it is felt that the general outline of the fog is valid.

Immediately after cruising out of the upwind edge of the fog at ~2230 on 3 August, ship's course was changed to 194°T; and the fog was reentered. Hence, very little is known about upwind conditions for this fog, and we can only speculate about its origin. Comparison of the surface features of this fog (Figure 7) with the detailed sea surface isotherm analysis shown in Figure 8 reveals a marked correlation between fog density and sea surface temperature. In the downwind direction from the upwind edge of the fog, visibility at the surface degraded as air advected toward colder water. Minimum visibilities were observed, in almost every instance, over or just downwind of the coldest water along ship's track.

FIGURE 7: CONTOURS OF VISIBILITY (M) FOR THE FOG OF 1030-2000 EDT, 3-4 AUGUST 1975.

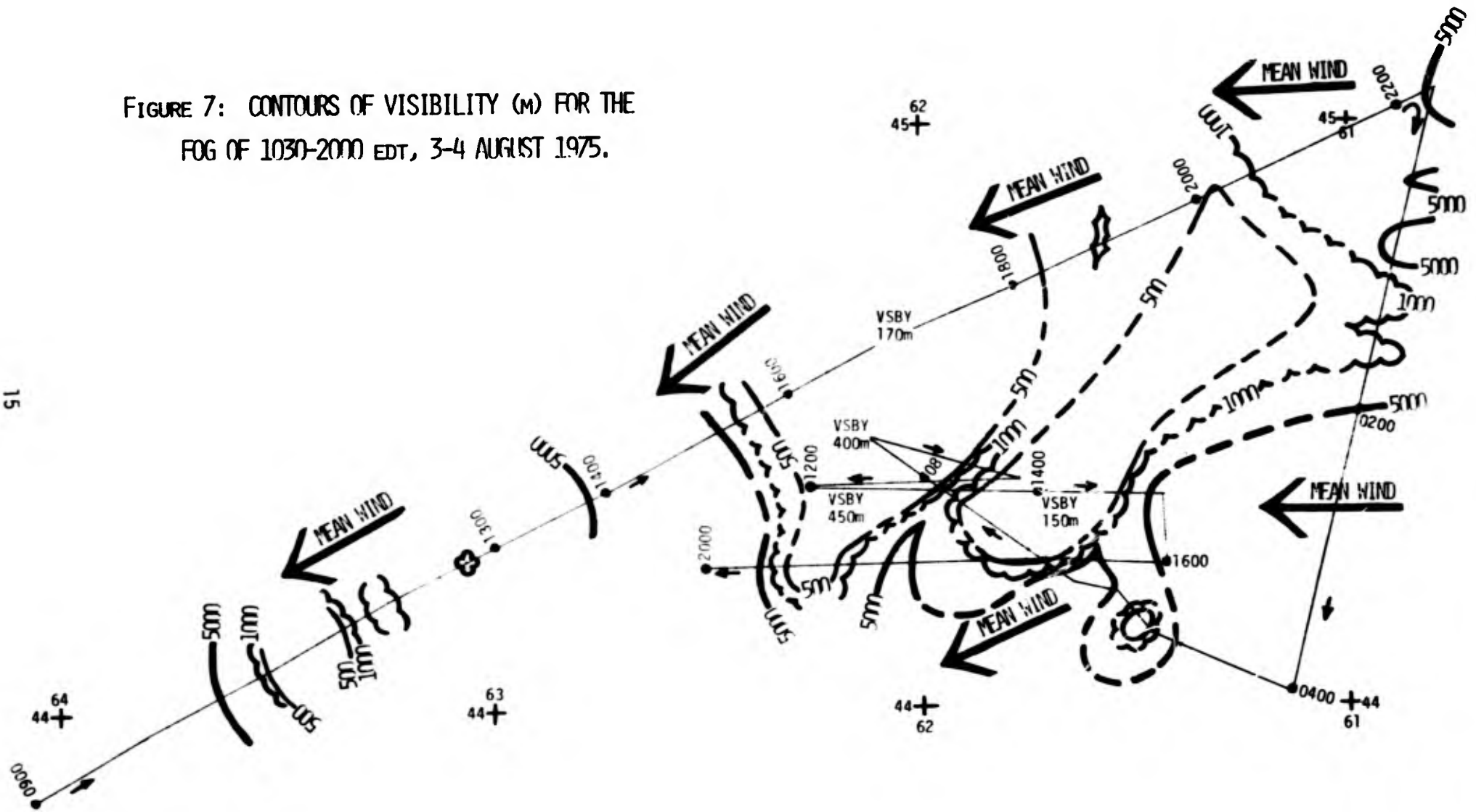

FIGURE 8: SEA SURFACE ISOTHERM (C) ANALYSIS FOR THE FOG SITUATION OF 1030-2000 EDT, 3-4 AUGUST 1975.

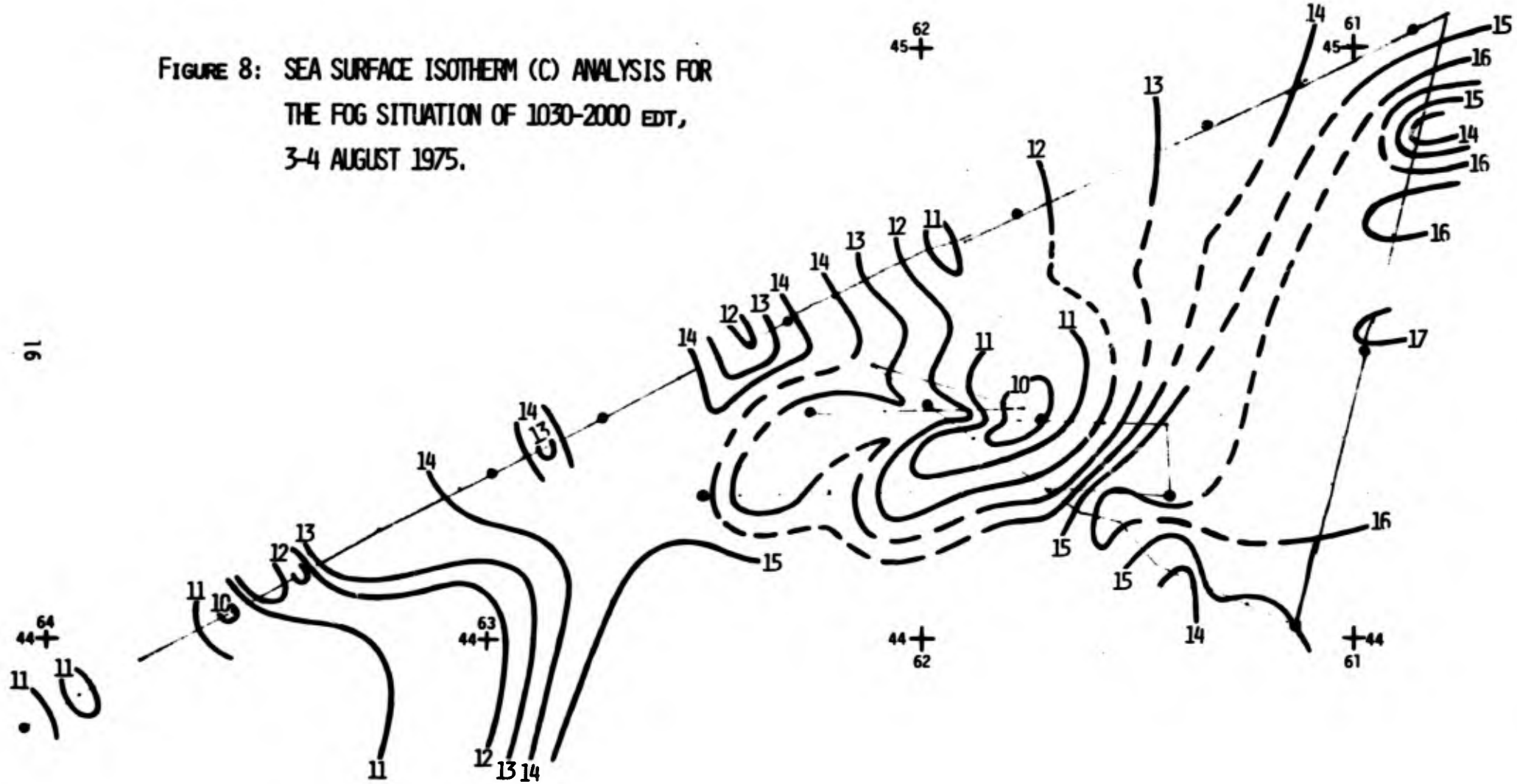

From a comparison of Figures 7 and 8, it is evident that the eastern portion of the fog dissipated at the surface (or lifted) at its downwind edge in response to the warmer sea surface downwind of the major cold water area. Over the warmer water, the air mass warmed rapidly while dew point remained constant, and the fog apparently evaporated in the layer next to the surface. (See Figures A-21, A-22 and A-23.) Low stratus remained overhead, and farther downwind fog reformed at the surface (Fog 2C) as the air again cooled over another area of cold water. (See Figures A-18 and A-19).

Microphysics data obtained in the central core of the fog may be summarized as follows: mean drop size varied between ~4.5 and 8.0 μm, averaging ~6.5 μm radius; droplet concentration ranged between ~40 and 100 cm^{-3} and averaged ~60 cm^{-3} in the denser central portion of the fog; liquid water content values varied between 0.06 and 0.17 g m^{-3}, averaging about 0.10 g m^{-3}. Minimum observed visibility was ~150 m. Details of the individual drop size distributions may be found in Figures A-26, A-29, A-32, and A-35.

In summary, it appears that the fog episode of 3-4 August 1975 could have formed via a stratus-lowering mechanism which was augmented by cooling due to the cold sea surface. Stratus were present at <u>all</u> locations immediately outside the boundaries of the fog, and considerable drizzle was present throughout much of the fog--both observations indicative of a deep layer of fog/cloud. Vertical soundings are not available to verify the depth of the mixed layer for this situation. However, complete obscuration of the sun and moon during the episode suggest a cloud layer well in excess of 150 m depth.

Vertical temperature profiles up to 27.5 m (from ship's instrumentation) show that lapsed conditions were prevalent (particularly outside the fog boundaries) except where an extremely cold sea surface cooled and modified the boundary layer. In a low stratus situation, a well-mixed layer, assisted by radiative cooling of the stratus cloud and subsequent instabilities, would be expected to exhibit a lapsed temperature profile. The data therefore suggest that this fog formed at least as a partial result of a thickening

stratus deck. The influence of cold sea surface on fog density is unmistakable. It appears likely that the presence of the stratus aloft (which in itself may be a result of air-sea boundary layer exchange processes) set the stage (or conditioned the air mass) for eventual fog formation at the surface through direct heat exchange with the cold sea surface.

2.3 The Fog Event of 4-5 August 1975

Fog event Number 6 (Figures A-41 through A-47) was observed between the hours of 2200, 4 August, and 1300, 5 August, in the cold water area located approximately south of the position of the prior Fog 2 (see Section 2.1) and southwest of Fog 4 (Section 2.2). During the period of observation of Fog 4 on the previous morning, winds were consistently from the E to ENE. By the time (and at the location) of Fog 6 winds had shifted, and for the duration of Fog 6 winds were from the W to NW direction.

Ship's track and the areal extent of Fog 6 are depicted in Figure 9. The sea surface isotherm analysis for the area bounded by ship's track for this situation is presented in Figure 10. Comparison of Figures 9 and 10 suggests a near direct relationship between the location of the cold water and the location of the fog. It is interesting to note that the tongue of very warm water intruding into the western edge of the area apparently had very little effect on surface-level visibility.

Since upwind conditions are unknown, it is difficult to assess with certainty the processes responsible for triggering this fog. Comparison of Figures 9 and 10 suggests that the five upwind extensions of Fog 6 were formed over cold water patches and subsequently grew and merged in the downwind direction. From visual observations, each of the middle three upwind extensions (labeled Fogs 6.1, 6.2 and 6.3 in Figure A-46) of Fog 6 was shallow (the sun and blue sky were visible in the vertical) and gave the impression of becoming more shallow and narrower in the upwind direction. Downwind, the fog patches appeared to grow in depth and merge near the horizon.

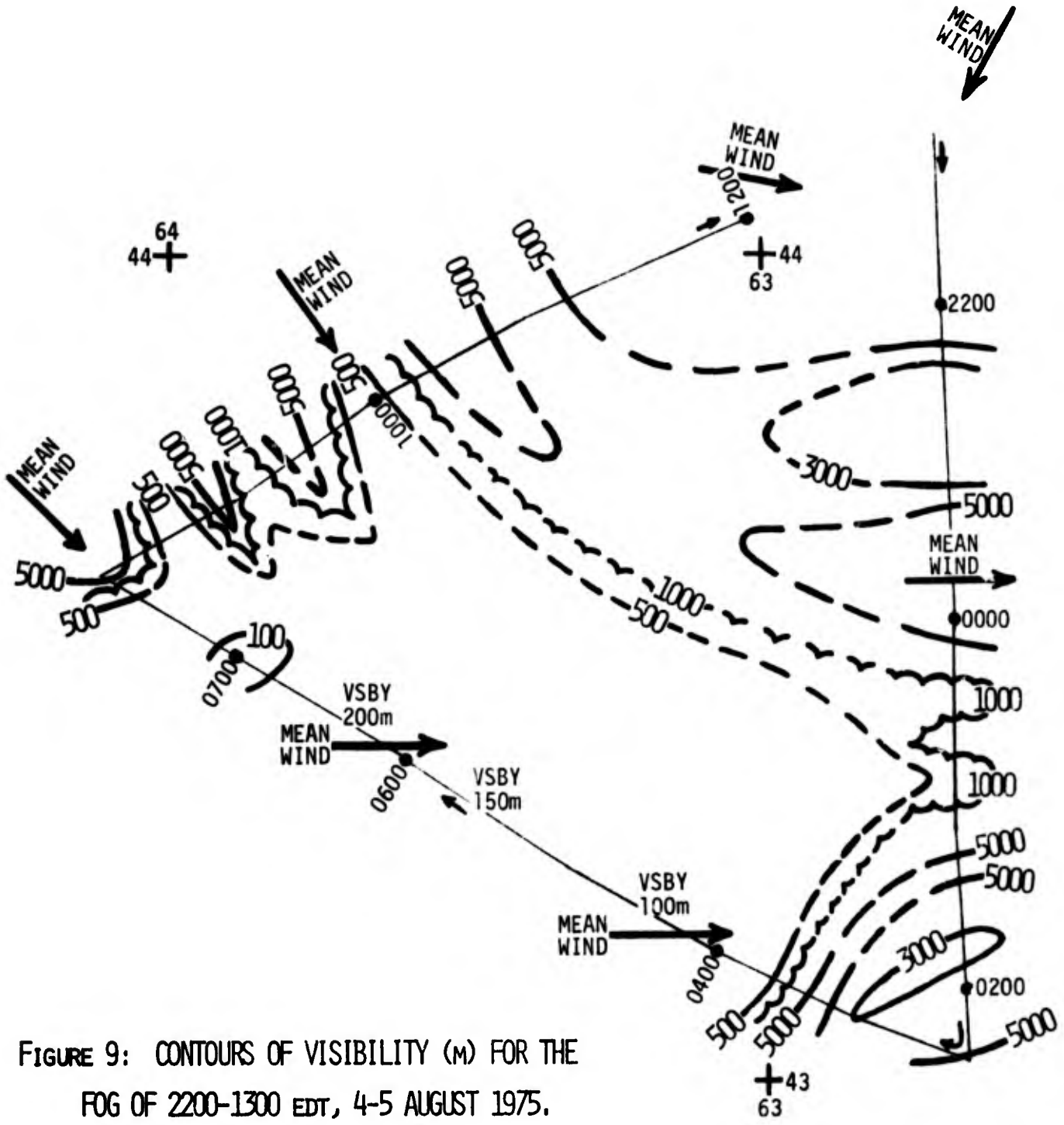

FIGURE 9: CONTOURS OF VISIBILITY (M) FOR THE FOG OF 2200-1300 EDT, 4-5 AUGUST 1975.

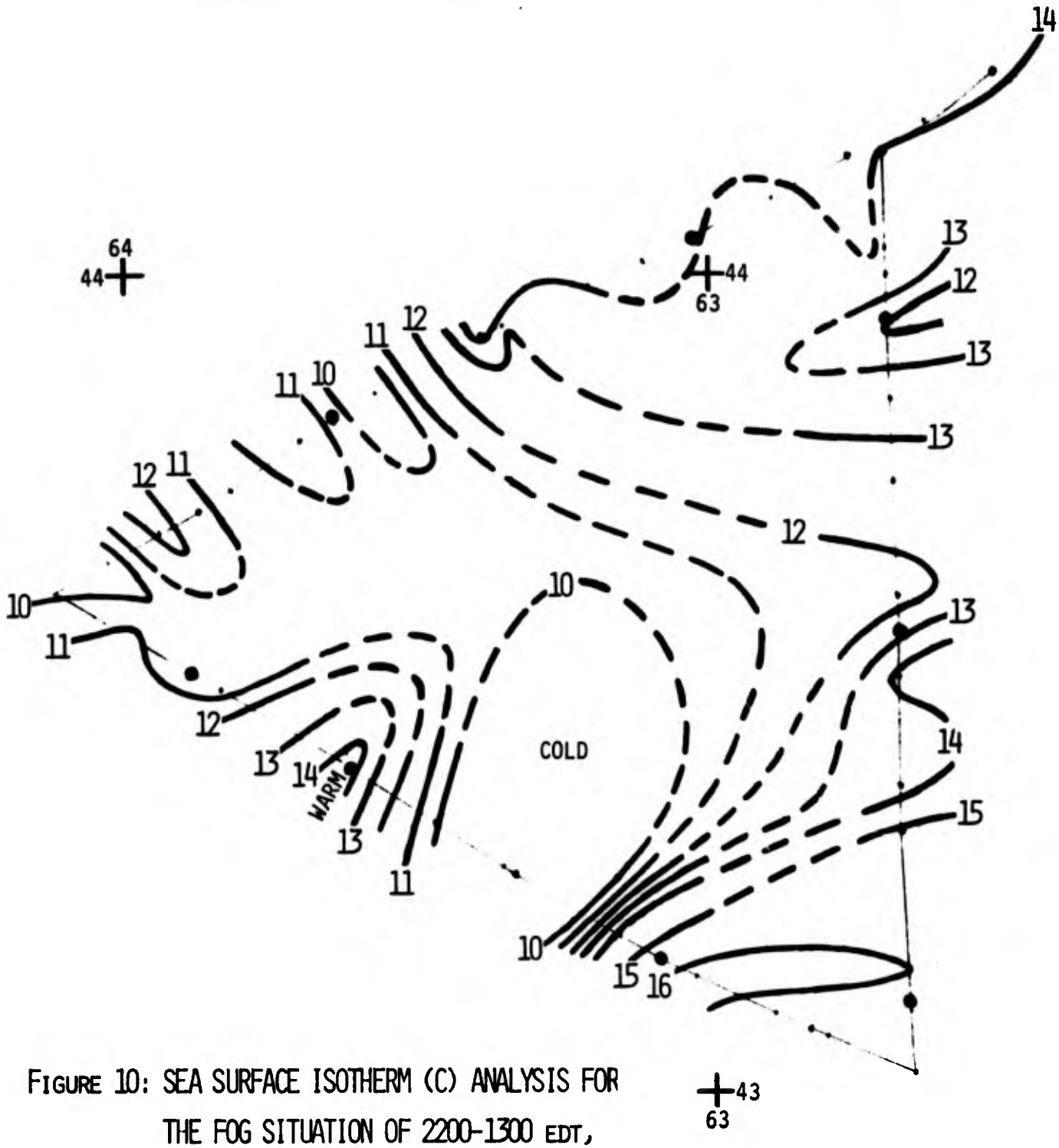

FIGURE 10: SEA SURFACE ISOTHERM (C) ANALYSIS FOR THE FOG SITUATION OF 2200-1300 EDT, 4-5 AUGUST 1975.

Some insight into the processes responsible for the growth and persistence of this fog may be gained from data acquired during the period 0230-0745 (5 August) along the ship's track heading 300°T. Since winds shifted from a direction of 270°T near the southern end of the track to a direction of 315°T at the northern end, the data acquired along the track provide an approximate downwind profile from the leading to the trailing edge of the fog. These data are provided in Figures A-42, A-43 and A-44 and are reproduced in a slightly different format in Figures 11 and 12. In Figure 11, air and sea surface temperatures are compared with visibility as functions of time along the track. In Figure 12 the relative dew point and selected vertical temperature profiles as functions of time are shown along with a reproduction of the visibility record. The synchronous fluctuation of temperature and dew point within the bounds of the fog suggests that saturated conditions existed at least at the 17 m level at all times in the fog.

With reference to Figures 11 and 12, the sequence of events in the development of Fog 6 from the upwind edge to the downwind edge was as follows: the upwind portion of the fog (between times 0740 and 0700 EDT) was located over water colder than the air, and inverted lapse conditions prevailed from the surface through 27.5 m. (A vertical temperature sounding obtained much later between Fogs 6.2 and 6.3 at 0930 EDT (Gathman, 1976) showed an inverted lapse of 5 Celsius degrees up to the 200 m height.) Like other previously-mentioned upwind extensions (Fogs 6.1, 6.2 and 6.3), the fog in the portion of this track upwind of the 0700 position was quite shallow, and it grew in depth in the downwind direction. At 0735 bright sunshine was filtering through the fog. Farther downwind at 0718, a solid fog structure previously visible to the southeast was becoming obscure, and at the 0708 position blue sky was only faintly visible in the vertical. By the 0700 position, only the faint brightness of the sky through the fog could be observed. Within a few kilometers farther downwind, the sky was totally obscured. Of course, some of the degradation in vertical visibility can be ascribed to the increasing density of the fog as shown by the visibility record at the top of Figure 11. That the fog was quite shallow in this region is clearly evidenced by the

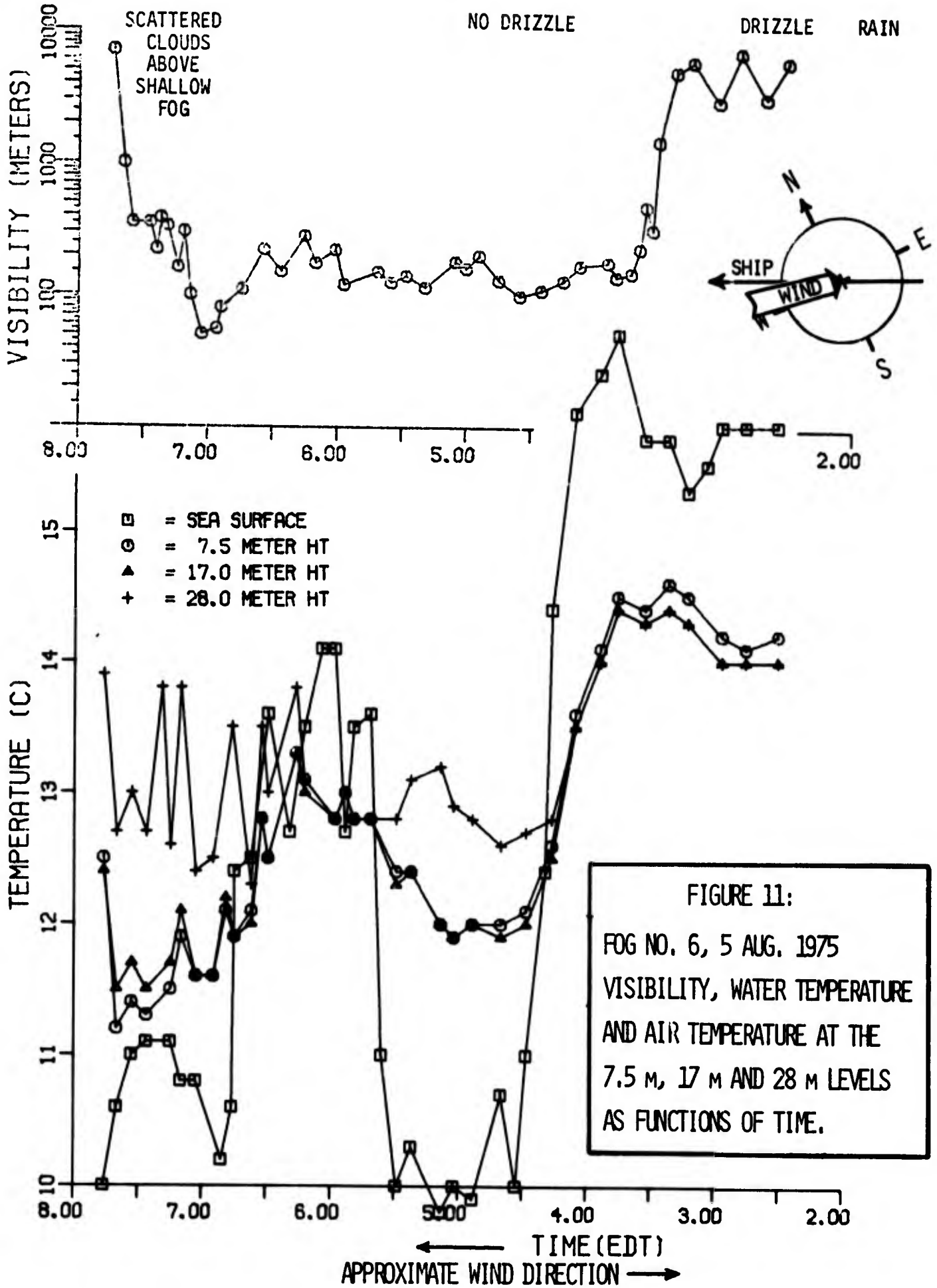

FIGURE 11:

FOG NO. 6, 5 AUG. 1975 VISIBILITY, WATER TEMPERATURE AND AIR TEMPERATURE AT THE 7.5 M, 17 M AND 28 M LEVELS AS FUNCTIONS OF TIME.

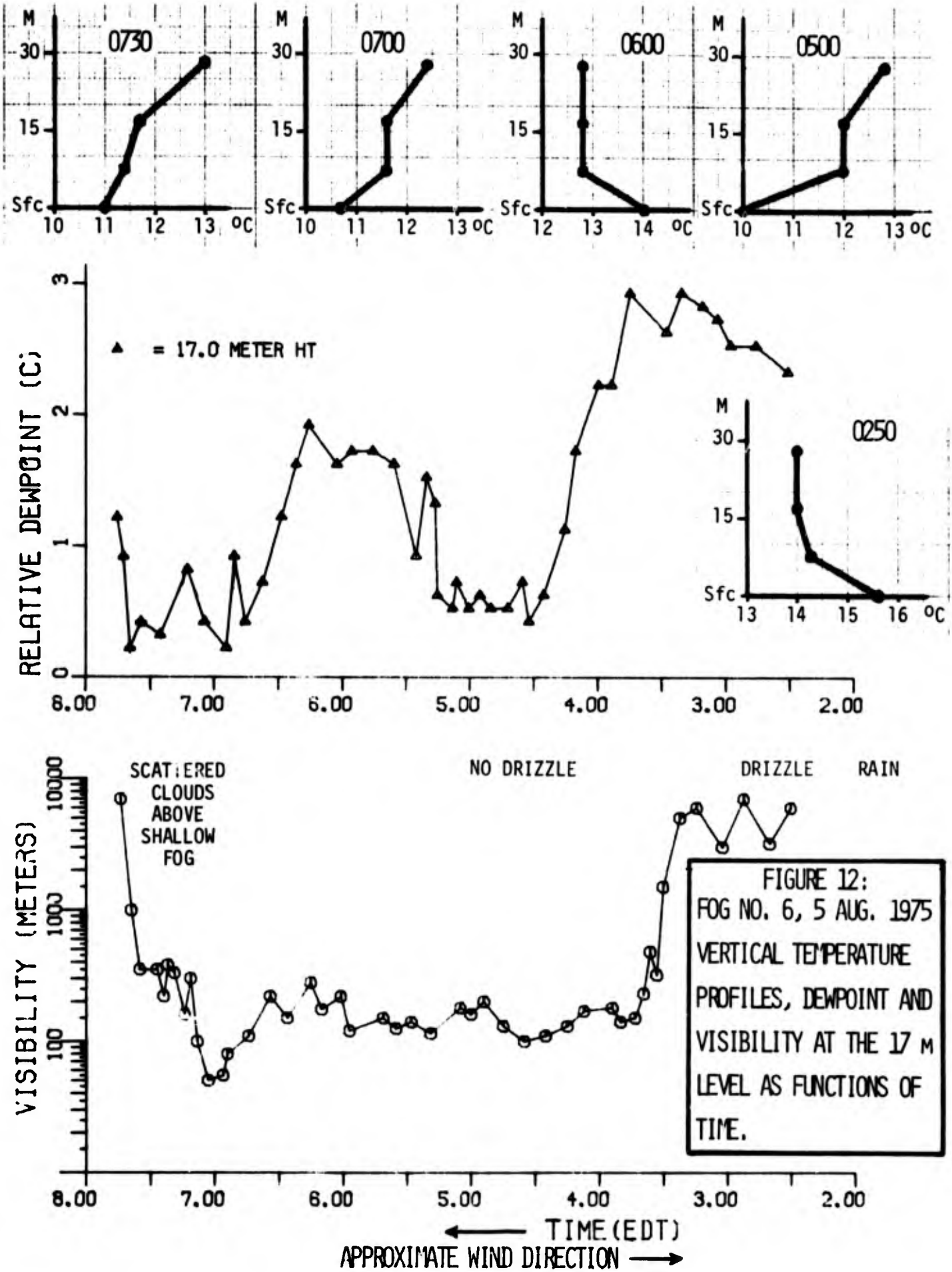

FIGURE 12:
FOG NO. 6, 5 AUG. 1975
VERTICAL TEMPERATURE PROFILES, DEWPOINT AND VISIBILITY AT THE 17 M LEVEL AS FUNCTIONS OF TIME.

fluctuating temperature record at 27.5 m--indicating that the temperature sensor at that level was alternately in and out of the fog top.

Data presented in Figure 11 show that for the initial period of fog development visibility rapidly degraded as the fog was apparently triggered over cold water. Visibility remained relatively constant (at ~300 m) as the fog advected over a slightly warming sea surface, and then visual range dropped rapidly to 60 m (at the 0705 position) as the fog advected toward cold water on the downwind side of the small, warm patch.

Immediately downwind of the shallow "formation zone" of Fog 6, the foggy air was advected over a steep gradient in sea surface temperature to water approximately 2°C warmer than the air and approximately 4°C warmer than water in the upwind area. Evidently the instabilities created by this situation caused enough vertical mixing of the air to bring the lowest 28 m into near isothermal conditions at the 0615-0540 EDT location. Immediately downwind of the abrupt gradient to warmer water, visibility improved from 60 m to 200 m--suggesting some dissipation of fog at the surface or perhaps some dilution as the foggy air was mixed to higher altitudes. The visual observations indicate that vertical visibility was increasingly restricted in the downwind direction over the warm water, in spite of the improvement in surface visibility. These observations lead to the conclusion that the warm water and resultant instabilities actually caused the fog to grow in depth probably by promoting mixing of cold, moist surface air with warm, moist air aloft. The actual depths to which this fog ultimately grew are unknown, but the temperature sounding by Gathman suggests that it couldn't grow much beyond the height of 200 m.

Farther downwind the fog advected over the other side of the warm tongue to the colder water. Air temperature in the lowest levels responded by cooling sufficiently to re-establish inverted lapse conditions below 28 m. Response to the cold water by the fog is evidenced by its increased density as visibility gradually dropped from 200 to 100 m. (That air temperature at the 27.5 level did not respond to the cold water may be indicative of the depth of the newly-formed mixing layer in the region over the cold water.)

At the 0430 EDT position, the fog finally advected out of the cold water area and over the dramatically warmer water existent farther to sea away from the region of upwelling. Over a distance of 15 km sea surface temperature increased by more than 6°C. Air temperatures quickly increased and visibility began to improve in response to the heating from below. Comparison of data in Figures 11 and 12 indicates that the fog finally dissipated at the surface after the air had been warmed to beyond the dew point. A stratus deck and considerable drizzle were all that remained of the fog farther downwind. Evidently the surface warming by more than 6°C was sufficient to overcome the original stability of the entire layer (see Gathman sounding), destroying the original inversion and lifting the entire fog layer off the surface and to a new equilibrium altitude.

In summary, the data from this situation provide striking evidence of the influence of warm water patches in promoting the persistence and growth of some marine fogs. Obviously, a balance between the stability of the boundary layer and the magnitude of a sea surface temperature increase over which the fog advects is a prerequisite for warm water to be a positive influence in the persistence of marine fog. If the temperature gradient is too great, it may overwhelm delicately balanced boundary layer structure, creating a new boundary layer of considerably greater depth and raising the condensation level off the surface.

2.4 The Fog Event of 6-7 August 1975

On 5-7 August the area of investigation was extended farther east by covering in three passes a strip 25 km wide and 150 km long approximately parallel to and 70 km off the shore of N.S. between 63° and 59° W (see Figure 13). In the eastern part of this area (E of 61°30' W), fogs #7, 8 and 9 were encountered during that time (see Figure 2). Collected data pertaining to this episode are illustrated in Figures A-56 through A-69 of the Appendix.

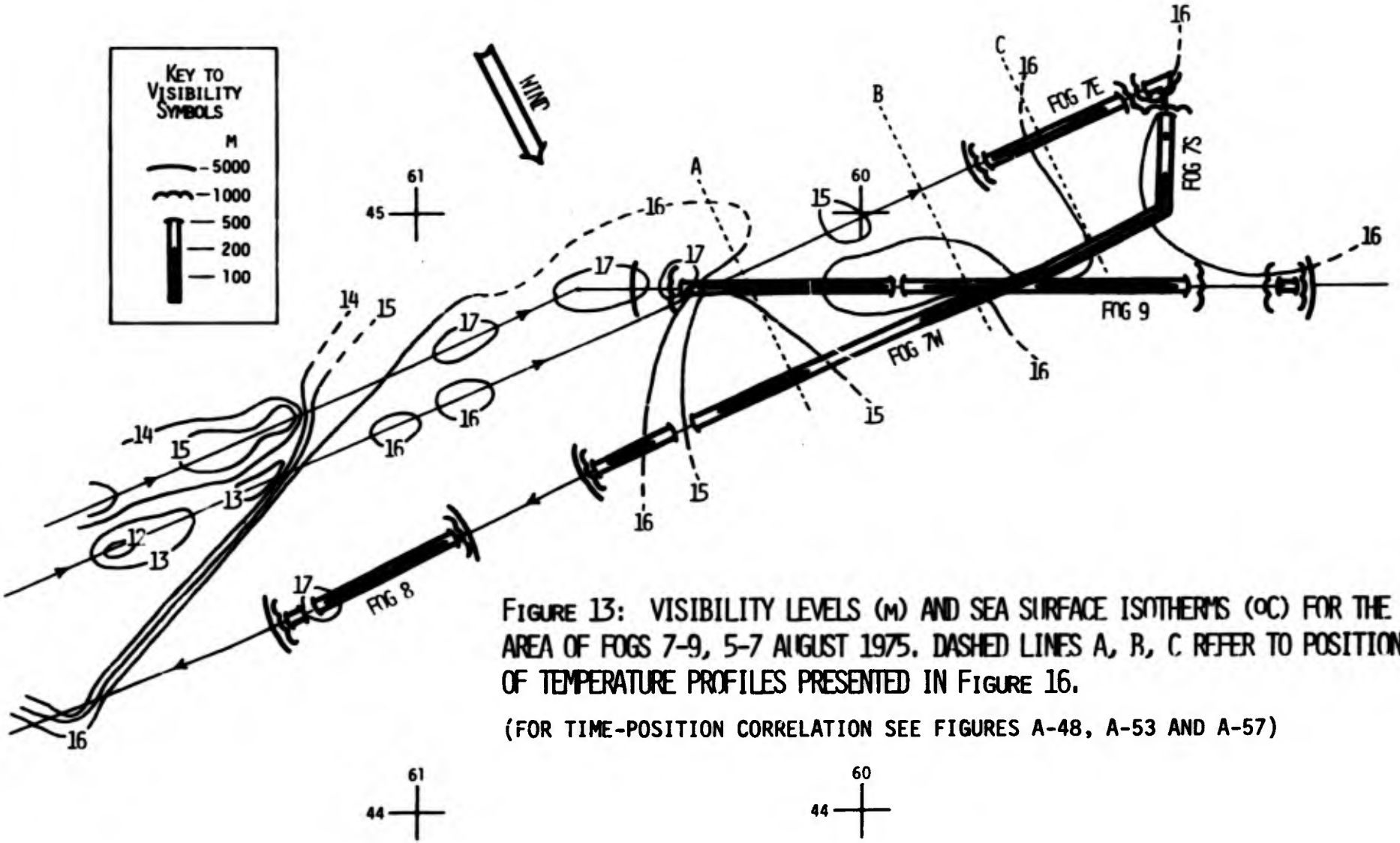

FIGURE 13: VISIBILITY LEVELS (M) AND SEA SURFACE ISOTHERMS (°C) FOR THE AREA OF FOGS 7-9, 5-7 AUGUST 1975. DASHED LINES A, B, C REFER TO POSITIONS OF TEMPERATURE PROFILES PRESENTED IN FIGURE 16.

(FOR TIME-POSITION CORRELATION SEE FIGURES A-48, A-53 AND A-57)

These three fogs are discussed here as one event because they all occurred over relatively warm water. In addition, they occurred within a 30-hr period in a relatively small area and under basically the same wind regime. (Fogs 4B and 15 were observed in the same general area but are separated from the presently discussed group by time and totally different wind directions.)

Figure 13 shows, in more detail than Figure 2, the ocean surface temperature distribution for the area in question. Whereas this figure takes into account only those temperatures measured along the tracks relating to Fogs No. 7-9, Figure 2 is based on all the tracks of this cruise, thus representing a temporal average. This explains the differences between the isotherms of Figures 2 and 13 and points to interesting temporal variations of the sea surface temperatures. The most important features of this water surface temperature map are the very moderate spatial variations in temperature in the warm water area where the Fogs 7-9 occurred and the extremely sharp decrease in sea temperature on the west side of the region.

The locations of the fogs are also shown in detail in Figure 13 where visibility values are entered along the ship's track. (Since part of Fog No. 9 was encountered in a position found free of fog on the previous pass, a composite delineation of the Fogs No. 7-9 seems inappropriate.)

In view of the fact that the predominant winds during this situation were from the NW quadrant (with the exception of a brief possible light SW wind in the middle of Fog 9), i.e., approximately perpendicular to the ship's tracks, it is difficult to interpret the present fog event with regard to possible formation mechanisms, since hardly any pertinent data upwind of the fogs are available.

In the case of Fog No. 8, available sea surface temperature data reach upwind for about 20 km owing to the northerly position of the other two passes. This distinctly cold area, which probably extended even further north (according to measurements during Fog No. 4A), may have conditioned

the lowest air layer sufficiently to trigger a "warm water fog" similar to the ones observed by these authors off the California coast (Mack et al., 1974). Figure 14, depicting temperature and visibility data combined along the track, shows the air temperature to be about .5°C colder than the water, both inside and out of the fog. The reason for the fog to be deeper on the east side than on the western portion could be attributed to the greater distance it advected over the warmer water. However, without direct upwind air data, this has to be mere speculation. The presence of a stratus layer being characteristic for this whole episode, it is tempting to consider the stratus-lowering mechanism as a possible source for these fogs. However, whenever it could be observed, the stratus, as indicated in Figures 14-17, appeared broken and scattered-- hardly substantial enough to trigger fog by a stratus-thickening process.

Fog No. 7 was far more extensive than Fog 8 from which it was separated by about 15 km of nearly cloudless sky. Within a few kilometers from its western edge (see Figure 14, ~0700-0800), this fog was similar in depth and vertical temperature distribution to the eastern edge of Fog 8. Farther to the east in Fog 7 over the area of coldest water, the low-level temperature profile shows a strong inversion accompanied by shallow fog (the structured base of a stratus could be seen through the fog at an estimated height of 400-600 m). The eastern half of 7W seemed less shallow (the farther east the more was drizzle noticeable), and the air temperature profile reverted to near adiabatic below 15 m and slightly inverted above 15 m, while the water temperature increased to about .5°C above that of the air. In an attempt to overcome the lack of upwind data, temperature profiles from the above-mentioned three areas were plotted (see Figure 16) with their upwind counterparts from along the northern track (Fog 7E, Figure 15). Whereas the profiles in Figure 16C from the portion of the area in fog are expectedly identical, Figure 16B also shows that similar profiles existed both out of fog upwind and in fog downwind. The cooling indicated in Figure 16A throughout the first 30 m parallelling a decrease in water temperature, suggests that that portion of the fog may have formed via the cold water. However, these data from single points upwind are not sufficient to determine the exact cause of fog formation.

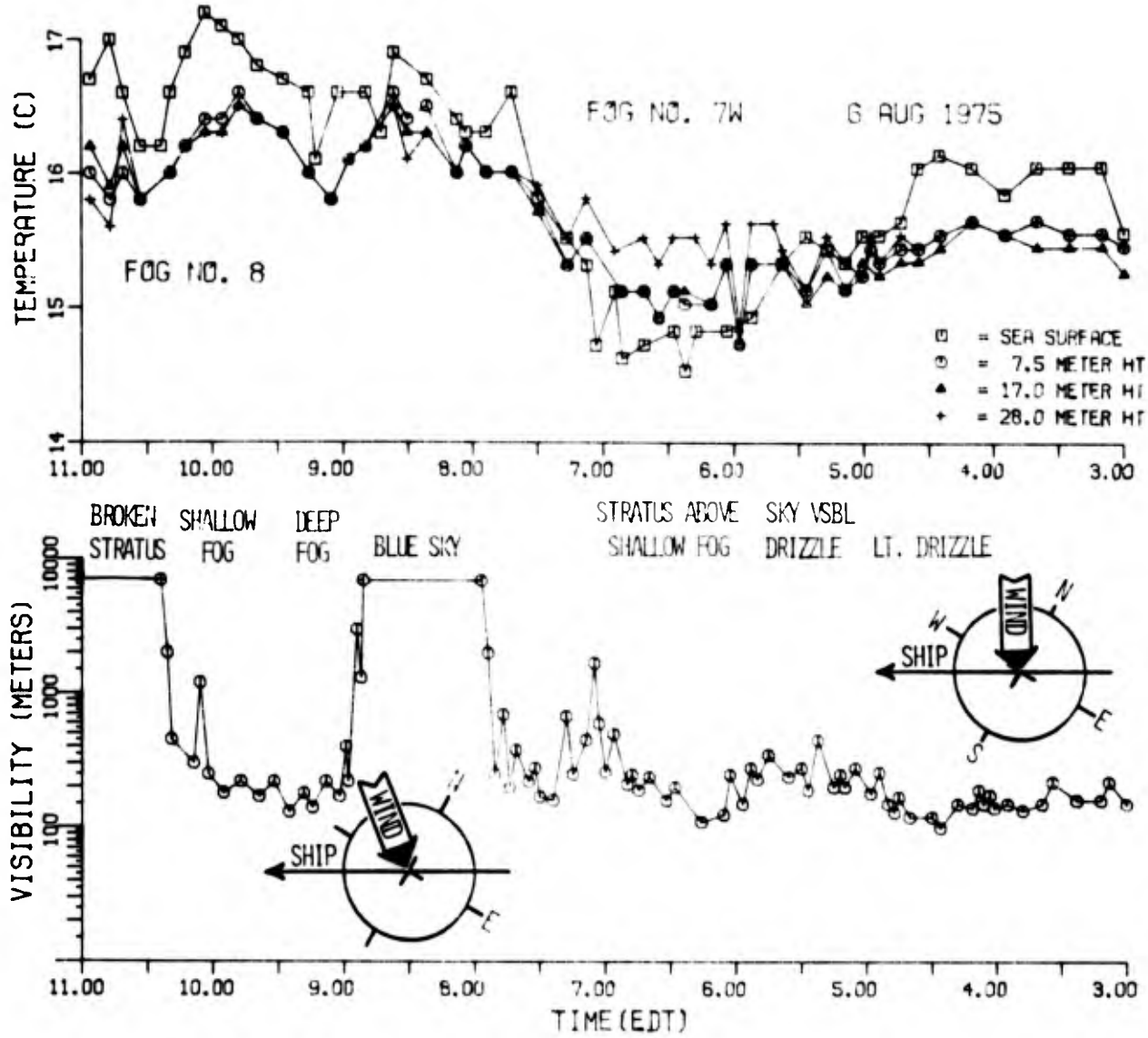

FIGURE 14: VISIBILITY, AIR AND SEA SURFACE TEMPERATURE VS. TIME
FOGS 8 AND 7W, 6 AUGUST 1975

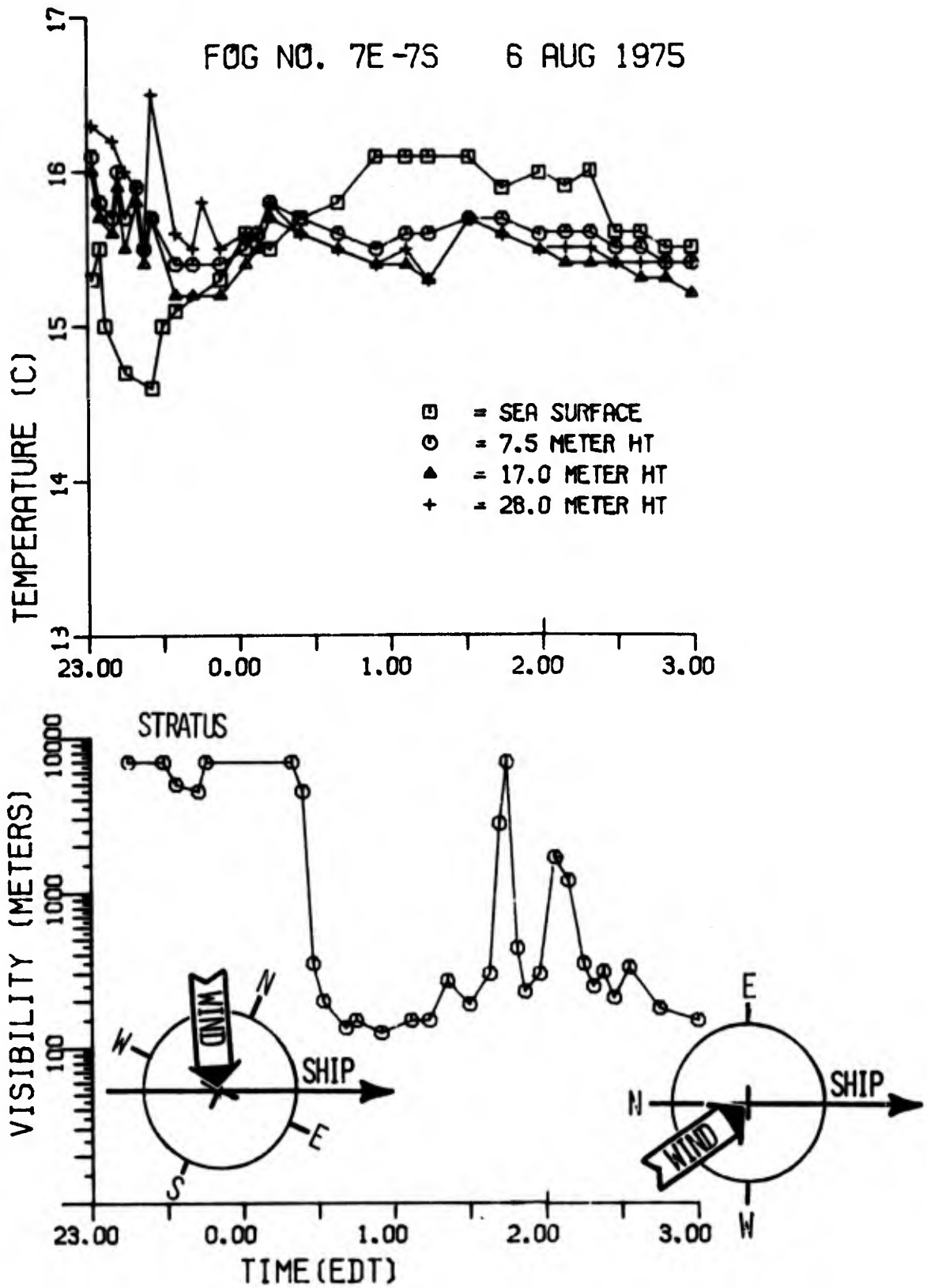

FIGURE 15: VISIBILITY, AIR AND SEA SURFACE TEMPERATURE VS. TIME. FOG 7E-S, 6 AUGUST 1975

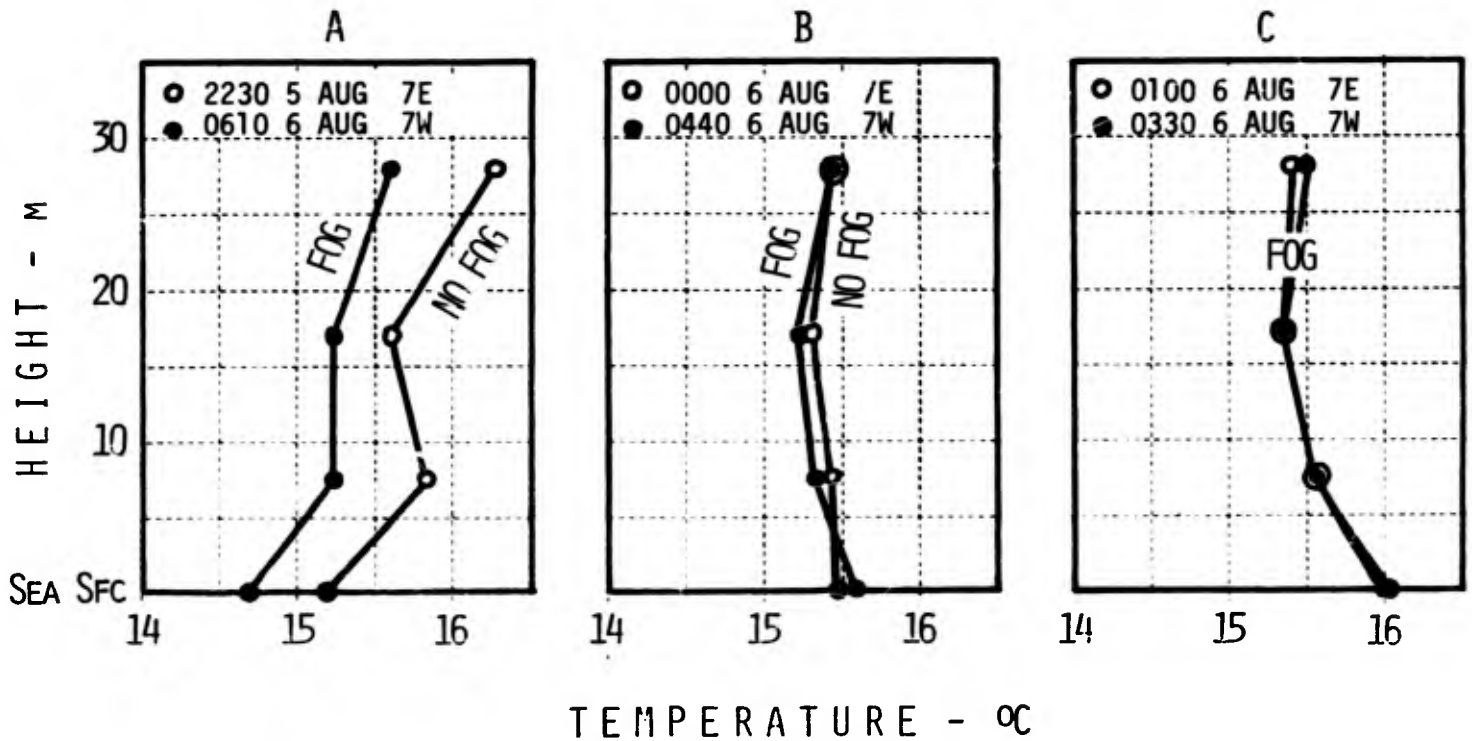

FIGURE 16: LOW LEVEL VERTICAL TEMPERATURE PROFILES FOR 3 SELECTED PAIRS OF LOCATIONS (A, B, C) ON TRACKS 7E (o, UPWIND) AND 7W (●, DOWNWIND) AS INDICATED ON FIGURE 13.

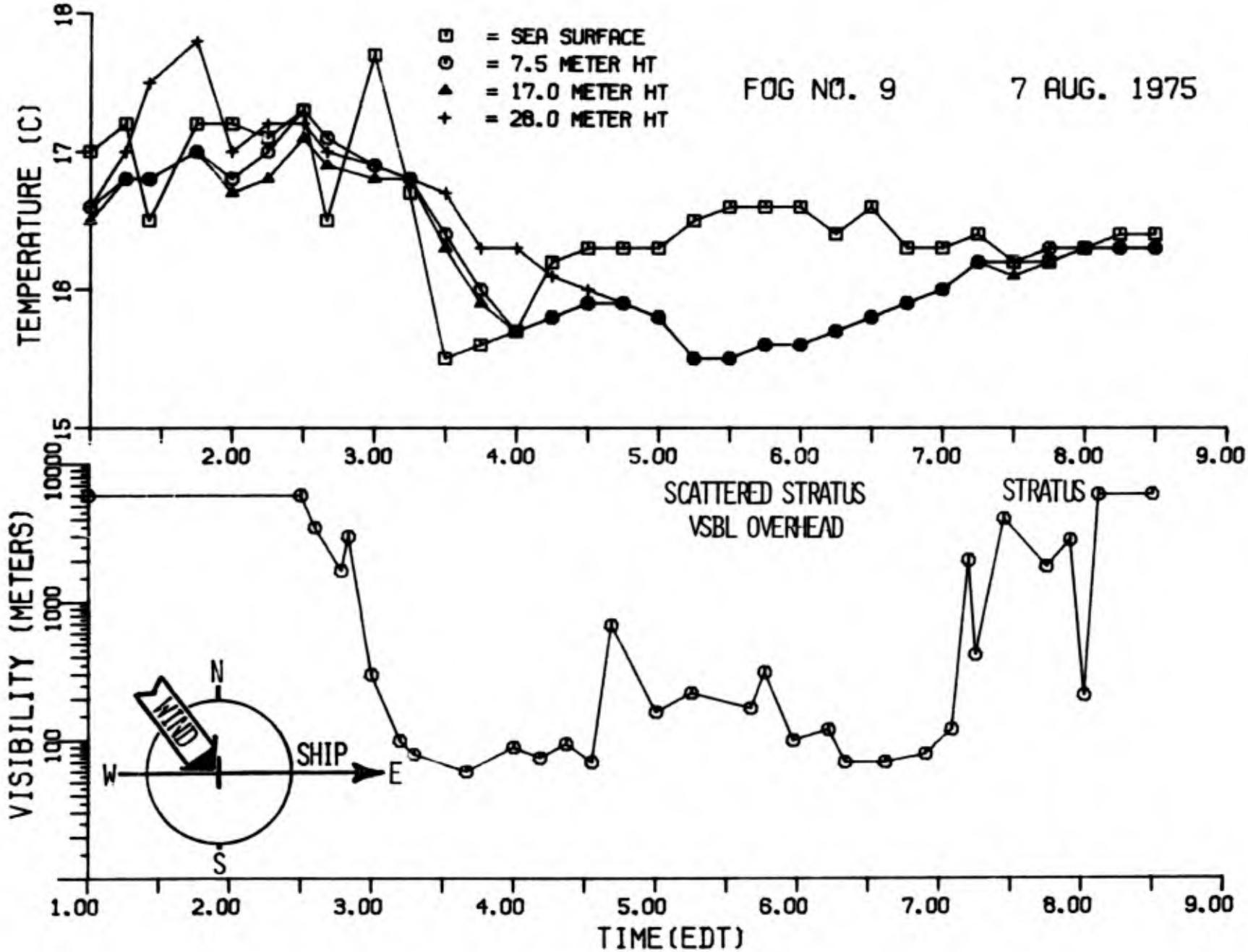

FIGURE 17: VISIBILITY, AIR AND SEA SURFACE TEMPERATURE VS. TIME -- FOG 9, 7 AUGUST 1975

Fog No. 9 for which temperatures and visibility are depicted in Figure 17 may be thought of as a later stage of Fog 7 modified by changes of wind to very light from WNW in the east and west portions of the fog and WSW for the center portion. The western edge of Fog 9, which lies farther west than the combined Fog 7W-7E boundary, shows temperature characteristics similar to those of Fog 7W, i.e., warm water and slightly colder air; however, in contrast to Fog 7W, the 2°C drop in water temperature in the eastern area coincides here with a deep and very dense (60 m visibility) fog. The middle portion of the fog over warmer water was less dense and quite shallow (permitting observation of scattered stratus above) with the air now being coldest (in this fog). Towards the eastern edge with the air temperature gradually increasing to that of the sea surface, a second deep and dense region of fog was encountered. (A fog depth of ~200 m is as suggested by the inversion height observed in a sounding by Gathman (1976) in the clearing near fog edge.) It is apparent that in Fog 9 perhaps three different air parcels were observed, each with a different (unknown) history of boundary layer modification.

In summary, although Fogs 7, 8 and 9 occurred in the same general area during a 30-hr period, over relatively warm water, and all under a similar wind regime, the available evidence does not indicate that they are portions of the same fog or even share a common mode of formation. Without information from the areas upwind, it is impossible to determine the formation mechanism(s) responsible for these three fogs.

2.5 The Fog Events of 7-10 August 1975

On 7 August the cruise activity was shifted substantially eastward to the area of the Banquereau Bank, where frequent fogs were to be expected. Indeed, while traversing the region between 7 and 10 August, Fogs 10 through 13 were encountered in an area of ~10,000 km^2 located between 56° and 57°W and 44.5° and 45.5°N (see Figures 2, 18, 19). The data acquired during that period are presented in Figures A-70 through A-90 of the Appendix. Selected portions of that material, some in slightly different form, accompany the following discussion.

Figures 18 and 19 illustrate the ship's track and the fog boundaries superimposed on the sea surface isotherm analysis (two figures are presented in order to avoid confusing overlaps). The area in question was

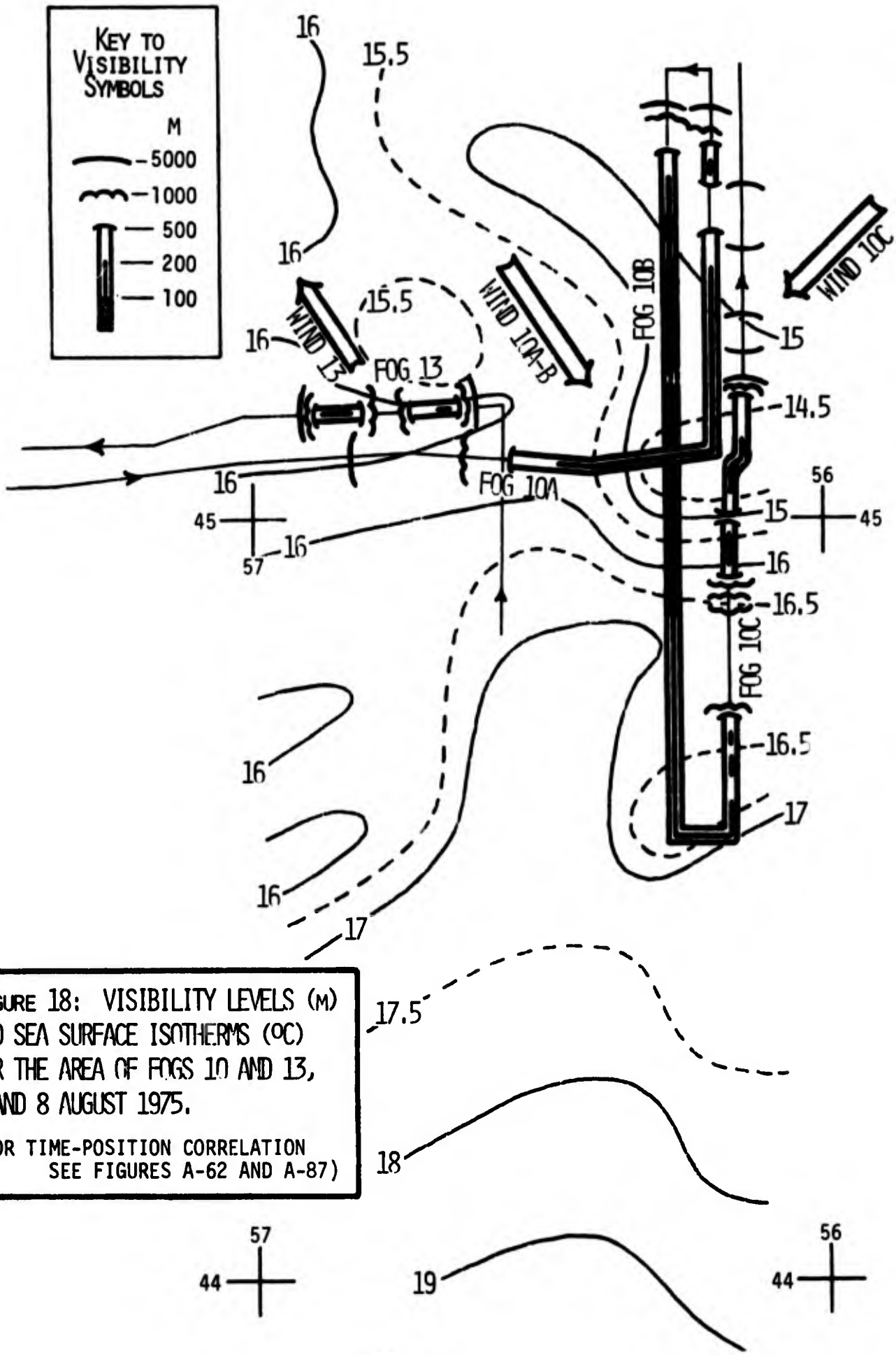

FIGURE 18: VISIBILITY LEVELS (M) AND SEA SURFACE ISOTHERMS (°C) FOR THE AREA OF FOGS 10 AND 13, 7 AND 8 AUGUST 1975.

(FOR TIME-POSITION CORRELATION SEE FIGURES A-62 AND A-87)

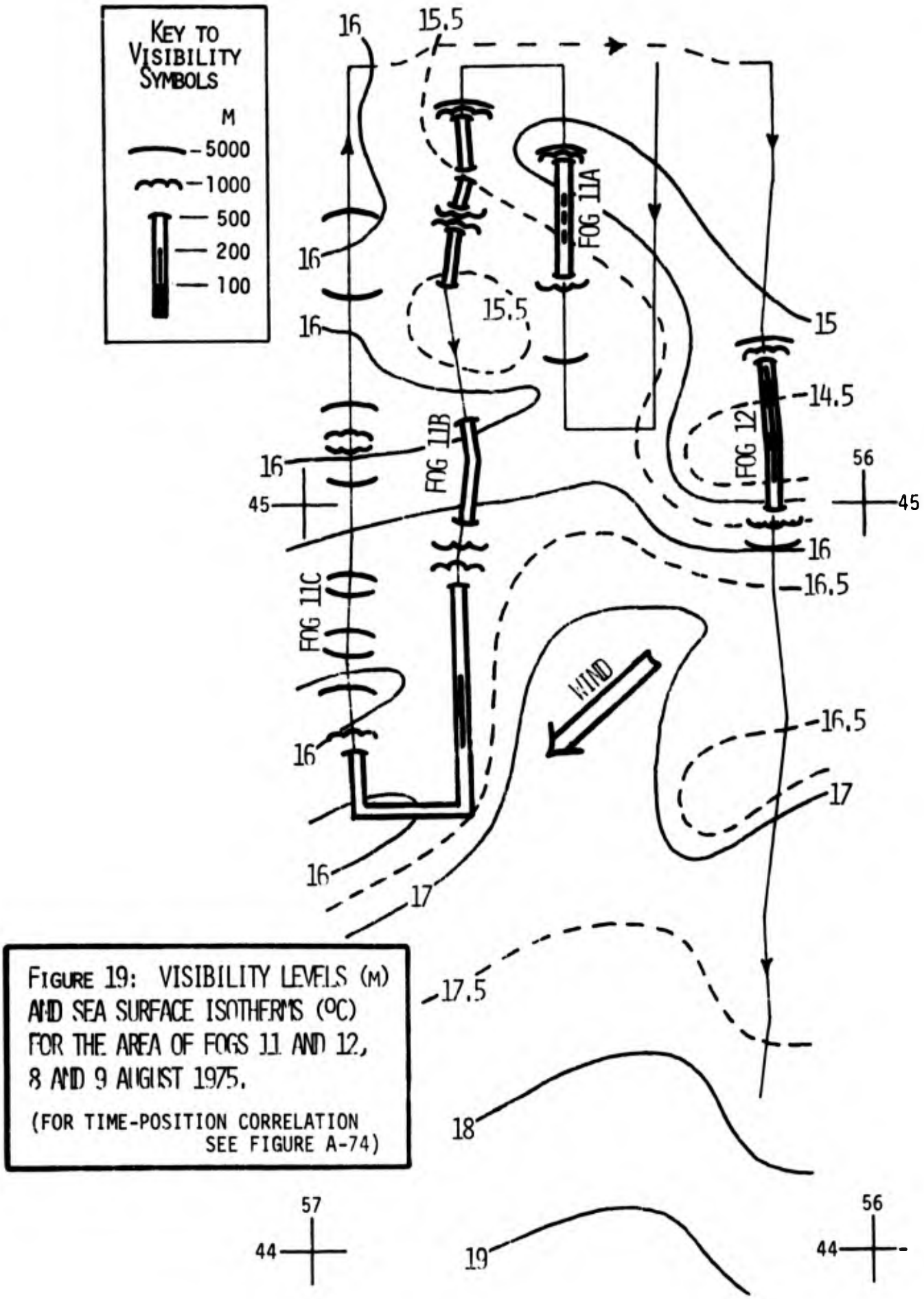

FIGURE 19: VISIBILITY LEVELS (M) AND SEA SURFACE ISOTHERMS (°C) FOR THE AREA OF FOGS 11 AND 12, 8 AND 9 AUGUST 1975.

(FOR TIME-POSITION CORRELATION SEE FIGURE A-74)

characterized by relatively warm waters (15-16°C) and a rather flat sea surface temperature distribution with the exception of a small cold spot (center, right on Figures 18 and 19) where a 2°C temperature drop occurred over a distance of about 20 km. The wind regime during the three-day period changed from NW (Fogs 10A, B) to NE (Fogs 10C, 11A, B, C) to SE (Fog 13).

Referring to Figures 18 and 20, Fog 10A was penetrated on an easterly course after cruising for hours under a nearly solid stratus in very hazy conditions. As Figure 20 indicates, visibility decreased gradually in fog of rather patchy nature. Simultaneously air and water temperature decreased; at the coldest spot the visibility reached a minimum of 100 m. Upon proceeding in a northerly direction, a slight but gradual increase in air and sea surface temperature was accompanied by gradual improvement in visibility and clearing, permitting occasional star sightings through the fog. At its northern edge, a gradual visibility increase from approximately 150 m to 5000 m took place over a distance of about 10 km under constant water and air temperatures but with decreasing dew point (Figure A-65). Visual observations indicated that at its northern upwind edge the fog layer was only slightly thicker than 30 m. (A sounding by Gathman (1976) just prior to reaching the densest portion of the fog at 1800 EDT shows an inversion with its base at about 100 m.) Throughout the fog lapsed conditions prevailed in at least the lowest 30 m.

The fog was re-entered on a track heading due south at a position 8 km to the west and similar temperature traces and lapsed conditions (see Figure 21, 10B) were recorded. However, the fog was much more uniform (visibility 100-200 m) and showed little correlation with the cold water patch (even more pronounced on this track), even though the cold water considerably modified the low-level temperature structure. While initiating another run northward (10C, Figure 22) at the same longitude as Fog 10A, a wind shift to NE probably contributed to the deterioration and eventual dissipation of the fog as illustrated by the visibility trace in Figure 22. Between 0700 and 0800 EDT, thin patchy fog was overlain by thin stratus (estimated to be ~150 m thick). It should be noted that north of the edge

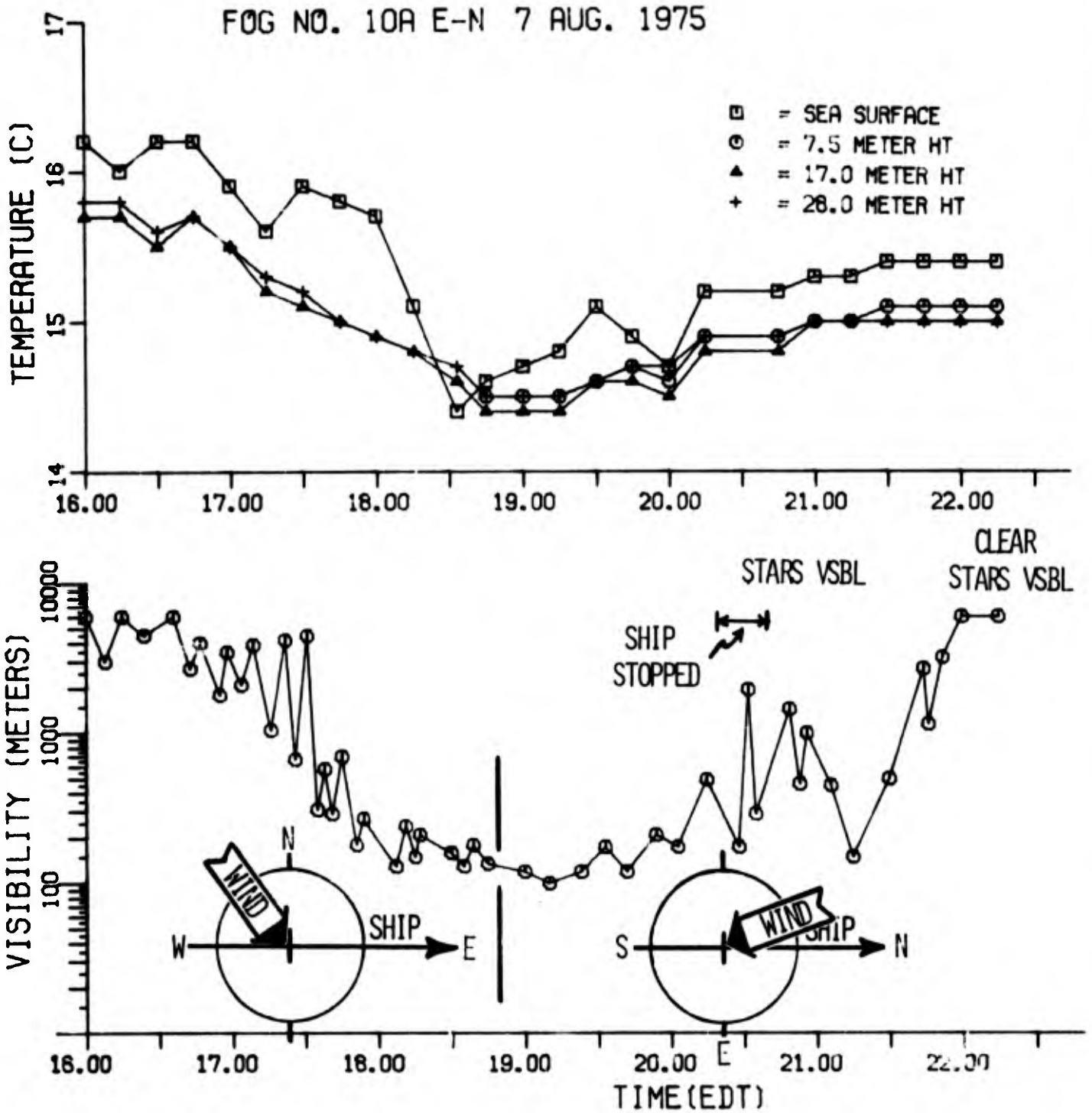

FIGURE 20: VISIBILITY, AIR AND SEA SURFACE TEMPERATURE VS. TIME
FOG 10A, 7 AUGUST 1975

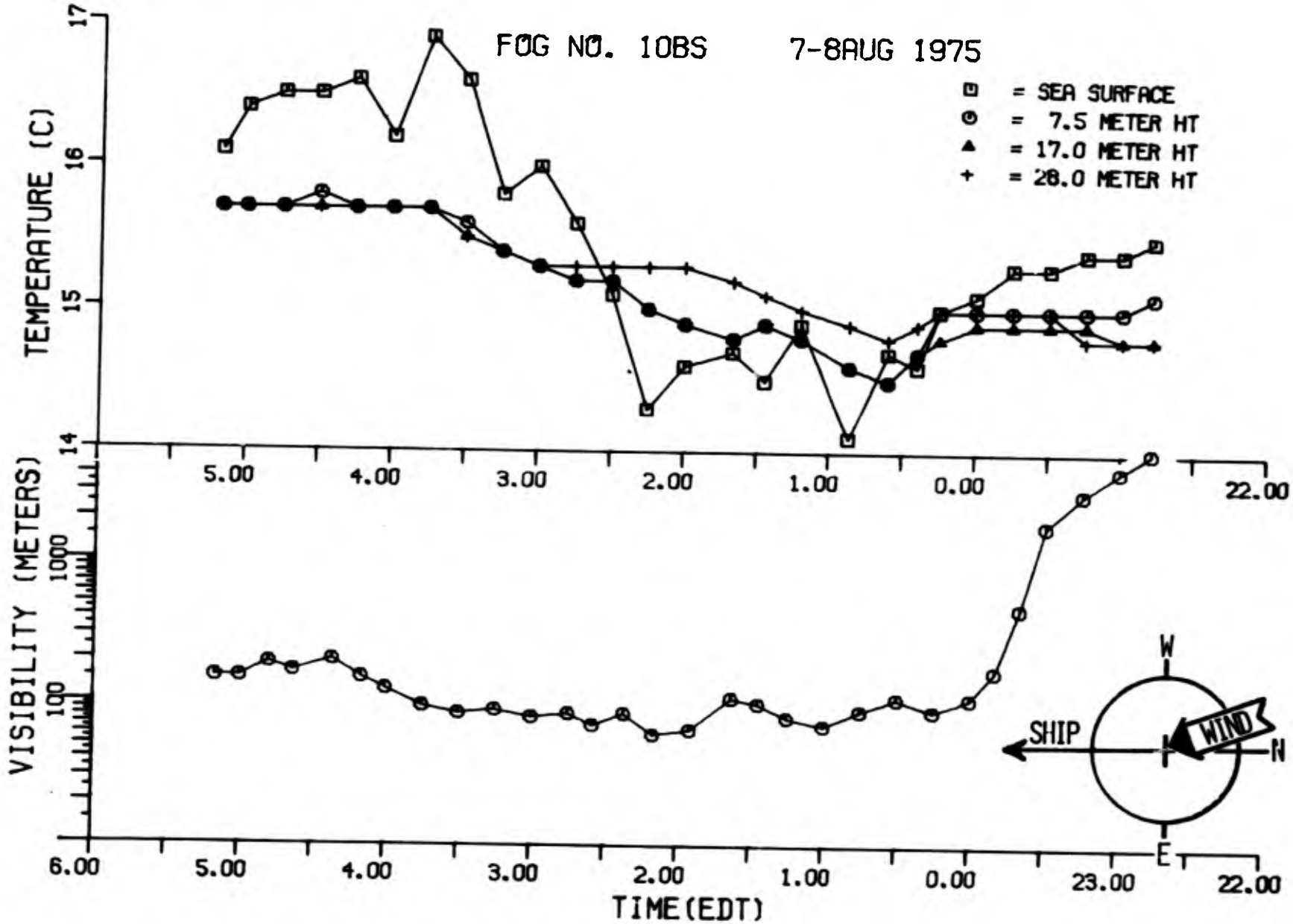

FIGURE 21: VISIBILITY, AIR AND SEA SURFACE TEMPERATURE vs. TIME -- FOG 10B, 7-8 AUGUST 1975

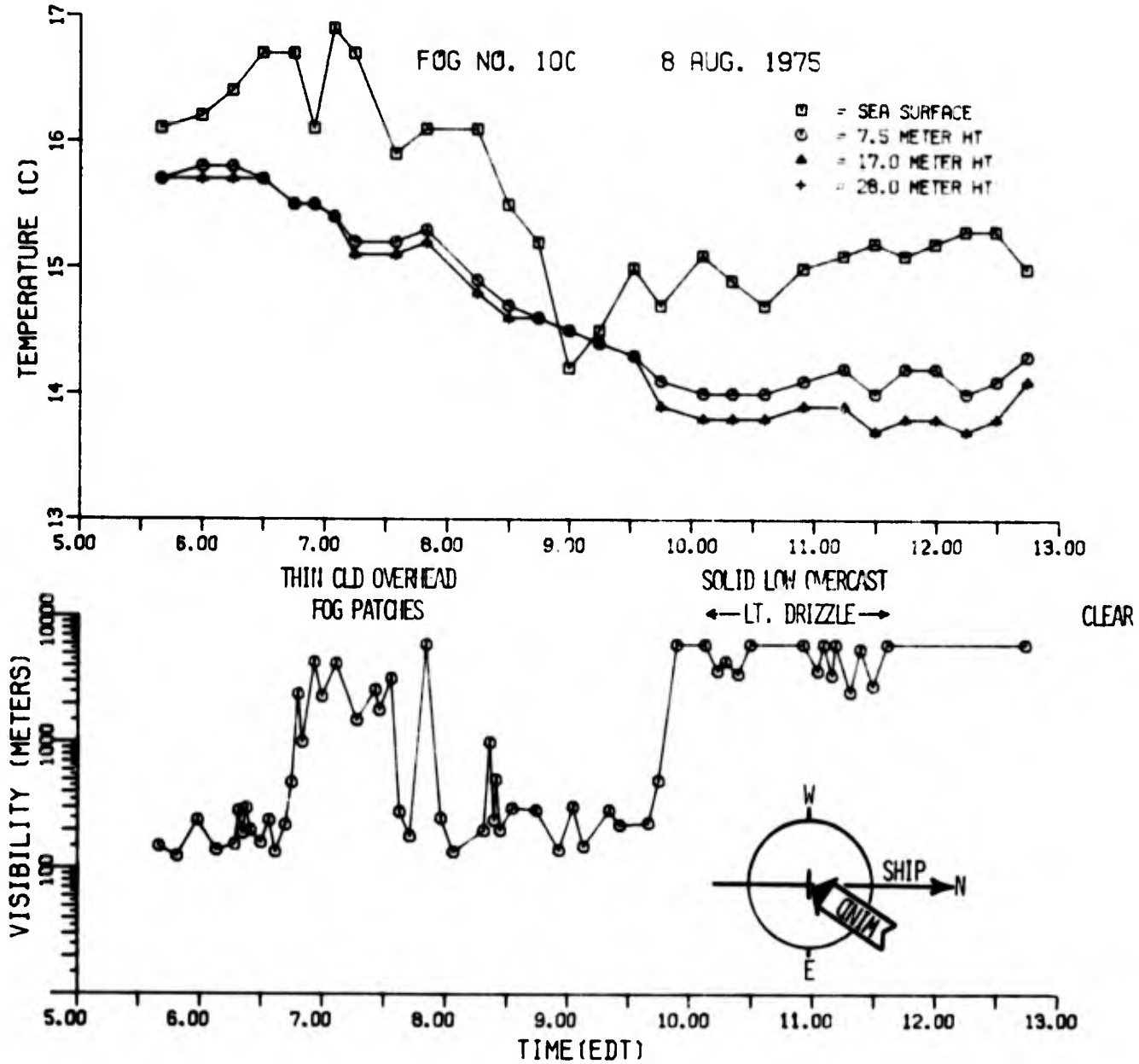

FIGURE 22: VISIBILITY, AIR AND SEA SURFACE TEMPERATURE VS. TIME

FOG 10C, 8 AUGUST 1975

of Fog 10C a solid, low overcast releasing some drizzle had replaced Fog 10A while the air temperature dropped markedly, possible due to evaporation of drizzle in the dryer air (as suggested by the sharp dew point increase (Figure A-73) in the drizzle area). A lapsed temperature structure in the lowest 30 m also prevailed throughout most of the track of Fog 10C.

There is little doubt that Fogs10A-10C represents the same fog and, concluding mainly from the low-level temperature structure and the visual observations of a low stratus closely associated with this fog, it appears to have formed by a stratus-lowering process. Since true upwind data are not available, it is difficult to positively identify the reason for the air to be colder than the water (except over the coldest spot) throughout this episode. However, the isotherm map (Figure 18) suggests that the air at the southernmost point of this fog could not have cooled to 15.7°C through heat exchange with the water surface. (The data for the track of Fog 10C, Figure 22, when compared with those of Fogs 10A and 10B suggest that the observed wind shift was accompanied by not only dryer but also cooler air.) In view of the lapsed temperature structure in Fogs 10A and 10C, radiational cooling appears to be the most satisfactory explanation for the observed cooling. Figures 20 and 21 also indicate that the cold water patch was not responsible for the presence of the fog, but may have contributed to its persistence or caused it to grow denser in that particular area.

Figure 19 shows the situation for the multiple fog encounter 11A-C. In a 20-hour period (1400, 8 August - 1100, 9 August), the indicated meander pattern of the ship's track covered the NE half of the area under study, the NS legs being spaced 15 to 20 km apart. As the isotherm analysis clearly shows, water temperature fluctuation amounted to only about 1°C throughout this episode. Winds were light from NE-ENE. During the first north-south (easternmost) leg, fog was not encountered; however, conditions changed from initially clear at the surface and sunny skies to a solid stratus from which sporadic drizzle emanated, limiting visibility to ~6000 m. It was also observed that occasionally the structured stratus base reached close to the

surface. On the following northward portion of the cruise, Fog 11A was encountered. Pertinent temperature and visibility data are presented in Figure 23. On its south edge, the fog was preceded by heavy drizzle which gradually subsided as the visibility decreased to 200 m over a period (distance northward) of one hour. The northern edge of the fog was sharply delineated with the low stratus extending about 10 km beyond that edge. The dryness of the air north and south of the fog manifests itself in dew point decreases and temperature increases.

The third north-south track, identified as Fog 11B and illustrated in Figure 24, extended over 100 km to the south, most of the time in fog. Here, the sharp northern edge of the fog is located in a zone of particularly cold air in contrast to 11A where the cold air was fog-free. The stratus protruded only about 2 km over the northern edge of Fog 11B. The visibility fluctuations along this track were considerable (between 200 m and 1000 m) with two brief, complete clearings. Drizzle, heavy at times, contributed to the visibility degradation. Most interesting is the steady air temperature increase toward the south, apparently not affecting the intensity of the fog; the most uniformly dense part of the fog was observed at the southern end of the track where the air was nearly as warm as the water surface. Before reaching the southern edge of the fog, a last cross section (heading northward) farther west was initiated. Data obtained on this northward track (11C) are depicted in Figure 25. It is evident that the fog had lifted off the surface quite extensively along the track where there were just small surface clearings at comparable locations on the previous track. Two patches of visibility degradation to ~1000 m associated with heavy drizzle at northerly locations along the track appear to correlate with local water temperature minima; however, the densest fog (at the southern end of the track) was again accompanied by relatively warm water and air temperatures.

It is quite obvious that Fogs 11A-C were formed as downward extensions of the same stratus. In order to assess the exact causes for the lowering in one area and not in another, a careful study of temperature and humidity along a streamline is required. Without data of this type, we cannot assess

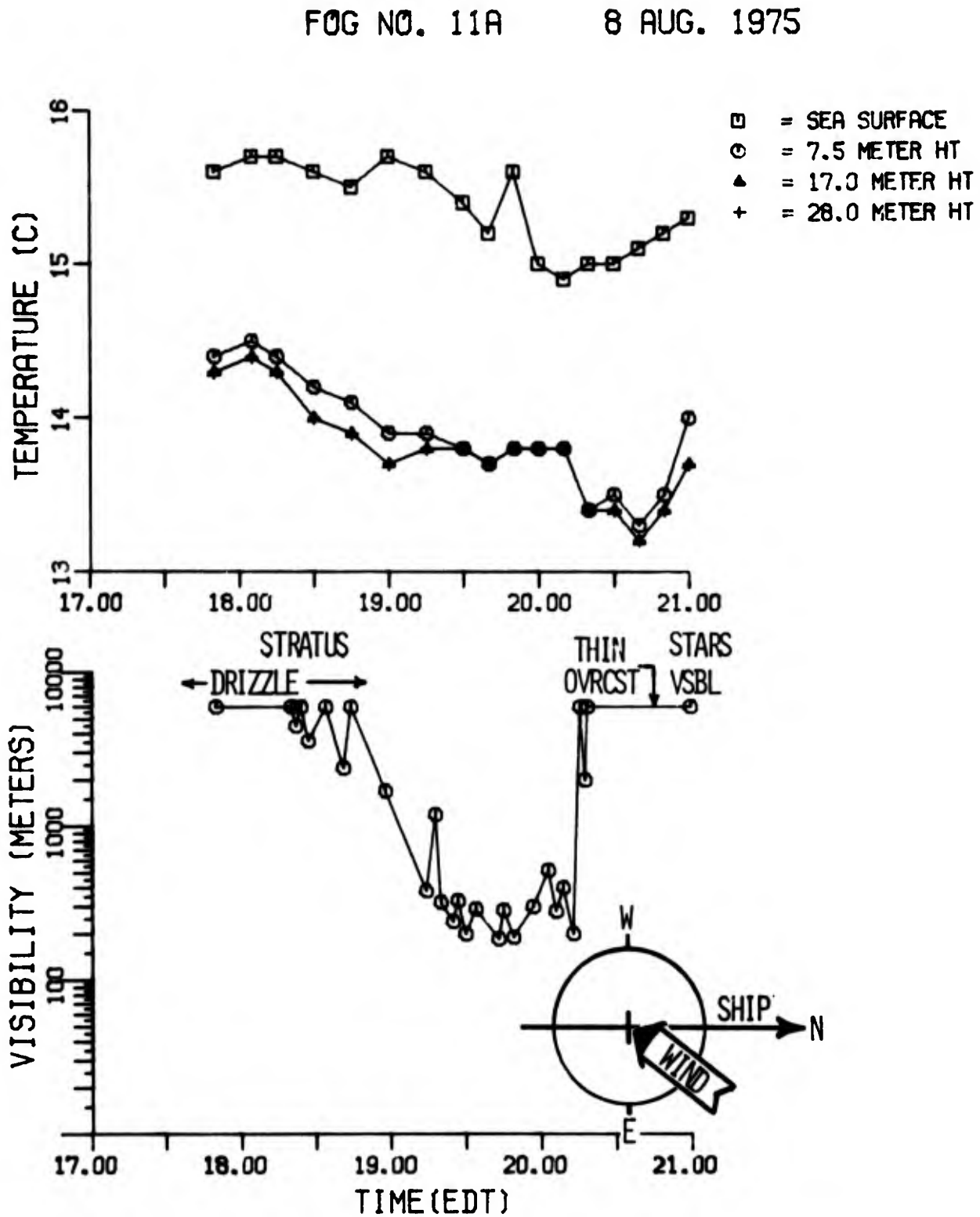

FIGURE 23: VISIBILITY, AIR AND SEA SURFACE TEMPERATURE VS. TIME
FOG 11A, 8 AUGUST 1975

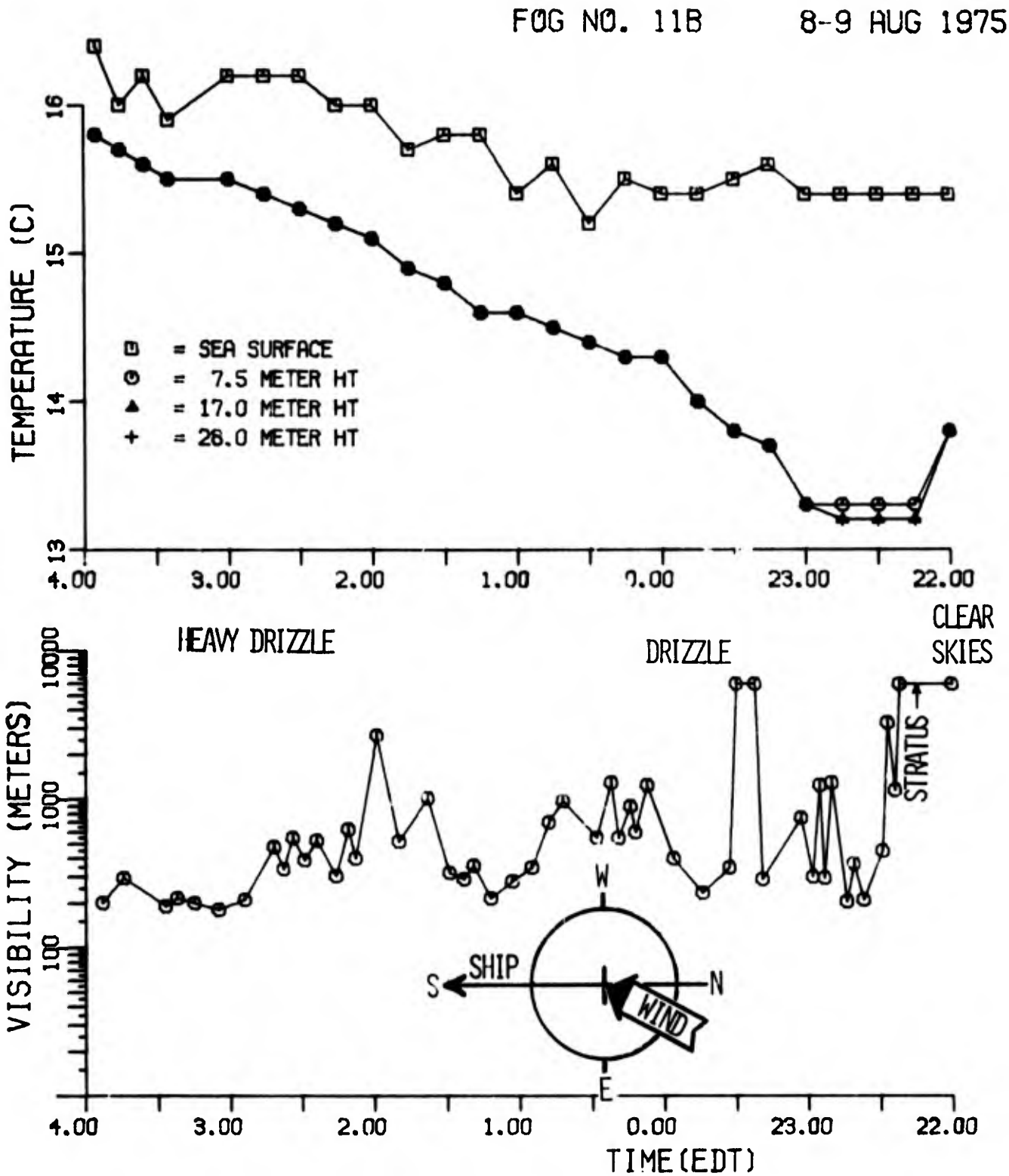

FIGURE 24: VISIBILITY, AIR AND SEA SURFACE TEMPERATURE vs. TIME
FOG 11B, 8-9 AUGUST 1975

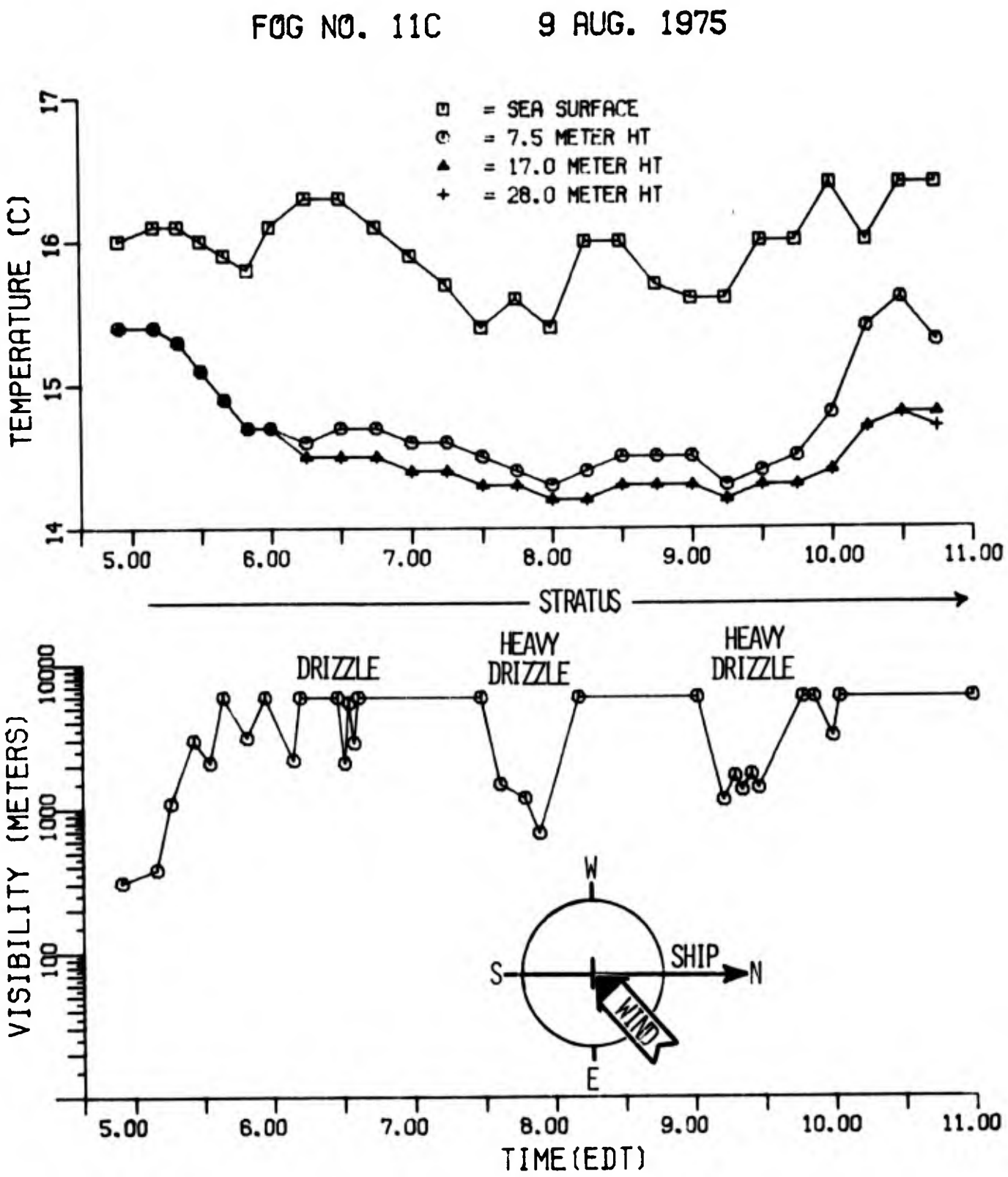

FIGURE 25: VISIBILITY, AIR AND SEA SURFACE TEMPERATURE VS. TIME
FOG 11C, 9 AUGUST 1975

the relative influences of spatial and temporal variations in the micrometeorology of the situation. Since direct upwind profiles were not obtained in this instance, a cross section constructed by using data along a streamline intersecting the four parallel tracks could be useful. However, wind direction is not known well enough; and since conditions changed considerably along the tracks, an effort of this type would not produce a meaningful result.

A subsequent further probing of the area of Fog 10 provided an additional cross section of a fog (Fog 12) located over the local cold water patch. The data, obtained under calm conditions, are shown in Figure 26. Fog 12 very much resembles the northern portion of Fog 10C except that the stratus on the north side of Fog 12 appeared thinner and (or, possibly, because) the air temperatures beneath it were about 1.5°C warmer than in the case of 10C. One might speculate that this fog was a remnant of Fog 10 (33 hrs later), its stability being favored by the water temperature minimum. Visual observation again confirmed that the fog consisted of portions of a low stratus descending to the surface.

In summary, the common features of Fogs 10-12 are their association with low-lying stratus, lapsed temperature structure, and air temperatures about 1°C colder than the sea surface temperature. Indications are that cold water spots enhanced the density or persistence of these fogs, but were most likely not a necessary condition for fog formation in this general area. The similarity of this group of fogs is also evident from the microphysics data (see Section 3.3 for details) which show nearly identical values of drop sizes, drop concentration, and LWC for Fogs 10 and 12. (Data are not available for Fog 11.)

Upon leaving the Banquereau Banks region on a westerly course on 10 August, Fog 13 was encountered in the same area where Fogs 10 and 11 had been previously observed (see Figure 18). The situation, though, was different from that of the previous fogs in more than one respect. The visibility

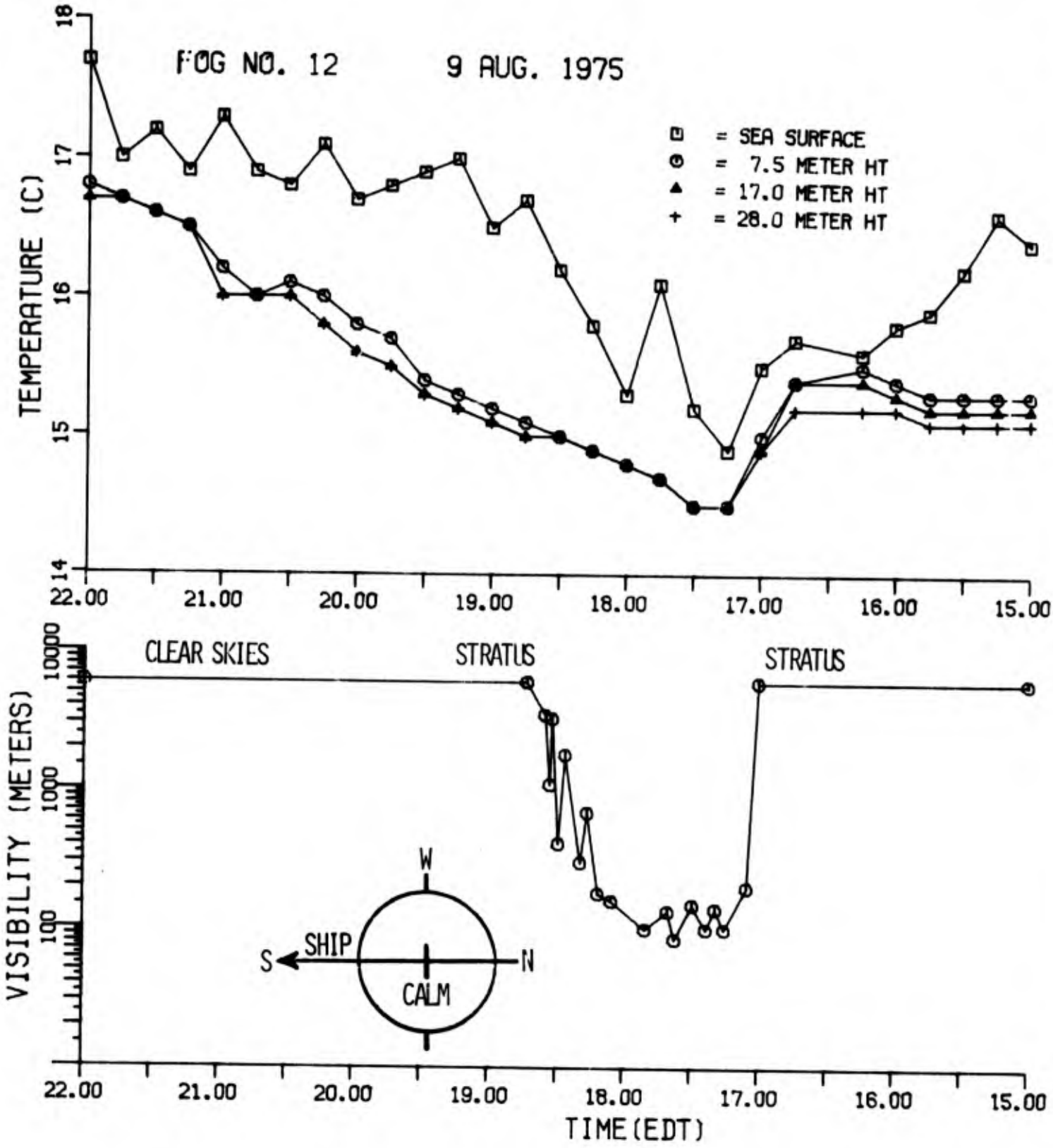

FIGURE 26: VISIBILITY, AIR AND SEA SURFACE TEMPERATURE VS. TIME
FOG 12, 9 AUGUST 1975

and temperature data presented in Figure 27 clearly show that, in this case, only within the fog was the air substantially colder than the sea surface. This is quite plausible since winds had shifted to the SE, and water temperatures had been found to gradually increase to the south (Figures 18 and 19). A second aspect in which Fog 13 differed from Fogs 10-11 was the lack of an extensive stratus system; in the general upwind direction, clear skies prevailed. The eastern half of Fog 13 consisted of shallow patches but farther to the west, the depth increased sufficiently to obscure the sun. Unrestricted surface visibility near the fog center and on its western edge was caused by lifting of the fog off the surface. The low cloud extended only a few kilometers to the west beyond the fog edge. In the absence of upwind profiles of temperature, humidity, and visibility, it is not clear through what mechanism this fog was initiated. Since a cold water surface potentially responsible for the cold air is not evident in the upwind direction, the relatively low air temperatures and lapsed vertical temperature structure in the fog has to be attributed to radiational cooling after fog formation.

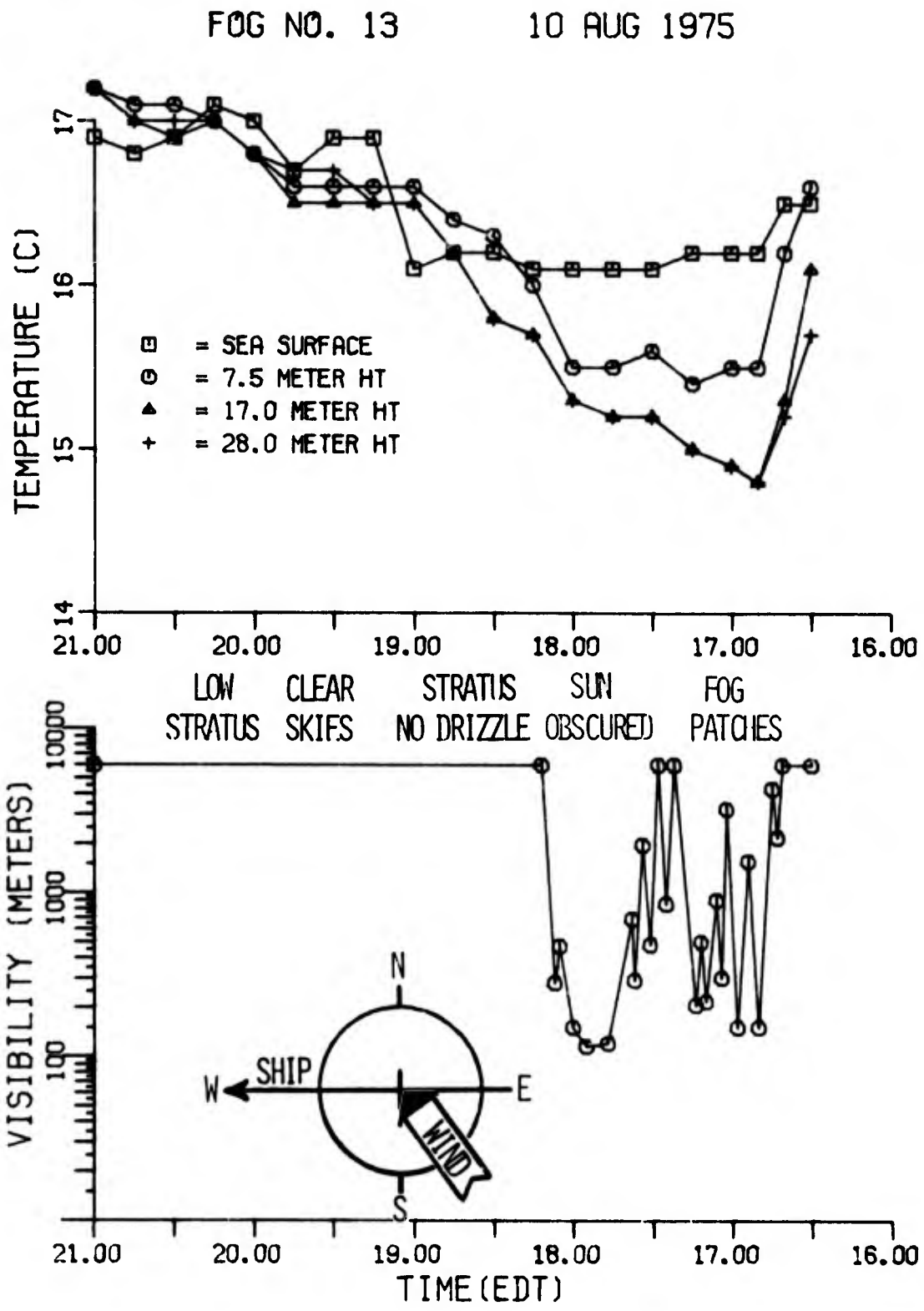

FIGURE 27: VISIBILITY, AIR AND SEA SURFACE TEMPERATURE VS. TIME
FOG 13, 10 AUGUST 1975

Section 3

THE INFLUENCE OF NON-MARINE AEROSOLS ON THE MICROPHYSICS OF FOGS OCCURRING OFF THE COAST OF NOVA SCOTIA

It is widely held that the chemical composition, size spectra, and concentration of condensation nuclei (CCN) play a direct role in determining the characteristics of the droplet population during the initial phases of fog and cloud formation. During the August 1975 HAYES cruise off the coast of Nova Scotia, a considerable quantity of data, including particulate and CCN concentrations, chemical composition of ambient aerosols, and chemical make-up of fog water, was collected in an effort to delineate the origin and effects of ambient aerosols on fog microphysics. These data, along with measurements of fog microphysics, are presented and discussed within this section. When compared with similar data from fogs formed in the relatively clean marine environment off the West Coast, these data demonstrate the close relationship between ambient aerosol characteristics and fog microphysics. As expected, aerosols of continental and anthropogenic origin were found to exert a marked influence on the microphysics of marine fogs formed off the coast of Nova Scotia during the observation period.

3.1 Characteristics and Chemical Composition of the Ambient Air Mass Aerosols

During non-fog periods on the cruise, samples of the ambient aerosol were collected twice daily over approximate eight-hour intervals. A few of the samples were obtained during fog episodes; and, except for minor losses of the air mass aerosol due to droplet fallout, these samples are considered representative of the characteristics of the ambient air mass aerosol. The samples were collected utilizing a hi-vol filter technique on 10 cm diamet . Tissuquartz filters and were subsequently analyzed by standard analytical techniques in Calspan's Chemistry Laboratory. Results of the chemical analyses of these samples are tabulated in Table A-2 and summarized in Table 1. A brief description of analytical techniques is provided in Appendix A.

Inspection of data in Table A-2 reveals several noteworthy features of the ambient aerosol existent along the East Coast and off the coast of Nova Scotia during the period of the cruise. The data for the period 29 July to 1 August were obtained while enroute from Virginia to Nova Scotia under a nominally SW wind regime and are probably representative of conditions found several hundred kilometers downwind of the industrialized East Coast. The data for the 1-8 August period were obtained in the region shown in Figure 1 within 160 km offshore from the western end of Nova Scotia to an area ~800 km to the ENE. Thus, the data in sequence for the period 1-8 August are approximately representative of conditions with increasing distance from the continent proper. The data show, as expected, that concentrations of all chemical components were highest downwind of the industrialized East Coast. Off the coast of Nova Scotia, concentrations of these materials were low and, in general, decreased with time and/or distance eastward from the continent through the period 1-8 August 1975.

During the observation period along the Nova Scotia coast, synoptic patterns and ship's position (and, hence, wind regimes) changed substantially. On 1 and 2 August, winds were from the SW to SE quadrant; on 3 and 4 August, winds were from the NE; from 5-7 August, winds shifted from W to NW; and on 8 August, winds were again from the NE. Thus, the data for the period 1-8 August are not truly representative of conditions directly downwind of the continent. Measurements of atmospheric radon during the cruise (Larson, 1976) show values reflecting the changing wind pattern which occurred during the period. Observed radon concentrations during the period 5-7 August suggest trajectories directly from the Nova Scotia land mass, while on all other days the data suggest residence times over the ocean of the order of one week for the air masses in question. Without detailed trajectory analysis (for which data are not available in the area of interest), it is difficult from the meteorological view to assess the origin of the observed aerosols or the reasons for the minor variations in chemical composition evident in Table A-2 for the period 1-8 August.

Because observed variations in the chemical composition of the aerosols were relatively minor compared to changes in prevailing winds, the results of the chemical analyses of the aerosol samples were summarized into two groups as presented in Table 1. At the top of Table 1, the average data (in micrograms per cubic meter of air) for the entire area traversed off the coast of Nova Scotia (1-8 August) are compared with the average of the data obtained off the East Coast while enroute to Nova Scotia. The data immediately reveal the differences in concentrations of the various chemical parameters between the aerosol existent downwind of the Washington to Boston coast and those which are found at more northerly latitudes. The most striking feature of the chemical make-up of the aerosol in both locations in the nearly complete absence of chlorides. Chlorides, which would be expected as a major component of the marine input to the aerosol population, were below minimum-detectable limits in every sample (i.e., airborne concentrations were $<0.02\ \mu g\ m^{-3}$). On the other hand, measurable concentrations of SO_4^{--}, NH_4^+ and aluminum, all presumably of continental origin, were found in every sample. The sulfate aerosol is partly a derivative of photooxidation of SO_2* plus other oxidative processes involving SO_2 and reactive intermediates, while aluminum would be expected as a component of continental soil dust.

In an effort to determine the molecular composition and origin of the observed aerosol, selected molar ratios of the aerosol components are compared at the bottom of Table 1 with textbook values of those for North American soil dust and sea water. It is readily seen that the ratios Ca/Mg, Ca/Al and K/Al in our samples closely approximate those of North American soil particulates. A second particulate source may be deduced by noting the following two factors: (1) the excess Na observed over that expected from soil suggests an additional source of Na; (2) for complete balance as ammonium

*During the cruise an attempt was made to measure ambient SO_2 concentration using absorption-train collection and colorimetric analysis techniques. The absorption-train was operated for 24-hr samples, but measured SO_2 concentrations were never observed at levels greater than the "noise level" for this technique. Therefore, average 24-hr concentration of SO_2 was never greater than 0.04 ppm during the period 1-10 August 1975.

TABLE 1.

AVERAGE DATA FROM CHEMICAL ANALYSES OF AEROSOL COLLECTED BY HI-VOL FILTER TECHNIQUE

ABSOLUTE CONCENTRATION ($\mu G/M^3$)

	Cl^-	Mg	Ca	K	SO_4^{--}	NH_4^+	Al	Na
Off Coast of Nova Scotia	<.02	.05	.09	.19	3.95	.66	.22	.87
Enroute; off Wash.-Boston Coast	<.02	.12	.13	.22	14.04	2.52	.26	1.34

MOLAR RATIOS

	Ca/Mg	Ca/Al	K/Al	K/Na	NH_4^+/SO_4^{--}	Na/SO_4^{--}
Off Coast of Nova Scotia	1.07	.27	.59	.14	.91	.92
North American Soil Dust	.76	.16	.23	1.22		
Sea Water	.19	>10	>10	.02		

sulfate, the NH_4^+/SO_4^{--} ratio would be 2. The ratios Na/SO_4^{--} and NH_4^+/SO_4^{--} together therefore suggest a nearly equimolar mixture of ammonium sulfate and sodium sulfate as a second aerosol component. The absolute concentrations of Na can almost exactly account for both the molar ratios required of the observed soil particulates and the sodium-ammonium sulfate aerosols.

Mohnen and Yue (1974) suggest a mechanism whereby the presence of NaCl in solution droplets would cause an increase in the oxidation rate of SO_2 and in the process release chlorine as hydrogen chloride to the atmosphere. Such a process, while perhaps a valid hypothesis, must certainly require long time periods and could not easily account for the complete absence of chloride aerosols in the marine air. (In the event of significant chloride aerosol production and destruction, an equilibrium would be established between continuous aerosol input and losses, and measurable quantities of chloride would still be observed in the air mass.) Therefore, it does not appear warranted or necessary to invoke such a mechanism to account for the absence of chloride in the observed aerosols. Even if the mechanism were operative, the input rate of NaCl aerosols would have had to have been very small.

In summary, the aerosols observed during the cruise appear to have originated from two major sources. One was sulfate aerosol probably derived from atmospheric oxidation of sulfur dioxide and of a chemical composition comprised mainly of a sodium-ammonium sulfate form ($NaNH_4SO_4$). The other source of aerosol appears to have been continental soil particles with chemical compositions primarily of a sodium-aluminosilicate form. (Silicates were reported in samples of the ambient aerosol obtained by Baier (1975).) The absence of chlorides is, in retrospect, perhaps not unexpected in view of the light winds (and absence of white caps) characteristic of the entire cruise. Obviously the air masses encountered during the cruise were of aged, continental character exhibiting very little evidence of aerosol modification (other than losses) by residence over the sea. Aerosol coagulation and losses due to setling, dilution and scavenging along with photochemical aerosol production probably combined to produce the bulk chemical features of the air mass aerosol.

These conclusions are, in part, substantiated by measurements of condensation nuclei (CCN) obtained during the cruise. The data, obtained at irregular intervals as time permitted, are presented in Table A-4 and summarized in Figure 28. In Figure 28 the data have been grouped and averaged for the three different periods and general locations during the cruise: CCN activity spectra are shown for the portion of the cruise enroute off the East Coast (29-31 July); for the area off the SW coast of Nova Scotia between 66 and 63 W longitude (1, 2, 5 August); and for the cruise region east of Nova Scotia between 61 and 56 W longitude (7-10 August). The activity spectra plotted in Figure 28 reveal a decided trend of decreasing number concentrations with distance from the continent, paralleling the decreasing airborne concentrations of the various chemical constituents discussed earlier.

The CCN concentrations observed in the Atlantic during the cruise were considerably greater than those typically observed at sea in the relatively clean air off the West Coast. In Figure 29 the average CCN activity spectrum from the portion of the cruise east of Nova Scotia is compared with average CCN spectra obtained with the same instrumentation on a previous study off the West Coast (Mack et al., 1975). It is seen from this comparison that nucleus concentrations even in the cleanest area off the Nova Scotia coast during the observation period lie between the concentrations measured in the urbanized Monterey Bay area and those observed in relatively clean marine air at sea off the West Coast--again suggesting a continental influence. CCN concentrations, in general, were a factor of 5 greater at 0.2% S off the coast of Nova Scotia than off the California coast.

In contrast, "haze" nuclei* which are found in concentrations typically of the order of 10-50 cm^{-3} in the clean marine air off the West Coast were virtually non-existent in the air masses off the Nova Scotia coast during the observation period. Off Nova Scotia, observed concentrations of haze

*Haze nuclei are those which grow to ~1 μm at 98% RH.

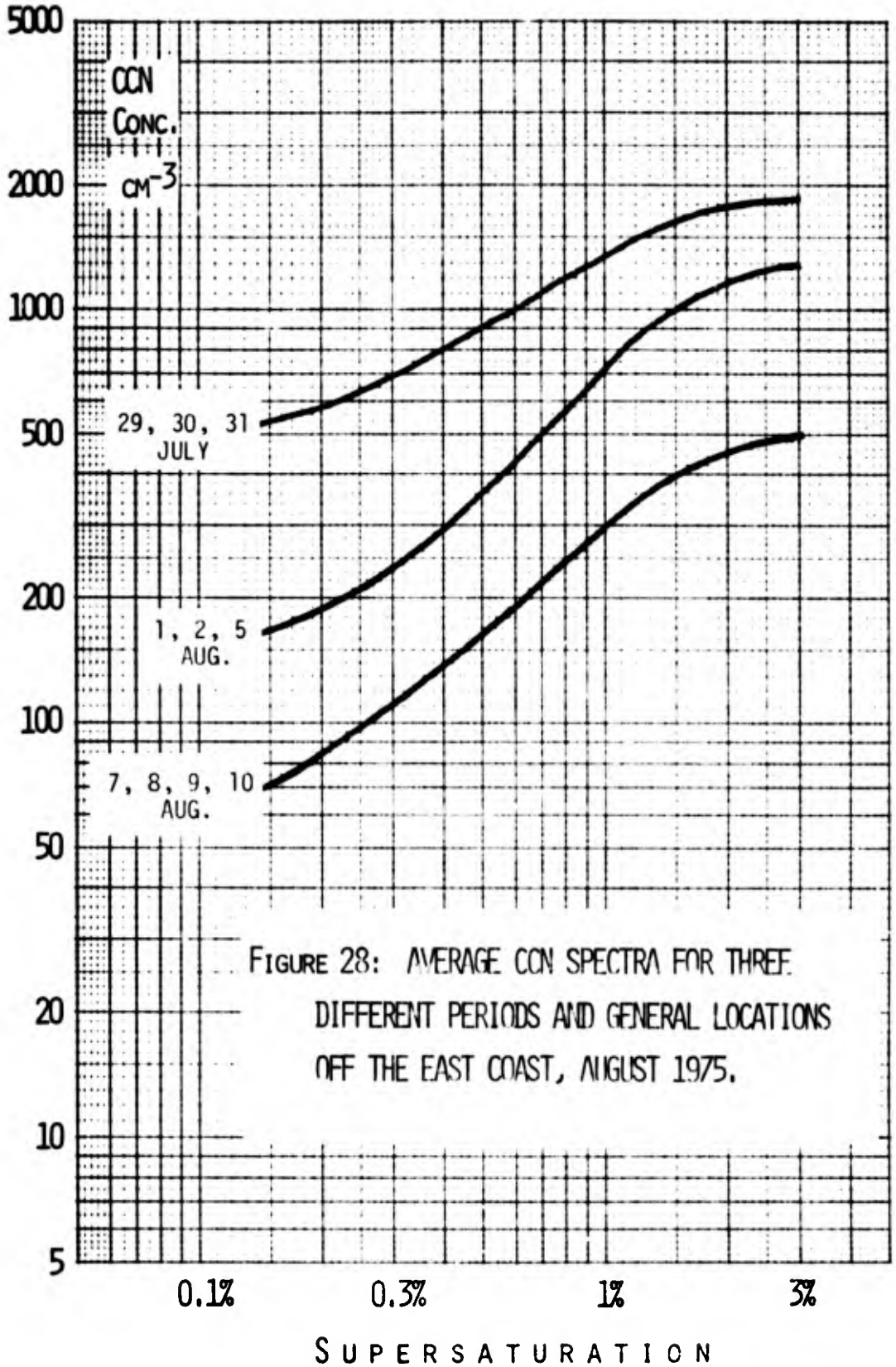

FIGURE 28: AVERAGE CCN SPECTRA FOR THREE DIFFERENT PERIODS AND GENERAL LOCATIONS OFF THE EAST COAST, AUGUST 1975.

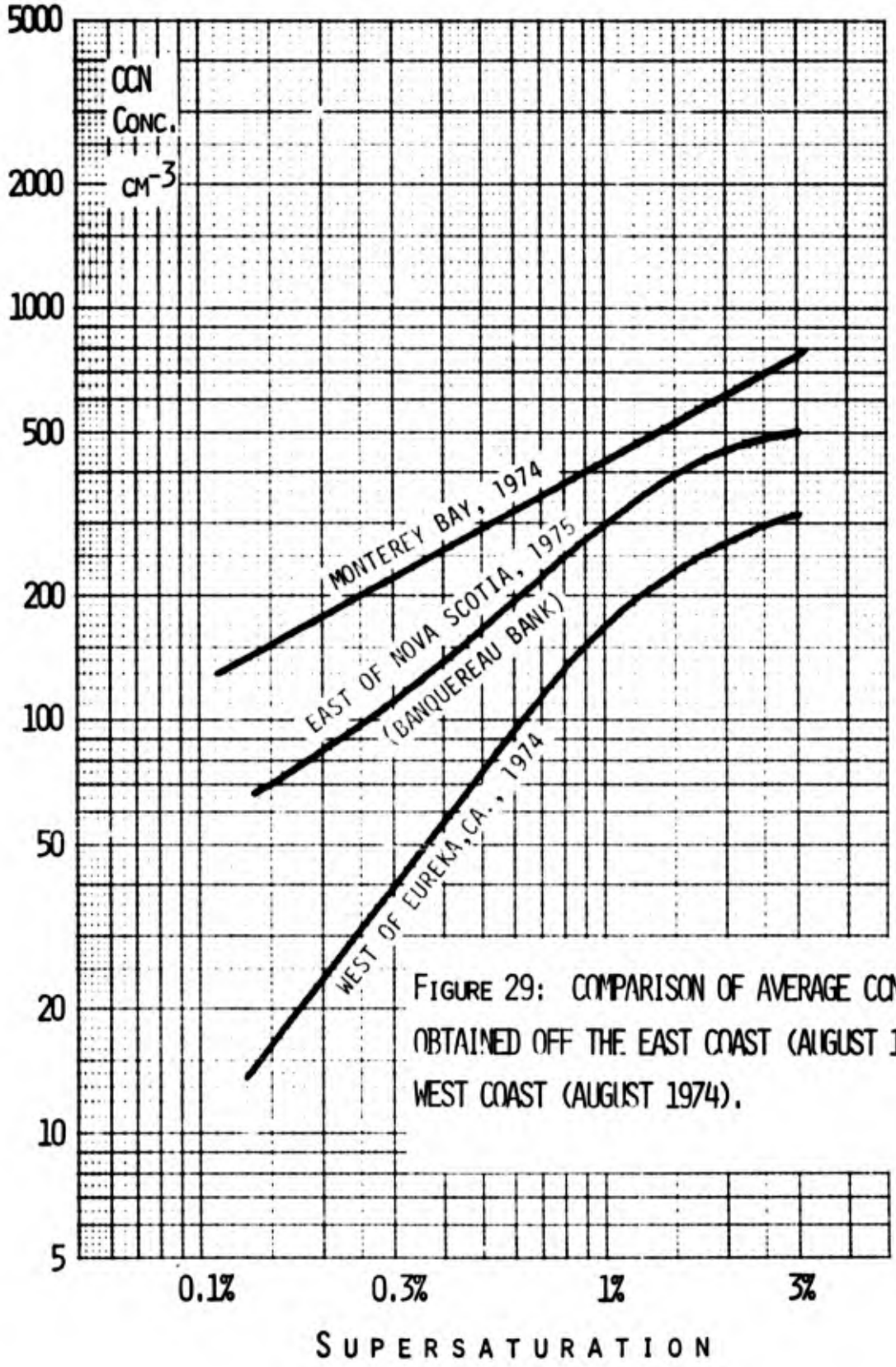

FIGURE 29: COMPARISON OF AVERAGE CCN SPECTRA OBTAINED OFF THE EAST COAST (AUGUST 1975) AND WEST COAST (AUGUST 1974).

nuclei were typically of the order of 0.1 cm^{-3}. Off the West Coast, the number concentrations of these particulates has always correlated favorably with droplet concentrations in fogs formed in the same air mass. The source of these nuclei has been attributed to local sea surface activity and has been substantiated by the high chloride concentrations found in fog water off the West Coast. The absence of particulates active at 98% RH in the area off Nova Scotia is indicative of the low wind and calm sea states which prevailed during the cruise and correlates well with the absence of chlorides in the samples of the ambient aerosol.

3.2 The Chemical Composition of Fog Water

During the cruise ~170 discrete 7 ml samples of fog water were collected with the Calspan Fog Water Collector for analysis of chemical composition. The samples were collected over 5-15 minute intervals, depending on fog density. Subsequent analysis at Calspan utilized the same analytical techniques as were used for the hi-vol filter samples of the ambient aerosol. For some fog events as many as 20 individual fog water samples were collected. Preliminary analysis of selected samples from each fog indicated that, as is the case in fogs off the West Coast, chemical composition is relatively constant throughout a given fog and that each fog differs slightly from the others. Therefore, the remaining samples were combined to form large composite samples for each fog event. Results of the analyses of the composite samples may be found in Table A-3 in Appendix A.

In accordance with the analyses presented in Section 2, the results of chemical analysis of the fog water were further categorized into groups corresponding to each of the major fog situations. These data are presented chronologically in Table 2. It is immediately evident that the data exhibit trends paralleling those of CCN concentration and component concentrations of the ambient aerosol--i.e., decreasing absolute concentration with time and/or distance eastward from the continent.

Table 2. RESULTS OF CHEMICAL ANALYSIS OF COMPOSITE FOG WATER SAMPLES COLLECTED OFF THE COAST OF NOVA SCOTIA

(μg/ml of fog water)

Fog Numbers	SO_4^{--}	NH_4^+	Na	K	Ca	Mg	Al	Cl^{-1}
2AB	22.5	0.52	28.5	2.0	1.38	0.94	<1	8.4
2C, 4	16.8	0.95	27.0	1.6	0.89	2.40	<1	9.0
6	9.0	1.30	26.1	1.5	0.80	0.55	<1	0.5
7, 8, 9	12.0	0.44	23.7	2.3	0.89	2.02	<1	0.3
10, 11	6.5	0.17	21.1	1.9	0.83	0.61	<1	0.2
12, 13, 14	2.6	0.16	20.3	1.7	0.77	0.51	<1	0.5

Details of the data presented in Table 2 show that the chemical composition of the collected fog water may be summarized as follows: (1) sulfate and ammonium concentrations were highest in the fogs located closest to the coast (i.e., fogs 2 through 9); (2) sodium and calcium concentrations were approximately the same in all fogs, trending toward lower values with distance from the continent; (3) magnesium and potassium concentrations fluctuated from fog to fog; (4) chloride concentrations were nearly negligible except in Fogs 2 and 4 in which the greatest wind speeds of the entire cruise were experienced; and (5) aluminum concentration was below the minimum detectable concentrations in all fogs.

In Table 3 the average chemical composition of fog water from Nova Scotia fogs is compared with that collected in California marine fogs and with that observed in inland fogs at Travis AFB (California). Although differences in absolute concentration of the constituents of fog water could be explained merely by differences in liquid water content and nucleus sizes, the substantially lower concentration of chloride in the Nova Scotia fogs (relative to that of California marine fog) is striking in view of the closely matched values for the other components of the fog water.

At the bottom of Table 3, the concentrations of the various components of the fog water are normalized with respect to Na concentration and are compared with that of sea water. (The sea water sample was obtained in the Pacific approximately 80 km off the coast of California.) It is immediately apparent that the normalized values of the components of fog water in California marine fogs closely resemble that of sea water--suggesting that the nuclei responsible for California marine fogs are primarily of sea salt origin. In contrast, the normalized values for Nova Scotia marine fogs more closely approximate those observed in the inland fogs. Presumably, sea salt nuclei were of only minor consequence in the nucleation of the observed Nova Scotia fogs.

TABLE 3. COMPARISON OF CHEMICAL COMPOSITION OF FOG WATER FROM FOGS OCCURRING AT DIFFERENT LOCATIONS

ABSOLUTE CONCENTRATION (μG/ML)

	CL^{-1}	Mg	Ca	K	Na	Al	SO_4^{--}	NH_4^+
Nova Scotia Coastal Fogs	.4-9.	1.2	0.9	1.8	24	<1	12	0.6
California Coastal Fogs	25-100	3.5	2.4	3.2	23	--	~10	---
Inland Fogs	1.2	0.1	0.7	6.7	1.3	--	~10	~30

SODIUM RATIOS (x/Na) (MASS RATIOS)

	CL^-	Mg	Ca	K	SO_4^{--}	NH_4^+
California Coastal Fogs	1.8	.14	.10	.14	~0.5	---
Nova Scotia Coastal Fogs	.02-.3	.05	.04	.08	0.5	.03
Inland Fogs	0.9	.07	.54	5.2	~7.7	~23
Sea Water (Textbook)	1.8	.12	.04	.04	.27	---
Sea Water (Sample)	1.8	.09	.02	.06	.18	$<10^{-6}$

Comparison of data from Tables 1, 2 and 3 provides some insight into factors responsible for nucleation of the Nova Scotia fogs. Applying observed liquid water contents of 0.1-0.4 g m^{-3} (see Section 3.3) and assuming that the Fog Water Collector collects fog water quantitatively*, the absolute values of sulfate concentration measured in the fog water give values of airborne sulfate concentration of about 1 to 8 μg m^{-3} and typically about 3.5 μg m^{-3}. Observed SO_4^{--} concentration averaged 3.9 μg m^{-3} in the ambient air masses (Table 1). Without quantitative measurements of all parameters from the same air volume, these are only estimates; but they do suggest that the sulfate aerosols were nearly quantitatively "scavenged" from the air by the fog droplets.

Additional information may be derived from a comparison of the constituents of the aerosol and the fog water when normalized with respect to sulfate concentration. These data are presented in Table 4 and show that with respect to the quantitatively "scavenged" sulfate component all other chemical constituents (except for Al and NH_4^+) were enriched in the fog water by a factor of ~10 over their relative concentrations in the "dry" aerosol. (Both Cl^{-1} in the "dry" aerosol and Al in the fog water were below minimum detectable concentrations.) Lower values of NH_4^+ may be attributable to conversion to gaseous ammonium and losses while the fog water samples were stored (~1 mo.) for analysis. It is seen from these data that along with the sulfate component, the fog selectively "scavenged" (at the exclusion of Al) quantities of materials containing Cl^{-1}, Mg, Ca, K, and Na, perhaps originating from sea salt. Since Al was not found in the fog water, it is concluded that the other constituents were incorporated in the fog water not by direct scavenging, but rather as direct participants in the nucleation processes of the fogs.

*The nominal 50% collection cutoff for the Fog Water Collector is ~3 μm radius (i.e., fewer than 50% of the droplets smaller than that size are collected). None of the droplets <1.5 μm radius are collected.

Table 4.

COMPARISON OF THE NORMALIZED (with respect to SO_4^{--}) AVERAGE CONCENTRATIONS OF THE CONSTITUENTS OF THE AMBIENT AEROSOL AND FOG WATER SAMPLES COLLECTED OFF NOVA SCOTIA

	SULFATE RATIOS (x/SO_4^{--})(mass ratios)						
	Cl^{-1}	Mg	Ca	K	Na	Al	NH_4^+
AMBIENT AEROSOL	---	.01	.02	.05	0.2	.06	.17
FOG WATER	.03-.7	.1	.08	.15	2.0	---	.05

Briefly summarizing, it has been shown that fogs, formed off Nova Scotia in air masses characterized by the aerosol constituents enumerated in Table 1, selectively "scavenged" certain of these components. The major chemical constituent of the fog water was found to be a sulfate salt; minor concentrations of other components (probably attributable to sea salt) were also found. The fact that Al (indicative of continental soil particulates) was not found in the fog water suggests that the sulfate aerosol was also not incorporated in the fog water by direct scavenging, but rather served as the primary nucleant for the fogs observed during the cruise. A minor contribution by sea salt aerosol also appears likely.

3.3 The Microphysical Characteristics of the Nova Scotia Marine Fogs

During fog events encountered on the cruise numerous measurements of the drop size distribution were obtained (at a height of 20m above the surface) with the Calspan Fog Drop Sampler* at intervals of from 5 to 30 min. The sample slides were later photomicrographed and analyzed manually. As many of the droplet samples as was feasible (within the limits of time and funds) were

*Impaction and gelatin replication technique

analyzed and details of the individual drop size distributions are included with their respective fog events in Appendix A. Also shown for each size distribution are calculated values of drop concentration and liquid water content.

In order to make a reasonable comparison of data from individual fogs, the microphysics for the "mature" stages* of the individual fog events are summarized and presented in Table 5. From these data it is evident that the microphysical characteristics of the Nova Scotia fogs differed by a factor of 2-3 between fogs. These differences probably reflect the different formation processes and intensities of the individual situations and, hence, the depths to which the fogs could grow and the resultant liquid water contents (LWC). While considerable drizzle accompanied many of the fogs, the greatest fraction of the droplet population was in sizes <20 μm radius. Typically 95-98% of the droplets were of a size <15 μm, in reasonable agreement with observations in West Coast fogs.

It has been shown that, in comparison to conditions prevailing off the West Coast, air masses off the coast of Nova Scotia (at least during early August 1975) were characterized by high concentrations of presumably smaller and hence less active CCN. The observed CCN were shown to be comprised primarily of sulfate aerosols probably formed through atmospheric oxidation of SO_2 arising from anthropogenic activities. Chlorides (i.e., sea salt nuclei) were found to be virtually non-existent during the period of observation in either the fogs or the air masses in which the fogs subsequently formed. The chemical composition of the fog water along with CCN data suggest that small sulfate aerosols served as the primary nucleants of the observed Nova Scotia fogs. Although this is <u>not</u> likely to always be the case, it is reasonable to expect that a large fraction of the CCN population in the area downwind of the North American continent will usually be comprised of sulfate aerosols.

---

*The mature stage is loosely defined as that period (position) within a fog encounter in which visibility is most uniformly dense.

TABLE 5: AVERAGE MICROPHYSICAL CHARACTERISTICS FOR THE MATURE STAGES OF MARINE FOGS OBSERVED OFF THE COAST OF NOVA SCOTIA, AUGUST 1975

Fog Number	Date	Mode Rad. (μm)	Mean Rad. (μm)	Drop Conc. (cm^{-3})	Avg. LWC ($g\ m^{-3}$)	Max. LWC ($g\ m^{-3}$)	Avg. Min. Vsby. (m)
2AB	2-3 Aug	5.1	5.2	55	0.04	0.23	100
4B	3-4 Aug	3.2	5.4	34	0.07	0.10	550
5	4 Aug	3.7	4.9	58	0.05	0.07	350
4C	4 Aug	4.8	6.2	55	0.10	0.17	200
4D	4 Aug	3.1	4.3	72	0.06	0.10	300
6	5 Aug	7.0	8.0	155	0.40	0.49	100
9	7 Aug	3.0/7.5	7.7	105	0.35	0.48	80
10	7-8 Aug	6.8	8.4	70	0.30	0.48	90
12	9 Aug	7.0	8.7	74	0.29	0.36	100
13	10 Aug	6.0	6.6	85	0.14	0.19	150
14	10-11 Aug	7.0	7.8	112	0.32	0.49	70

Off the West Coast, in contrast to conditions observed off Nova Scotia, the CCN population is generally characterized by substantially fewer of the smaller particles (lower by a factor of ~5) active at supersaturations > 0.1% S. In addition, much higher concentrations of larger, more effective "haze" nuclei (higher perhaps by a factor of 100) are also found. The number concentration of these locally-produced, larger "haze" nuclei has always correlated well with the droplet concentrations in subsequent fogs. Further fog water off the West Coast has been found to be comprised primarily of materials in the same ratio as found in sea water--suggesting that sea salt aerosols (perhaps the "haze" nuclei) serve as the primary nucleants of most fogs occurring off the West Coast.

In view of the major differences in the respective aerosol populations (i.e., larger concentrations of smaller nuclei of different chemical composition off Nova Scotia) it would seem reasonable to expect that the microphysical features of fog occurring off Nova Scotia would also differ from those of West Coast fogs. Because the formation mechanisms of most of the Nova Scotia fogs cannot be precisely specified, the microphysics of California and Nova Scotia marine fogs cannot be directly compared on the basis of fog type. Instead, we have chosen to average the data from the Nova Scotia fogs according to the average minimum visibilities (i.e., the "mature" stage) characteristic of the fogs, using visibility as a measure of the strength of the driving mechanisms responsible for the fog. The average microphysics as functions of visibility levels* for the Nova Scotia fogs are presented at the bottom of Table 6 and compared with average data from California fogs at the top of the Table.

The similarities in LWC values of the California and Nova Scotia fogs within the visibility groupings (i.e., <150m and 200-600m) suggest that the driving mechanisms for fog formation and persistence are of comparable

---

*The visibility levels quoted here are not meant to be used quantitatively with individual LWC data to compute other droplet parameters; they are smoothed values of a continuous record, whereas LWC data are averages of instantaneous values obtained only occasionally within the highly variable microstructure common to fog.

TABLE 6: AVERAGE MICROPHYSICAL CHARACTERISTICS OF MARINE FOGS

CALIFORNIA COASTAL FOGS

1971 - 1974

	MEAN RADIUS (μM)	DROP CONC (CM^{-3})	AVG MAX LWC ($G\ M^{-3}$)	AVG MIN VSBY (M)
COASTAL FOGS (CONVERGENCE)	10.0	25	.16	100
COASTAL RADIATION-VALLEY FOGS	9.5	60	.30	100
STRATUS-LOWERING FOGS	9.0	10	.08	300-1000
FOG PATCHES (OVER WATER TEMP. DISCONTINUITIES)	6.5	30	.08	200
SHALLOW COASTAL FOGS	4.8	45	.03	300

NOVA SCOTIA COASTAL FOGS - 1975

	MODE RADIUS (μM)	MEAN RADIUS (μM)	DROP CONC (CM^{-3})	AVG MAX LWC ($G\ M^{-3}$)	AVG MIN VSBY (M)
DENSE FOG	6.6	7.5	95	.27	<150
MODERATE FOG	4.0	5.6	55	.09	200-600

magnitudes off both coasts. However, major differences in the fog microphysics are readily apparent when comparing mean drop sizes and droplet concentrations. Note that within the given visibility-LWC categories, droplet concentrations are greater and droplet sizes are smaller in the Nova Scotia fogs. It would appear that observed differences in the CCN population (between the offshore areas of California and Nova Scotia) are responsible for the observed differences in the resultant fog drop size distributions. For a given quantity of liquid water, the higher concentrations of presumably smaller sulfate nuclei apparently gave rise to the higher concentrations of smaller droplets observed in marine fogs occurring off the coast of Nova Scotia. Conversely, for a given LWC, a droplet population comprised of greater numbers of smaller drops would produce a lower visibility than would drop spectra of fewer but larger droplets. Indeed, the extremely low visibility levels (i.e., 50-80m) experienced in some of the marine fogs off Nova Scotia are uncommon to West Coast fogs.

In making these comparisons, it should be noted that, as stated several times in this section, we believe that the absence of sea salt nuclei observed near N.S. was due largely to the very light winds encountered during the Atlantic cruise. The microphysical characteristics of fog reported here reflect that lack of sea salt nuclei. There is no reason to believe that these microphysical characteristics are representative of all fogs in the Atlantic or near Nova Scotia.

Section 4

CONCLUSIONS

The following principal conclusions have been derived as a result of this study of marine fogs which occurred off the coast of Nova Scotia during early August 1975:

(1) Areas of very cold water (of mesoscale dimensions) are a major contributing factor in the development of most fogs (at the surface), and spatial variations in sea surface temperature are directly responsible for spatial fluctuations in surface-level characteristics of the fogs.

(2) Shallow fogs of mesoscale dimensions can apparently be triggered and maintained by advection of air over cold water. The "cold water" processes that we observed appear to function on a time scale on the order of hours, and no doubt represent the final stages of fog formation as suggested by Taylor (1917) to occur over time periods measured in days. The shallow "cold water" fog observed on this field study closely approximates conditions predicted by some numerical models (Rogers et al., 1975; Eadie et al., 1976) except with respect to time scale.

(3) Fog development and persistence off the East Coast can also occur or be promoted by at least two processes previously identified as operative off the West Coast: by the thickening of a stratus cloud and by advection over warmer water. In some stratus-lowering fogs, the cold underlying sea surface contributed substantially, augmenting the stratus-lowering mechanism to produce saturated conditions at the surface.

(4) The aerosol populations of the air masses prevailing downwind of the continent during the observation period were essentially (and are expected to always be to some extent) of continental character. Analyses of CCN data, aerosol samples, and fog water samples suggest that high number concentrations of sulfate aerosols served as the primary nucleants for the

fogs observed off the coast of Nova Scotia during August 1975, a period of light wind and calm sea. In contrast, sea salt aerosols in low concentrations have been found to serve as the primary fog droplet nuclei in the clean marine air off the West Coast. In periods of strong winds in the Nova Scotia region, we would expect a substantial contribution by sea salt in the nucleation process.

(5) Differences in the nucleus populations apparently gave rise to differences in the resultant droplet populations off the two coasts. Off the East Coast with many more smaller nuclei competing for comparable quantities of condensable water, the resultant droplet spectra were comprised of greater numbers of droplets and were shifted to smaller sizes than has been typically observed in fogs at sea off the West Coast. Again, under different wind conditions in the Atlantic, we would expect different nuclei spectra and different drop size distributions.

REFERENCES

Baier, R.E., 1975: Surface-Active and Infrared-Detectable Matter in North Atlantic Aerosols, Sea Fogs, and Sea-Surface Films, Calspan Corporation, Buffalo, N.Y. 14221.

Eadie, W.J., C.W. Rogers, and E.J. Mack, 1976: The Calspan Advection Fog Model Using Prognostic Equations for Turbulent Energy, Project SEA FOG: Fourth Annual Summary Report, Part 2, Report No. CJ-5756-M-2, Calspan Corporation, Buffalo, N.Y. 14221.

Gathman, S.G., 1976: Boundary Layer Measurements of Temperature, Water Vapor and Pressure During the 1975 Fog Cruise of the USNS HAYES, Compilation of Data from the 1975 USNS HAYES Fog Cruise, Naval Research Laboratory Report No. 7___, (in press).

Larson, R.E., 1976: Radon 222 Measurements During the 1975 Nova Scotia Marine Fog Cruise, Compilation of Data from the 1975 USNS HAYES Fog Cruise, Naval Research Laboratory Report No. 7___, (in press).

Mack, E.J., R.J. Pilié and W.C. Kocmond, 1973: An Investigation of the Microphysical and Micrometeorological Properties of Sea Fog, Project SEA FOG: First Annual Summary Report, Rept. No. CJ-5237-M-1, Calspan Corporation, Buffalo, N.Y. 14221.

Mack, E.J. and R.J. Pilié, 1973a: The Microstructure of Radiation Fog at Travis AFB, Rept. No. CJ-5076-M-2, Calspan Corporation, Buffalo, N.Y. 14221.

Mack, E.J., U. Katz, C.W. Rogers, and R.J. Pilié, 1974: The Microstructure of California Coastal Stratus and Fog at Sea, Project SEA FOG: Second Annual Summary Report, Calspan Rept. No. CJ-5404-M-1, Calspan Corporation, Buffalo, N.Y. 14221.

Mack, E.J., R.J. Pilié, and U. Katz, 1975: Marine Fog Studies Off the California Coast, Project SEA FOG: Third Annual Summary Report, Rept. No. CJ-5607-M-1, Calspan Corporation, Buffalo, N.Y. 14221.

Mohnen, V.A. and G.K. Yue, 1974: Free HCl Acid in the Atmosphere Resulting from Scavenging Processes, Precipitation Scavenging (1974), U.S. Atomic Energy Commission Symposium Series (in press).

Rogers, C.W., W.J. Eadie, U. Katz, and W.C. Kocmond, 1975: A Numerical Model of Advection Fog, PROJECT FOG DROPS V, NASA CR-2633, National Aeronautics and Space Admin., Wash., D.C. 20546, 79 pp., $4.75.

Taylor, G.I., 1917: The Formation of Fog and Mist, Quart. J. Royal Meteor. Soc., 43, pp. 241-268.

APPENDIX A*

REDUCED DATA FROM CALSPAN'S PARTICIPATION IN THE USNS HAYES CRUISE OFF THE COAST OF NOVA SCOTIA, 29 JULY - 12 AUGUST 1975

*PREPARED FOR INCLUSION IN AN NRL-EDITED DATA VOLUME FOR THE CRUISE OF THE USNS HAYES, AUGUST 1975.

LIST OF FIGURES

REDUCED DATA FROM CALSPAN'S PARTICIPATION IN THE USNS HAYES CRUISE OFF THE COAST OF NOVA SCOTIA, 29 JULY - 12 AUGUST 1975

BY

EUGENE J. MACK, ULRICH KATZ, AND JOHN Y. YANG

FEBRUARY 1976

INTRODUCTION

A major objective of Calspan's participation in the Summer 1975 cruise aboard the USNS HAYES was to obtain data describing the micrometeorological and microphysical characteristics of marine fogs occurring in the area off the Southeast coast of Nova Scotia. Calspan's participation in the cruise was limited to the period from departure at Williamsburg, Virginia on 28 July to arrival at Halifax on 12 August 1975. The cruise was highly successful, having encountered approximately 18 distinct fog occurrences and logging approximately 95 hours of observations in fog with visibility <5000 m, including 65 hours of dense fog (visibility <1000 m). The major portion of Calspan data obtained during the cruise is presented in this volume in reduced form with minimal interpretation for objective use by other participants of the cruise. The remaining Calspan data on surface chemistry were acquired under a different contract and are reported separately.

INSTRUMENTATION

Calspan instrumentation mounted aboard the HAYES is listed in Table 1. A 4 m high tower-platform (1.5 x 1.8 m on the sides) was constructed and installed on the flying bridge to provide for exposure of fog microphysics instrumentation adequately above the level of ship's influence. The drop sampler, fog water collector, air sampling apparatus, and visibility monitor were mounted atop the tower. The base of the tower was enclosed to provide shelter for the nucleus chambers and various recorders.

A specially-designed vehicle, housing a temperature sensor, was constructed from a 0.5 m length of 2.5 inch pipe and towed between the twin hulls of the ship to provide a continuous measure of surface water temperature. Air temperature was measured at three heights (7.5, 17 and 28 m) above the sea surface and dew point temperature was monitored at two levels (17 and 28 m).

During the cruise, fog was encountered almost nightly for a ten-day period beginning on 2 August. Visibility, air and water temperature, and dew point* were monitored continuously; in excess of 450 measurements of drop size distribution and over 160 samples of fog water were also obtained. Many additional samples of fog water were provided to other researchers participating in the cruise. Numerous measurements of the cloud nucleus spectrum and hi-vol samples of atmospheric aerosols (for chemical analysis) were also acquired during periods between fog events, providing data on the characteristics of the air masses in which the fogs formed.

---

*Calspan temperature instrumentation is always field calibrated, but similar calibrations for dew point sensors are not possible in the field. As a result, dew point temperatures are offset from air temperature, and the offset increased gradually (due to instrument drift) with time throughout the duration of the cruise. However, the data from individual sensors are good to approximately $\pm$0.4°C in a relative sense over periods of hours, and we have chosen to show the dew point data in terms of "relative dew point." We believe that in very dense fog (i.e., visibility <300 m) saturated conditions exist, and therefore the dew point records for individual fogs should be adjusted so that air temperature and dew point match at their respective heights when visibility is <300 m. Care should be taken in making this adjustment because visibility was measured only at the height of the lowest dew point sensor (about 20 m) and occasionally fog depth did not extend up to the level of the upper dew point sensor (28 m).

Table A-1.

CALSPAN INSTRUMENTATION INSTALLED ON USNS HAYES, AUGUST 1975

Instrument*	Height Above Sea Surface
Temperature Sensors (Foxboro)	sea surface, 7.5, 17, 28 m
Dew Point Sensors (Foxboro)	17, 28 m
Forward Scatter Visibility (EG&G)	21 m
Drop Sampler (Calspan)	20 m
Fog Water Collector (Calspan)	20 m
Air Chemistry (Hi-Vol Sampler)	18 m
Cloud Nucleus Chamber (Calspan)	18 m
Haze Nucleus Chamber (Calspan)	18 m

*Detailed descriptions of individual instruments may be found elsewhere (e.g., Mack et al., 1972, A Field Investigation and Numerical Simulation of Coastal Fog; and Mack et al., 1973, An Investigation of the Microphysical and Micrometeorological Properties of Sea Fog).

THE DATA

Ship's Track

Our interpretation of the position of ship's track throughout the 11-day portion of the cruise off the coast of Nova Scotia is shown in a modified version of a plot supplied by G. Schacher (Naval Postgraduate School) in Figure A-1. Our exact interpretations of ship's track are shown in later figures preceding the set of figures for each fog episode. On Figure A-1, the numbers 1 through 11 denote ship's position at the 0000 (EDT) hour of those respective days in August 1975.

Sea Surface Temperature

Our continuous record of sea surface temperature was transferred to the plot of ship's track by picking off min- and max- temperatures from the

FIGURE A-1. PLOT OF THE TRACK OF THE USNS HAYES OFF THE COAST OF NOVA SCOTIA FOR THE PERIOD 1-11 AUGUST 1975.

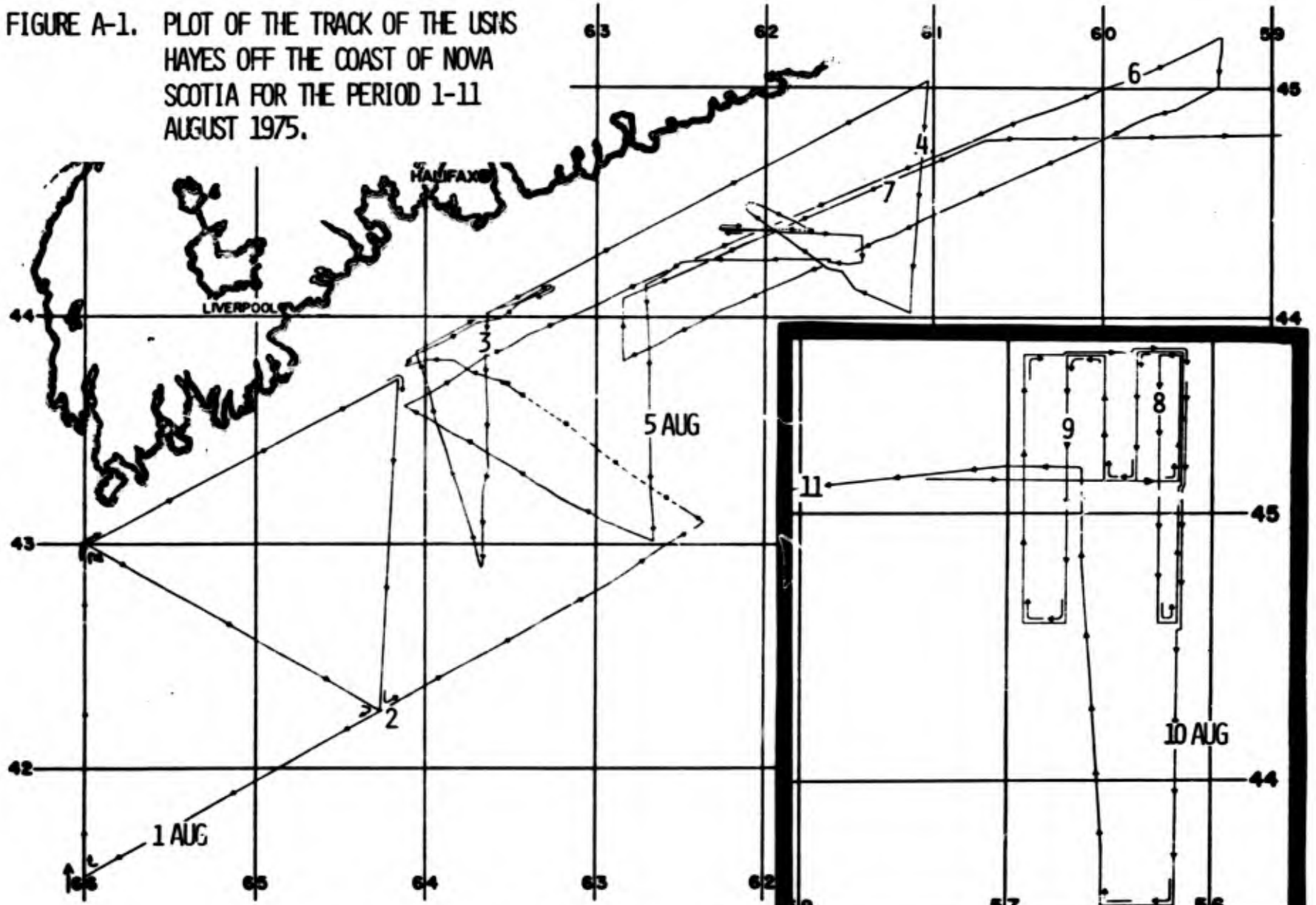

NRL CRUISE, USNS HAYES, AUGUST 1975
(AFTER G. SCHACHER, NPS)

original strip chart records. These data were then isoplethed to provide the chart of sea surface temperature shown in Figure A-2. The shaded areas superimposed on the sea surface temperature chart represent the portions of ship's track during which visibility (at the 21 m height) was reduced to less than 1000 m.

Fog Numbering System

During the initial analysis, fog events were numbered consecutively, and the same numbers were retained (with letters of the alphabet) for successive encounters with what was thought to be the same fog. To avoid confusion, the Calspan fog numbers were used to label various data from that portion of the ship's track which included the specific fog event. Figure A-3 is a reproduction of Figure A-2 showing the fog numbering system. Later interpretation suggested 18 separate fog occurrences which do not precisely coincide with the numbering system, but the system has been retained for convenience. The separate fog occurrences are delineated in Table A-3.

Cloud Nucleus Spectra

Individual measurements of cloud nucleus spectra obtained with Calspan's static thermal diffusion chamber are shown in Figure A-4. These measurements were obtained during "non-fog" periods in the ambient air masses in which fogs later formed. Haze nucleus* concentrations (not shown on the figure) were typically much less than one per sensitive volume (i.e., $<<10\ cm^{-3}$).

Chemistry of Air Mass Aerosol

Throughout the cruise, hi-vol samples of the ambient aerosol were collected over approximate 8-hour intervals during "non-fog" periods, if possible, in the air masses in which fogs later formed. Some indicated samples were

*Haze nuclei are measured with a modified thermal diffusion chamber and are those particles which grow to ~1 μm at 98% RH.

FIGURE A-2. ISOPLETHS OF SEA SURFACE TEMPERATURE (°C) AND REGIONS OF REDUCED VISIBILITY (<1000 M DUE TO FOG) ALONG SHIP'S TRACK

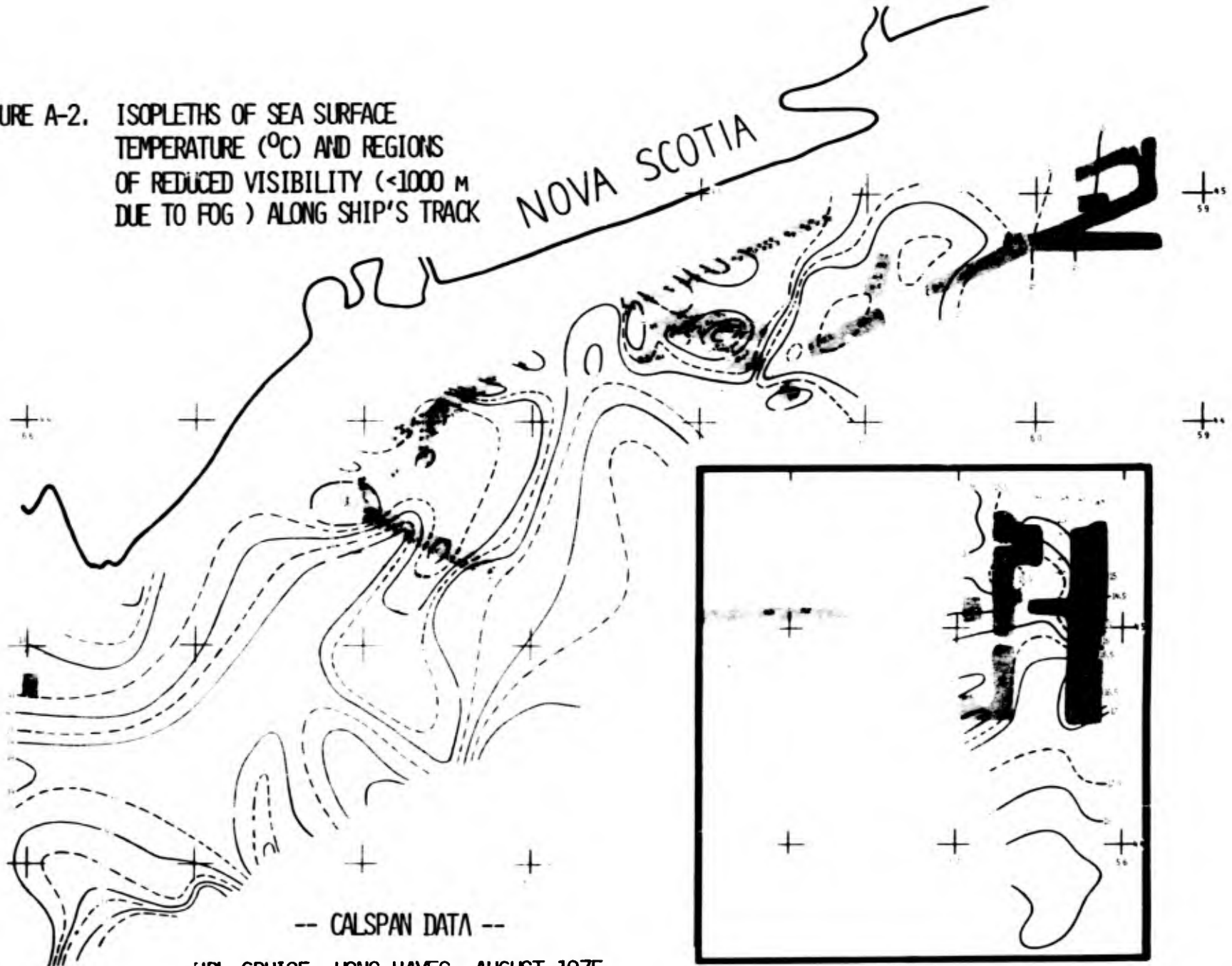

FIGURE A-3. FOG NUMBERING SYSTEM.

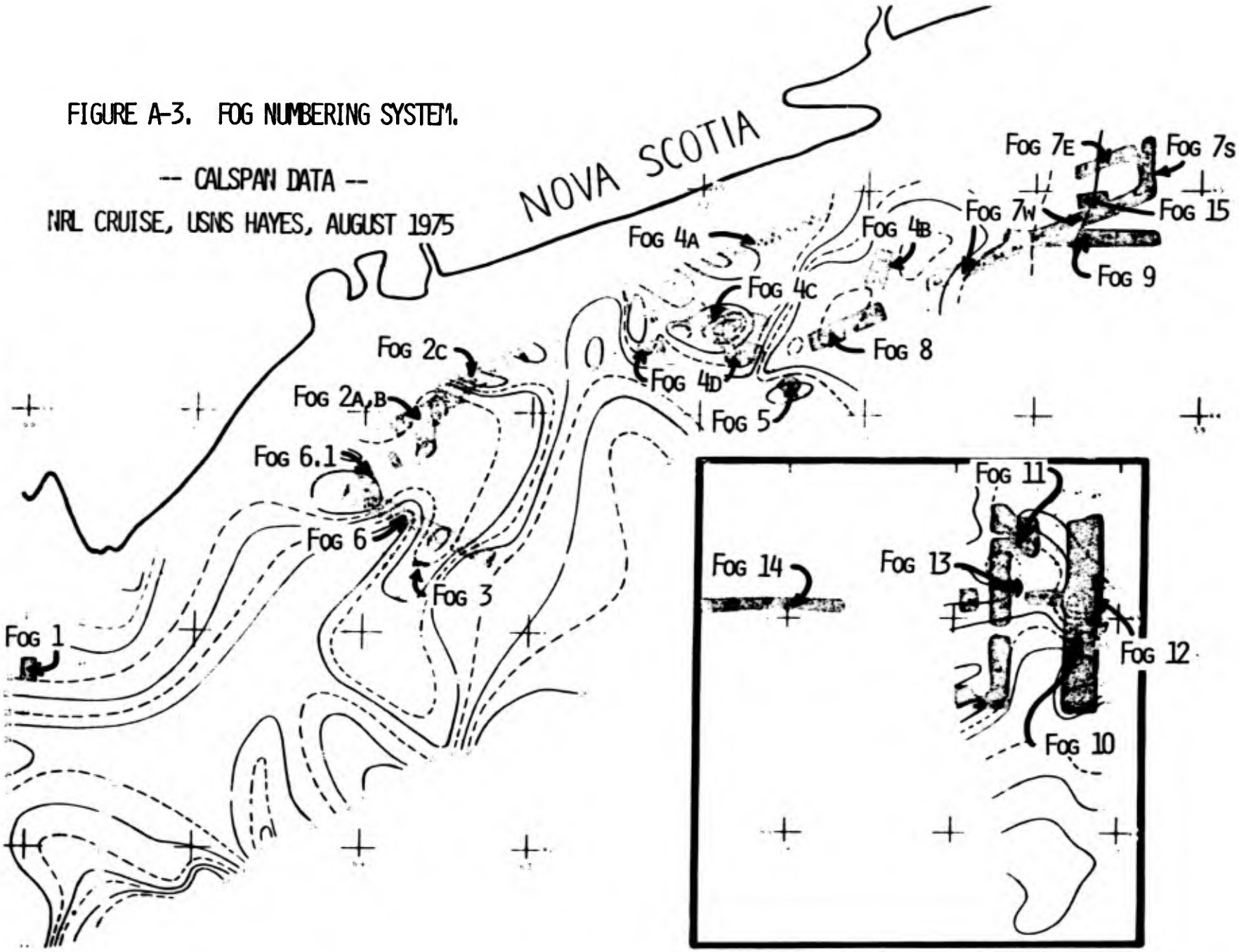

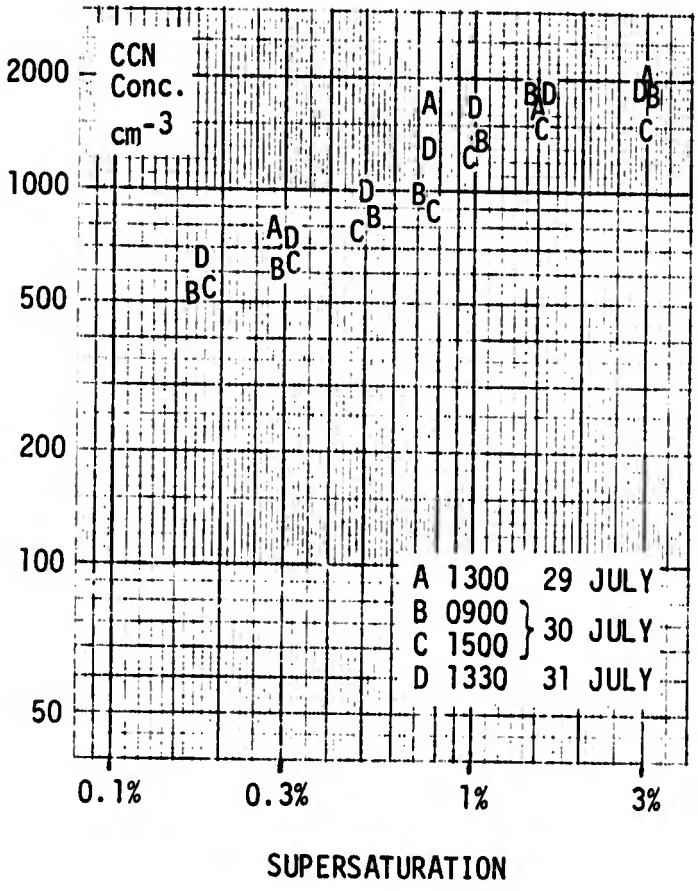

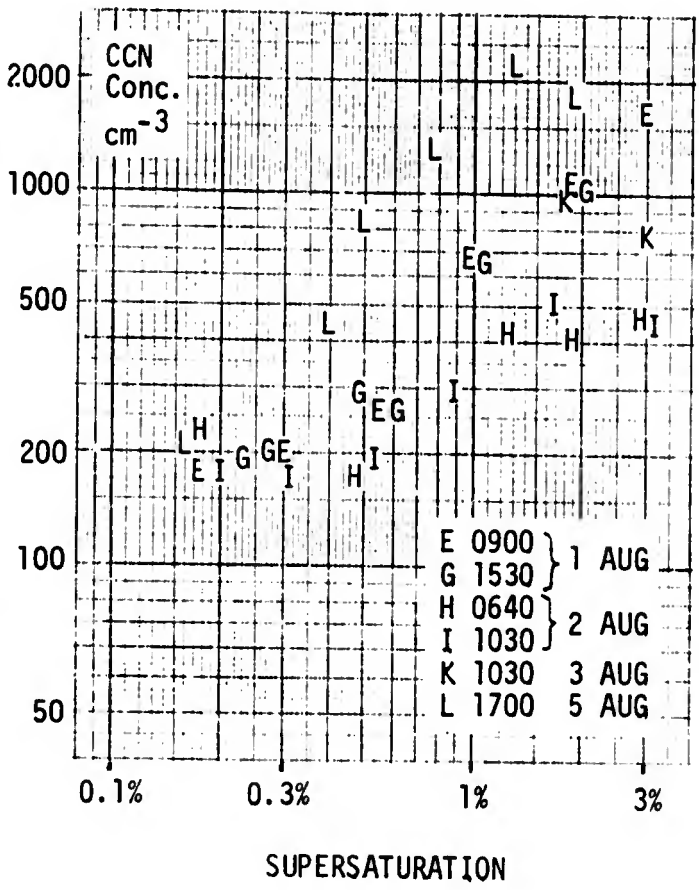

NRL CRUISE, USNS HAYES, AUGUST 1975

-- CALSPAN DATA --

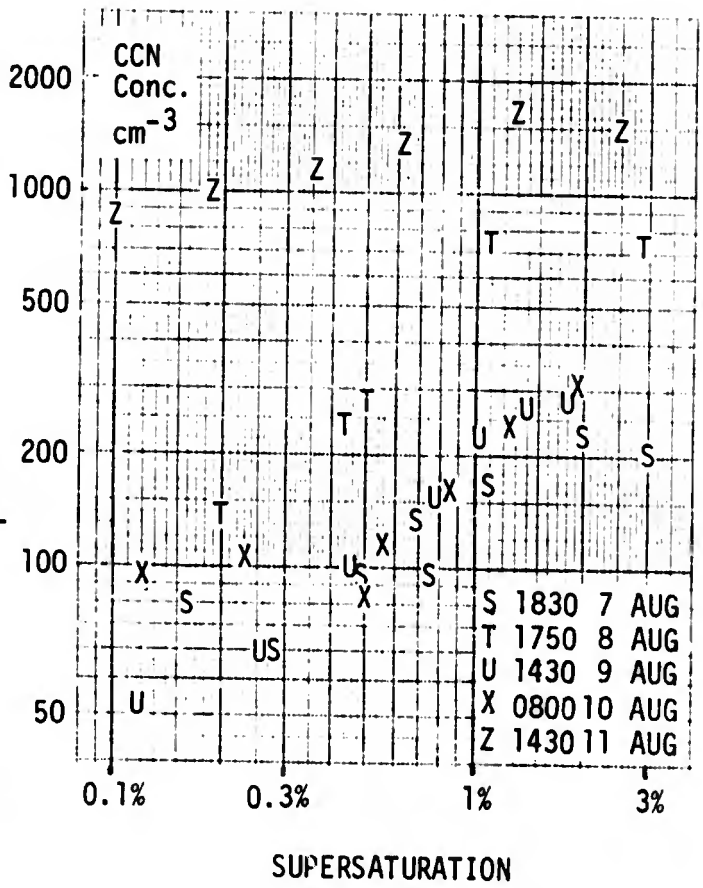

FIGURE A-4. OBSERVATIONS OF CLOUD NUCLEUS CONCENTRATIONS vs. SUPERSATURATION

unavoidably obtained during fog episodes; and except for minor losses due to droplet fallout, these samples should be representative of the ambient air mass characteristics.

The aerosol particulate samples were collected on 4" diameter Tissuquartz filters (Pallflex Corporation 2500 QAO). Each filter disc was cut into two halves and digested over low heat in two small beakers, each containing 20 ml triple distilled water and adjusted respectively to alkaline and acid pH with sodium hydroxide or sulfuric acid. The filter digestion solution was then filtered under suction and the filtrate reduced by evaporation to 10 ml. Desired analyses* were performed with aliquots of the individual samples, and these data are presented in Table A-2.

Chemistry of Fog Water

During the cruise, 168 discrete 7 ml samples of fog water were collected and retained for later analysis at Calspan; many additional samples were provided to other researchers. The samples were obtained at the 20 m height (to minimize influence by sea spray), and individual samples were collected over periods of from 4 to 15 minutes depending on fog density.

Initial analyses indicated that fog water chemistry did not vary substantially within individual fogs and that each fog, on the average, was slightly different from the others. The remaining samples were then composited into 14 groups corresponding to 14 of the 18 distinct fog occurrences encountered during the cruise. These data, delineation of the 18 fog events, and chemical analysis of their respective fog water may be found in Table A-3. (Quantities of fog water sufficient for chemical analysis were not obtained in fogs numbered 1, 3, 5 and 15.) The analysis techniques used for the ambient aerosol samples were also used for the fog water samples.

*Metal ion analyses were performed by atomic absorption; chloride and ammonium ion analyses were performed by specific ion electrode; and sulfate analyses were performed by barium perchlorate titration with Thorin indicator.

Table A-2. CHEMICAL ANALYSIS OF HI-VOL AMBIENT AEROSOL SAMPLES COLLECTED OFF THE COAST OF NOVA SCOTIA

($\mu g/m^3$ of air)

Date	Time	SO_4^{--}	NH_4^+	Na	K	Ca	Mg	Al	Cl^{-1}
29 Jul	1200-2000	25.3	5.34	1.43	0.33	0.17	0.12	0.44	<.02
30 Jul	1100-1800	14.3	1.84	0.49	0.18	0.11	0.04	0.18	<.02,
31 Jul	0000-0800	10.4	1.66	1.93	0.19	0.12	0.15	0.23	<.02
31 Jul	1200-2000	12.3	1.86	2.23	0.25	0.22	0.23	0.27	<.02
1 Aug	0000-0800	7.89	1.92	0.64	0.16	0.04	0.05	0.19	<.02
1 Aug	1200-2000	3.03	0.64	0.44	0.12	0.03	0.02	0.15	<.02
2 Aug	0000-0800	4.71	0.76	0.58	0.13	0.05	0.03	0.18	<.02
2 Aug	1030-1300 1530-1930	3.88	0.75	0.64	0.14	0.11	0.04	0.17	<.02
2-3 Aug	2000-0100 FG*	4.68	0.94	0.68	0.26	0.06	0.02	0.24	<.02
3 Aug	1230-1630	4.42	1.30	1.40	0.38	0.19	0.11	0.38	<.02
4 Aug	0930-1530 FG	3.49	0.55	1.51	0.25	0.07	0.10	0.25	<.02
5 Aug	0000-0800 FG	2.90	0.46	0.63	0.13	0.04	0.04	0.16	<.02
5 Aug	1200-2000 FG	6.65	0.78	1.80	0.17	0.15	0.10	0.34	<.02
6 Aug	0000-0800 FG	2.46	0.44	0.47	0.15	0.10	0.04	0.23	<.02
6 Aug	1200-2020	3.25	0.54	0.42	0.13	0.03	0.02	0.19	<.02
7 Aug	1200-2000 FG	5.45	0.49	1.16	0.18	0.22	0.11	0.32	<.02
8 Aug	0000-0800 FG	3.30	0.48	0.41	0.15	0.03	0.02	0.12	<.02
8 Aug	1200-2000	3.08	0.41	1.20	0.14	0.09	0.06	0.12	<.02

*FG indicates fog was present during a portion of the sampling period.

Table A-3. CHEMICAL ANALYSIS OF FOG WATER SAMPLES COLLECTED OFF THE COAST OF NOVA SCOTIA

(μg/ml of fog water)

Fog	Date	SO_4^{--}	NH_4^+	Na	K	Ca	Mg	Al	Cl^{-1}
2AB	2 Aug	22.5	0.52	28.5	2.03	1.38	0.94	<1	8.4
2C	3 Aug	21.0	1.20	14.0	0.83	0.68	1.52	<1	5.5
4A	3 Aug	24.0	0.85	36.0	1.85	1.22	3.62	<1	16.0
4B	4 Aug	17.3	1.70	25.0	1.53	0.68	3.28	<1	11.0
4CD	4 Aug	5.3	0.05	32.9	2.3	0.99	1.18	<1	3.3
6	5 Aug	9.0	1.30	26.1	1.5	0.80	0.55	<1	0.5
7	6 Aug	16.5	0.65	27.3	2.7	0.99	0.96	<1	0.4
8	6 Aug	10.5	0.43	23.7	2.1	0.82	0.54	<1	0.2
9	7 Aug	9.0	0.25	20.0	2.1	0.87	0.52	<1	0.2
10	7-8 Aug	8.0	0.28	21.8	2.3	0.90	0.60	<1	0.1
11	8-9 Aug	5.0	0.06	20.4	1.5	0.77	0.63	<1	0.3
12	9 Aug	2.3	0.21	17.6	1.6	0.65	0.36	<1	0.2
13	10 Aug	3.0	0.08	23.4	2.6	1.07	0.64	<1	0.6
14	10 Aug	2.5	0.20	20.0	1.0	0.59	0.53	<1	0.7

The Micrometeorology and Microphysics of the Fogs

For analysis purposes, each portion of the ship's track which included a fog penetration was given a "Fog Number." To the extent possible, all data acquired during each fog penetration (including those outside the fog boundaries) were analyzed and computer plotted. These data are provided here in groups corresponding to the fog numbering system shown in Figure A-3. Detailed plots of ship's track, including the 5000 m visibility boundaries of the fog, visibility as a function of time along the track, air, dew point, and sea surface temperatures along the track and drop size distributions* obtained in the fog are grouped for each fog penetration and are presented in Figures A-5 through A-97.

The computer plots are annotated with pertinent observations and an estimate of wind direction relative to the ship's heading. The wind directions shown are our estimates based on data provided by NRL and modified by our own observations. Because of uncertainties in the precise determination of ship's heading and spatial and temporal changes in the light wind patterns encountered, the winds are believed good only to $\pm 30°$.

*Computed values of drop concentration and liquid water content are provided for each drop size distribution.

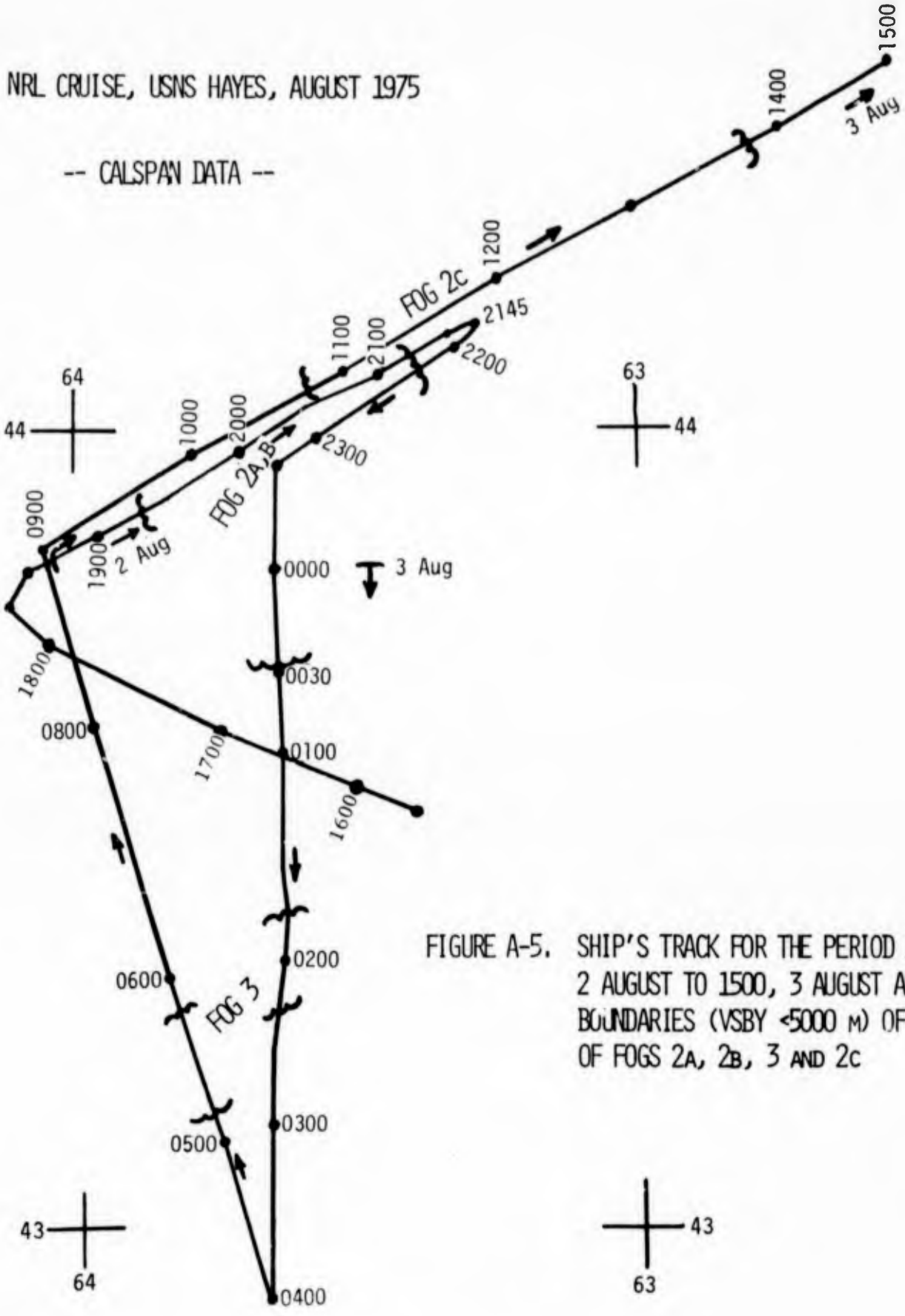

FIGURE A-5. SHIP'S TRACK FOR THE PERIOD 1800, 2 AUGUST TO 1500, 3 AUGUST AND BOUNDARIES (VSBY <5000 M) OF OF FOGS 2A, 2B, 3 AND 2C

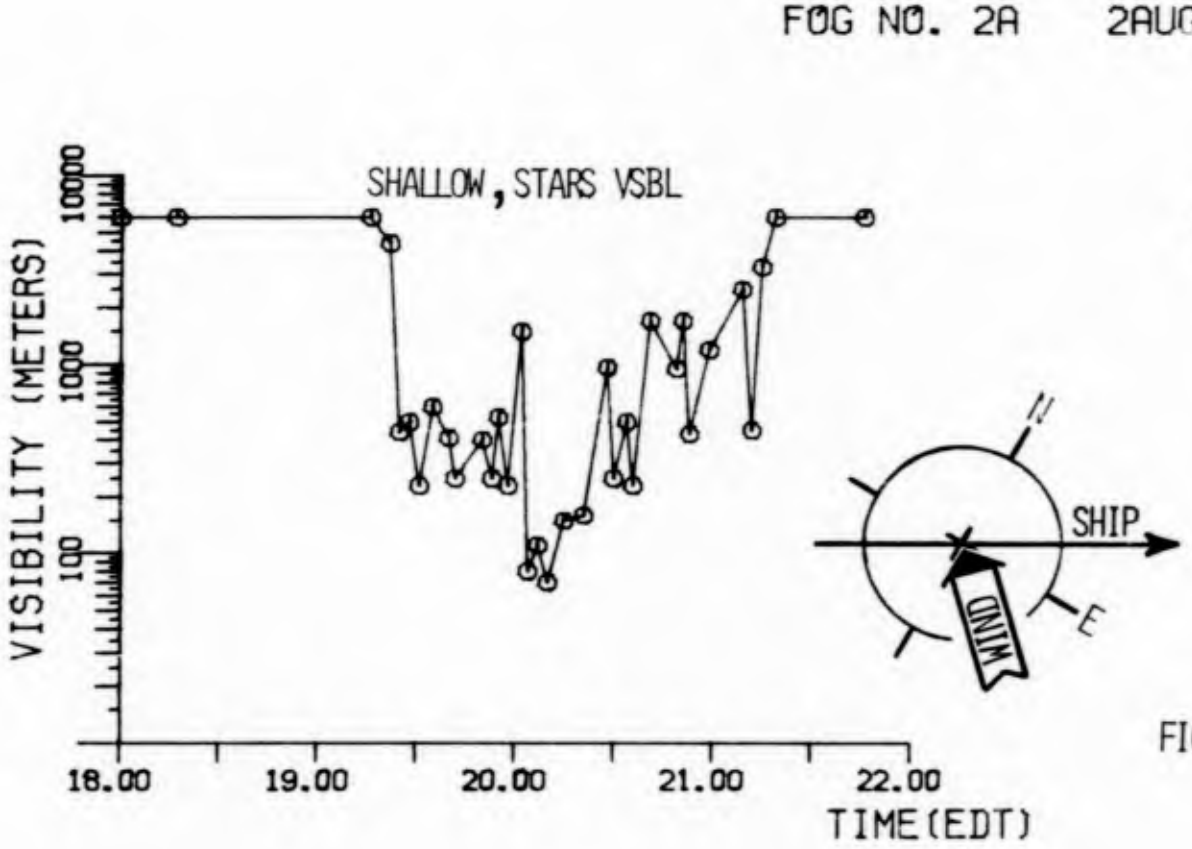

NRL CRUISE, USNS HAYES, AUGUST 1975

-- CALSPAN DATA --

FIGURE A-6. VISIBILITY vs. TIME -- FOG 2A, 2 AUGUST 1975

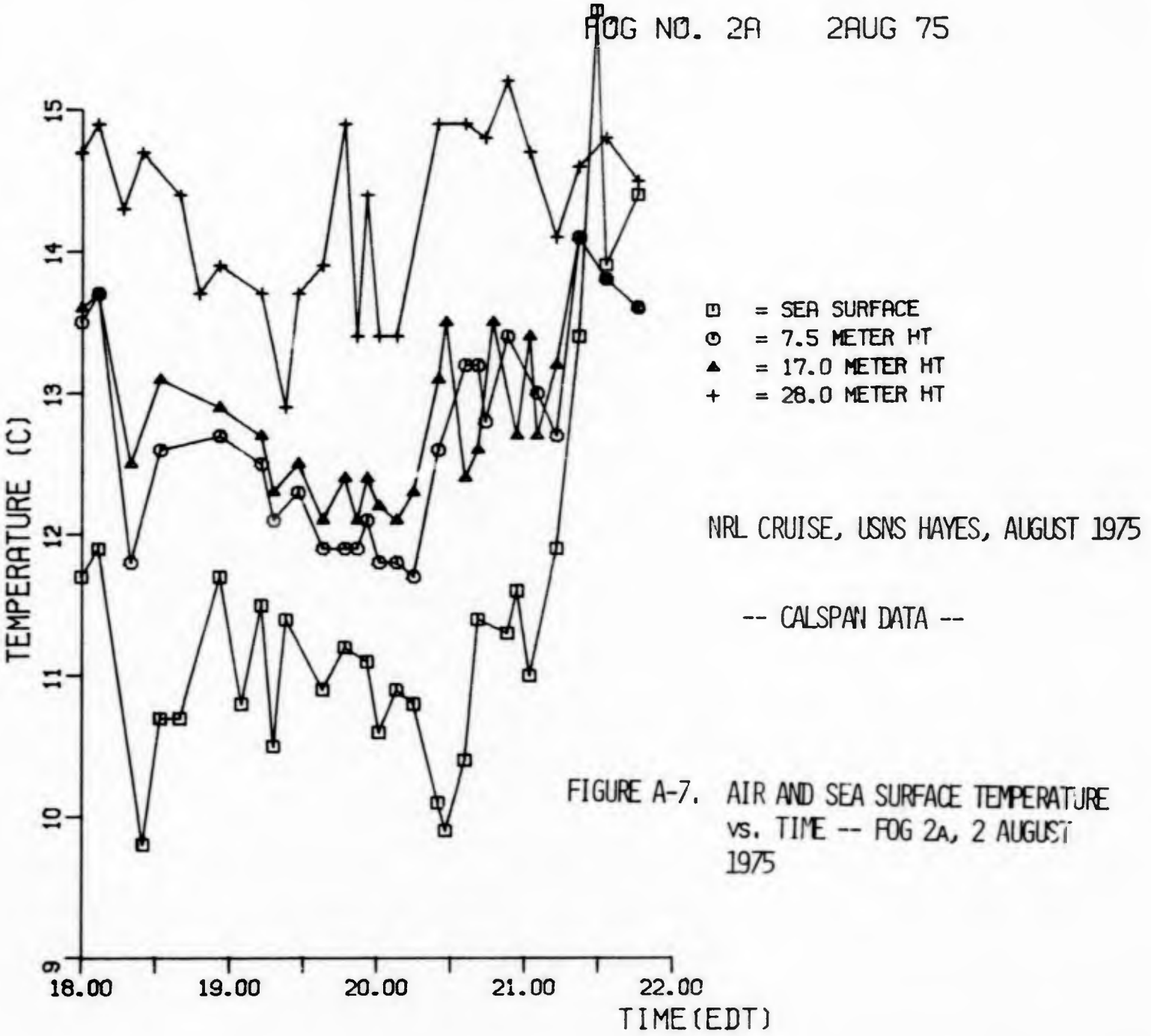

FIGURE A-7. AIR AND SEA SURFACE TEMPERATURE vs. TIME -- FOG 2A, 2 AUGUST 1975

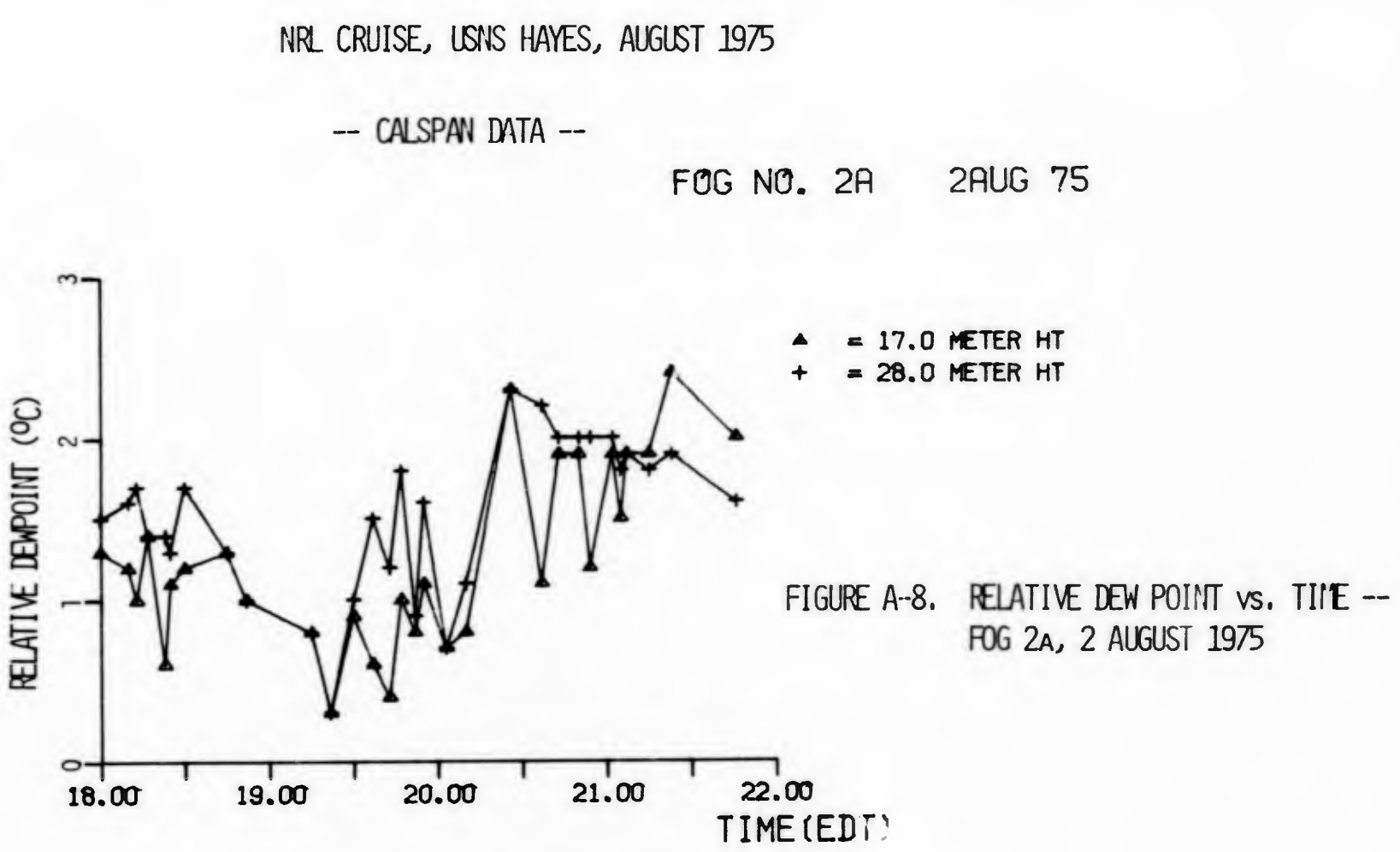

FIGURE A-8. RELATIVE DEW POINT vs. TIME -- FOG 2A, 2 AUGUST 1975

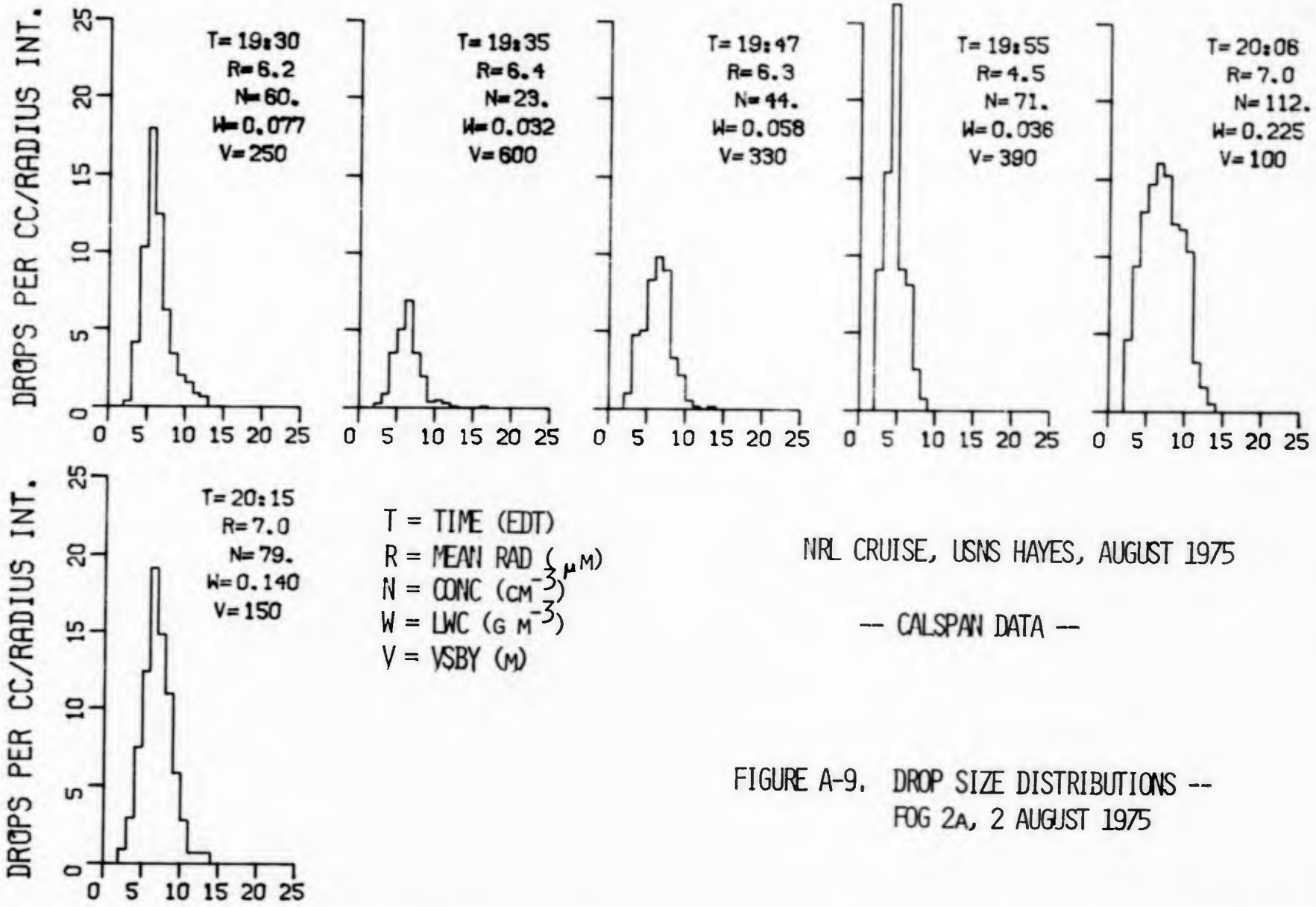

NRL CRUISE, USNS HAYES, AUGUST 1975

-- CALSPAN DATA --

FIGURE A-9. DROP SIZE DISTRIBUTIONS --
FOG 2A, 2 AUGUST 1975

2AUG75 NO. 2A

FOG NO. 2B 2-3AUG. 1975

NRL CRUISE, USNS HAYES, AUGUST 1975

-- CALSPAN DATA --

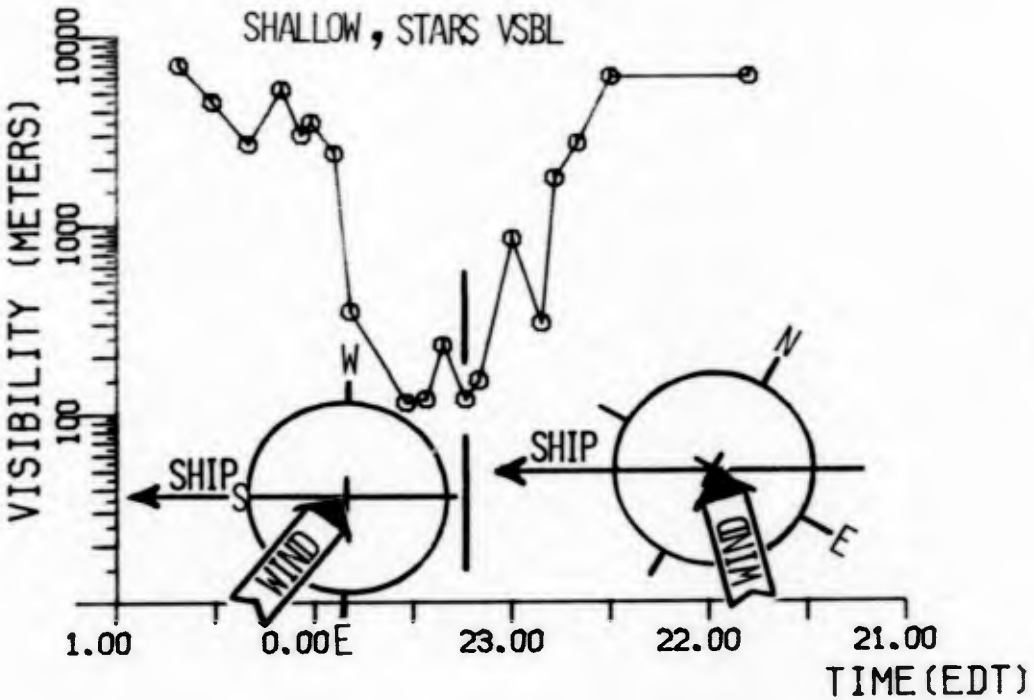

FIGURE A-10. VISIBILITY vs. TIME -- FOG 2B, 2-3 AUGUST 1975

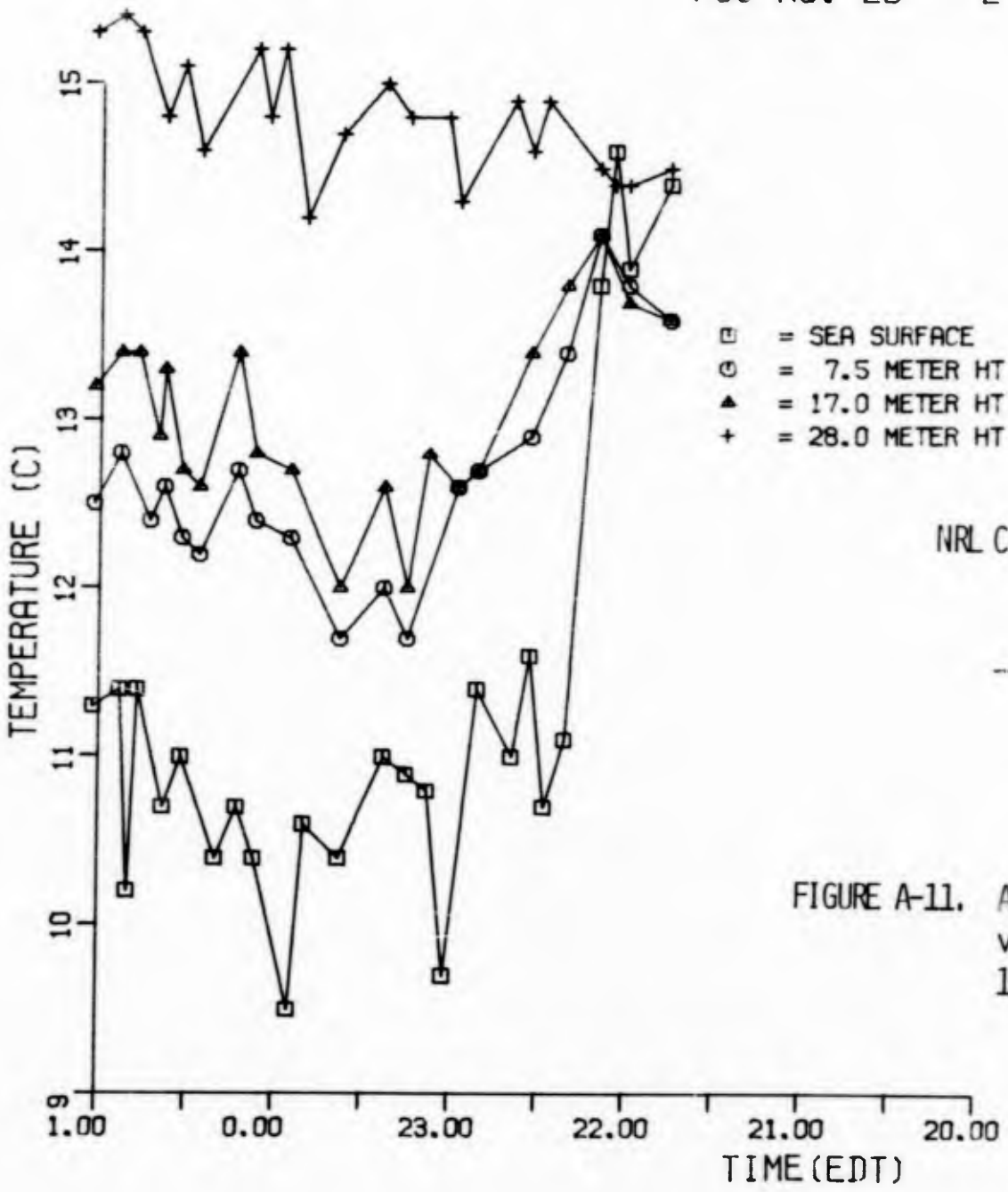

FIGURE A-11. AIR AND SEA SURFACE TEMPERATURE vs. TIME -- FOG 2B, 2-3 AUGUST 1975

FOG NO. 2B 2-3AUG 1975

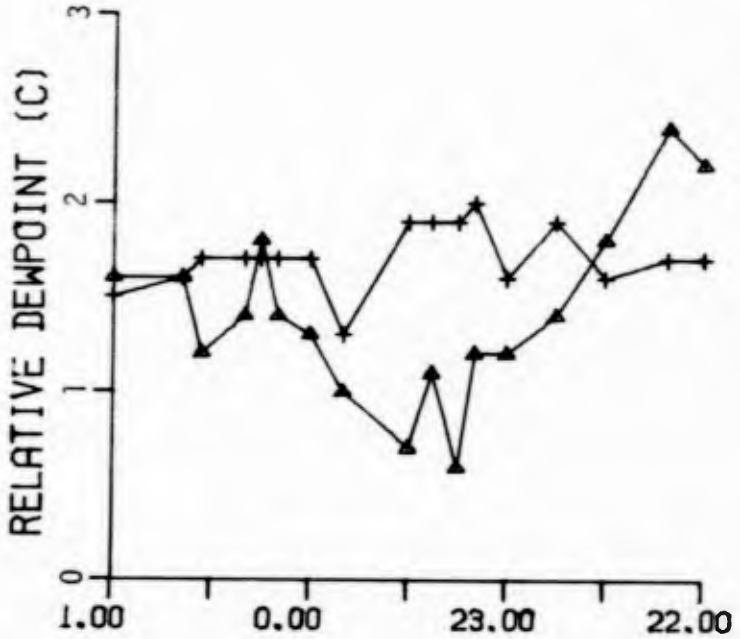

▲ = 17.0 METER HT
\+ = 28.0 METER HT

NRL CRUISE, USNS HAYES, AUGUST 1975

-- CALSPAN DATA --

FIGURE A-12. RELATIVE DEW POINT vs. TIME -- FOG 2B, 2-3 AUGUST 1975

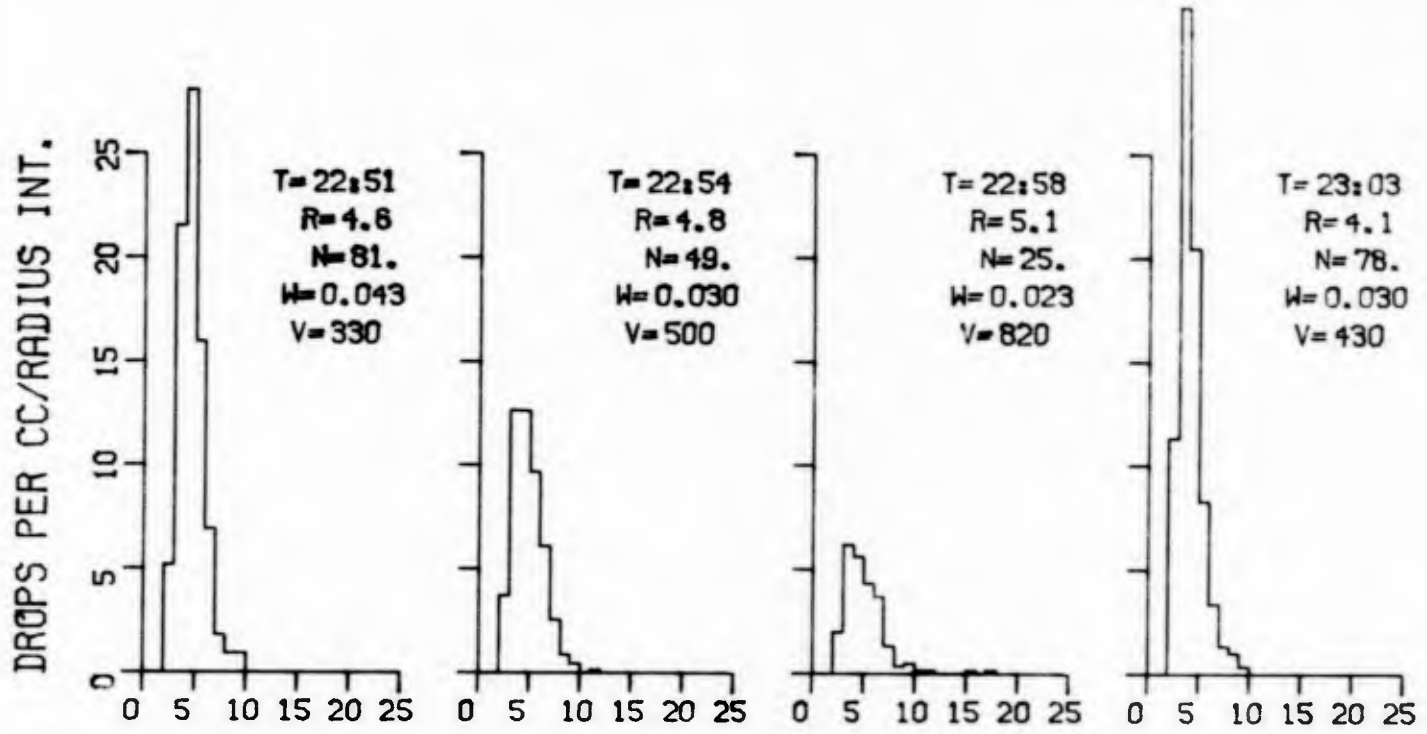

T = TIME (EDT)
R = MEAN RAD (μM)
N = CONC (CM^{-3})
W = LWC ($G\ M^{-3}$)
V = VSBY (M)

NRL CRUISE, USNS HAYES, AUGUST 1975

-- CALSPAN DATA --

FIGURE A-13. DROP SIZE DISTRIBUTIONS -- FOG 2B, 2-3 AUGUST 1975

RADIUS (MICRONS)

2AUG75 NO. 2B

FOG NO. 3A 3 AUG. 1975

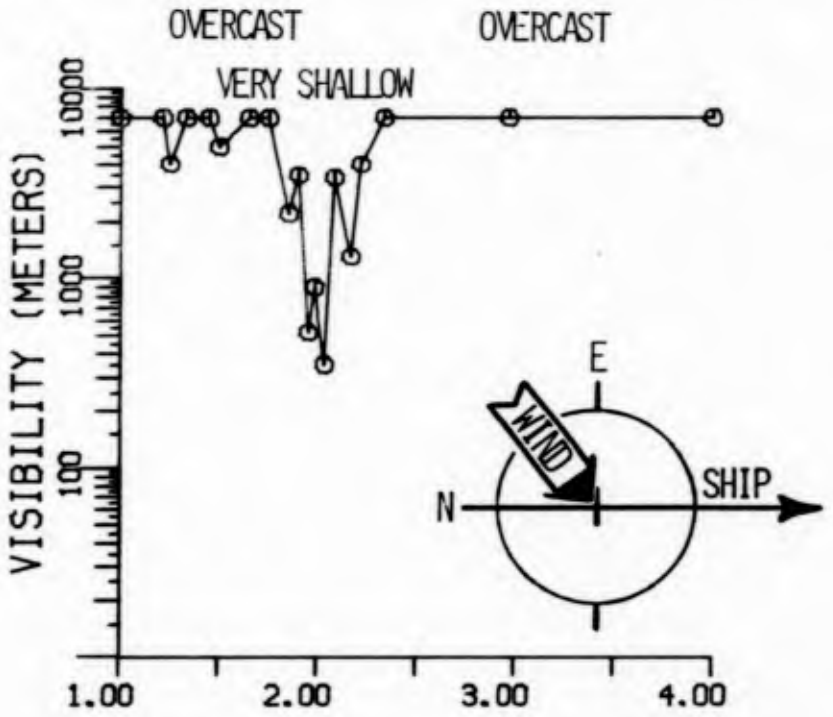

NRL CRUISE, USNS HAYES, AUGUST 1975

-- CALSPAN DATA --

FIGURE A-14. VISIBILITY vs. TIME -- FOG 3A, 3 AUGUST 1975

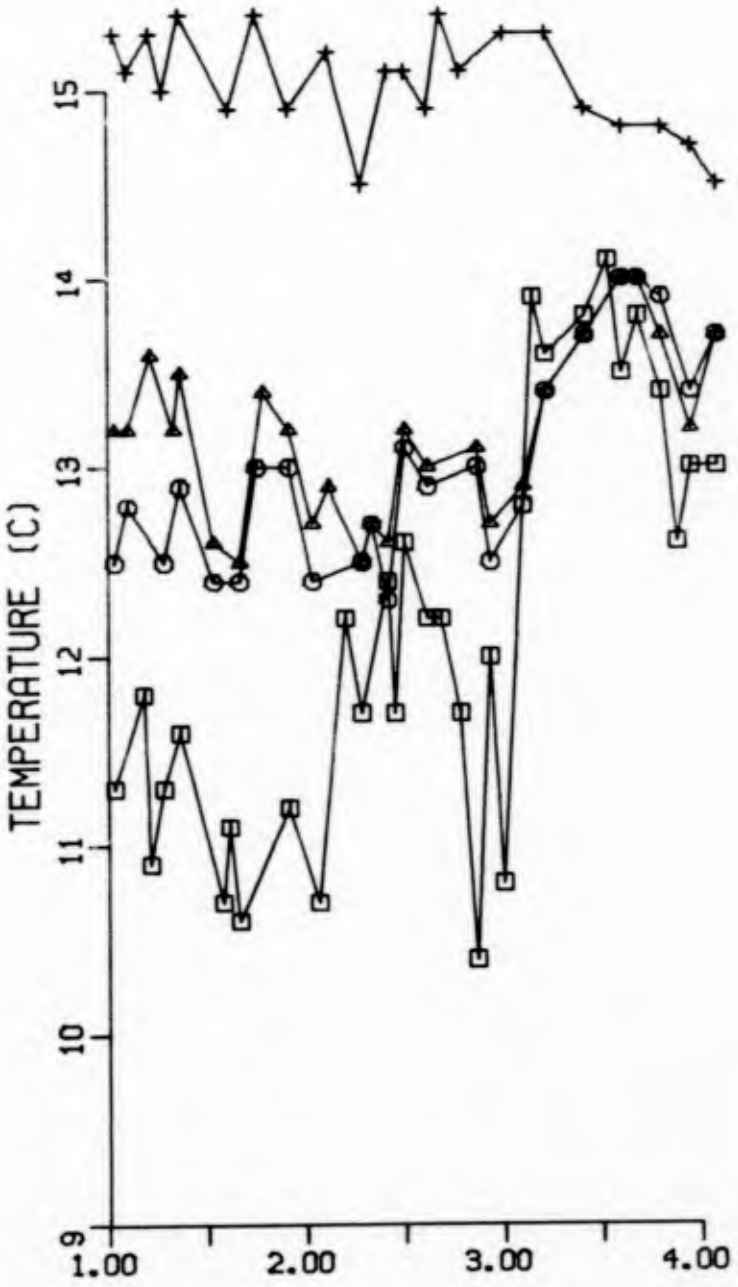

FIGURE A-15. AIR AND SEA SURFACE TEMPERATURE vs. TIME -- FOG 3A, 3 AUGUST 1975

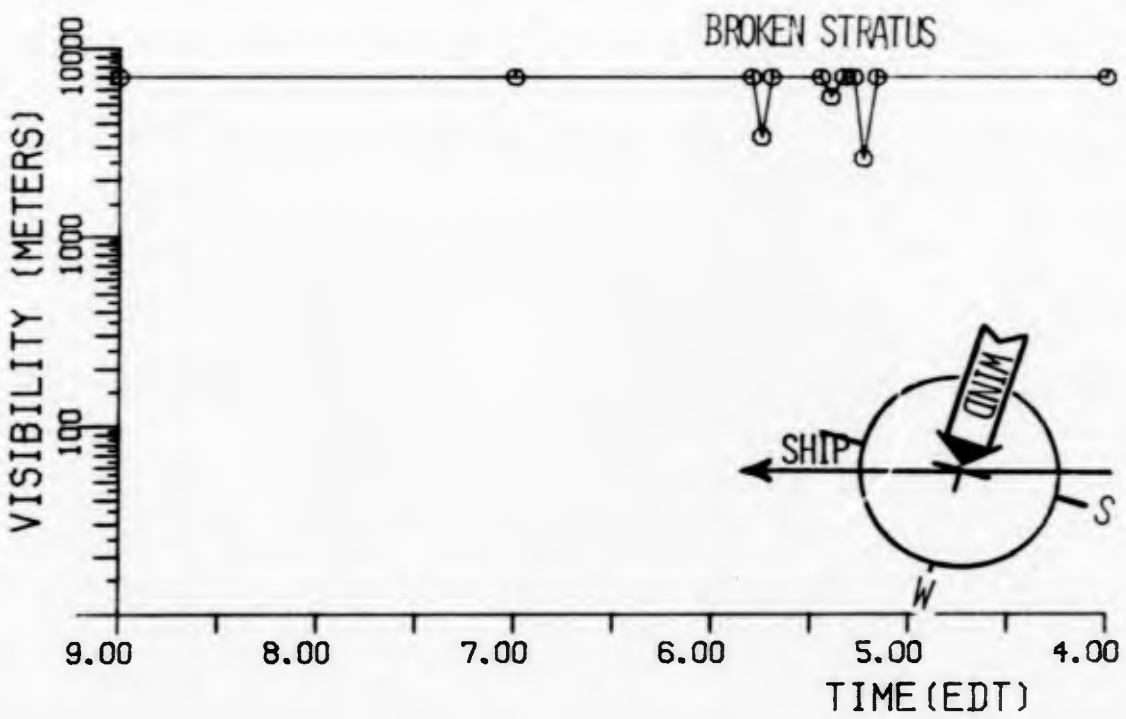

NRL CRUISE, USNS HAYES, AUGUST 1975

-- CALSPAN DATA --

FIGURE A-16. VISIBILITY vs. TIME -- FOG 3B, 3 AUGUST 1975

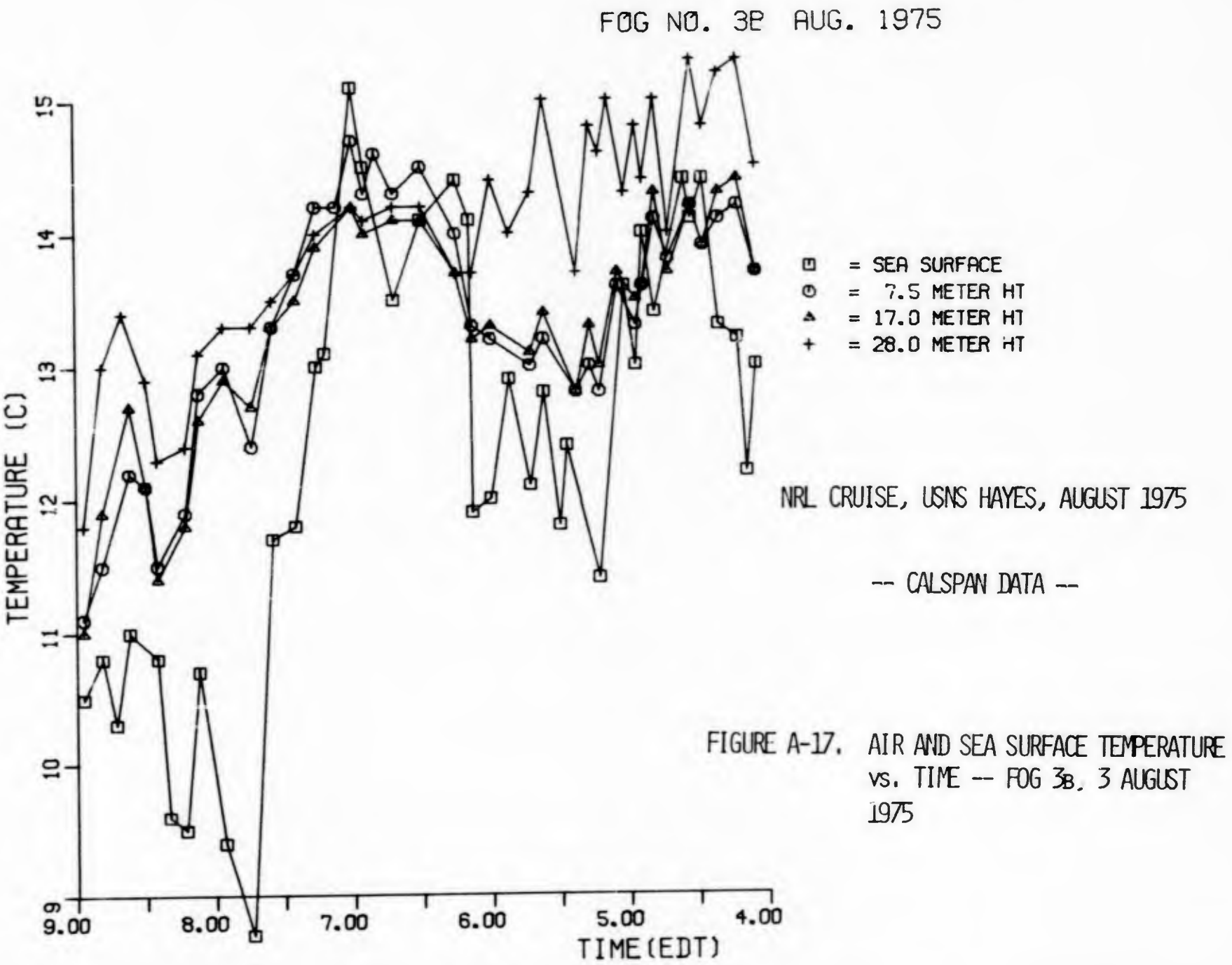

FIGURE A-17. AIR AND SEA SURFACE TEMPERATURE vs. TIME -- FOG 3B, 3 AUGUST 1975

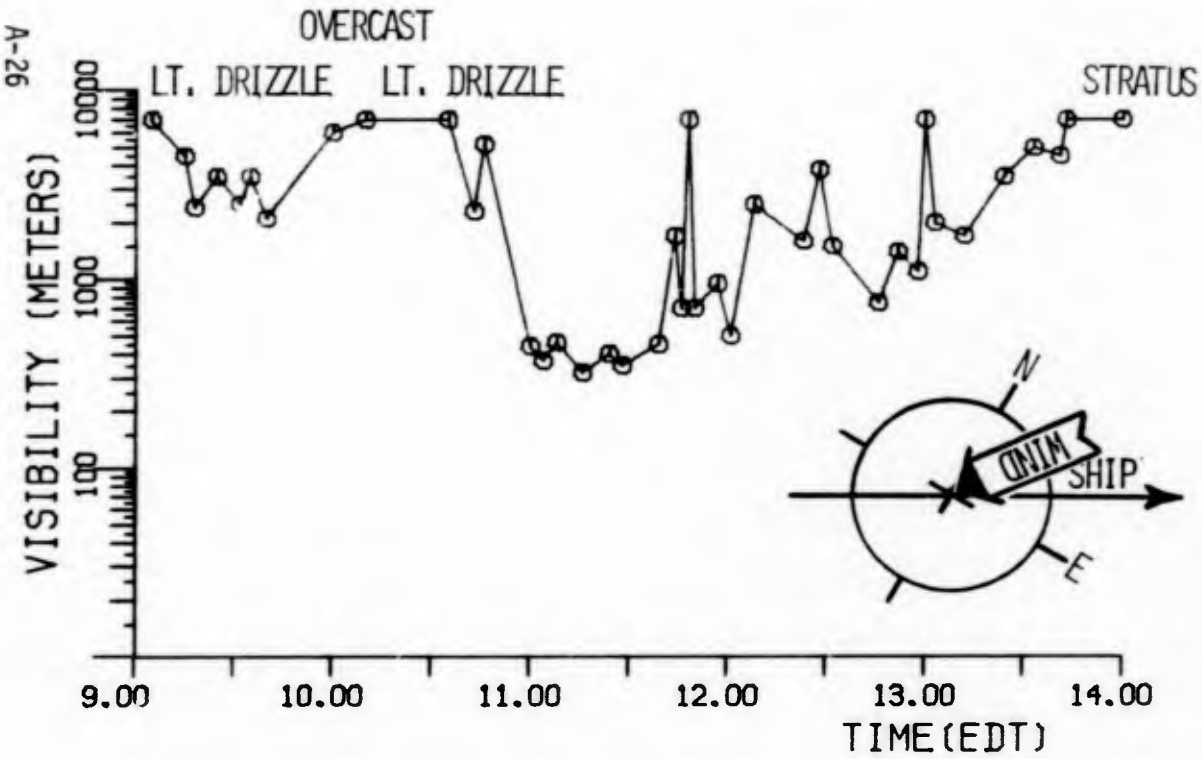

NRL CRUISE, USNS HAYES, AUGUST 1975

-- CALSPAN DATA --

FIGURE A-18. VISIBILITY vs. TIME -- FOG 2c, 3 AUGUST 1975

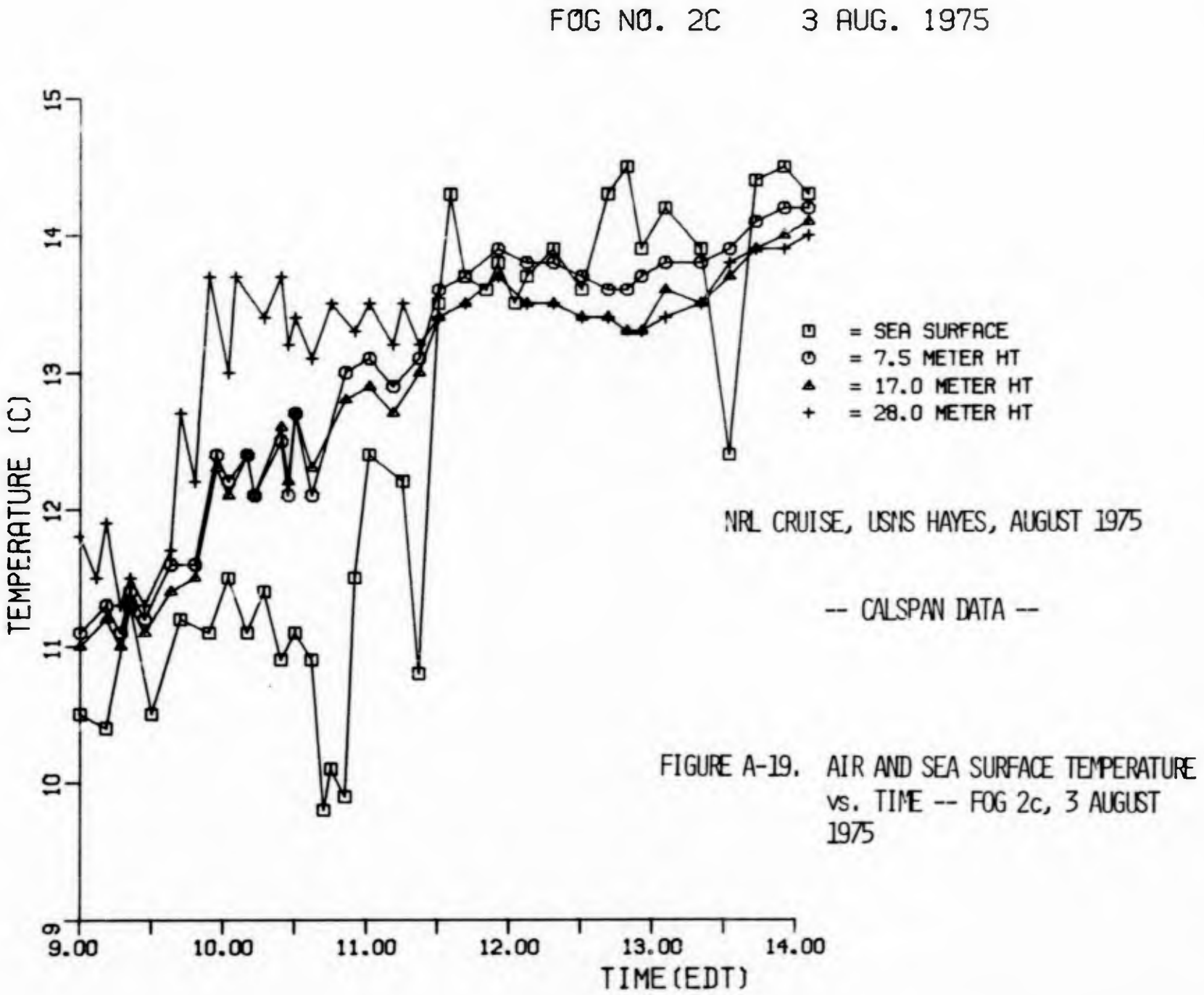

FIGURE A-19. AIR AND SEA SURFACE TEMPERATURE vs. TIME -- FOG 2c, 3 AUGUST 1975

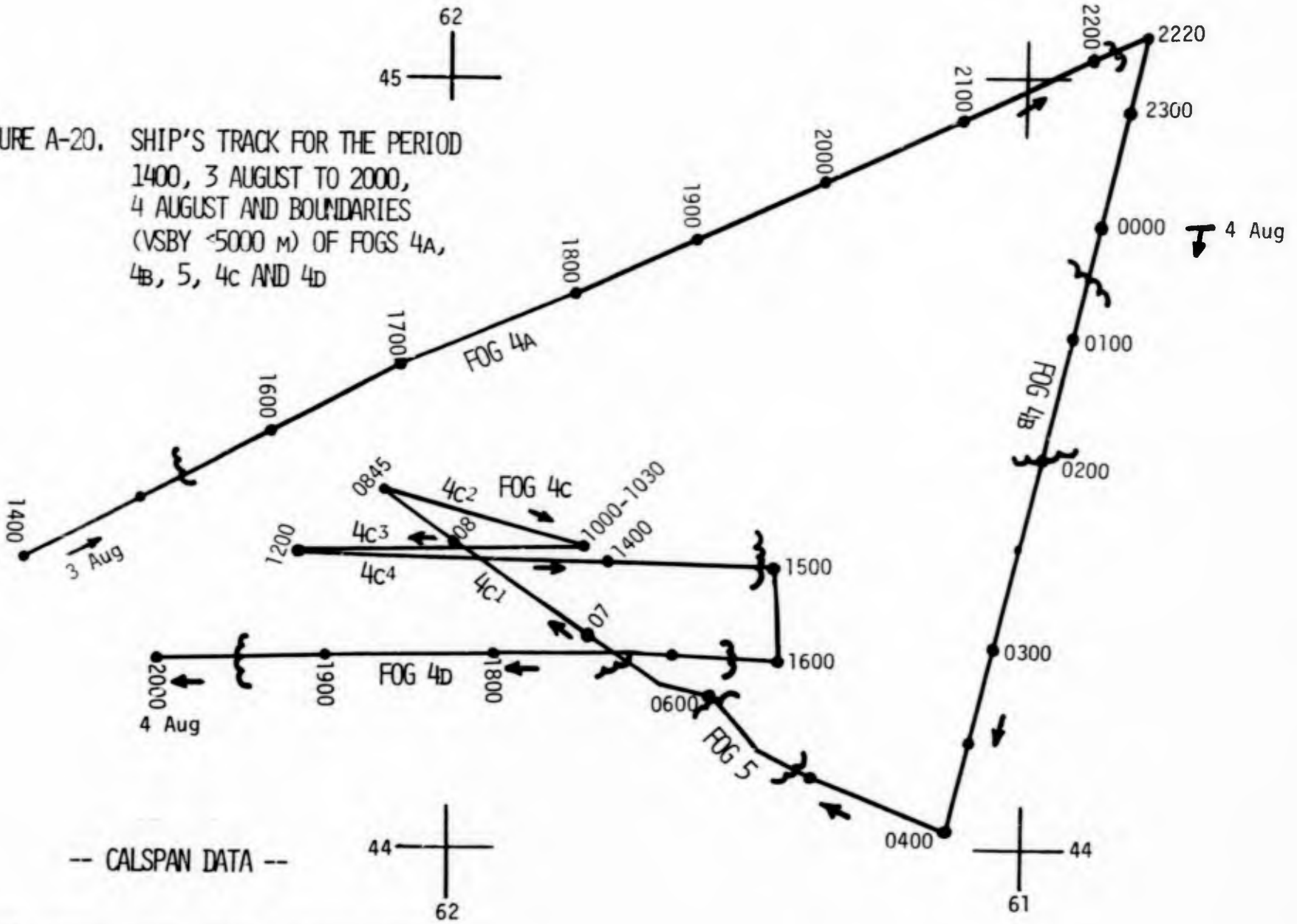

FIGURE A-20. SHIP'S TRACK FOR THE PERIOD 1400, 3 AUGUST TO 2000, 4 AUGUST AND BOUNDARIES (VSBY <5000 M) OF FOGS 4A, 4B, 5, 4C AND 4D

NRL CRUISE, USNS HAYES, AUGUST 1975

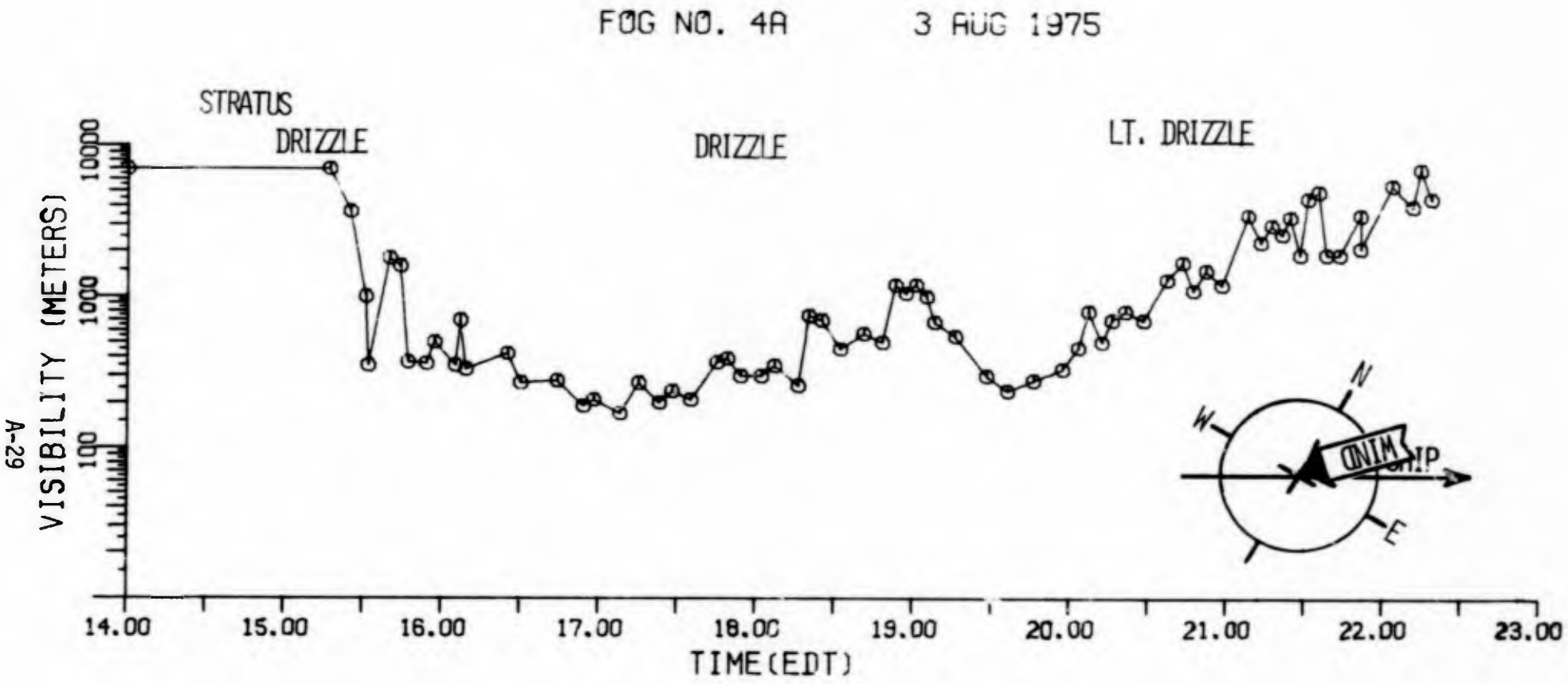

FIGURE A-21. VISIBILITY vs. TIME -- FOG 4A, 3 AUGUST 1975

NRL CRUISE, USNS HAYES, AUGUST 1975

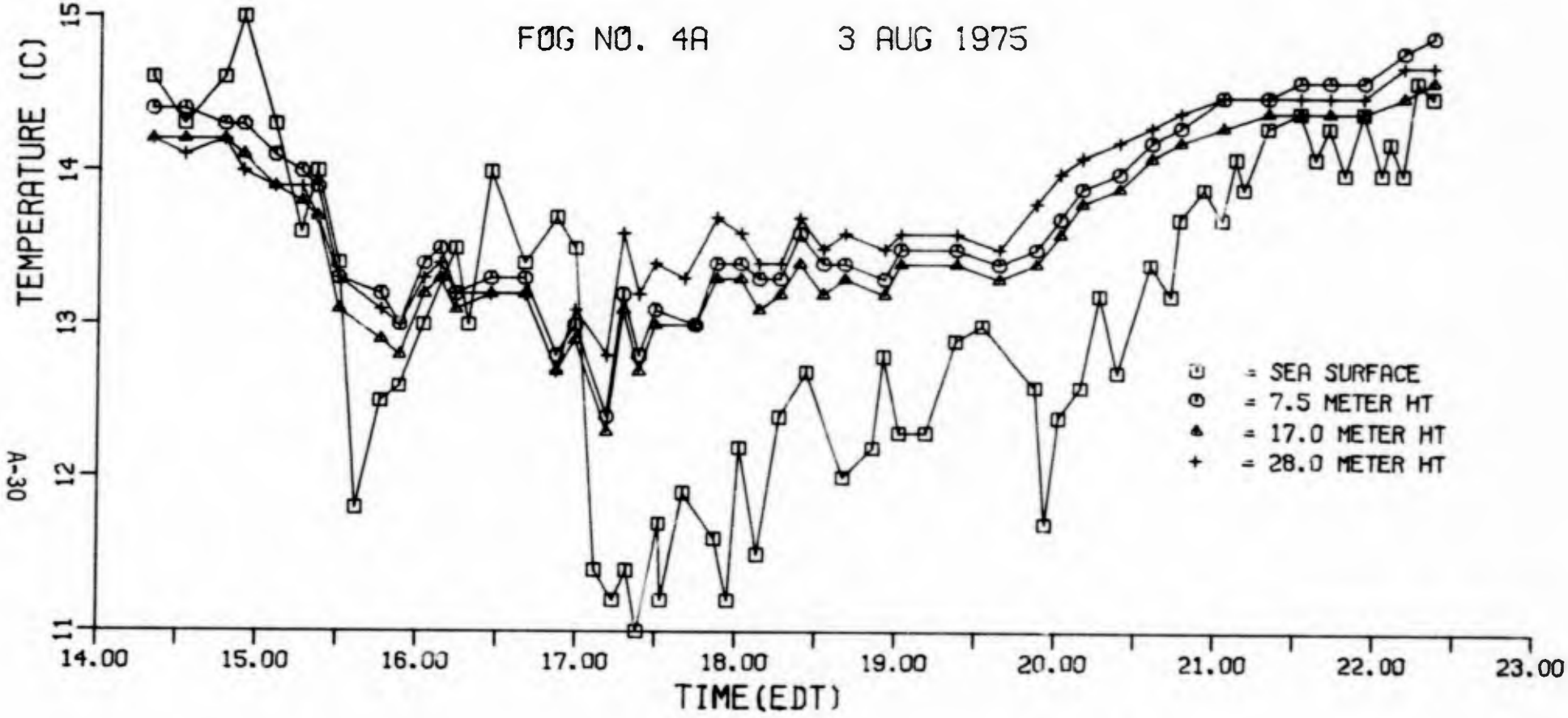

FIGURE A-22. AIR AND SEA SURFACE TEMPERATURE vs. TIME -- FOG 4A, 3 AUGUST 1975.

NRL CRUISE, USNS HAYES, AUGUST 1975

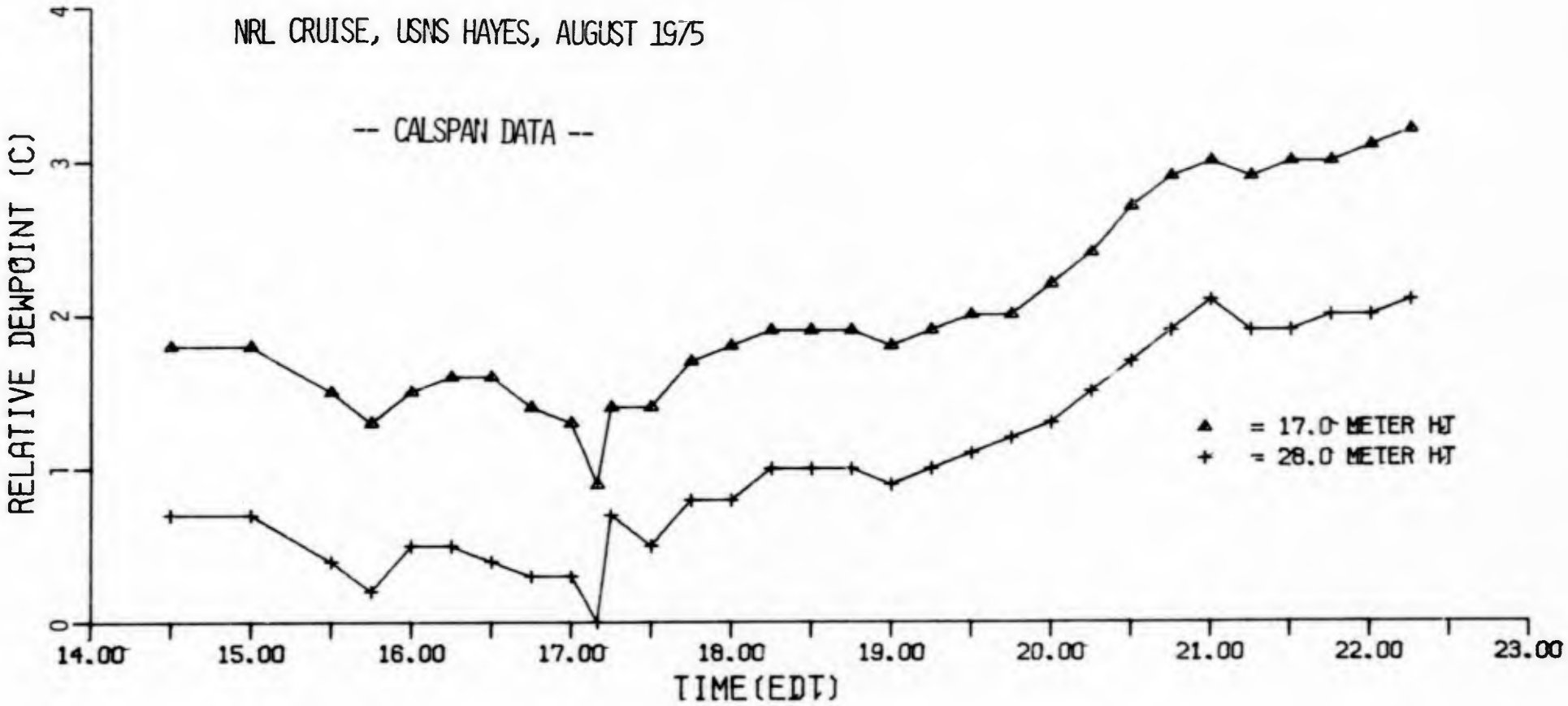

FIGURE A-23. RELATIVE DEW POINT vs. TIME --
FOG 4A, 3 AUGUST 1975

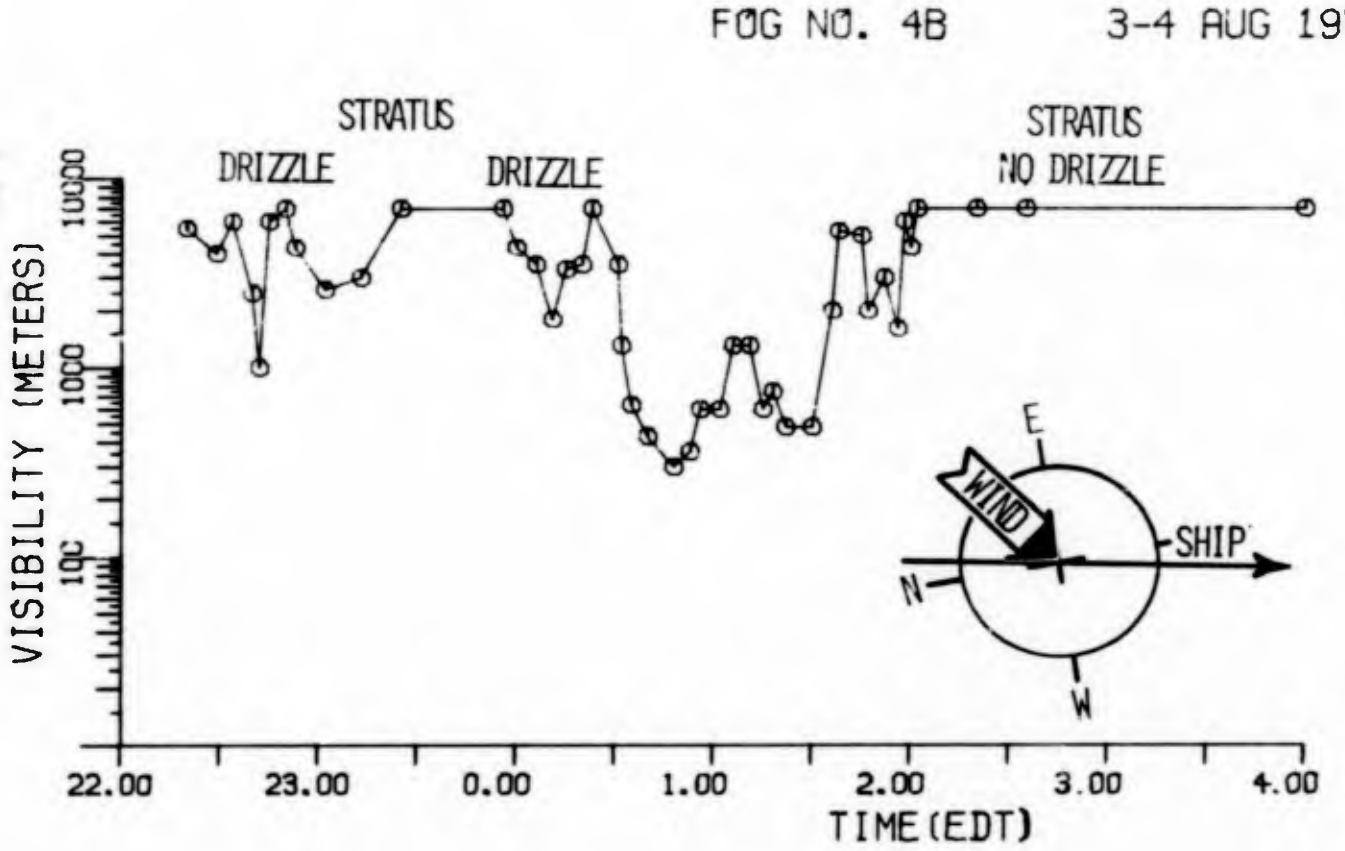

NRL CRUISE, USNS HAYES, AUGUST 1975

-- CALSPAN DATA --

FIGURE A-24. VISIBILITY vs. TIME -- FOG 4B, 3-4 AUGUST 1975

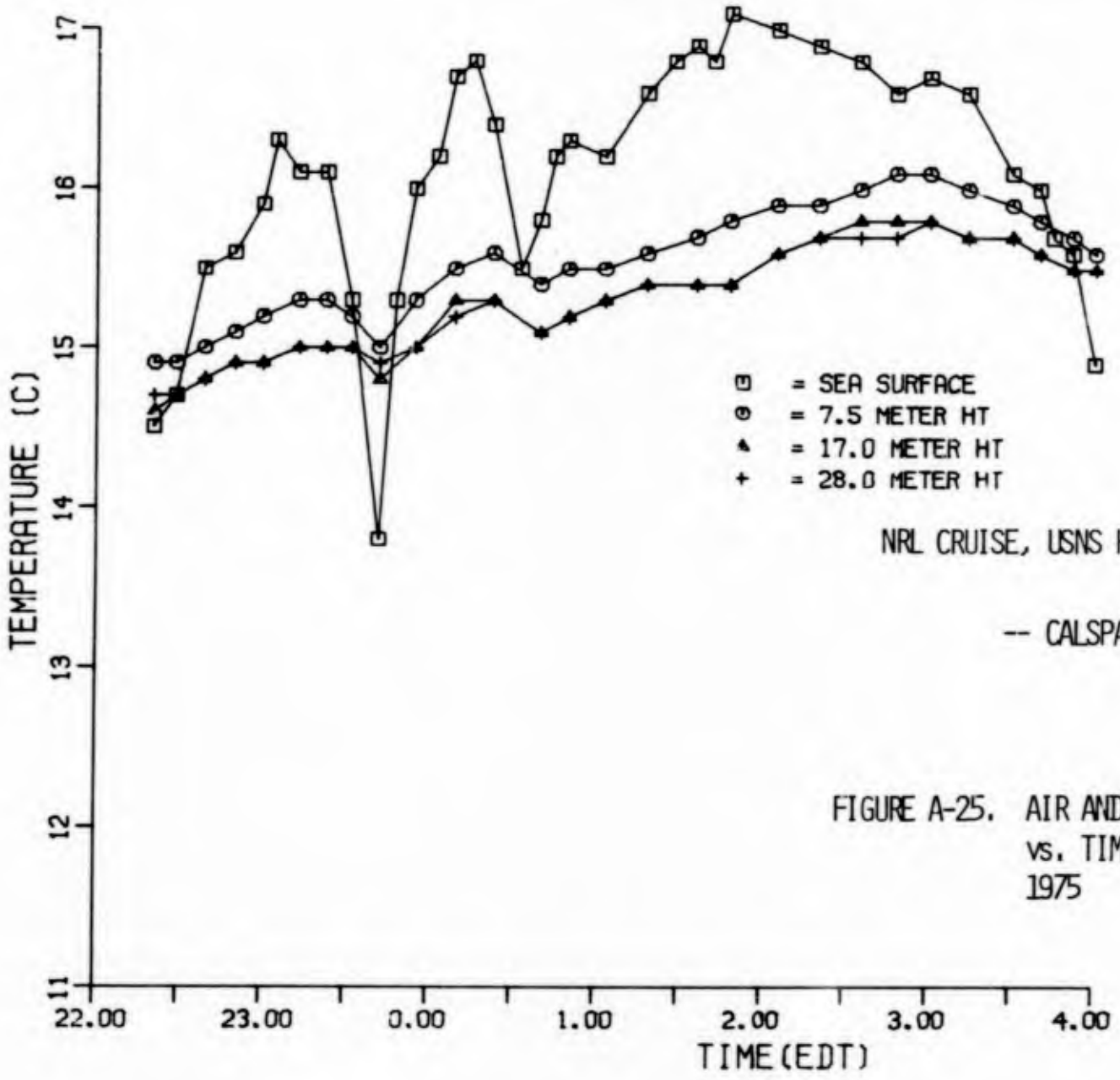

FIGURE A-25. AIR AND SEA SURFACE TEMPERATURE vs. TIME -- FOG 4B, 3-4 AUGUST 1975

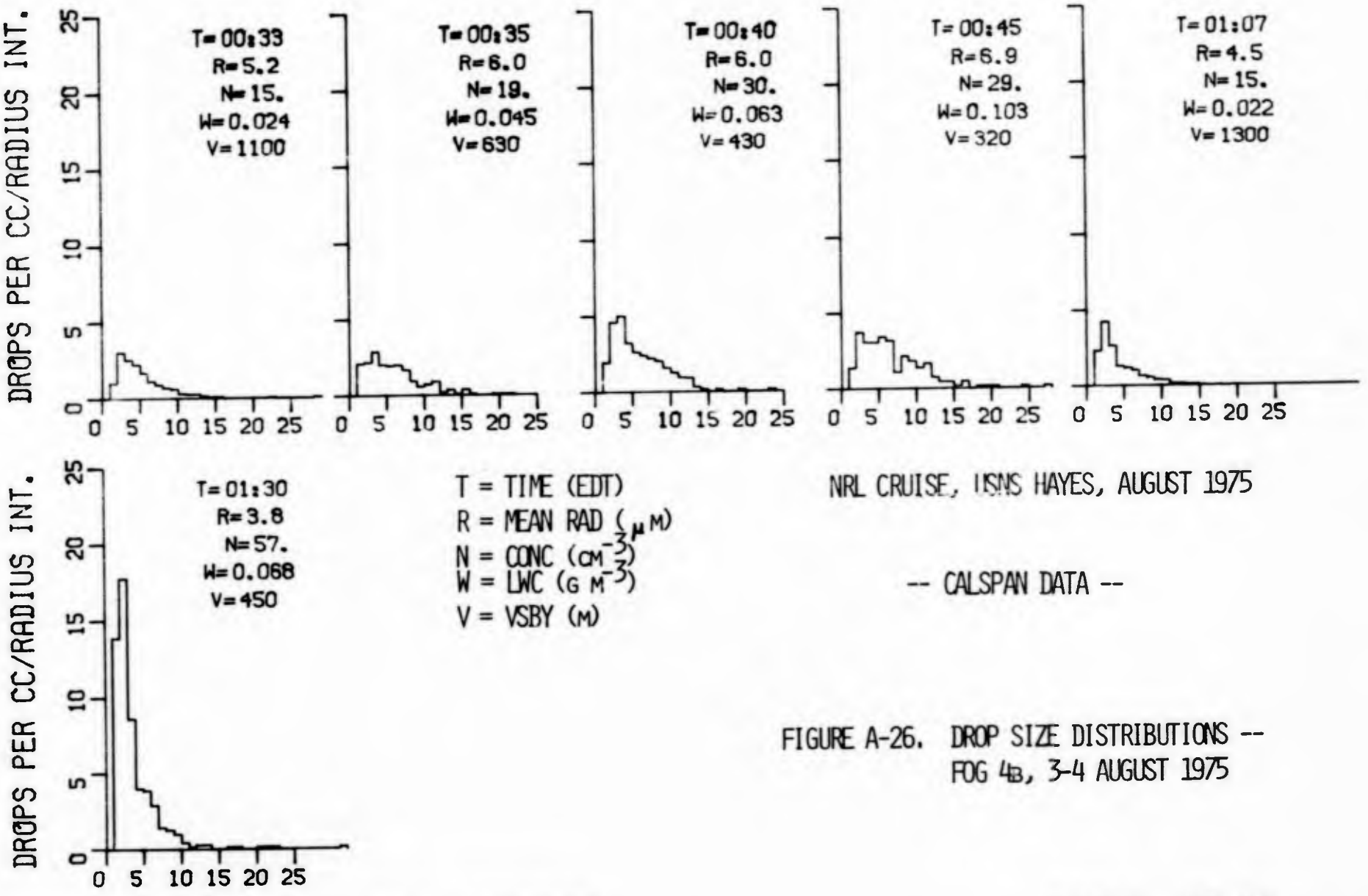

FIGURE A-26. DROP SIZE DISTRIBUTIONS -- FOG 4B, 3-4 AUGUST 1975

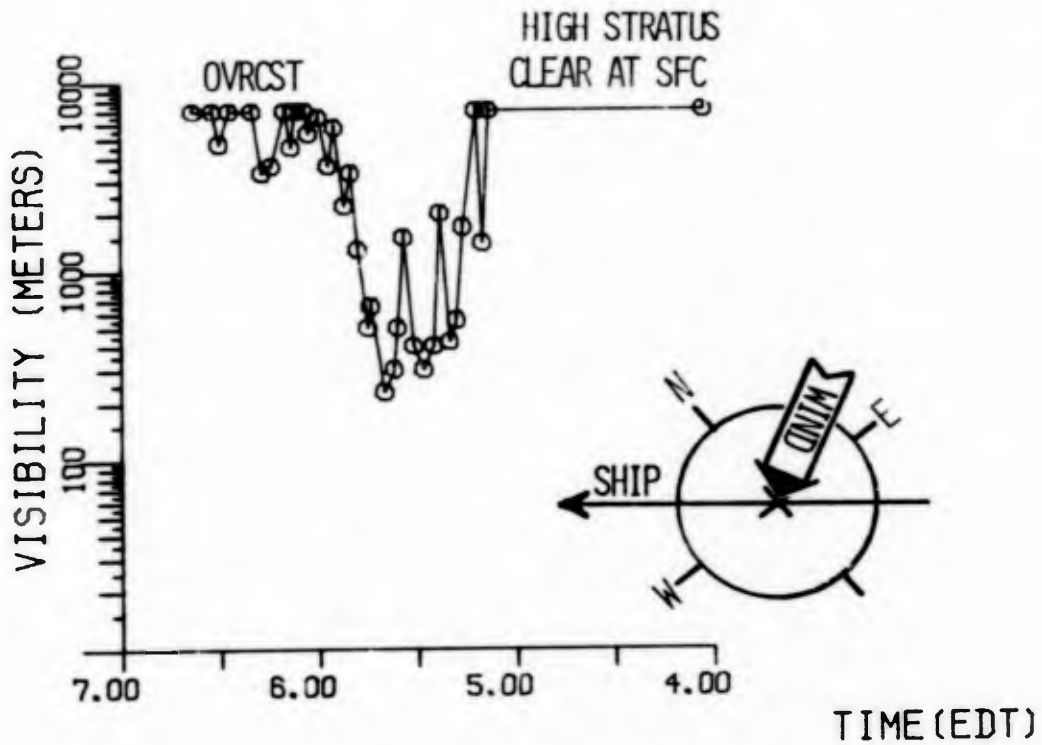

NRL CRUISE, USNS HAYES, AUGUST 1975

-- CALSPAN DATA --

FIGURE A-27. VISIBILITY vs. TIME -- FOG 5, 4 AUGUST 1975

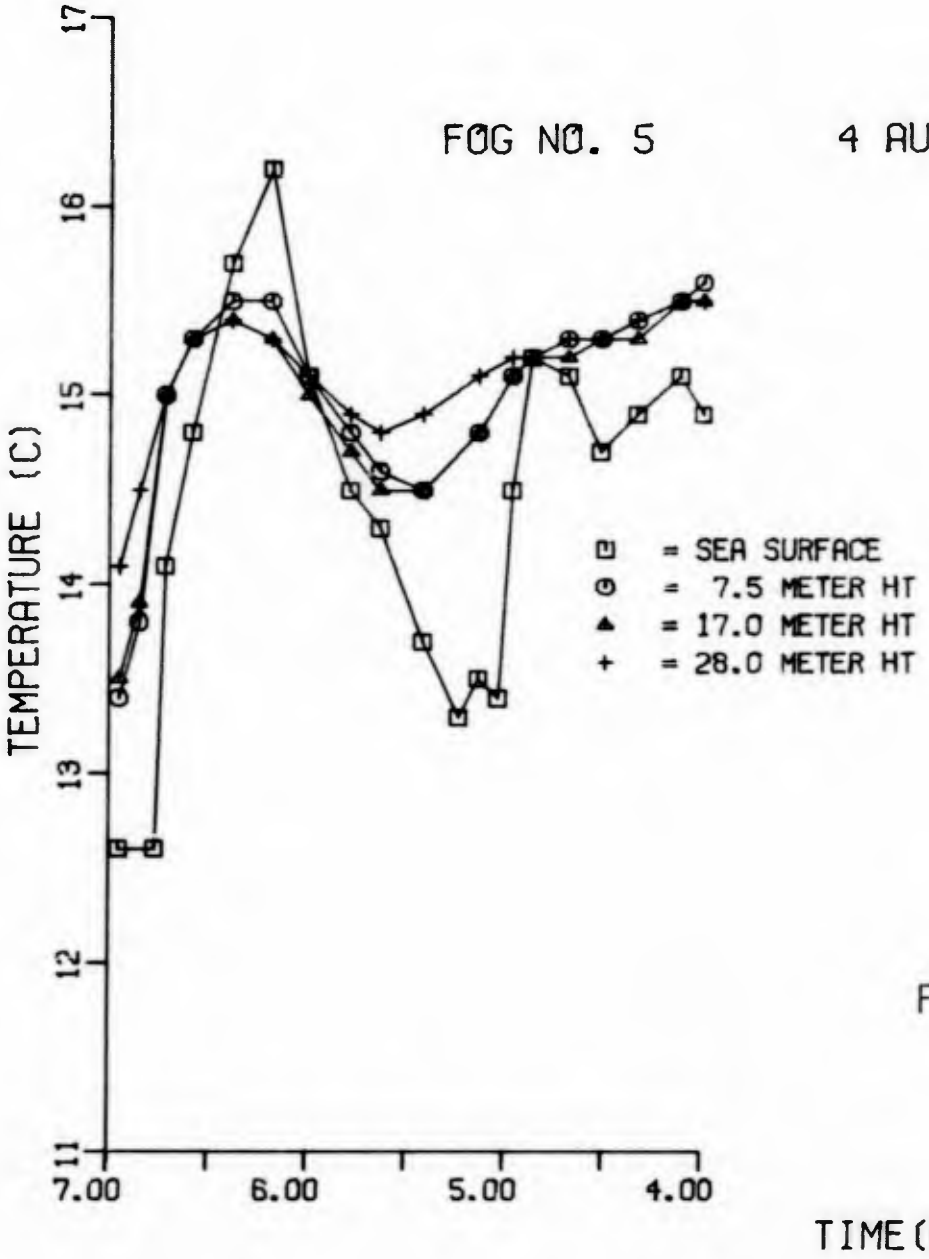

NRL CRUISE, USNS HAYES, AUGUST 1975

-- CALSPAN DATA --

FIGURE A-28. AIR AND SEA SURFACE TEMPERATURE vs. TIME -- FOG 5, 4 AUGUST 1975

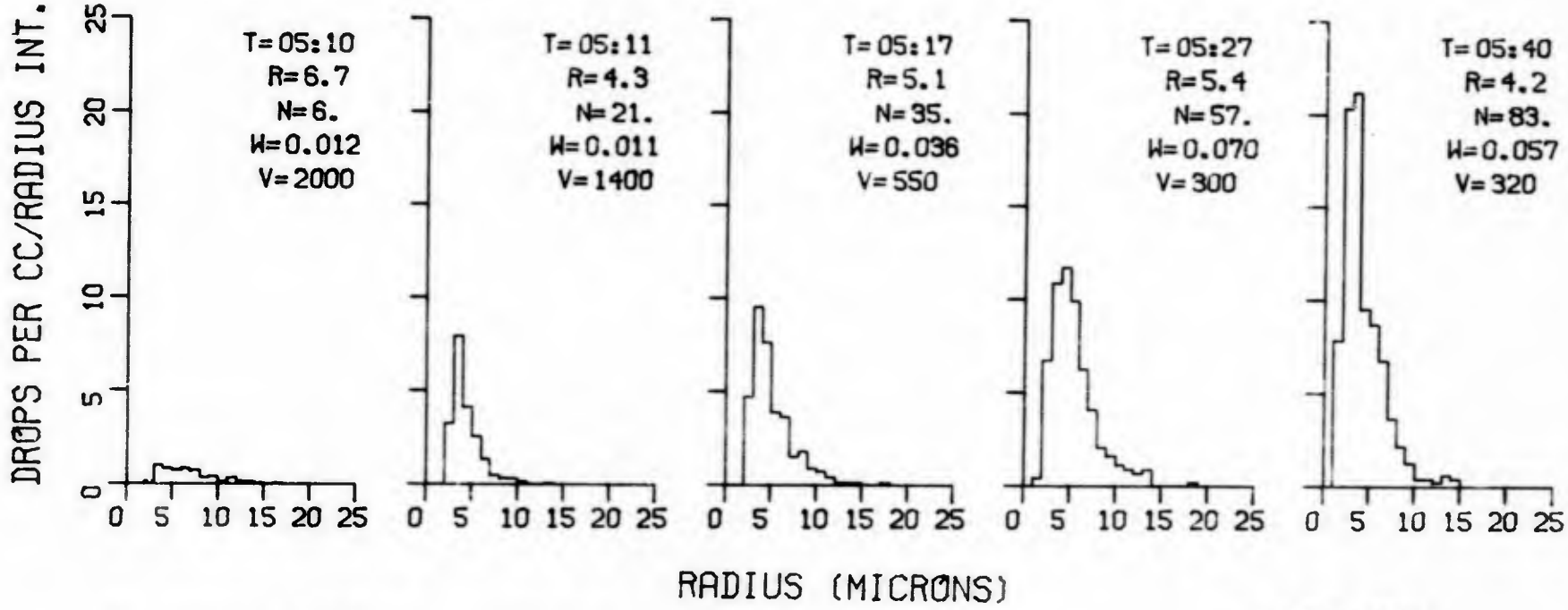

NRL CRUISE, USNS HAYES, AUGUST 1975

-- CALSPAN DATA --

T = TIME (EDT)
R = MEAN RAD (μM)
N = CONC (cm^{-3})
W = LWC ($g\ m^{-3}$)
V = VSBY (M)

FIGURE A-29. DROP SIZE DISTRIBUTIONS -- FOG 5, 4 AUGUST 1975

FOG NO. 4C1 4 AUG 1975

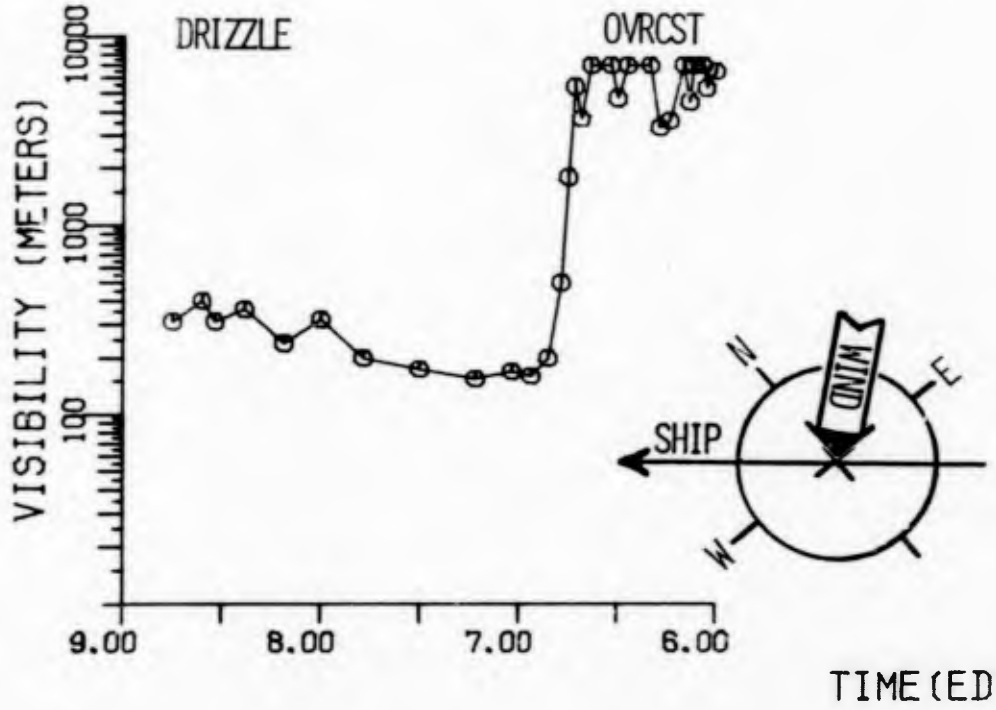

NRL CRUISE, USNS HAYES, AUGUST 1975

-- CALSPAN DATA --

FIGURE A-30. VISIBILITY vs. TIME -- FOG $4c_1$, 4 AUGUST 1975

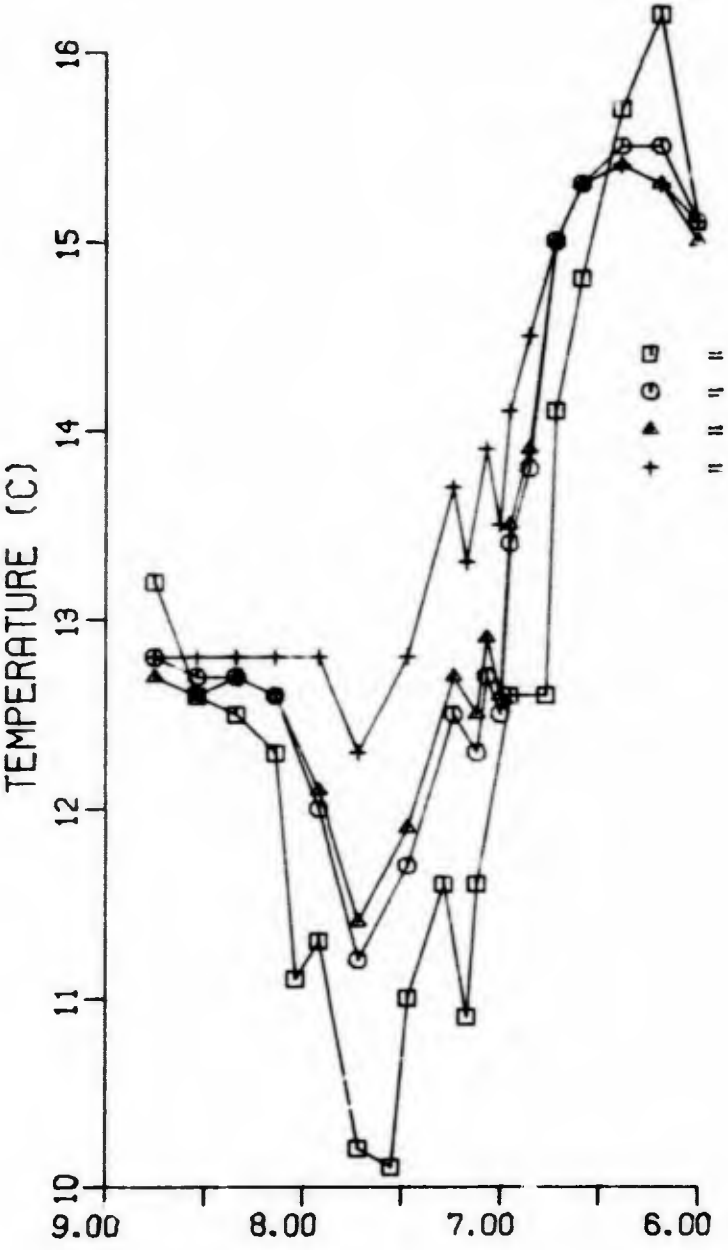

FIGURE A-31. AIR AND SEA SURFACE TEMPERATURE vs. TIME -- FOG $4c_1$, 4 AUGUST 1975

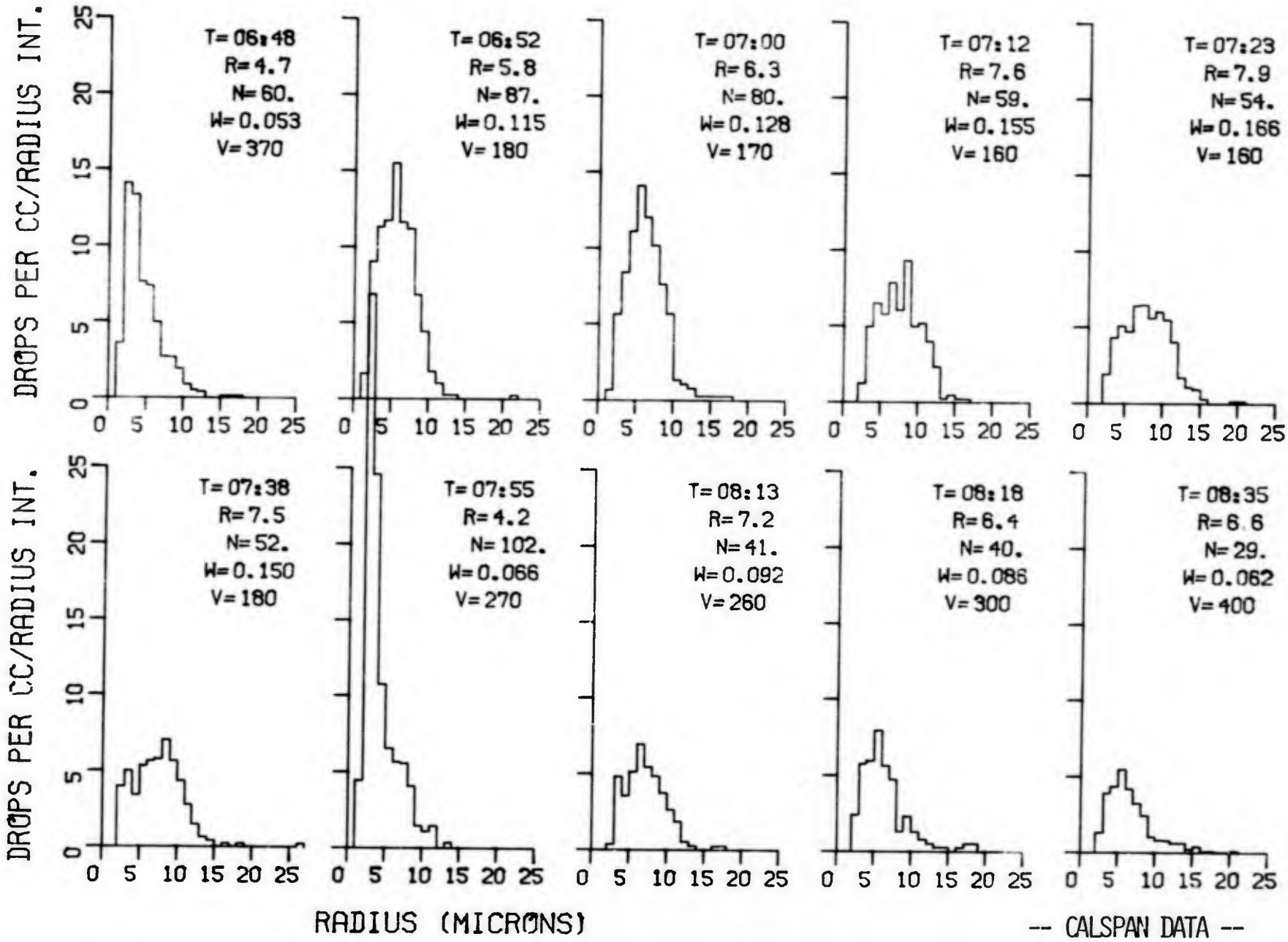

FIGURE A-32. DROP SIZE DISTRIBUTIONS -- FOG $4c_1$, 4 AUGUST 1975

NRL CRUISE, USNS HAYES, AUGUST 1975

4 AUG 1975

FOG NO. 4C2

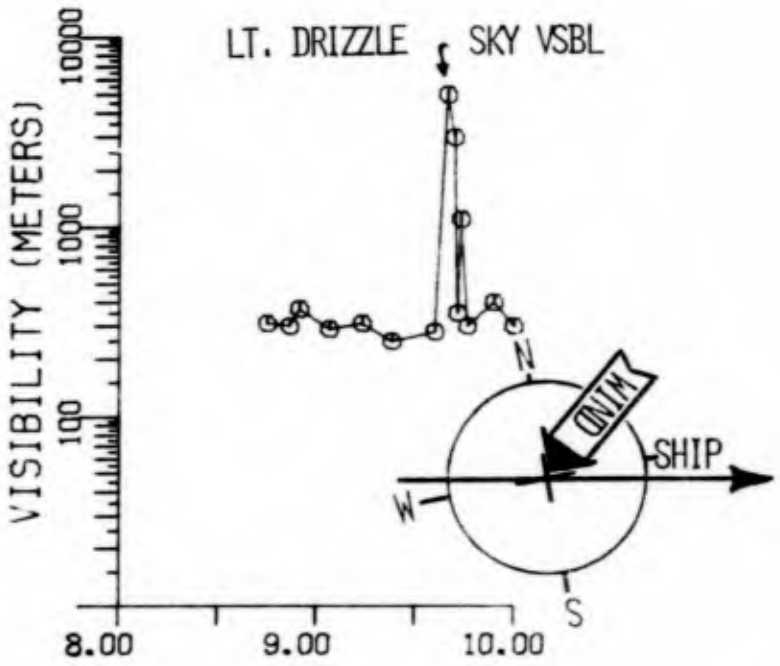

FOG NO. 4C3

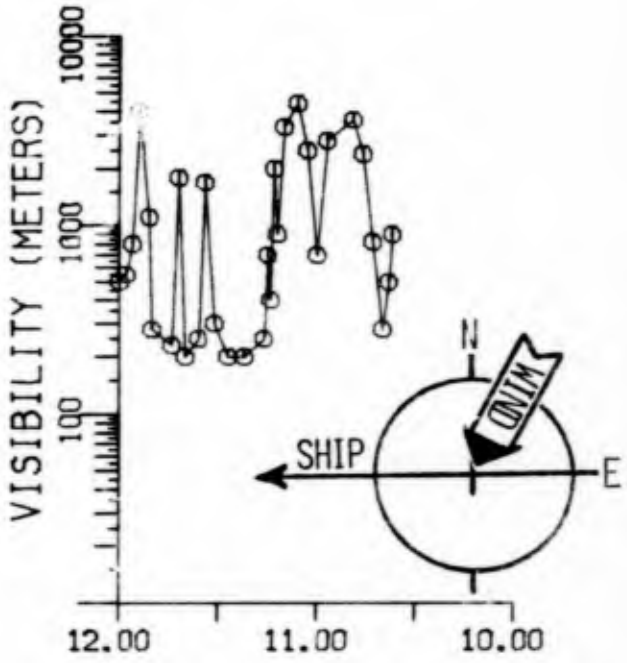

TIME (EDT)

NRL CRUISE, USNS HAYES, AUGUST 1975

FIGURE A-33. VISIBILITY VS. TIME -- FOGS $4c_2$ AND $4c_3$, 4 AUGUST 1975

-- CALSPAN DATA --

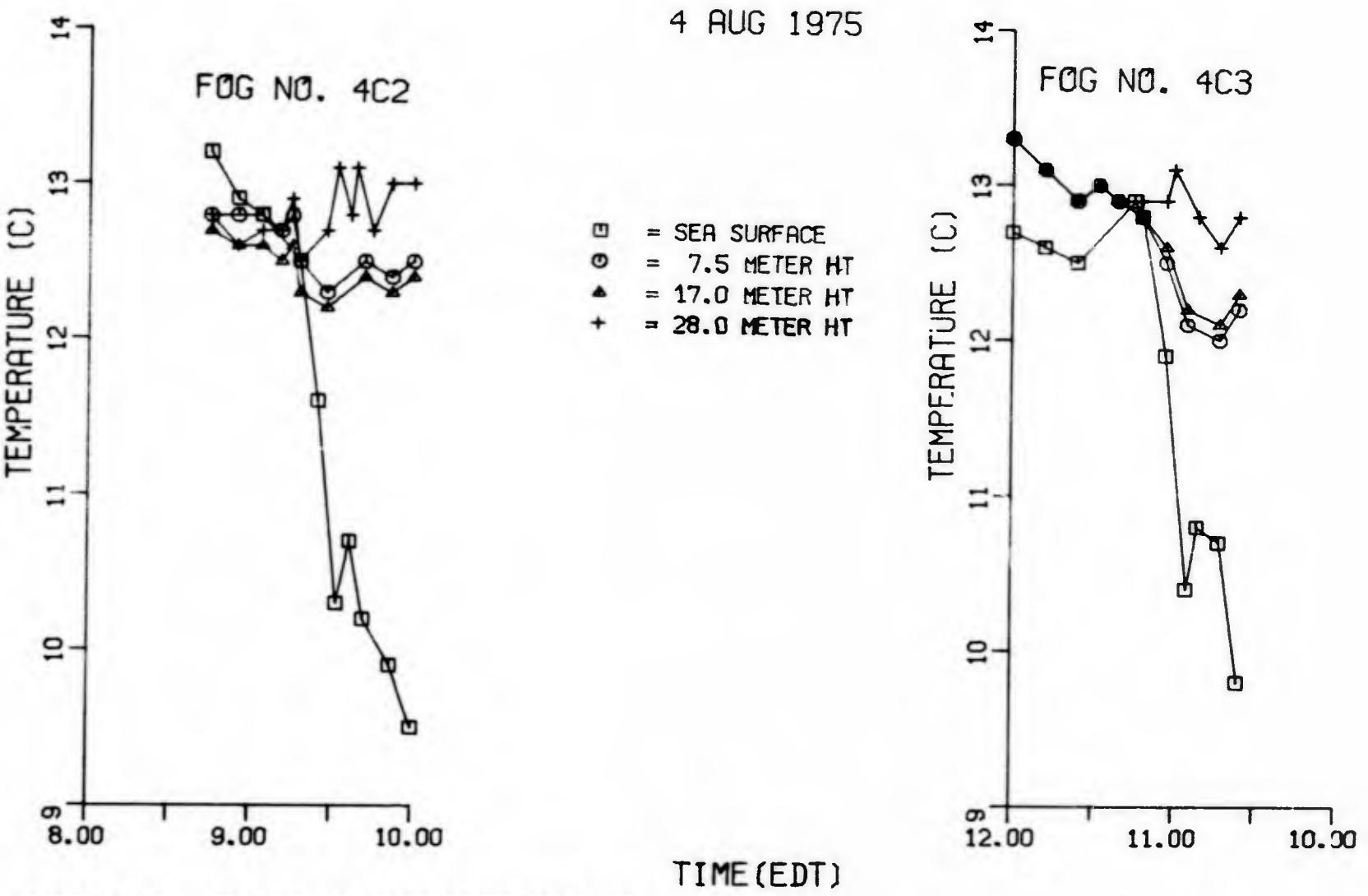

FIGURE A-34. AIR AND SEA SURFACE TEMPERATURE vs. TIME -- FOGS $4c_2$ AND $4c_3$, 4 AUGUST 1975

NRL CRUISE, USNS HAYES, AUGUST 1975

-- CALSPAN DATA --

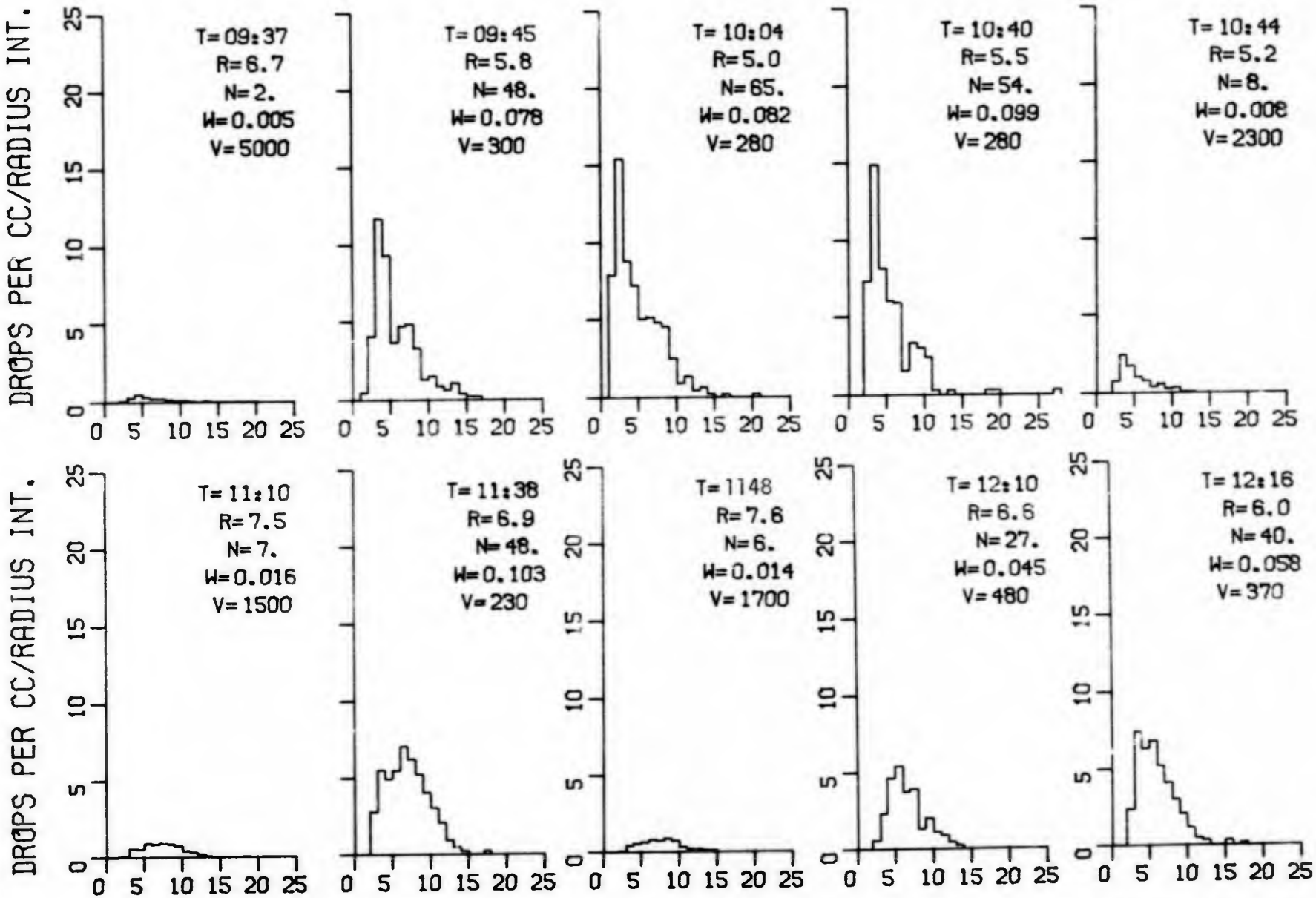

FIGURE A-35. DROP SIZE DISTRIBUTIONS -- FOGS $4c_2$, $4c_3$, AND $4c_4$, 4 AUGUST 1975

-- CALSPAN DATA --

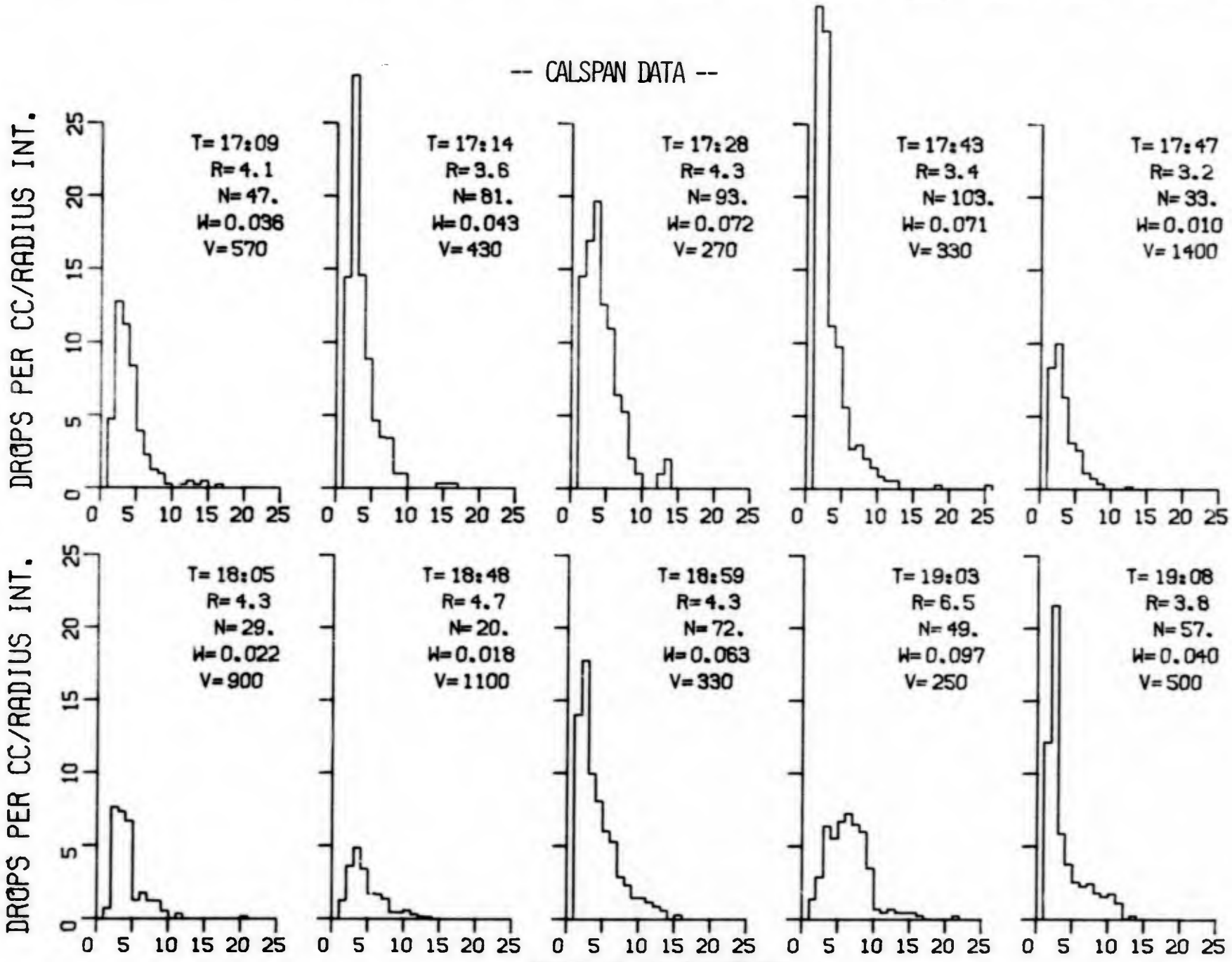

FIGURE A-40. DROP SIZE DISTRIBUTIONS -- FOG 4D, 4 AUGUST 1975

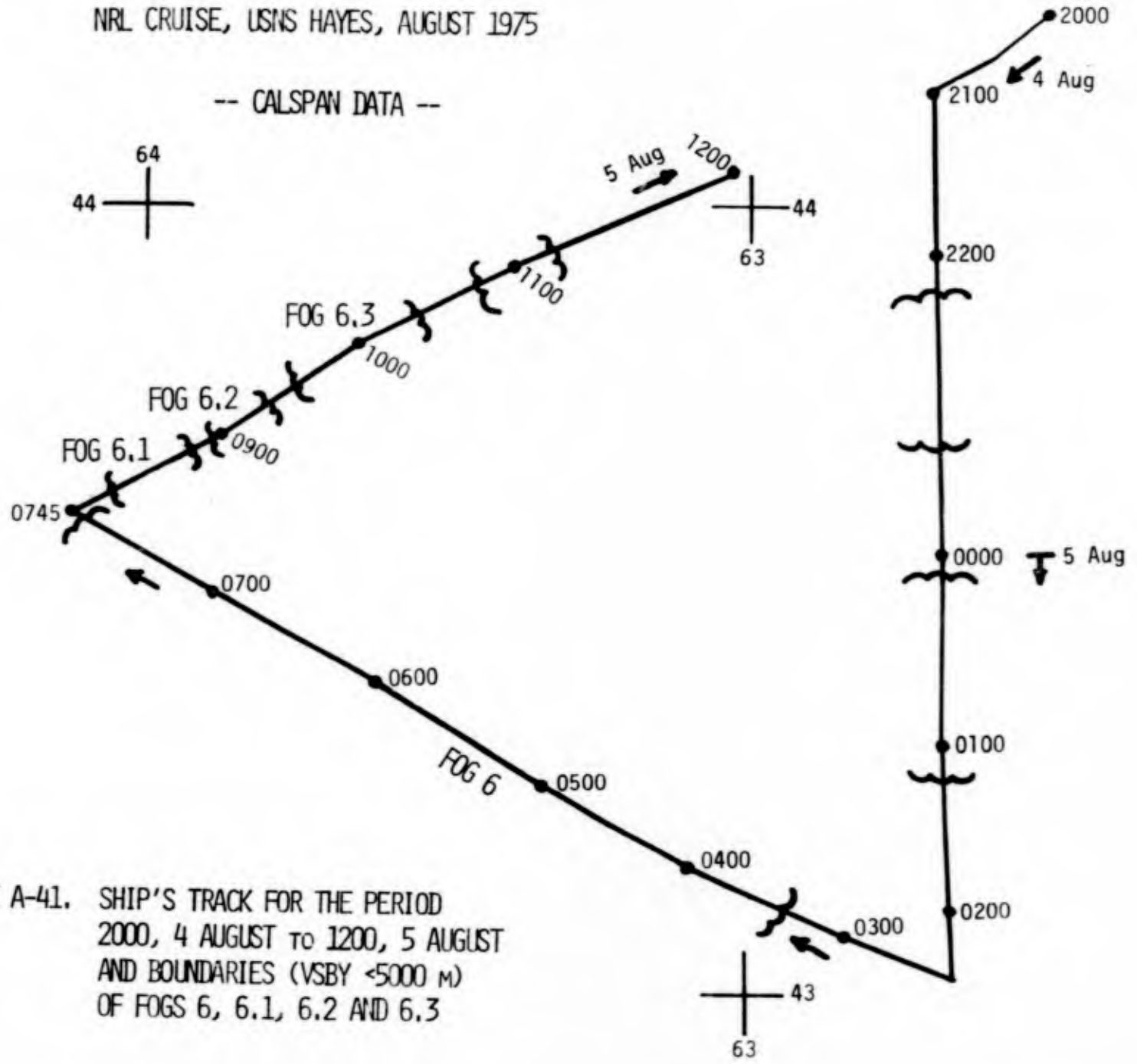

FIGURE A-41. SHIP'S TRACK FOR THE PERIOD 2000, 4 AUGUST TO 1200, 5 AUGUST AND BOUNDARIES (VSBY <5000 M) OF FOGS 6, 6.1, 6.2 AND 6.3

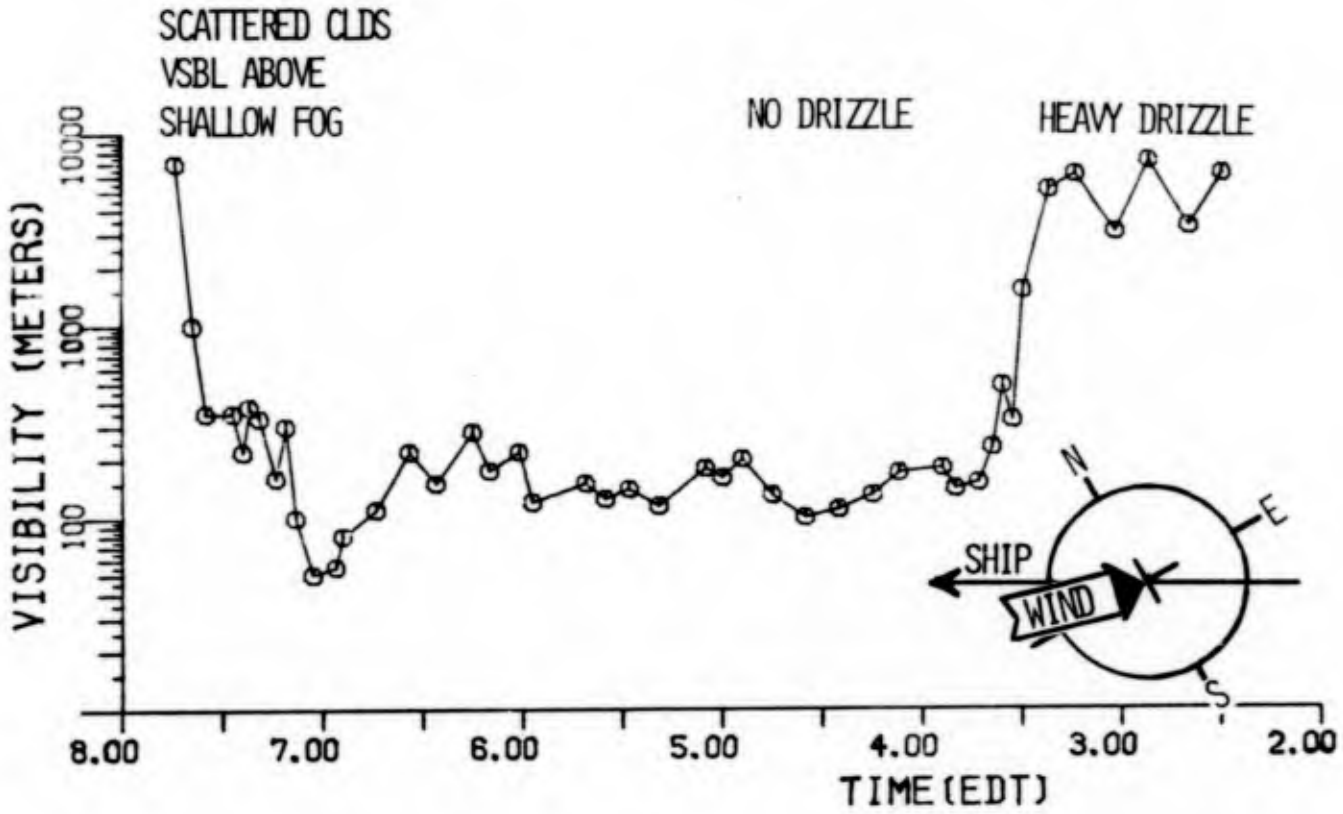

NRL CRUISE, USNS HAYES, AUGUST 1975

FIGURE A-42. VISIBILITY vs. TIME --
FOG 6, 5 AUGUST 1975

-- CALSPAN DATA --

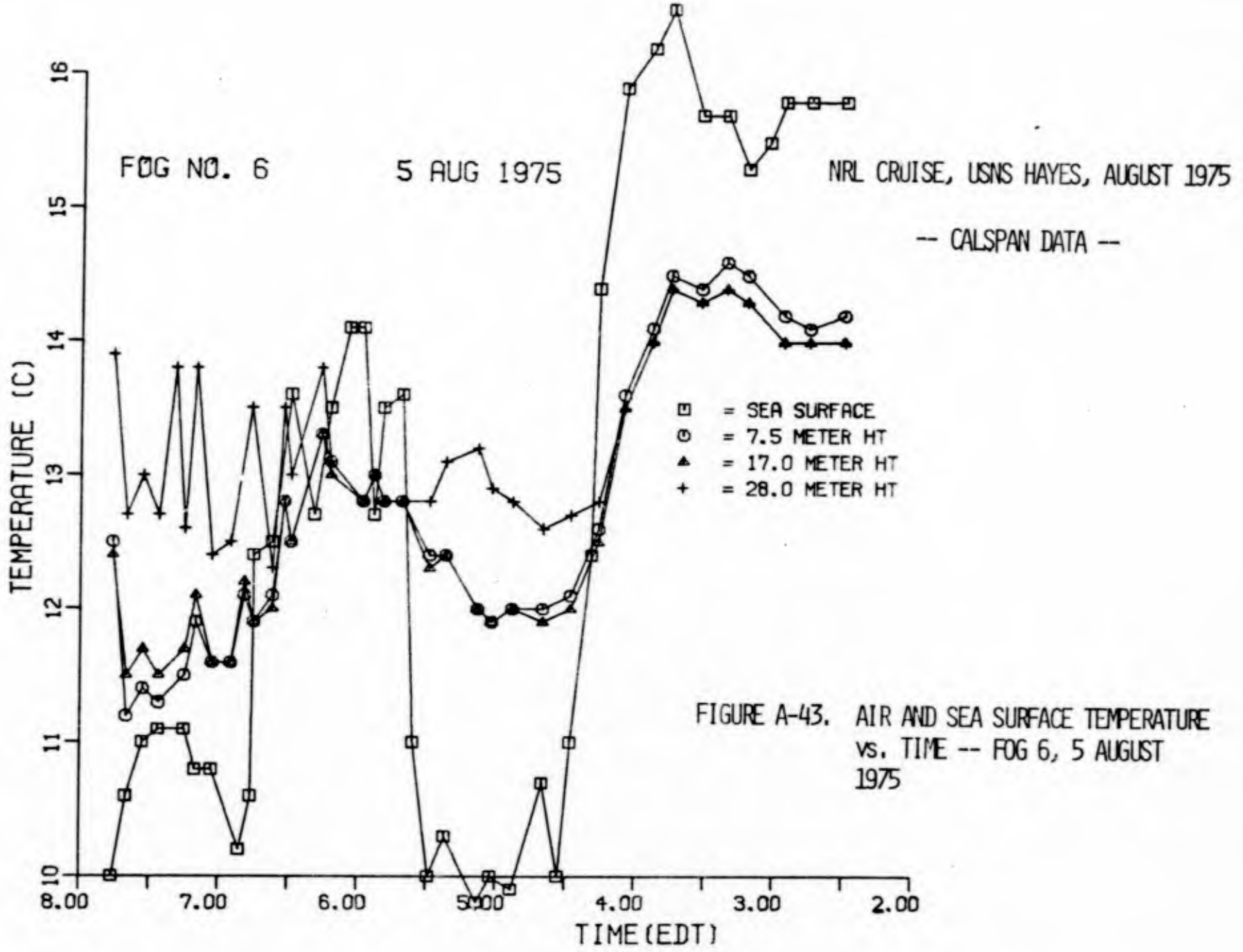

FIGURE A-43. AIR AND SEA SURFACE TEMPERATURE vs. TIME -- FOG 6, 5 AUGUST 1975

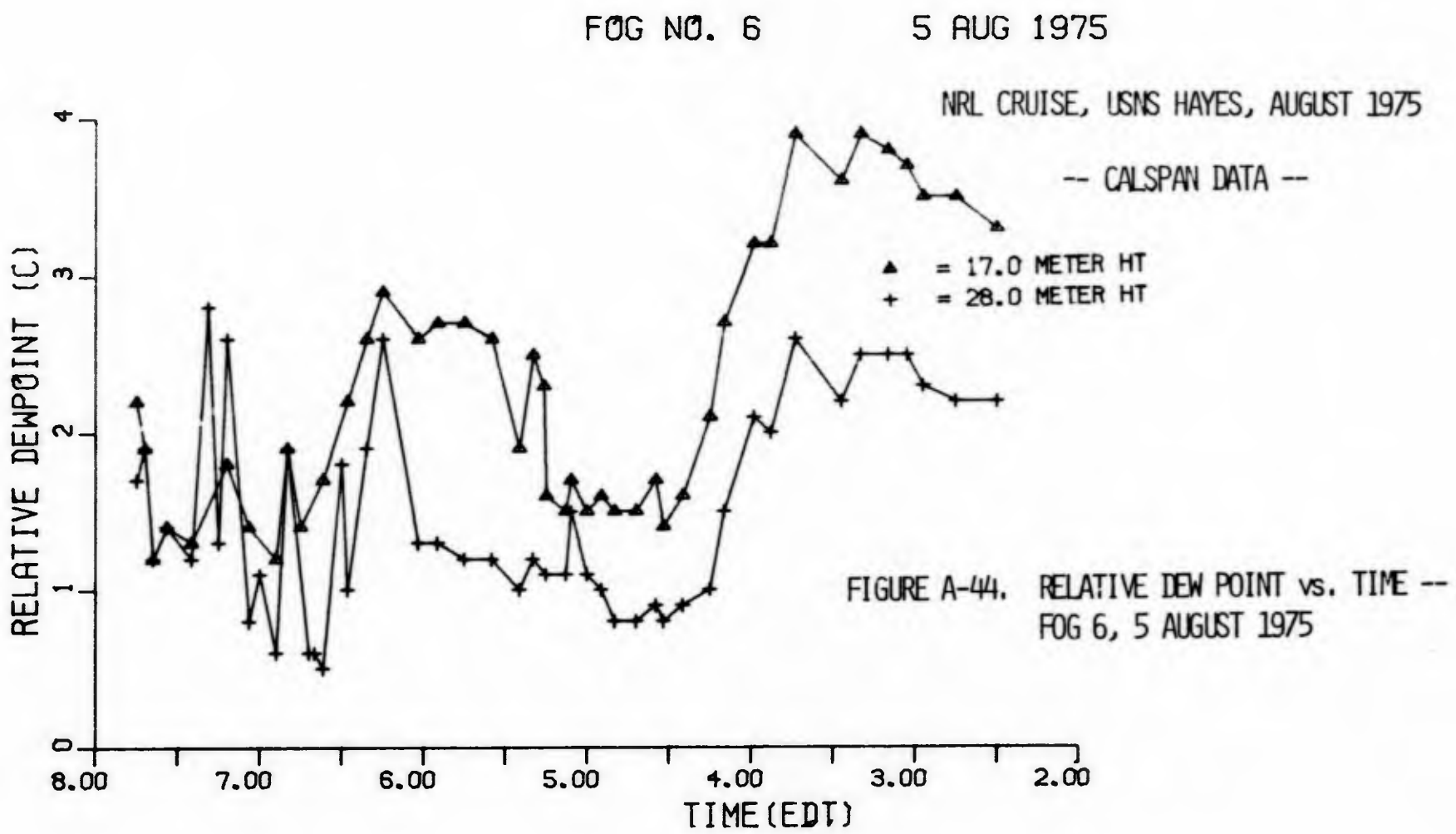

FIGURE A-44. RELATIVE DEW POINT vs. TIME -- FOG 6, 5 AUGUST 1975

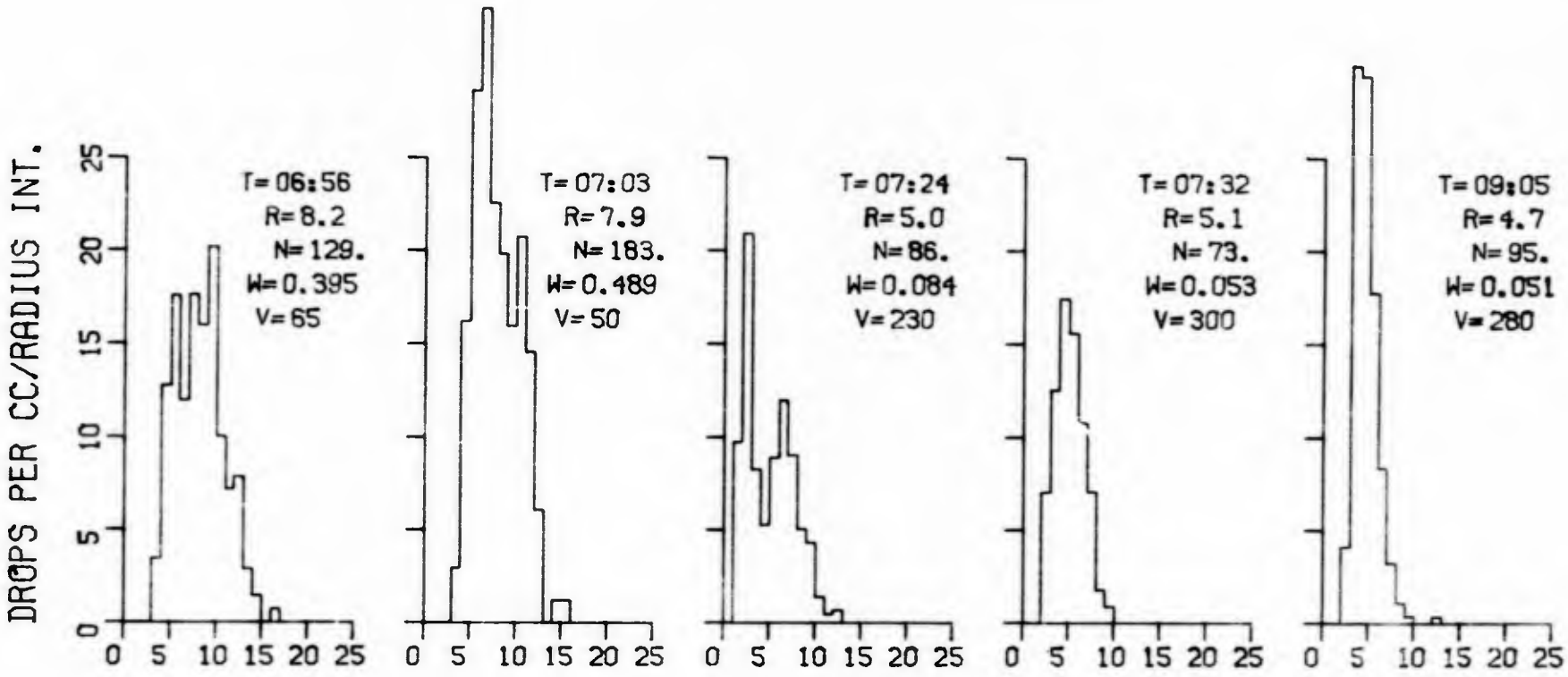

T = TIME (EDT)
R = MEAN RAD (μM)
N = CONC (CM^{-3})
W = LWC ($G\ M^{-3}$)
V = VSBY (M)

NRL CRUISE, USNS HAYES, AUGUST 1975

-- CALSPAN DATA --

FIGURE A-45. DROP SIZE DISTRIBUTIONS -- FOG 6, 5 AUGUST 1975

FOG NO. 6.1-6.3 5 AUG 1975

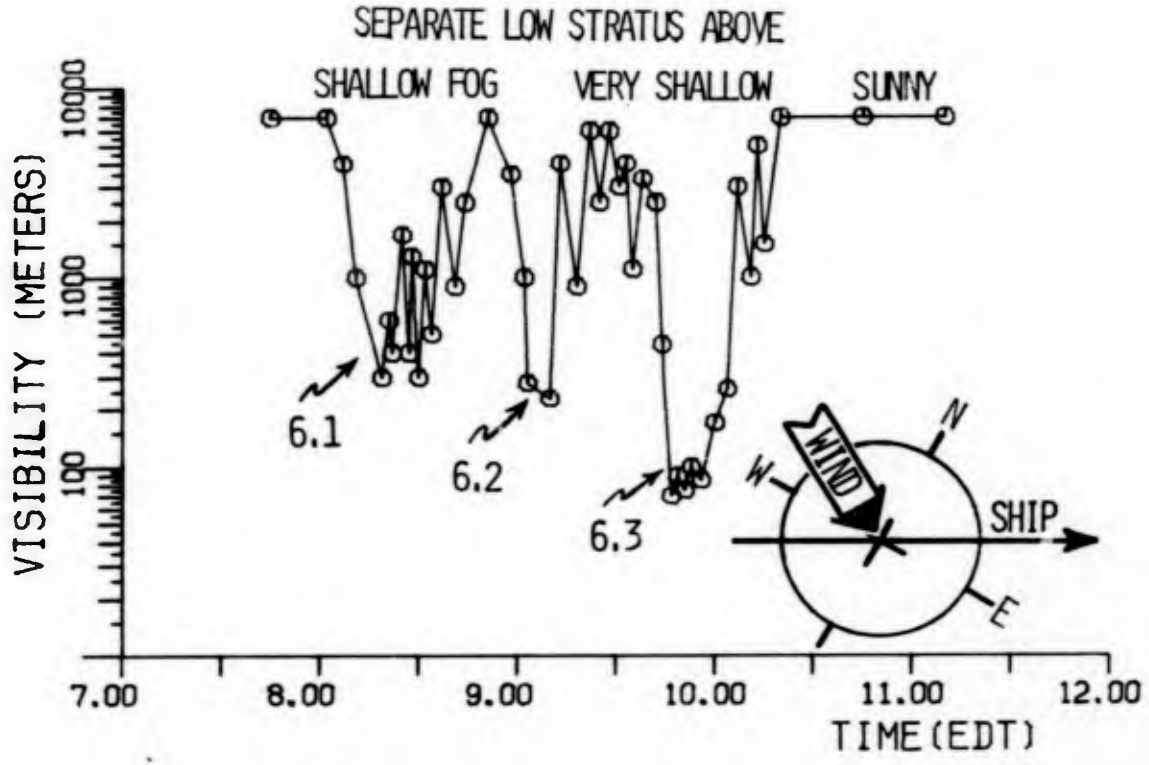

NRL CRUISE, USNS HAYES, AUGUST 1975

-- CALSPAN DATA --

FIGURE A-46. VISIBILITY vs. TIME -- FOGS 6.1, 6.2 AND 6.3, 5 AUGUST 1975

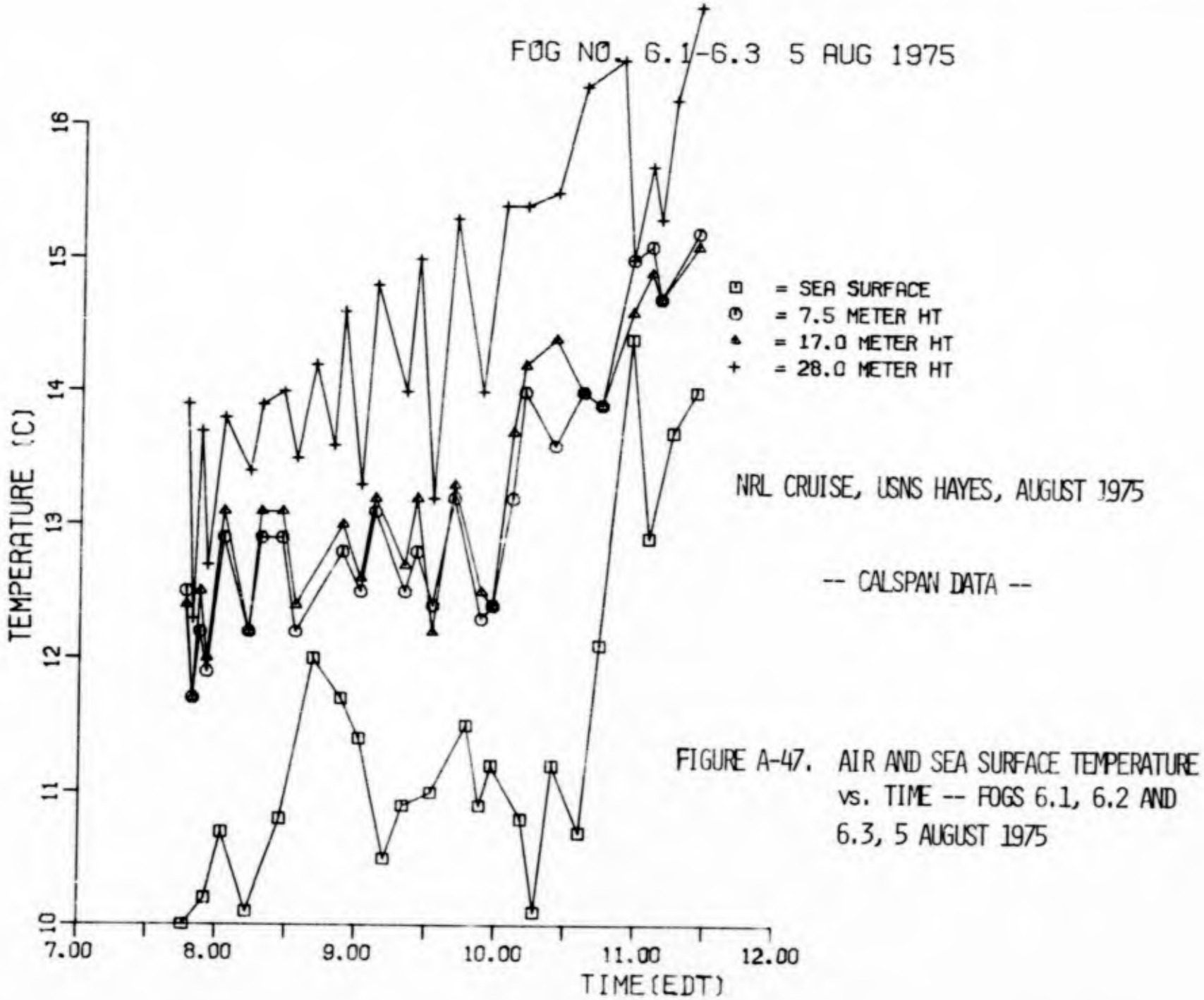

FIGURE A-47. AIR AND SEA SURFACE TEMPERATURE vs. TIME -- FOGS 6.1, 6.2 AND 6.3, 5 AUGUST 1975

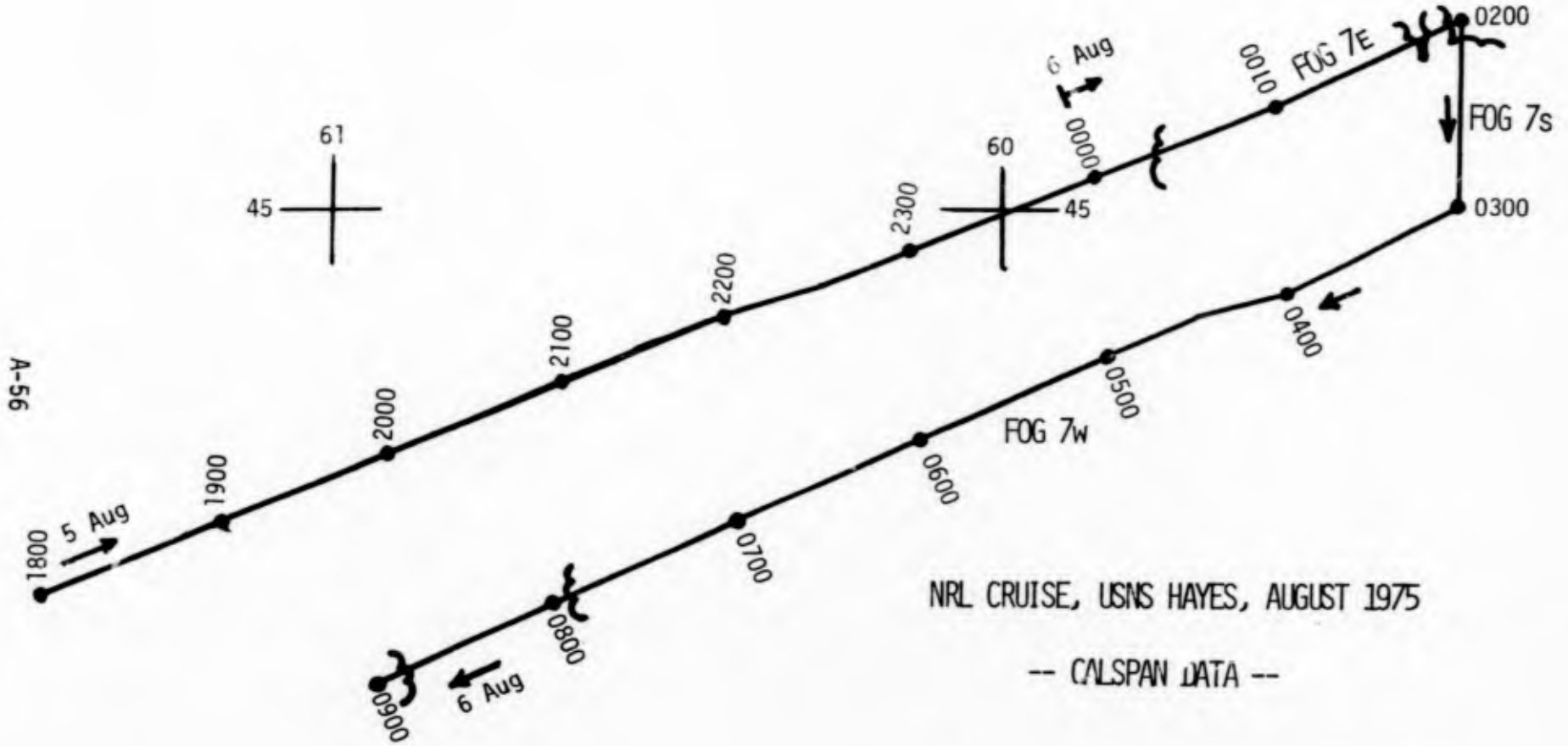

FIGURE A-48. SHIP'S TRACK FOR THE PERIOD 1800, 5 AUGUST TO 0900, 6 AUGUST AND BOUNDARIES (VSBY <5000 M) OF FOG 7

FOG NO. 7E

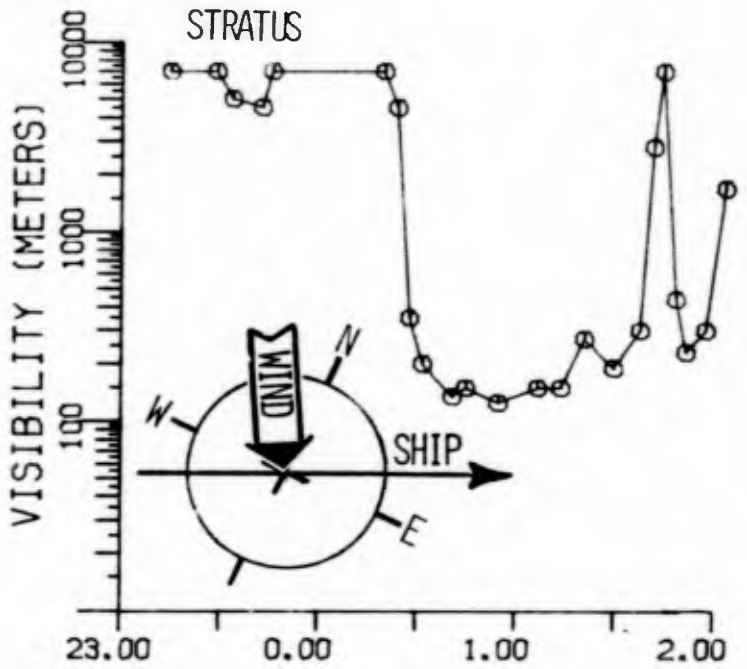

FOG NO. 7S

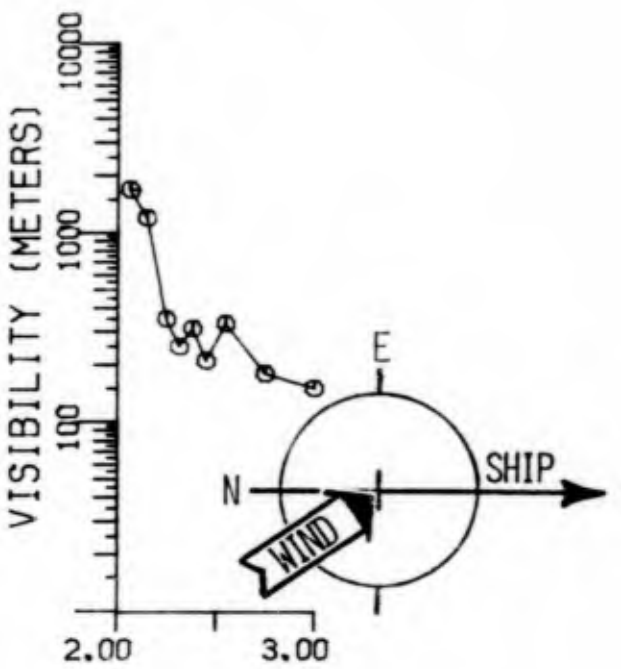

TIME (EDT)

FIGURE A-49. VISIBILITY vs. TIME -- FOG 7E AND 7S, 6 AUGUST 1975

NRL CRUISE, USNS HAYES, AUGUST 1975

-- CALSPAN DATA --

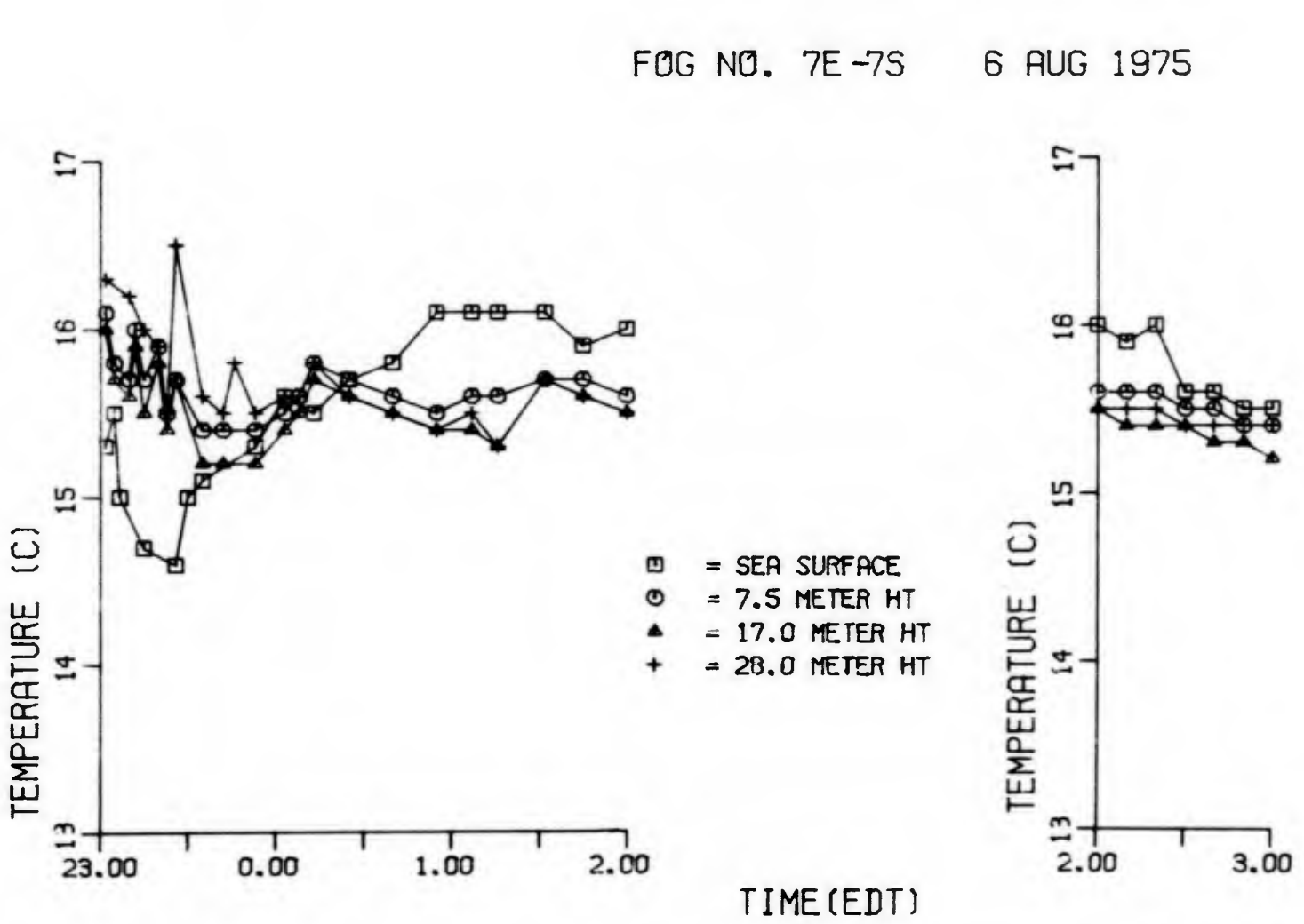

FIGURE A-50. AIR AND SEA SURFACE TEMPERATURE vs. TIME -- FOGS 7E AND 7S, 6 AUGUST 1975

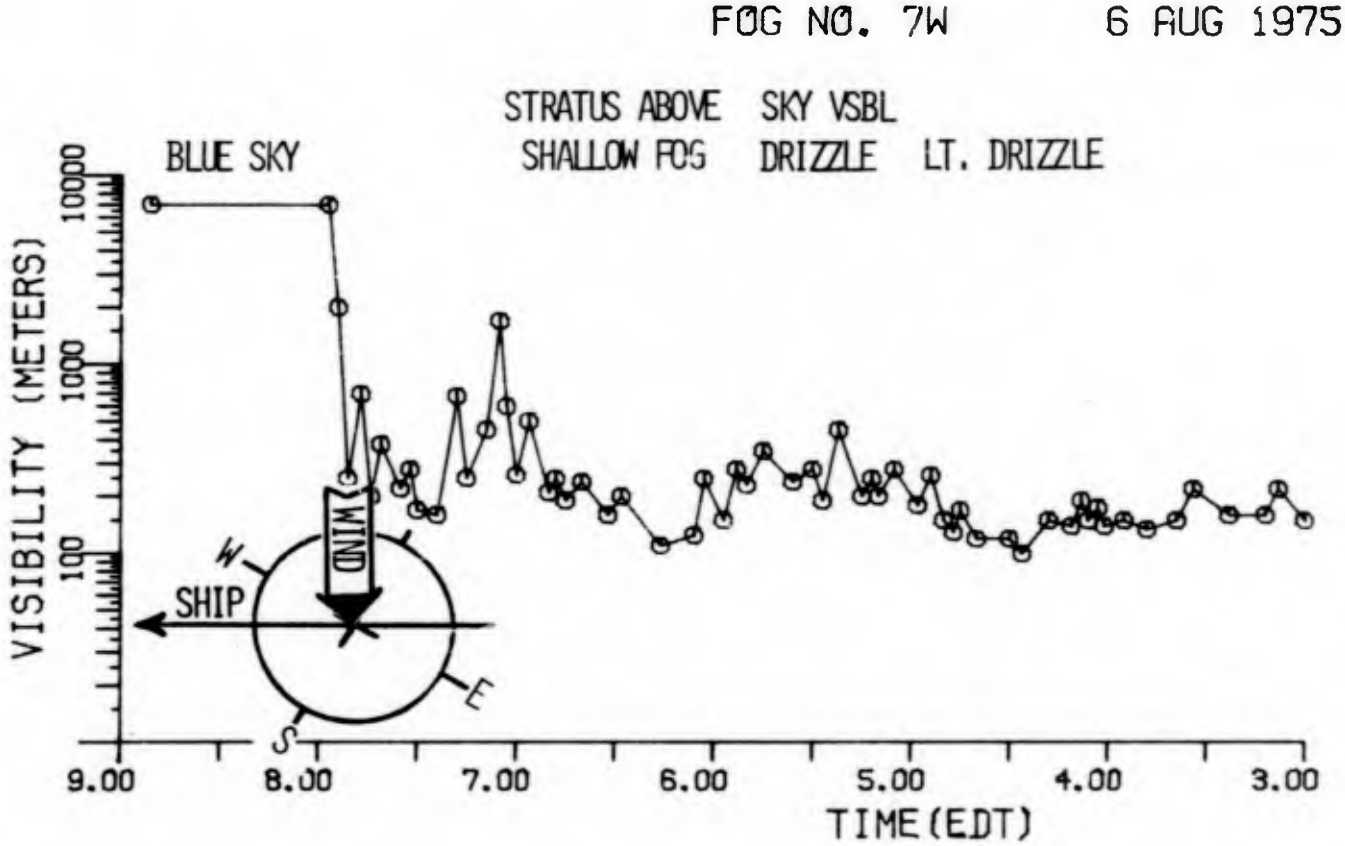

NRL CRUISE, USNS HAYES, AUGUST 1975

FIGURE A-51. VISIBILITY vs. TIME -- FOG 7w, 6 AUGUST 1975

-- CALSPAN DATA --

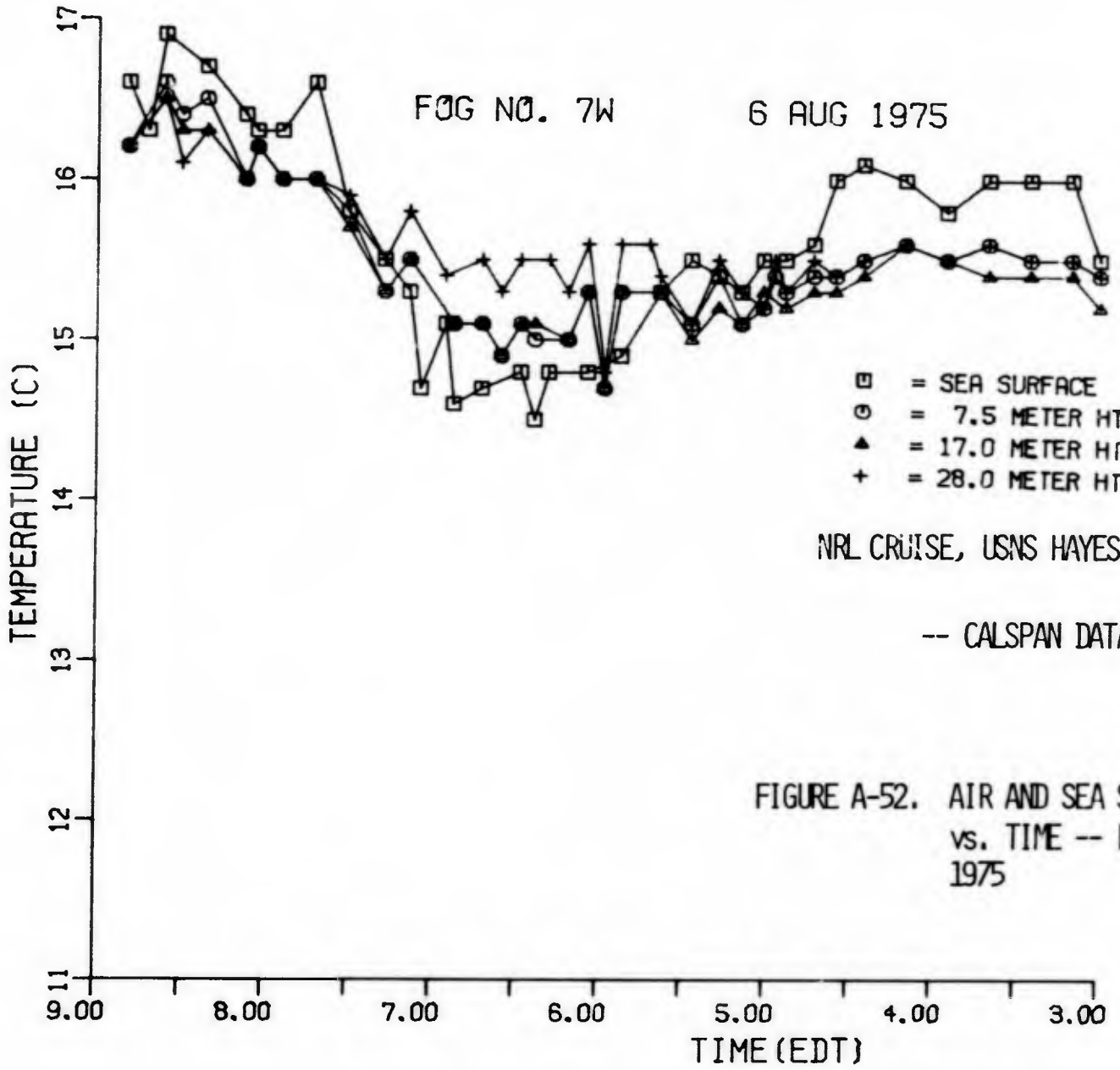

FIGURE A-52. AIR AND SEA SURFACE TEMPERATURE vs. TIME -- FOG 7w, 6 AUGUST 1975

FIGURE A-53. SHIP'S TRACK FOR THE PERIOD 0800, 6 AUGUST TO 0230, 7 AUGUST AND BOUNDARIES (VSBY <5000 M) OF FOG 8

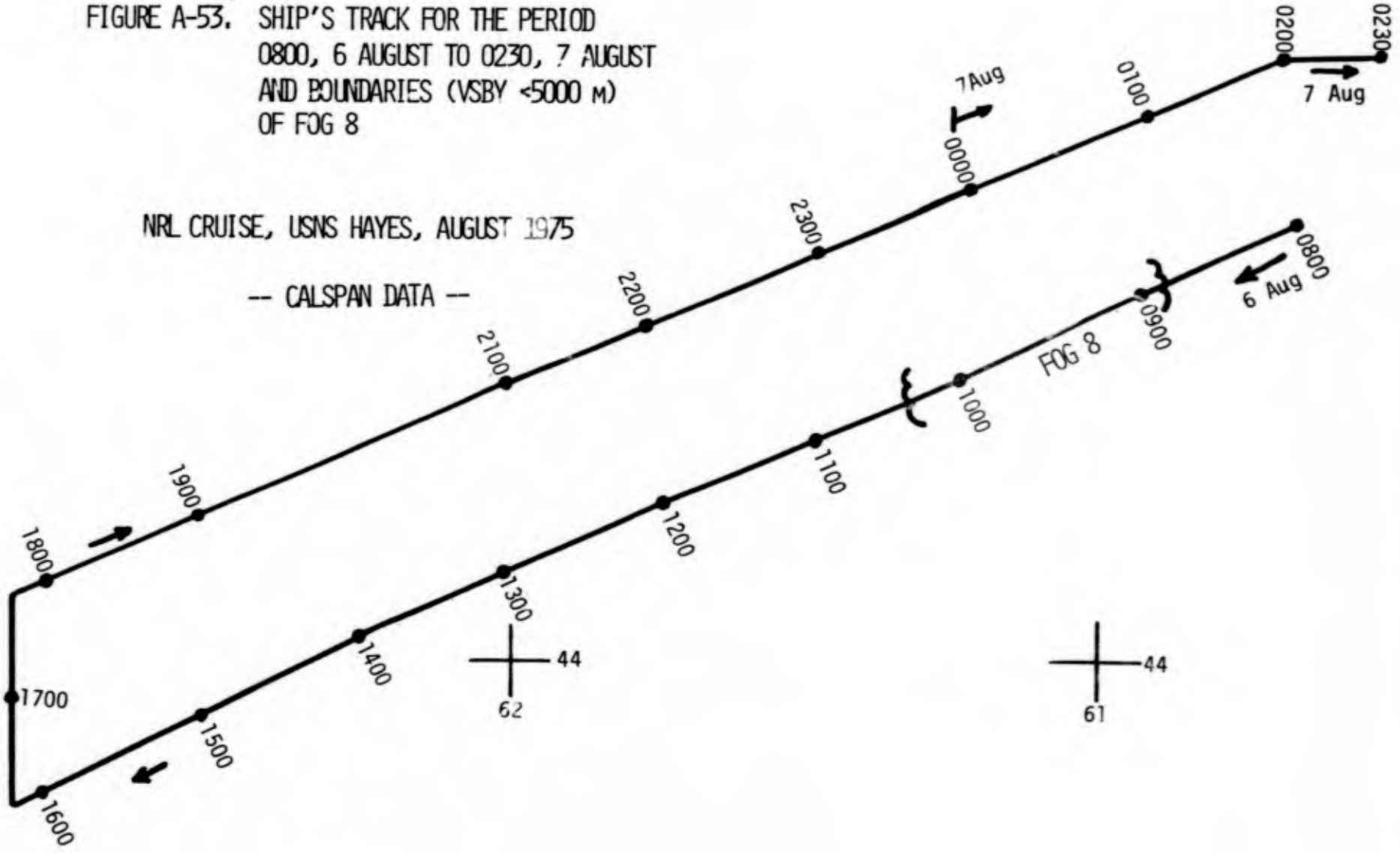

FOG NO. 8 6 AUG 1975

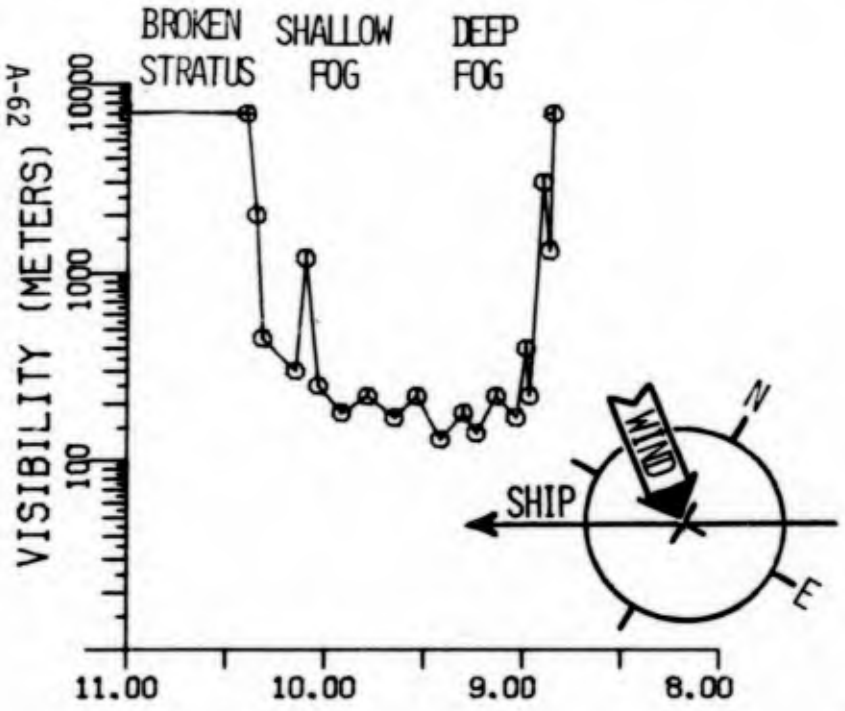

NRL CRUISE, USNS HAYES, AUGUST 1975

-- CALSPAN DATA --

FIGURE A-54. VISIBILITY vs. TIME -- FOG 8, 6 AUGUST 1975

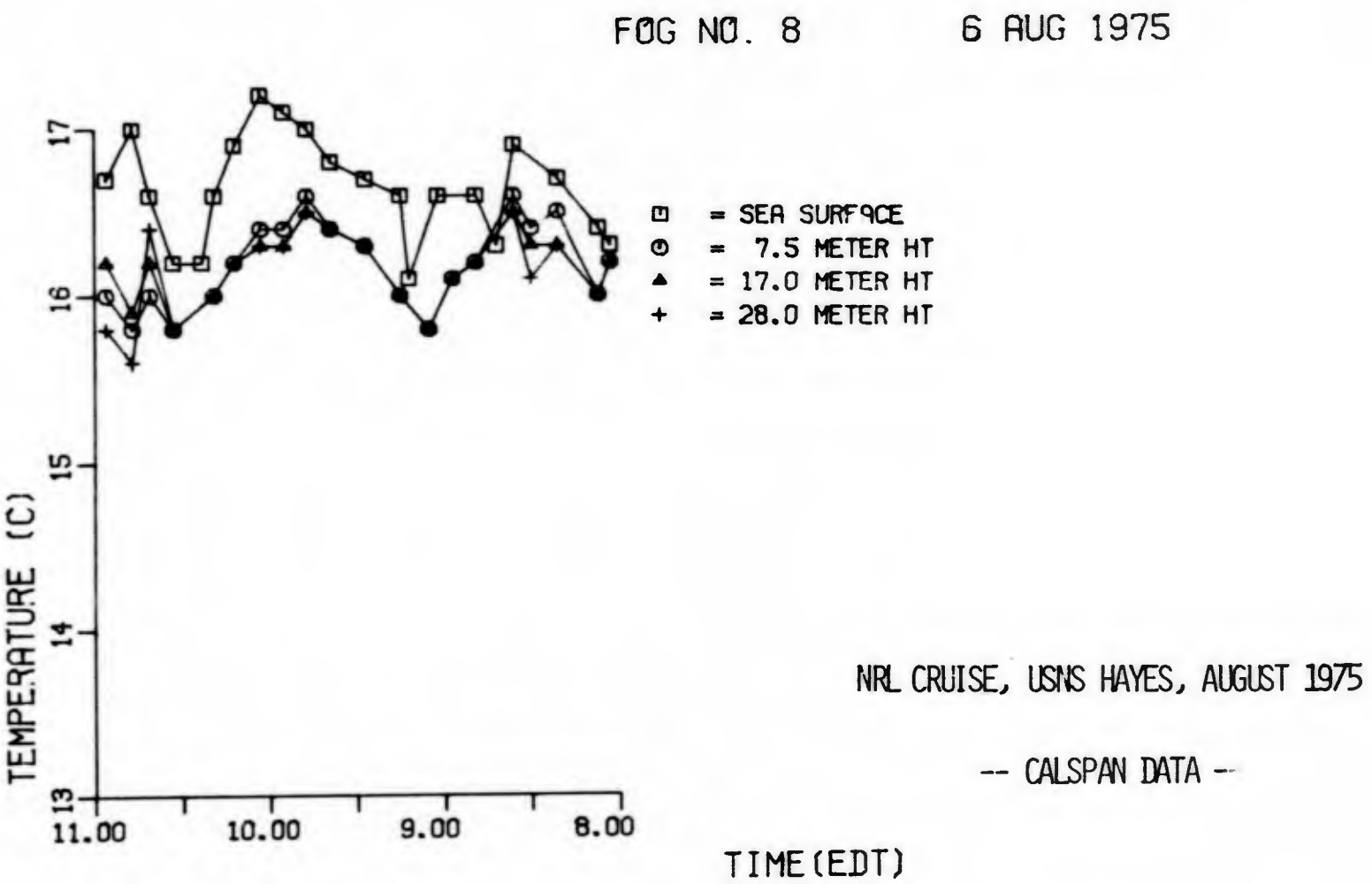

FIGURE A-55. AIR AND SEA SURFACE TEMPERATURE vs. TIME -- FOG 8, 6 AUGUST 1975

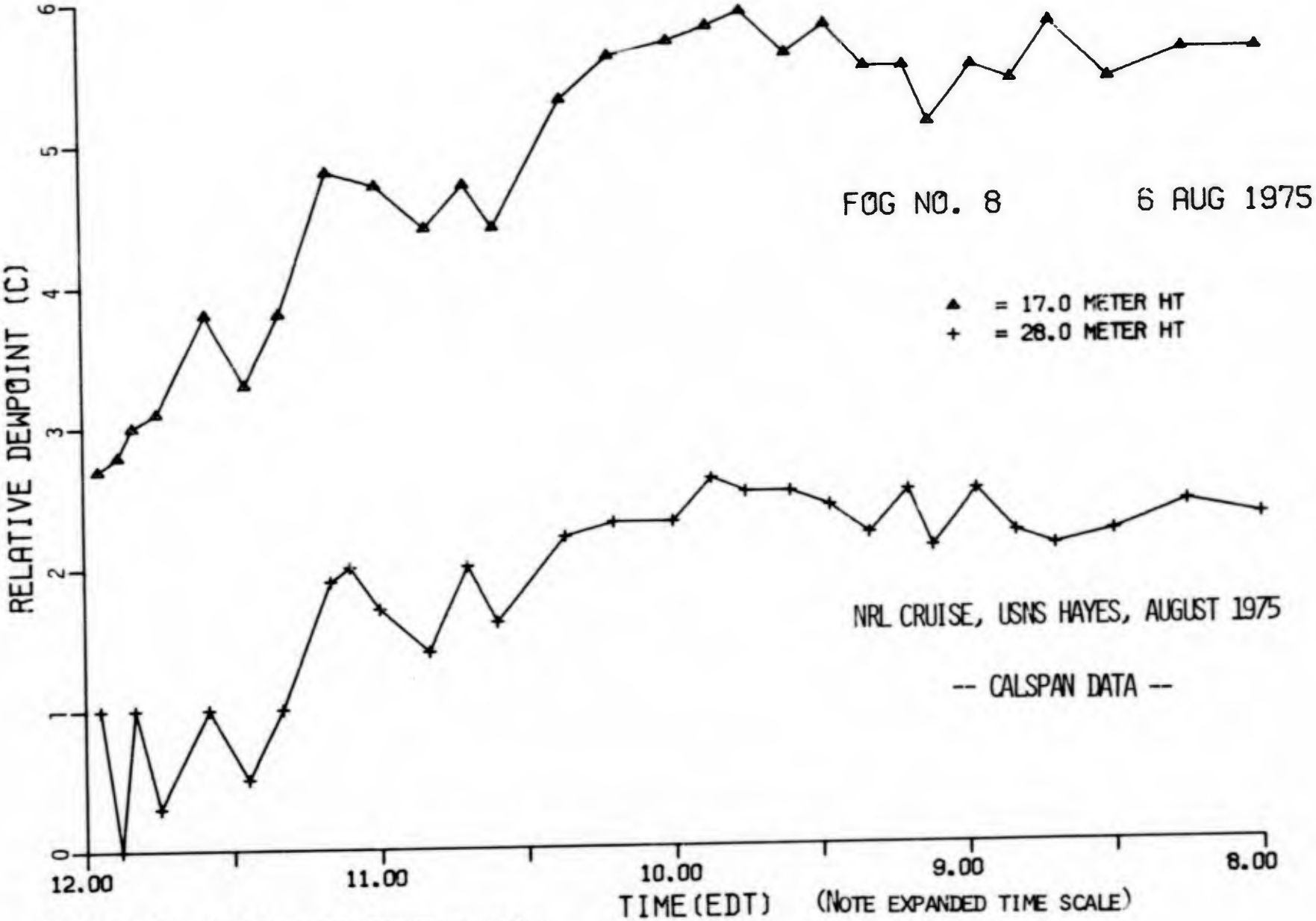

FIGURE A-56. RELATIVE DEW POINT vs. TIME -- FOG 8, 6 AUGUST 1975

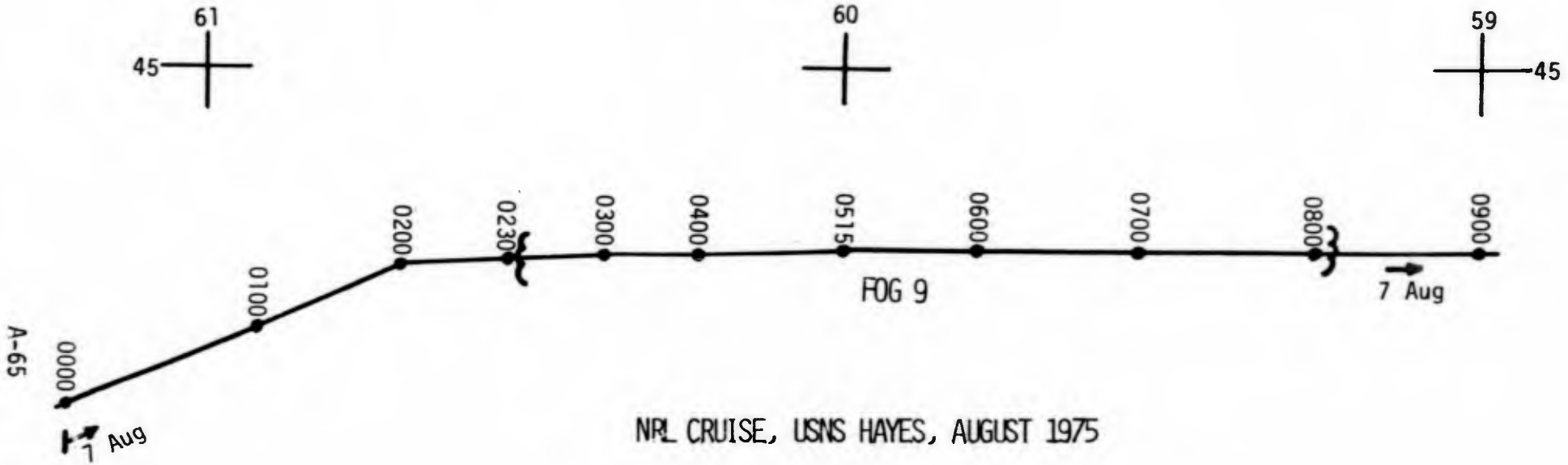

FIGURE A-57. SHIP'S TRACK FOR THE PERIOD 0000, 7 AUGUST TO 0900, 7 AUGUST AND BOUNDARIES (VSBY <5000 M) OF FOG 9

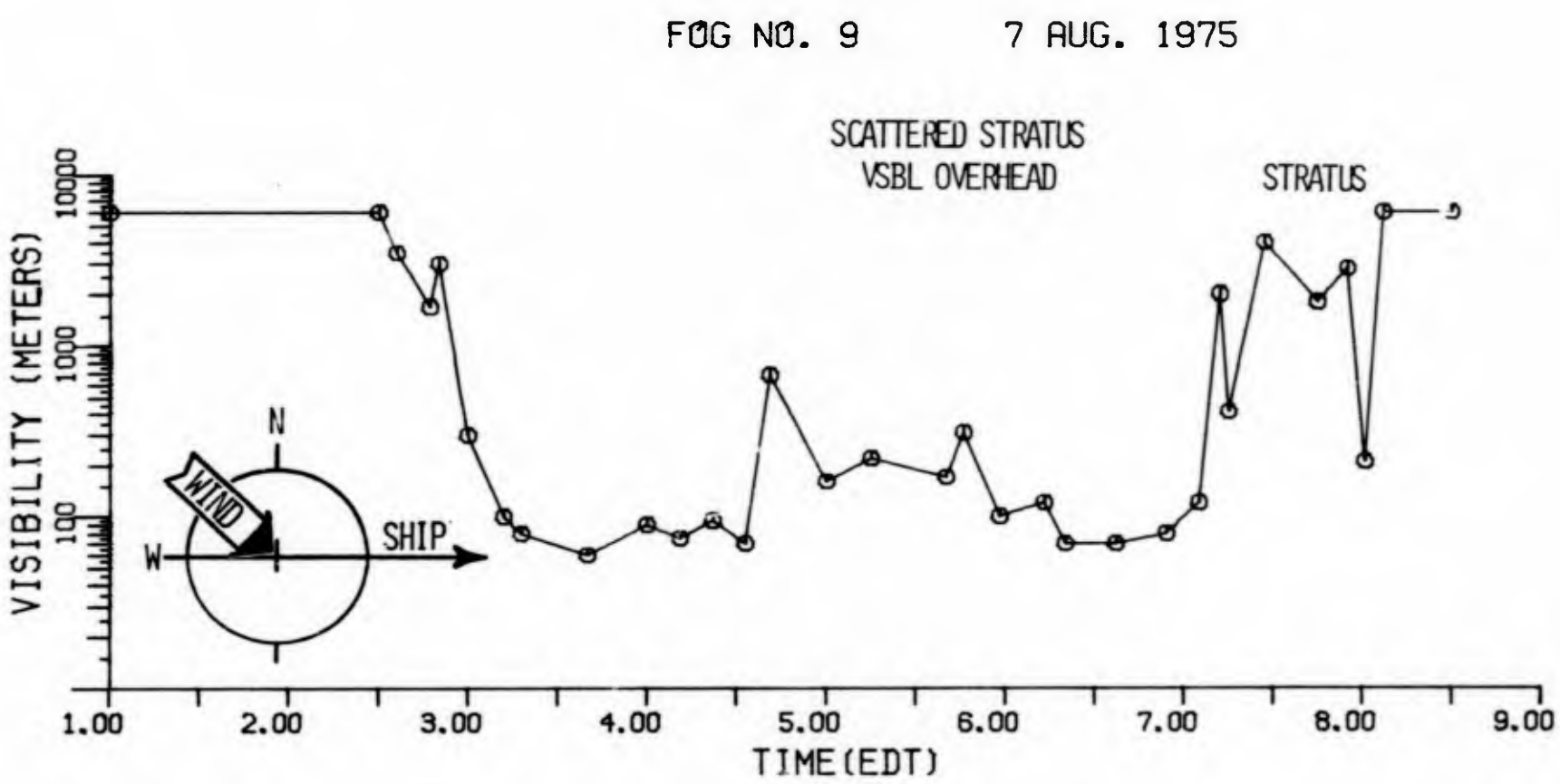

FIGURE A-58. VISIBILITY vs. TIME -- FOG 9, 7 AUGUST 1975

-- CALSPAN DATA --

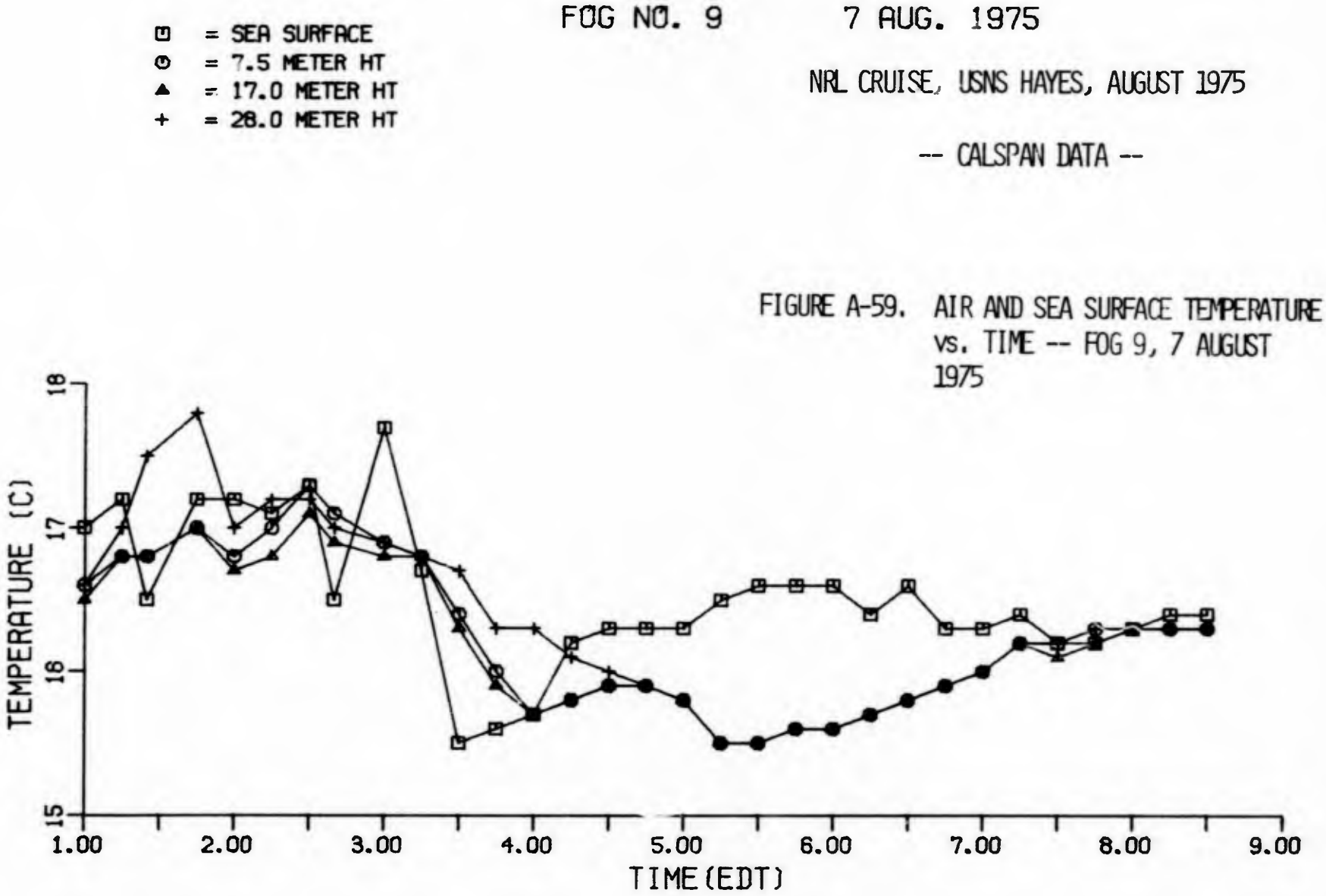

FIGURE A-59. AIR AND SEA SURFACE TEMPERATURE vs. TIME -- FOG 9, 7 AUGUST 1975

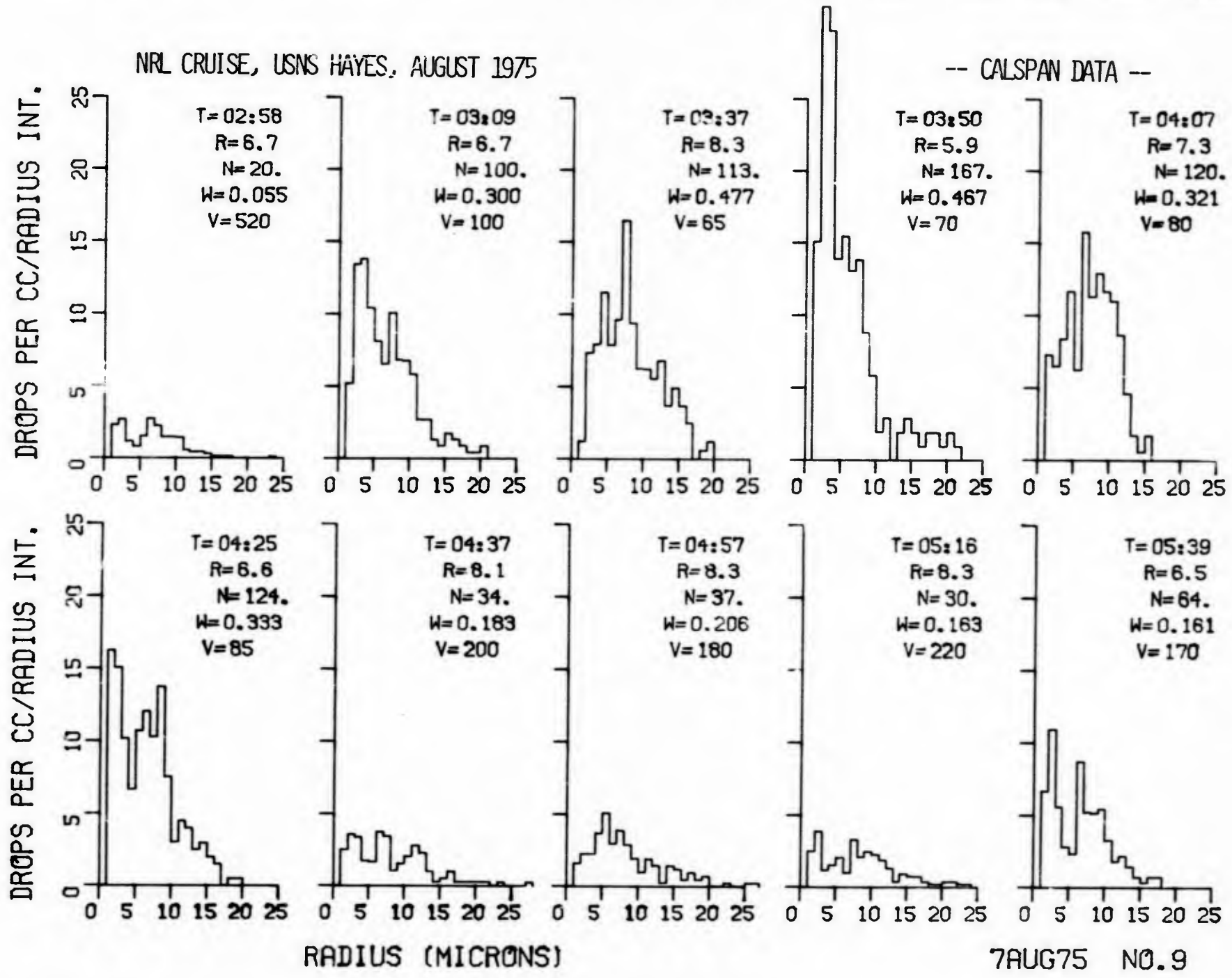

FIGURE A-60. DROP SIZE DISTRIBUTIONS -- FOG 9, 7 AUGUST 1975

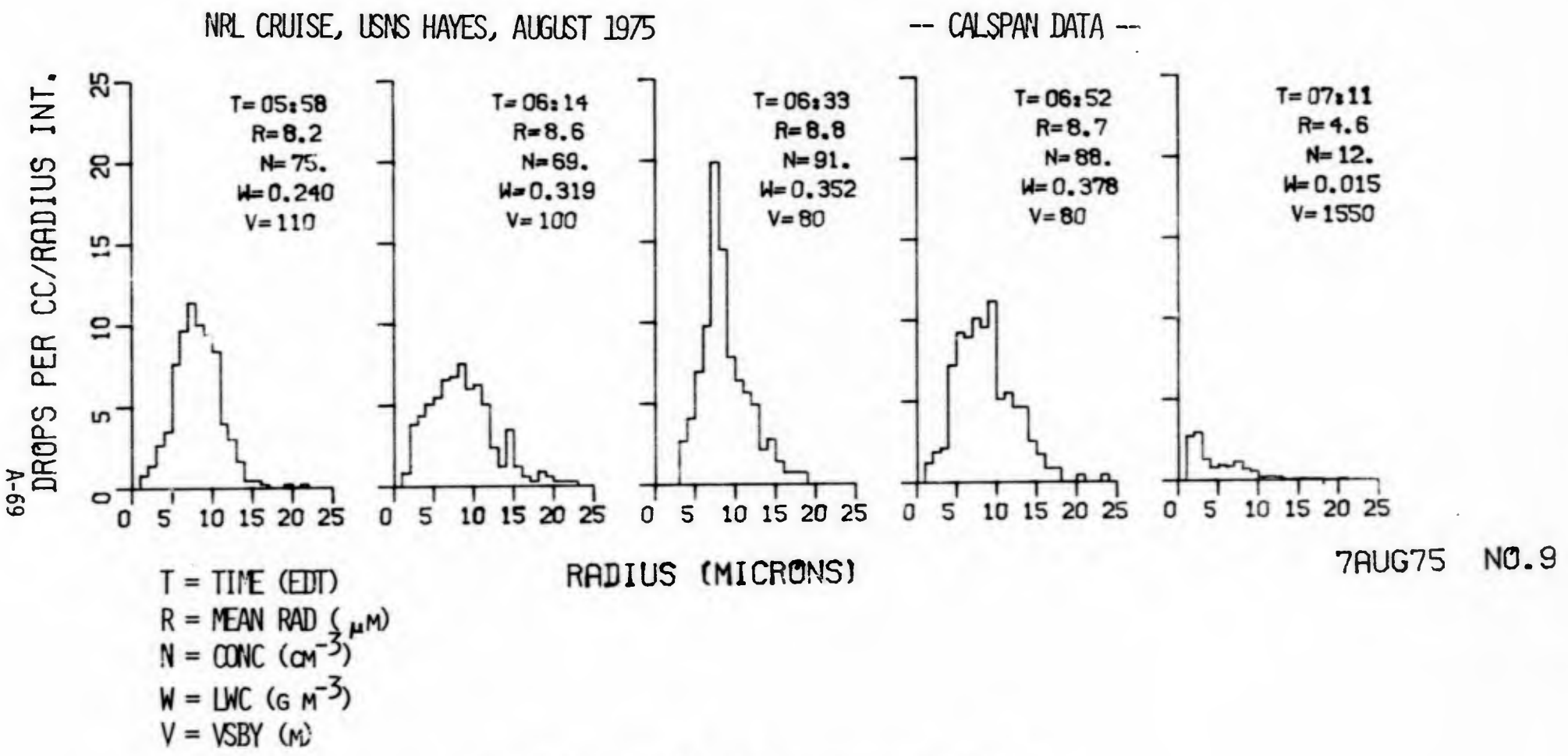

FIGURE A-61. DROP SIZE DISTRIBUTIONS (CONT.)
-- FOG 9, 7 AUGUST 1975

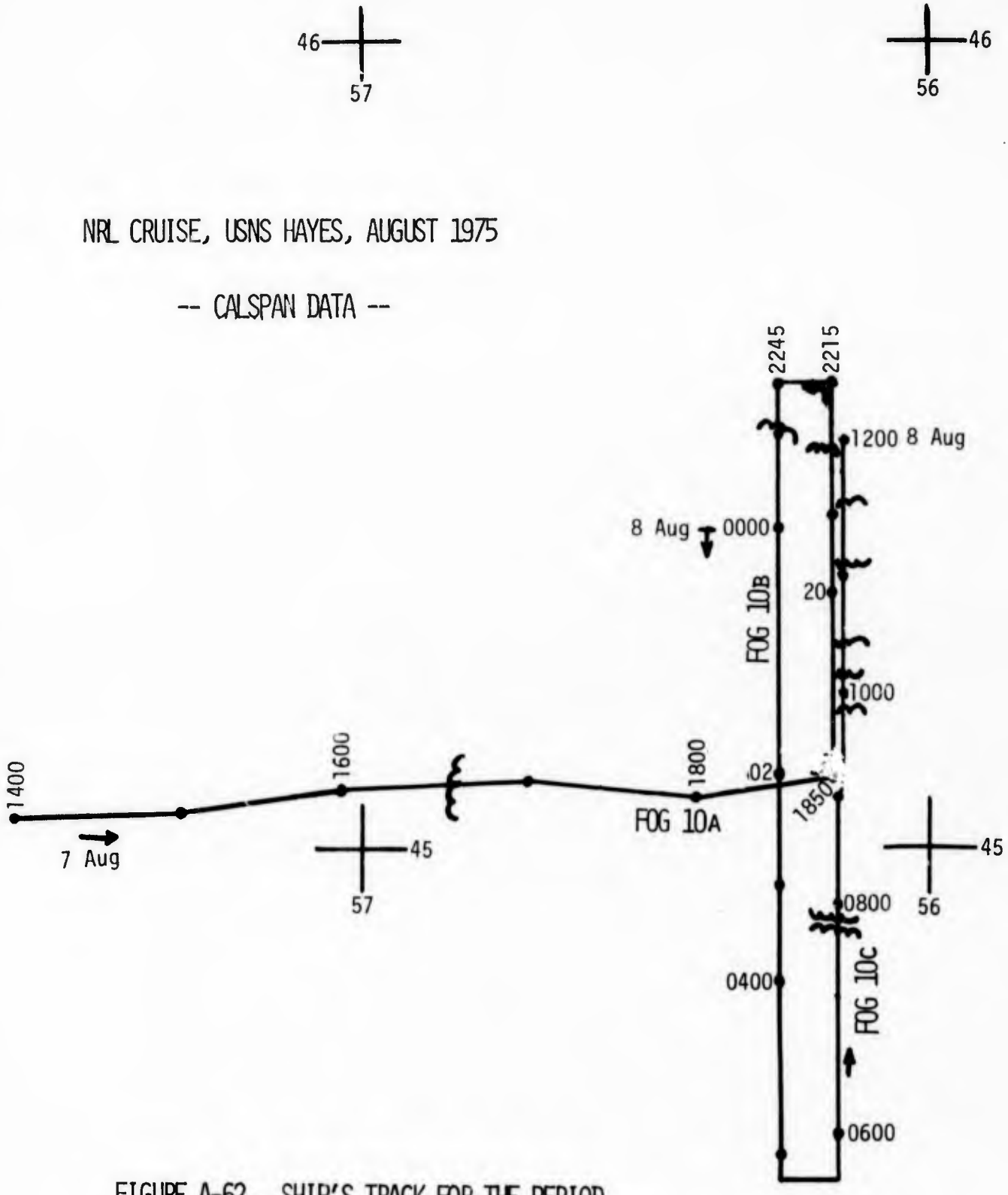

FIGURE A-62. SHIP'S TRACK FOR THE PERIOD 1400, 7 AUGUST TO 1200, 8 AUGUST AND BOUNDARIES (VSBY <5000 M) OF FOG 10

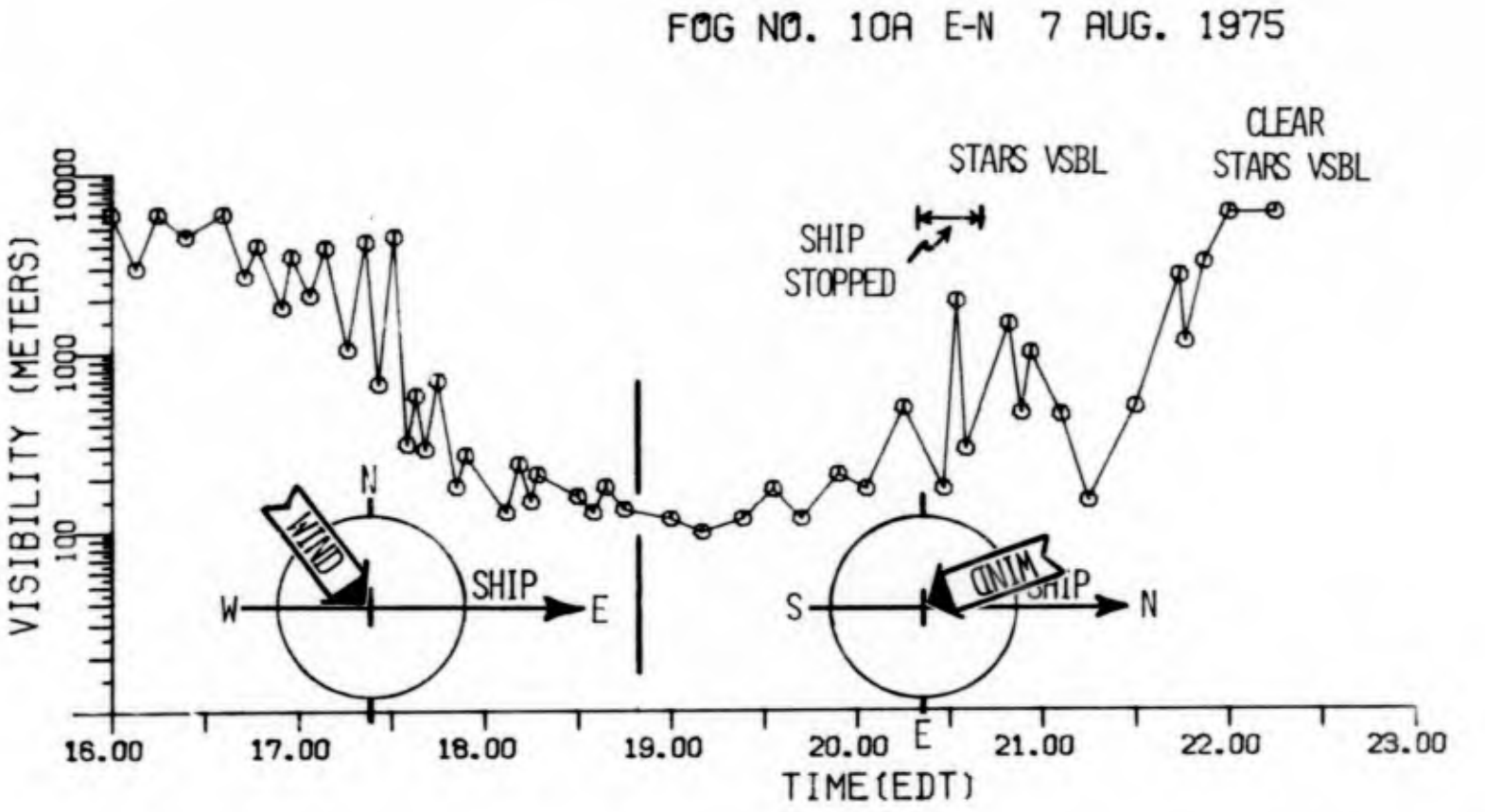

NRL CRUISE, USNS HAYES, AUGUST 1975

FIGURE A-63. VISIBILITY vs. TIME --
FOG 10A, 7 AUGUST 1975

-- CALSPAN DATA --

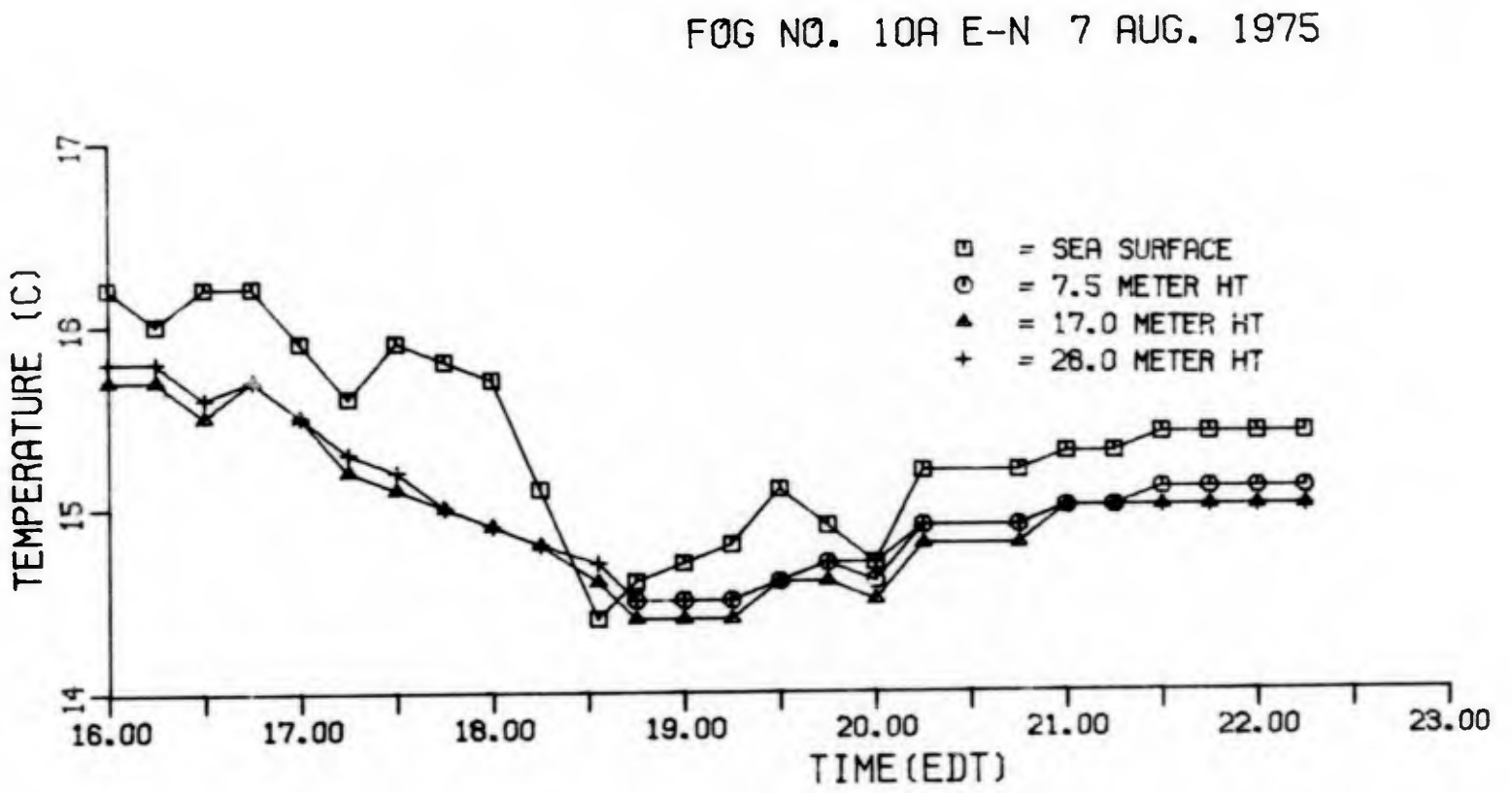

FIGURE A-64. AIR AND SEA SURFACE TEMPERATURE vs. TIME -- FOG 10A, 7 AUGUST 1975

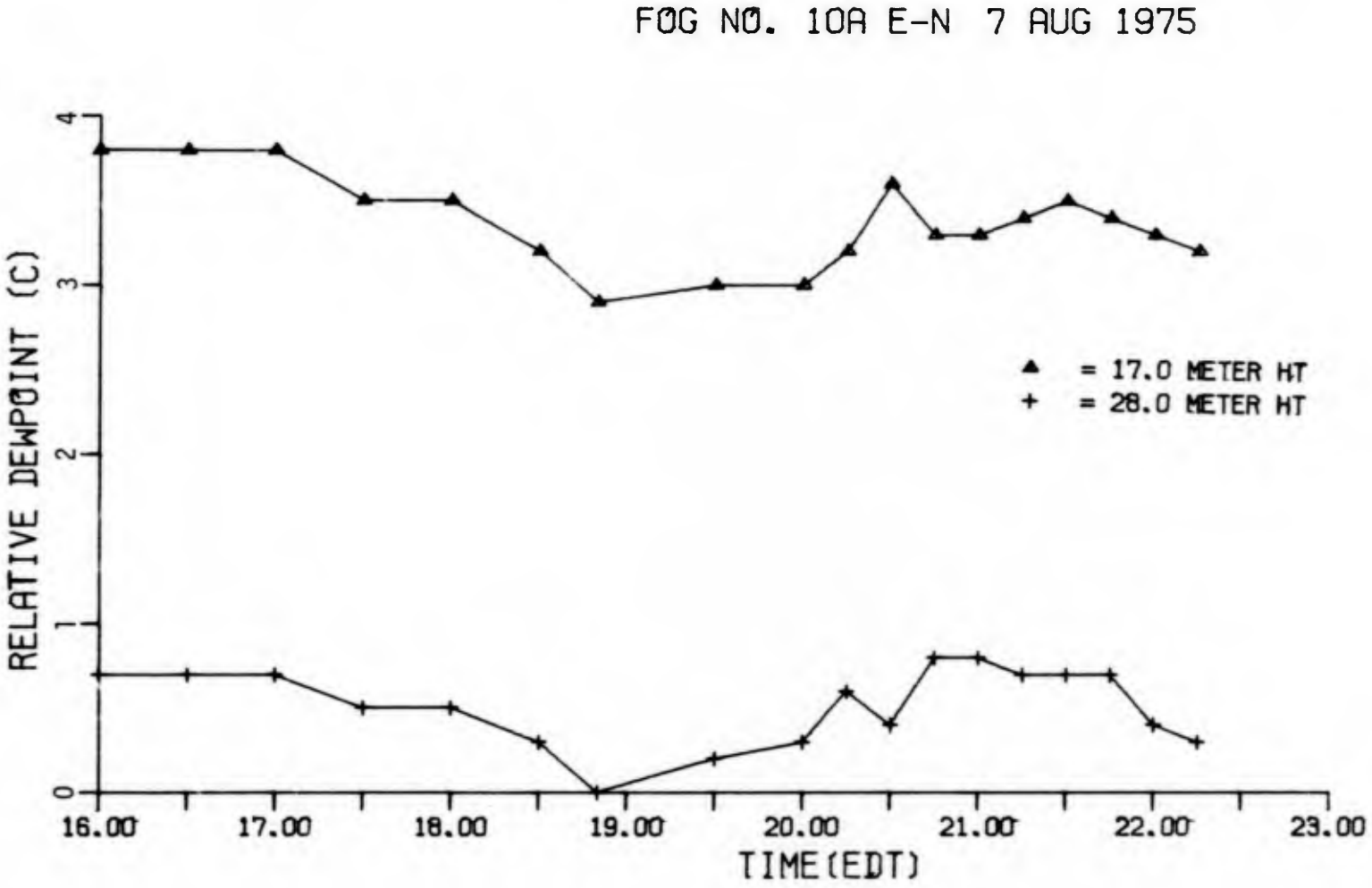

NRL CRUISE, USNS HAYES, AUGUST 1975

FIGURE A-65. RELATIVE DEW POINT vs. TIME -- FOG 10A, 7 AUGUST 1975

-- CALSPAN DATA --

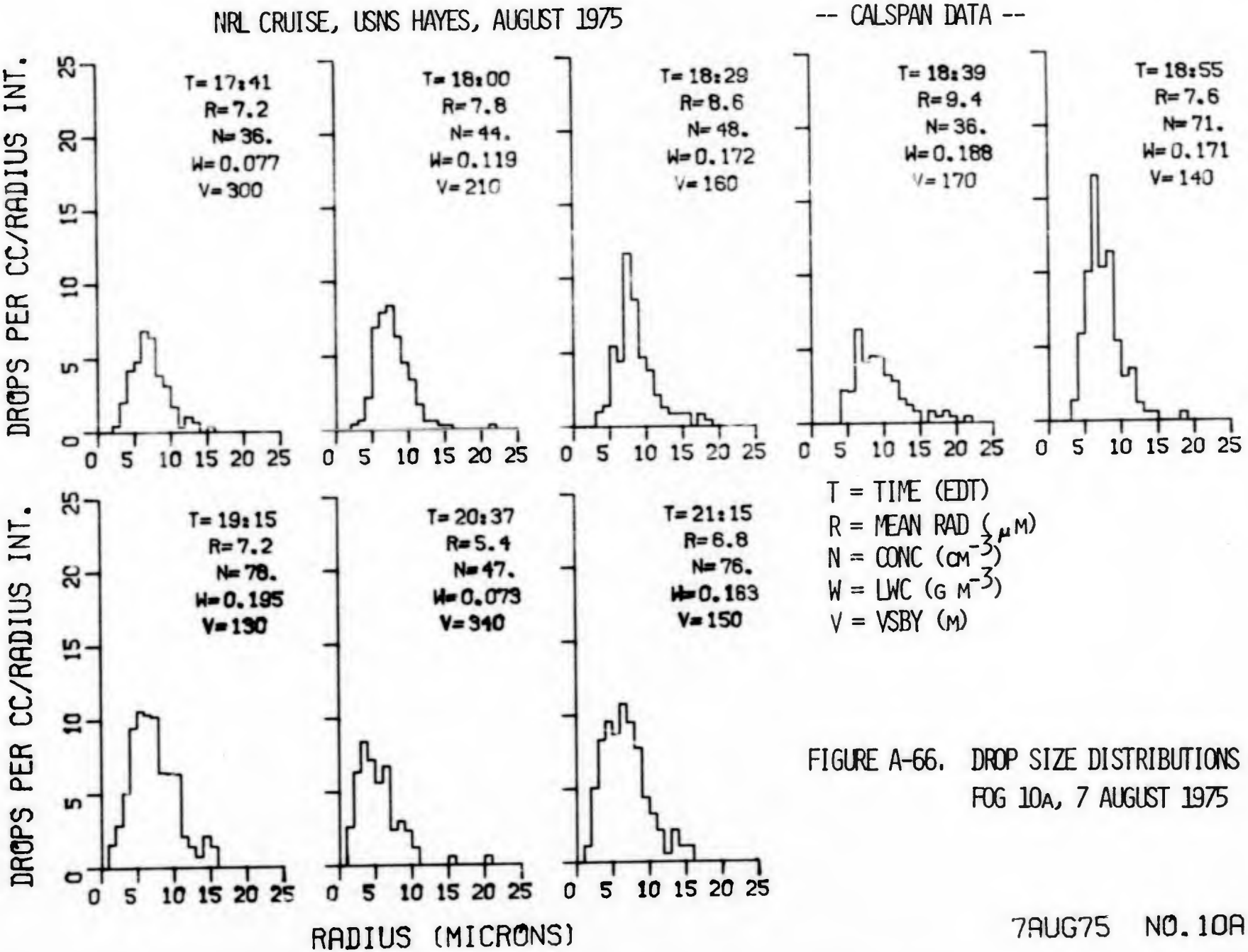

FIGURE A-66. DROP SIZE DISTRIBUTIONS -- FOG 10A, 7 AUGUST 1975

7AUG75 NO. 10A

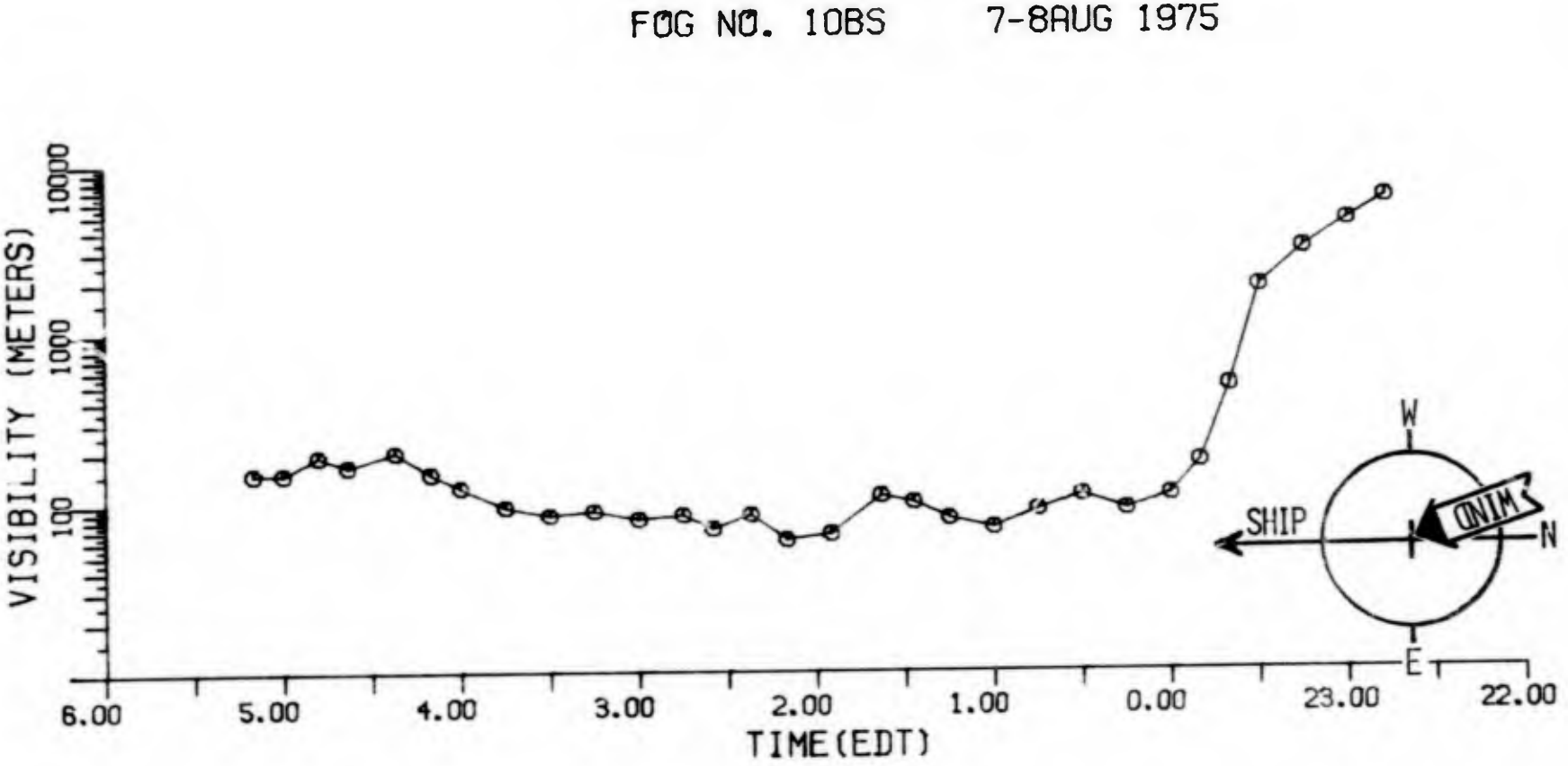

NRL CRUISE, USNS HAYES, AUGUST 1975

FIGURE A-67. VISIBILITY vs. TIME --
FOG 10B, 7-8 AUGUST 1975

-- CALSPAN DATA --

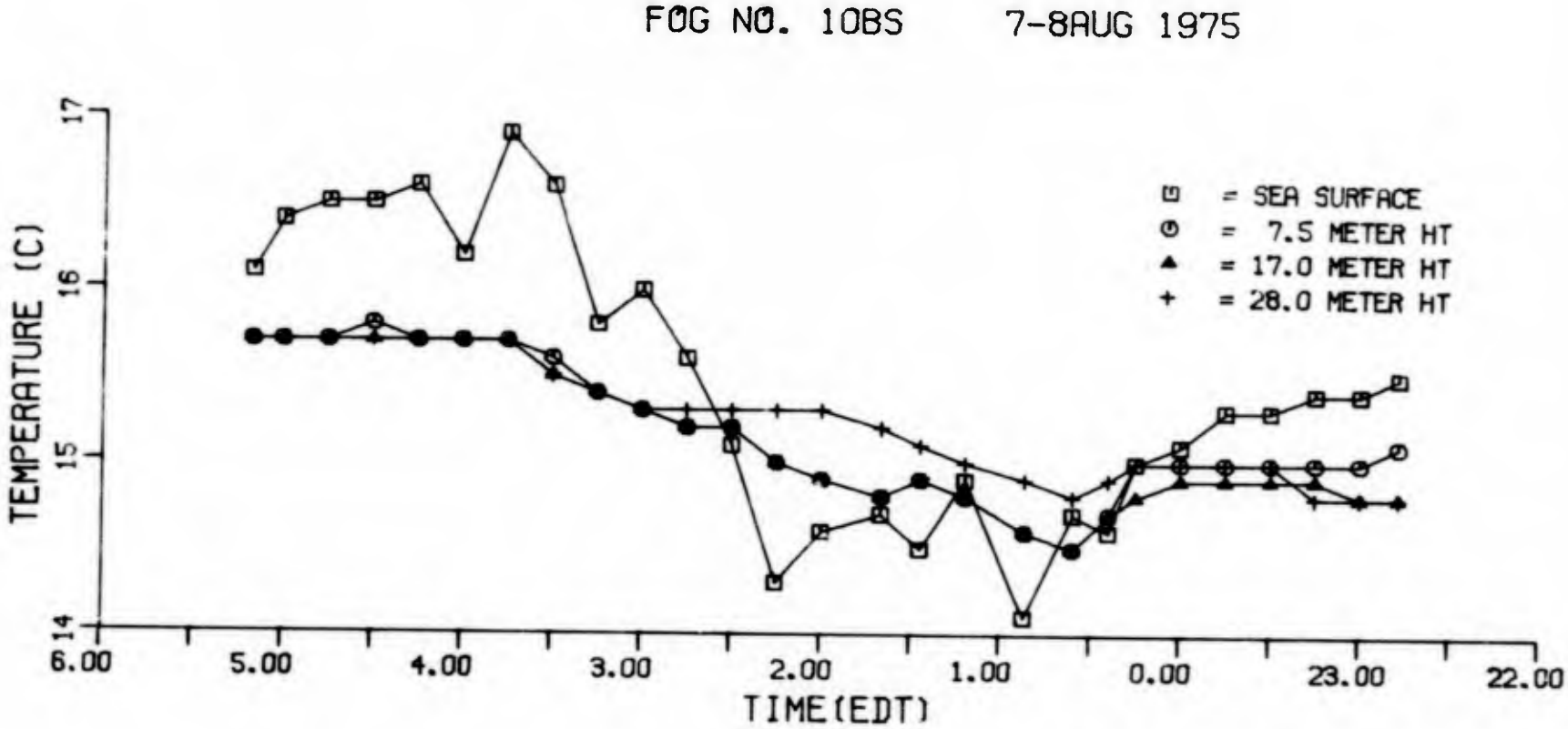

NRL CRUISE, USNS HAYES, AUGUST 1975

FIGURE A-68. AIR AND SEA SURFACE TEMPERATURE vs. TIME — FOG 10B, 7-8 AUGUST 1975

-- CALSPAN DATA --

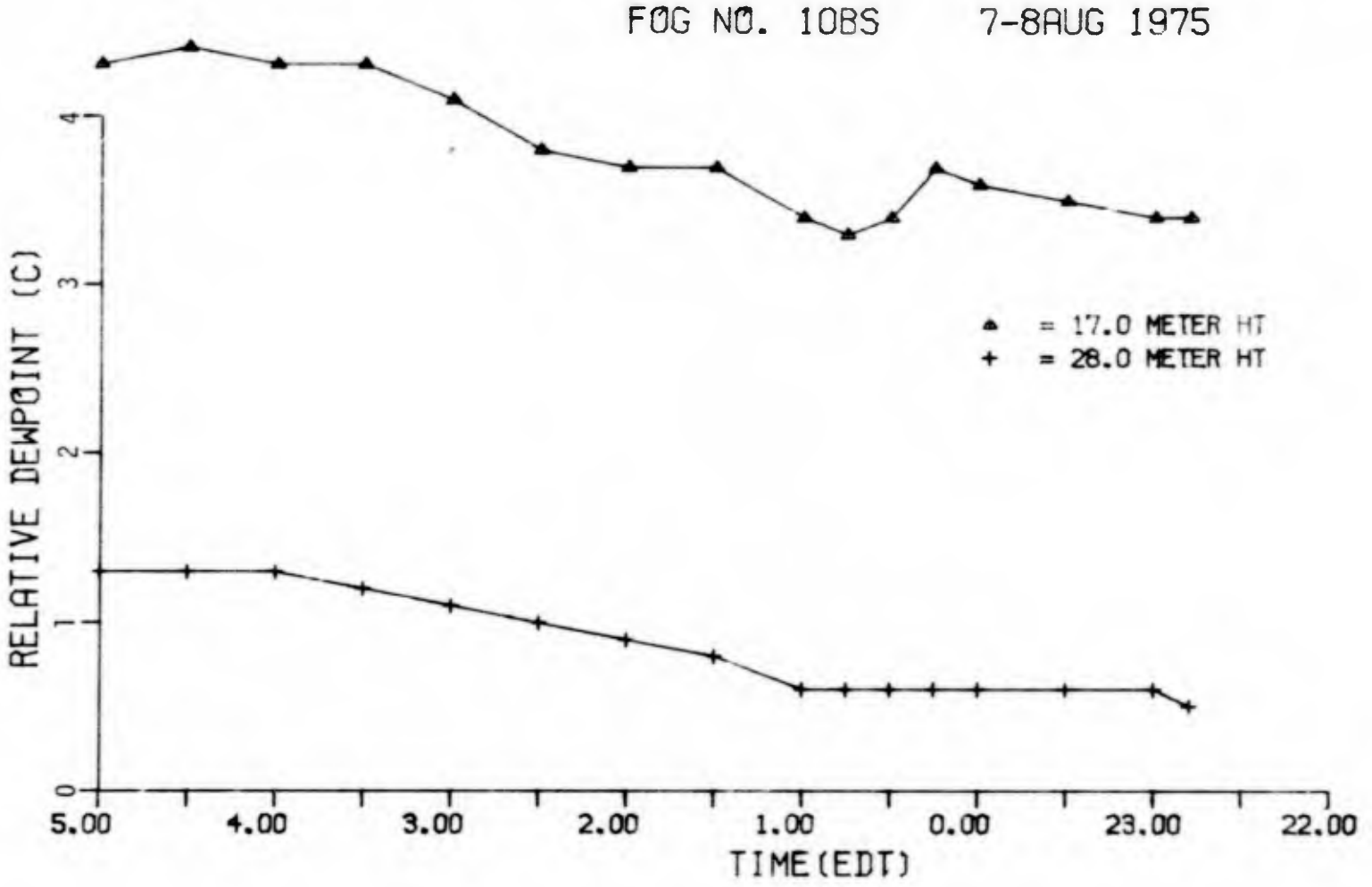

NRL CRUISE, USNS HAYES, AUGUST 1975

FIGURE A-69. RELATIVE DEW POINT vs. TIME -- FOG 10B, 7-8 AUGUST 1975

-- CALSPAN DATA --

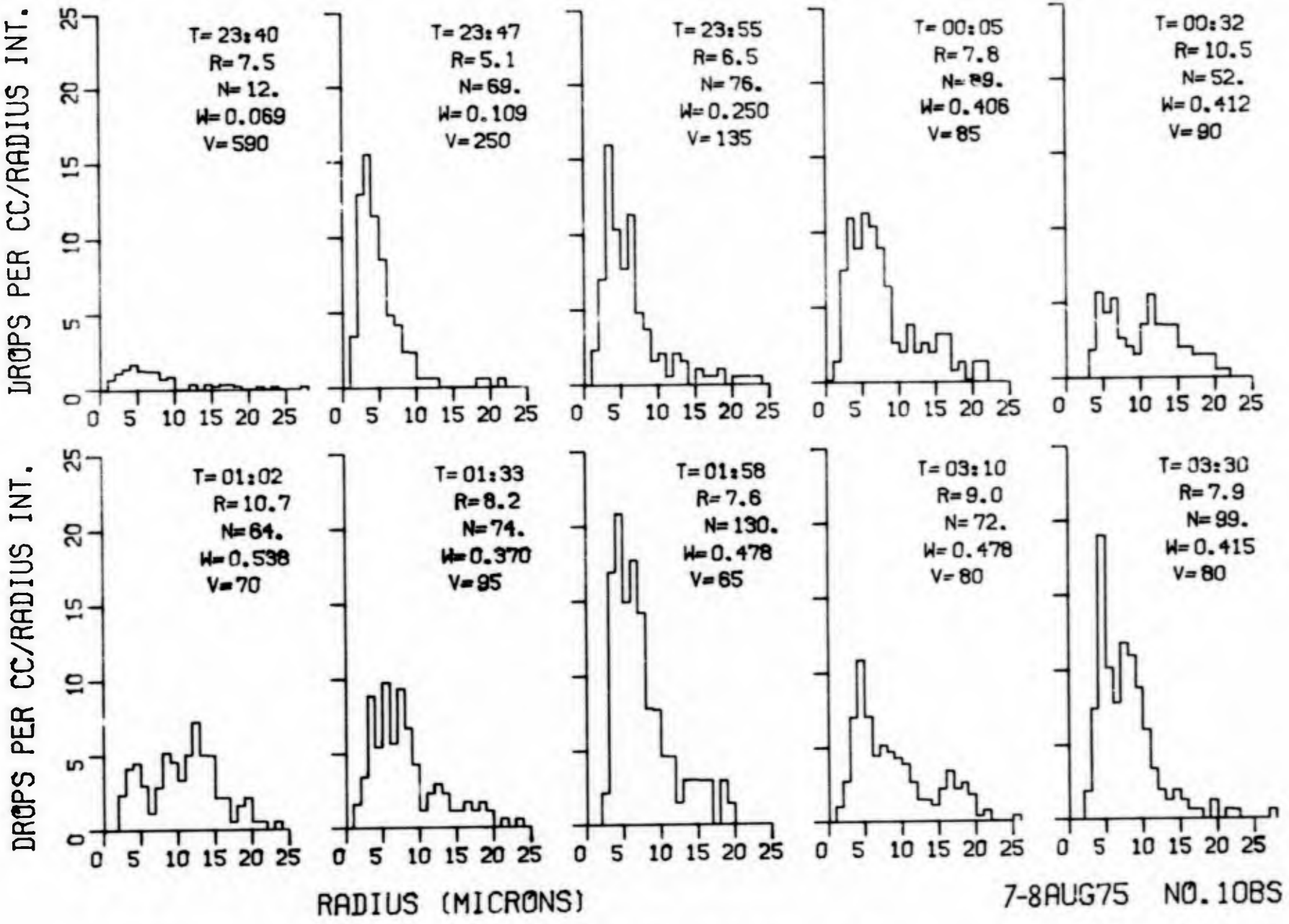

FIGURE A-70. DROP SIZE DISTRIBUTIONS -- FOG 10B, 7-8 AUGUST 1975

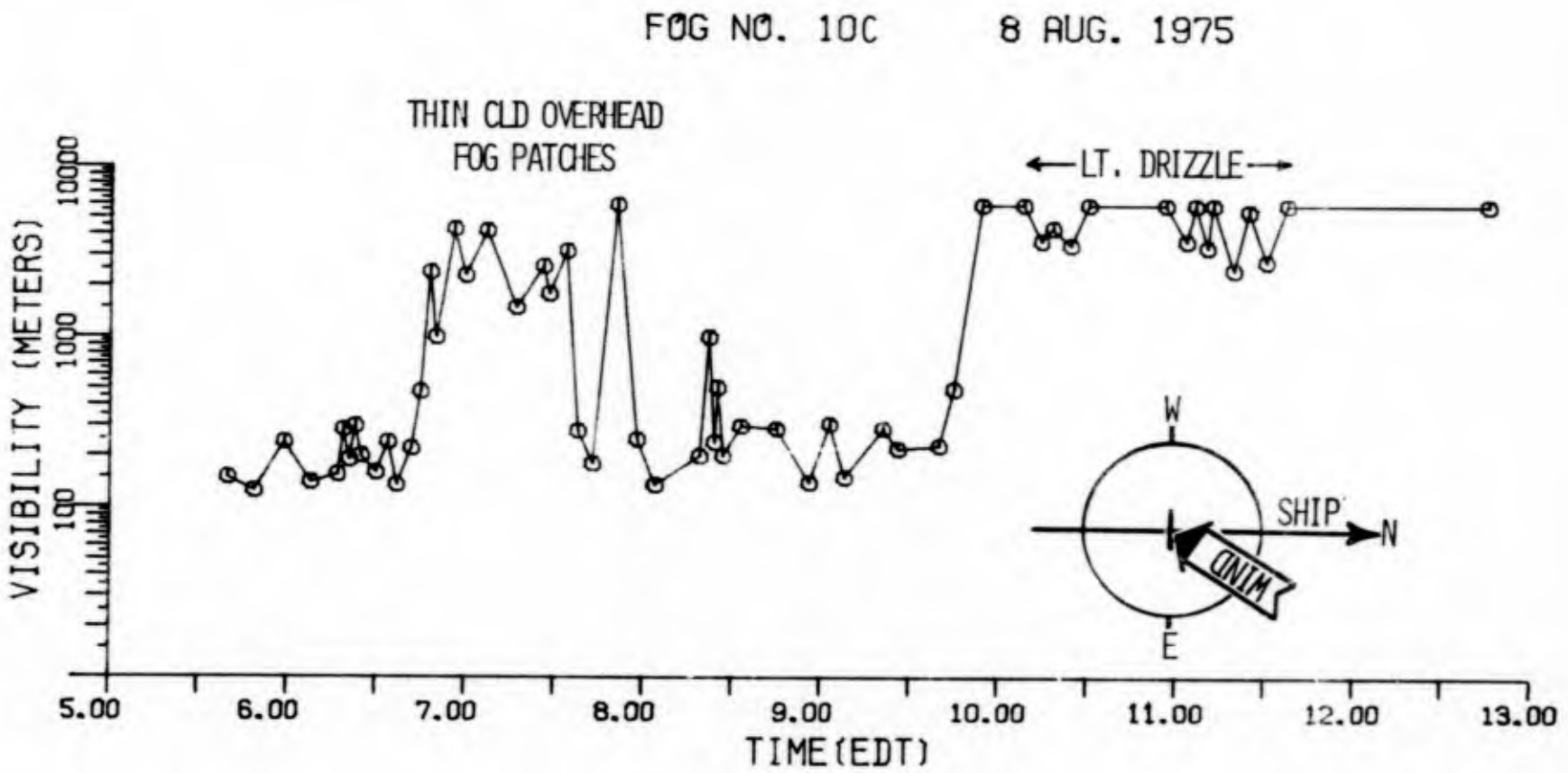

FIGURE A-71. VISIBILITY vs. TIME --
FOG 10c, 8 AUGUST 1975

-- CALSPAN DATA --

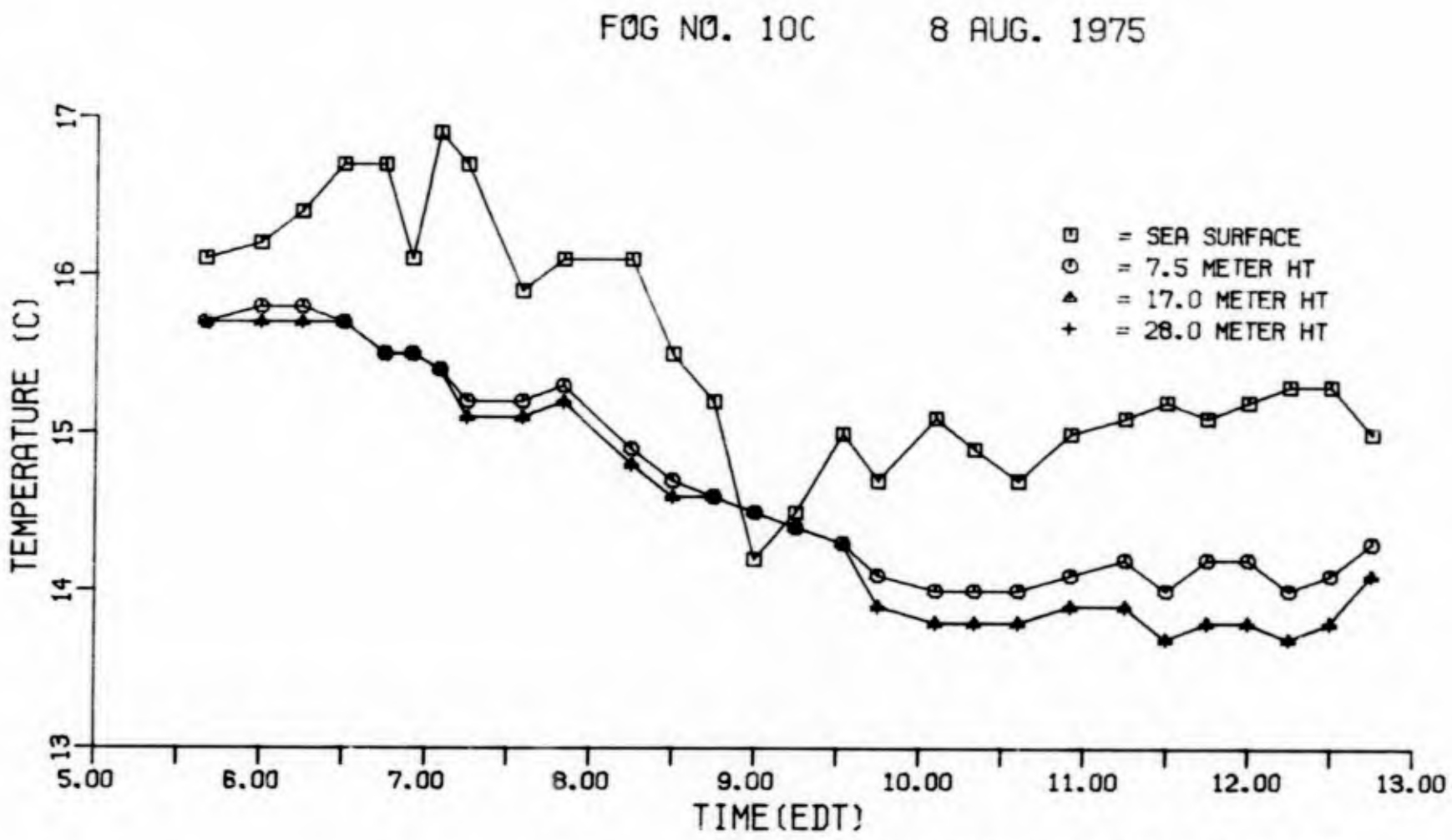

FIGURE A-72. AIR AND SEA SURFACE TEMPERATURE vs. TIME -- FOG 10c, 8 AUGUST 1975

-- CALSPAN DATA --

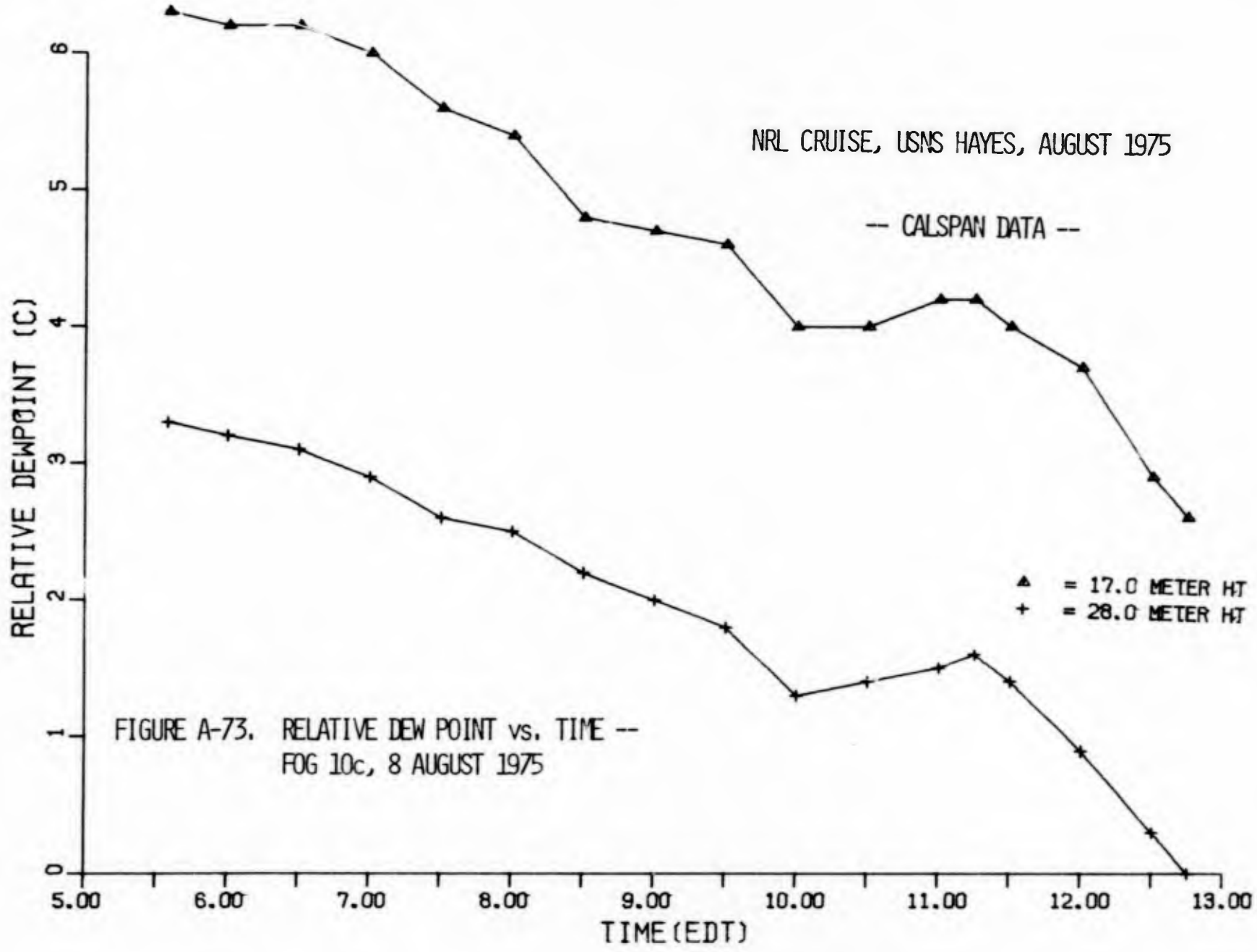

FIGURE A-73. RELATIVE DEW POINT vs. TIME --
FOG 10c, 8 AUGUST 1975

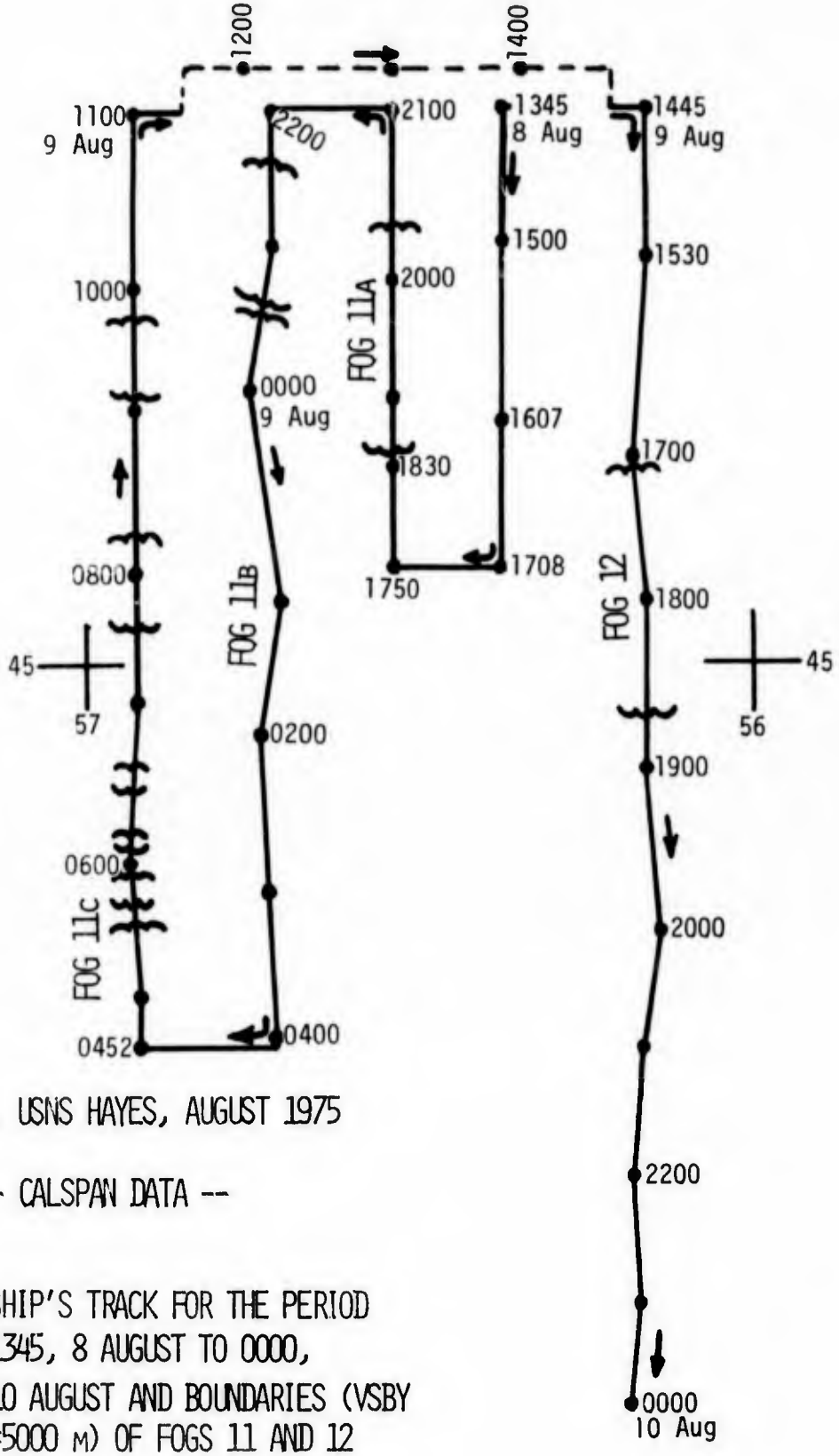

NRL CRUISE, USNS HAYES, AUGUST 1975

-- CALSPAN DATA --

FIGURE A-74. SHIP'S TRACK FOR THE PERIOD 1345, 8 AUGUST TO 0000, 10 AUGUST AND BOUNDARIES (VSBY <5000 M) OF FOGS 11 AND 12

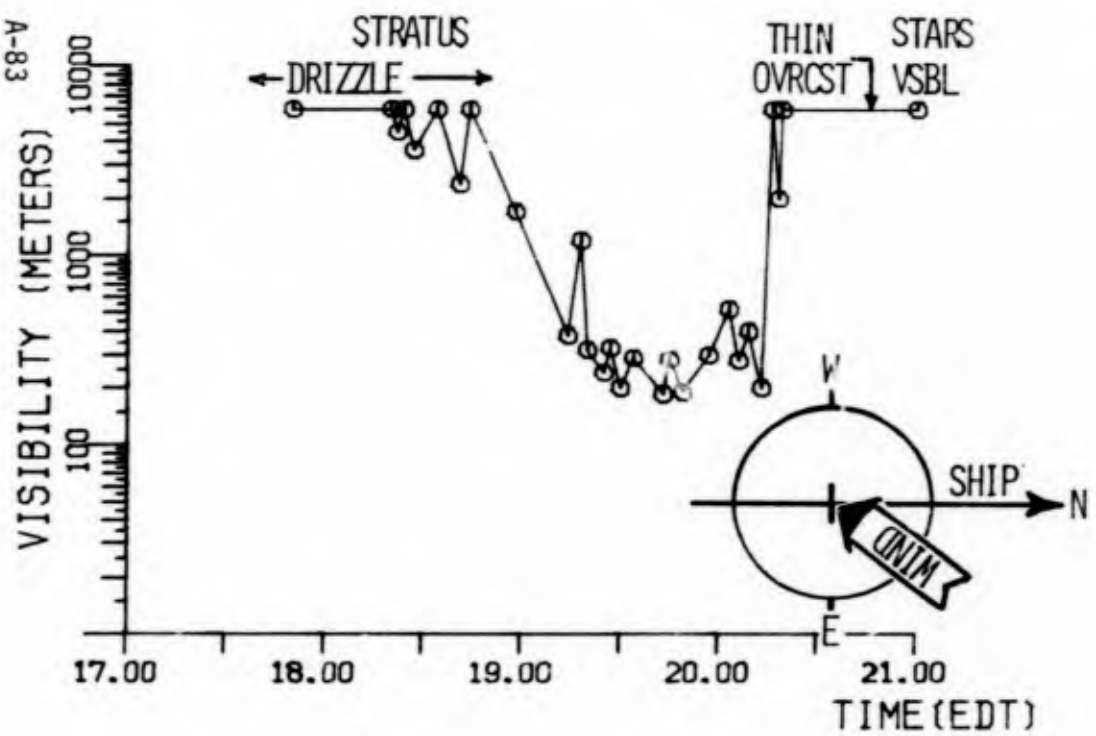

NRL CRUISE, USNS HAYES, AUGUST 1975

-- CALSPAN DATA --

FIGURE A-75. VISIBILITY vs. TIME -- FOG 11A, 8 AUGUST 1975

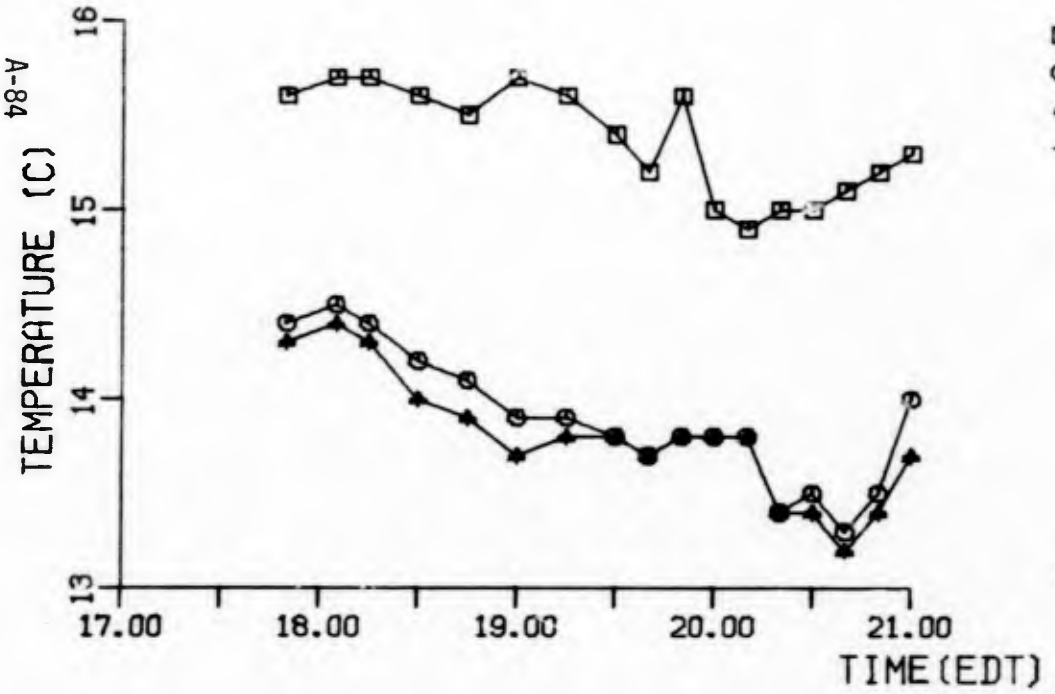

FIGURE A-76. AIR AND SEA SURFACE TEMPERATURE vs. TIME -- FOG 11A, 8 AUGUST 1975

FØG NØ. 11A 8 AUG 1975

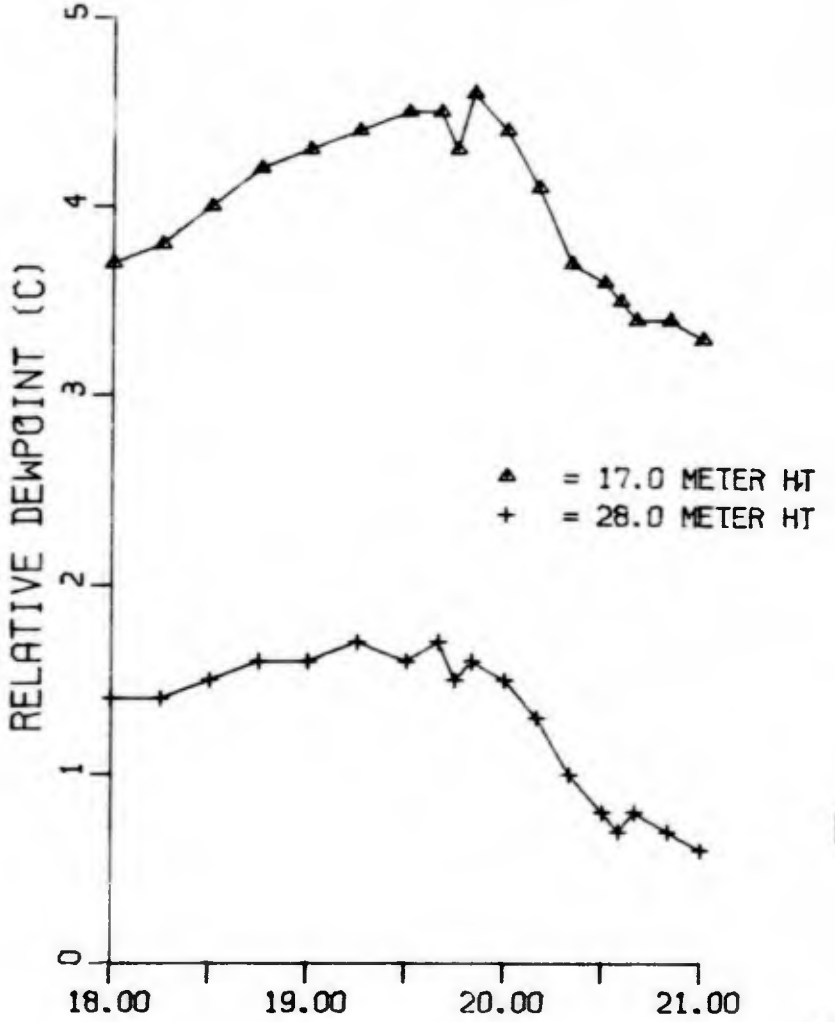

NRL CRUISE, USNS HAYES, AUGUST 1975

-- CALSPAN DATA --

FIGURE A-77. RELATIVE DEW POINT vs. TIME-- FOG 11A, 8 AUGUST 1975

FOG NO. 11B 8-9 AUG 1975

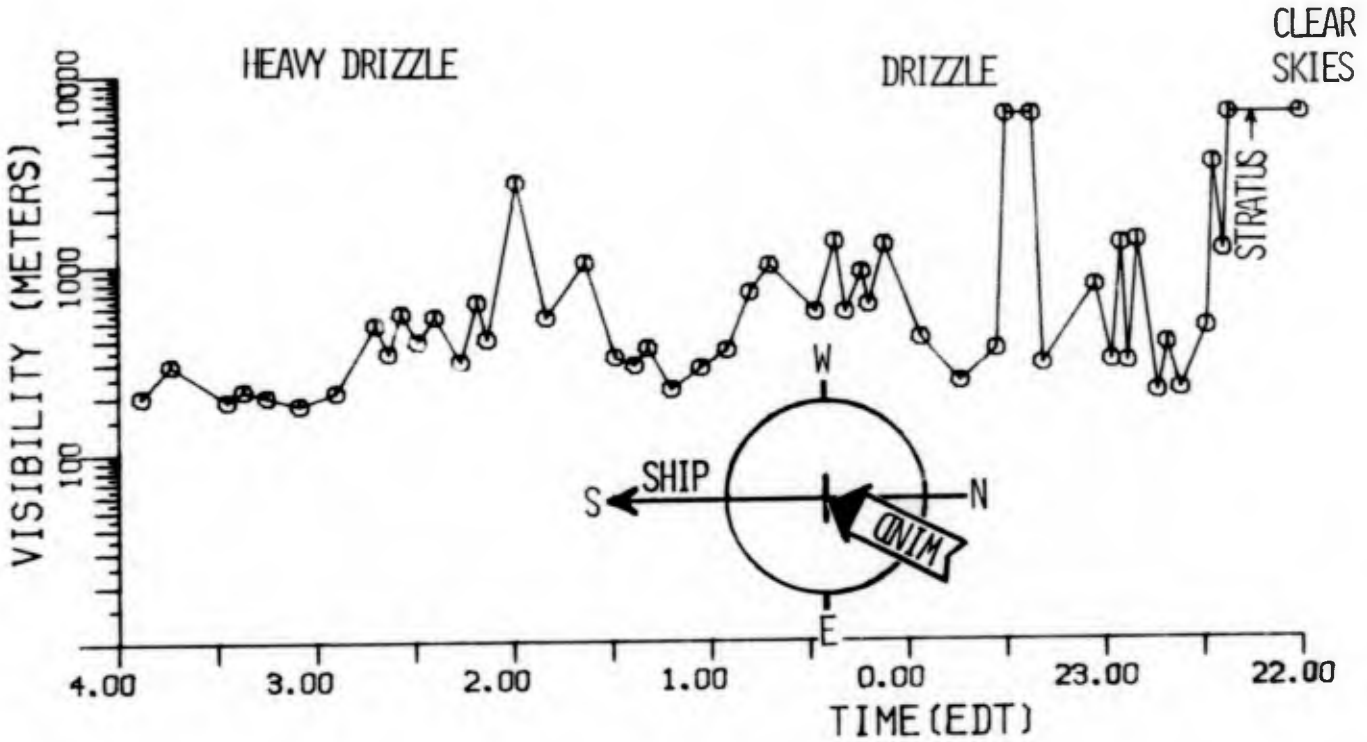

NRL CRUISE, USNS HAYES, AUGUST 1975

FIGURE A-78. VISIBILITY vs. TIME --
FOG 11B, 8-9 AUGUST 1975

-- CALSPAN DATA --

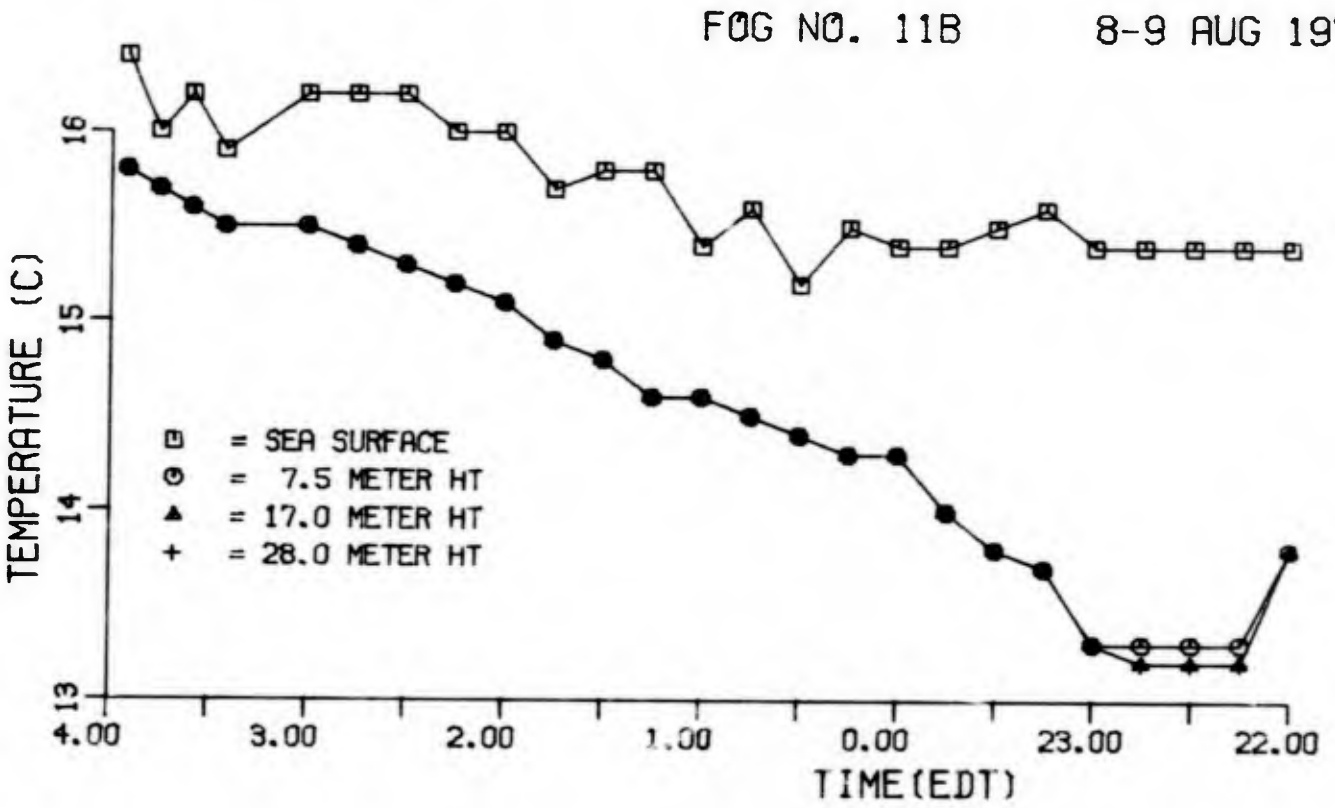

NRL CRUISE, USNS HAYES, AUGUST 1975

-- CALSPAN DATA --

FIGURE A-79. AIR AND SEA SURFACE TEMPERATURE vs. TIME -- FOG 11B, 8-9 AUGUST 1975

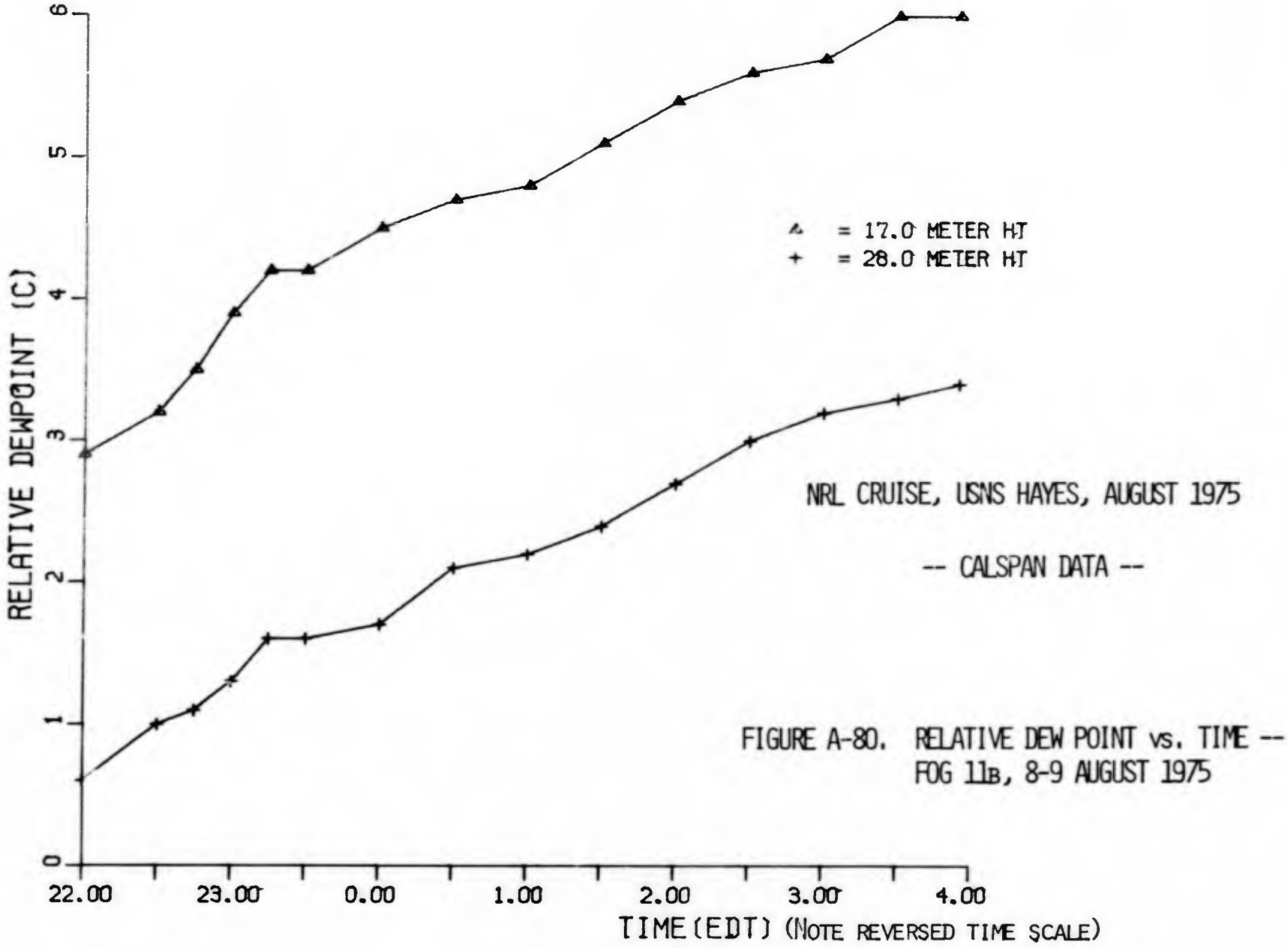

FIGURE A-80. RELATIVE DEW POINT vs. TIME -- FOG 11B, 8-9 AUGUST 1975

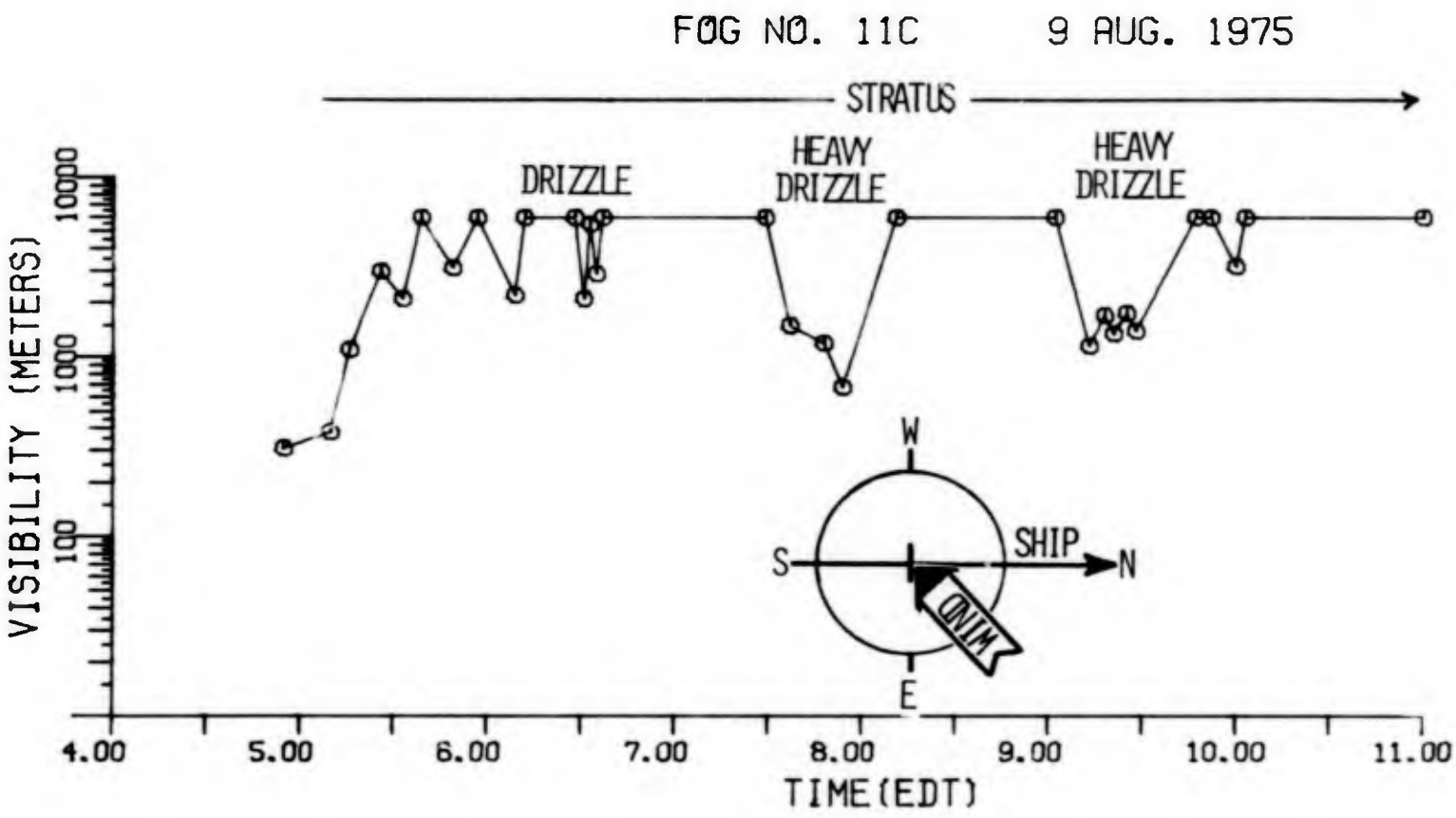

NRL CRUISE, USNS HAYES, AUGUST 1975

FIGURE A-81. VISIBILITY vs. TIME -- FOG 11c, 9 AUGUST 1975

-- CALSPAN DATA --

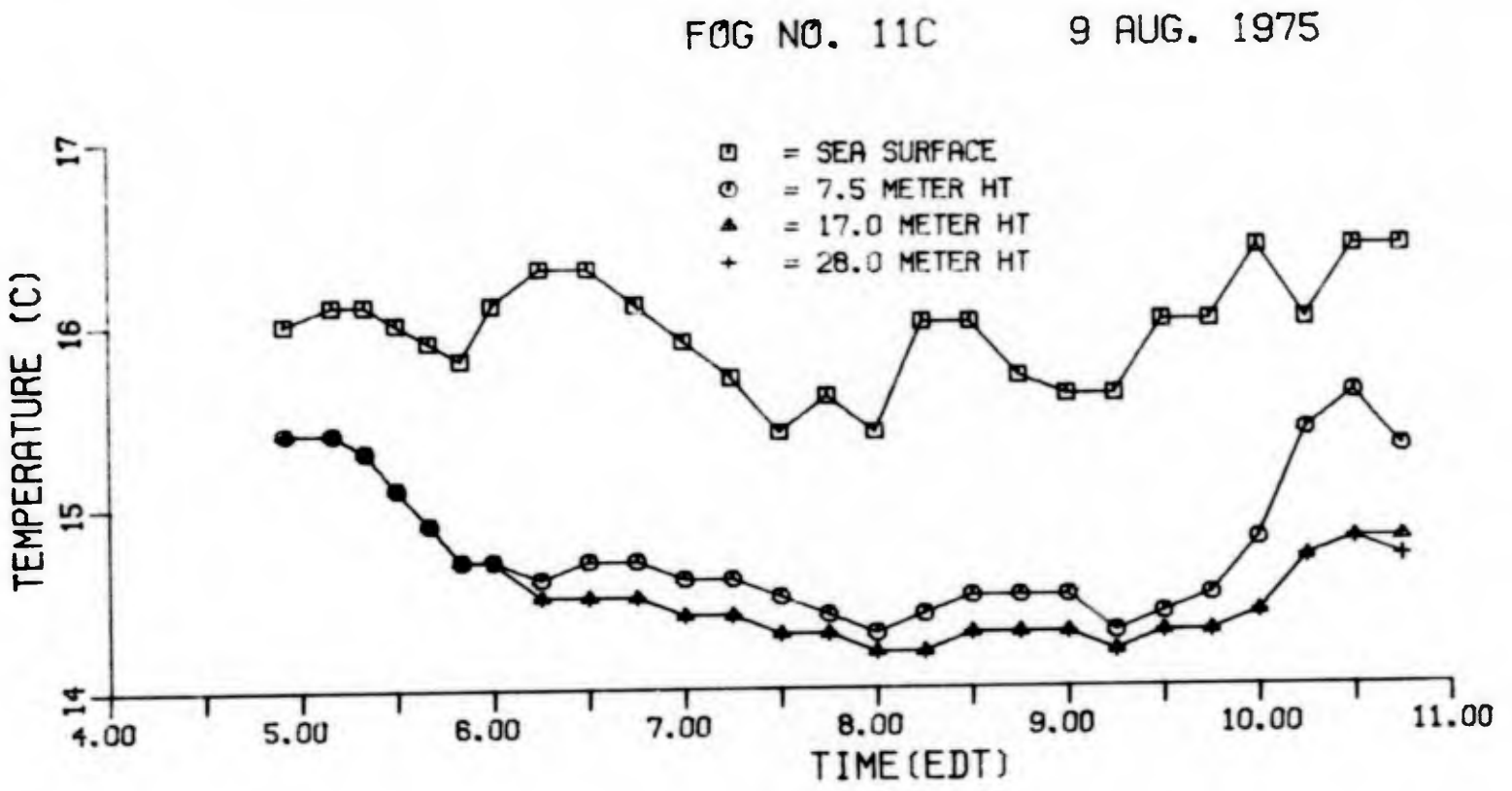

NRL CRUISE, USNS HAYES, AUGUST 1975

-- CALSPAN DATA --

FIGURE A-82. AIR AND SEA SURFACE TEMPERATURE vs. TIME -- FOG 11c, 9 AUGUST 1975

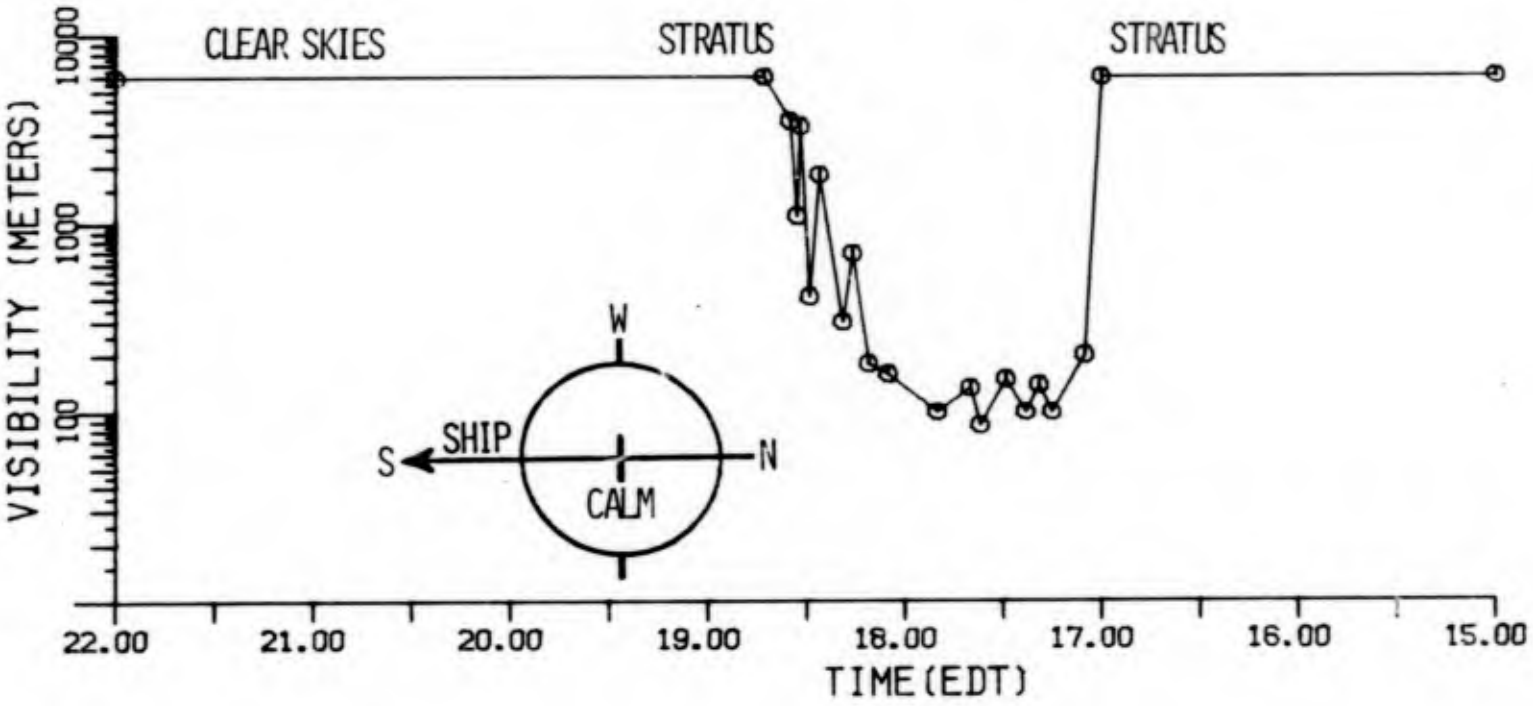

NRL CRUISE, USNS HAYES, AUGUST 1975

FIGURE A-83 VISIBILITY vs. TIME -- FOG 12, 9 AUGUST 1975

-- CALSPAN DATA --

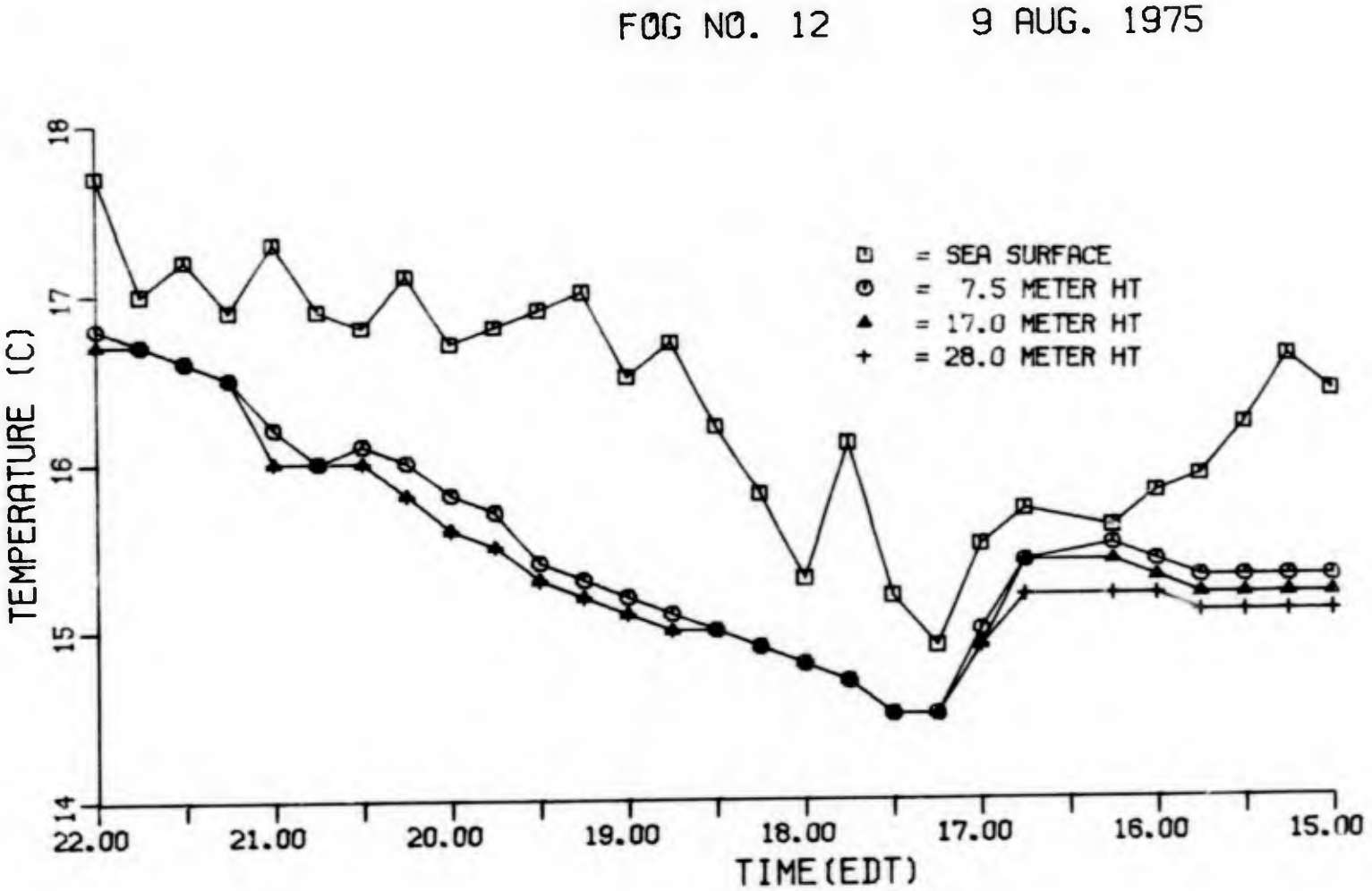

NRL CRUISE, USNS HAYES, AUGUST 1975

FIGURE A-84 AIR AND SEA SURFACE TEMPERATURE vs. TIME -- FOG 12, 9 AUGUST 1975

-- CALSPAN DATA --

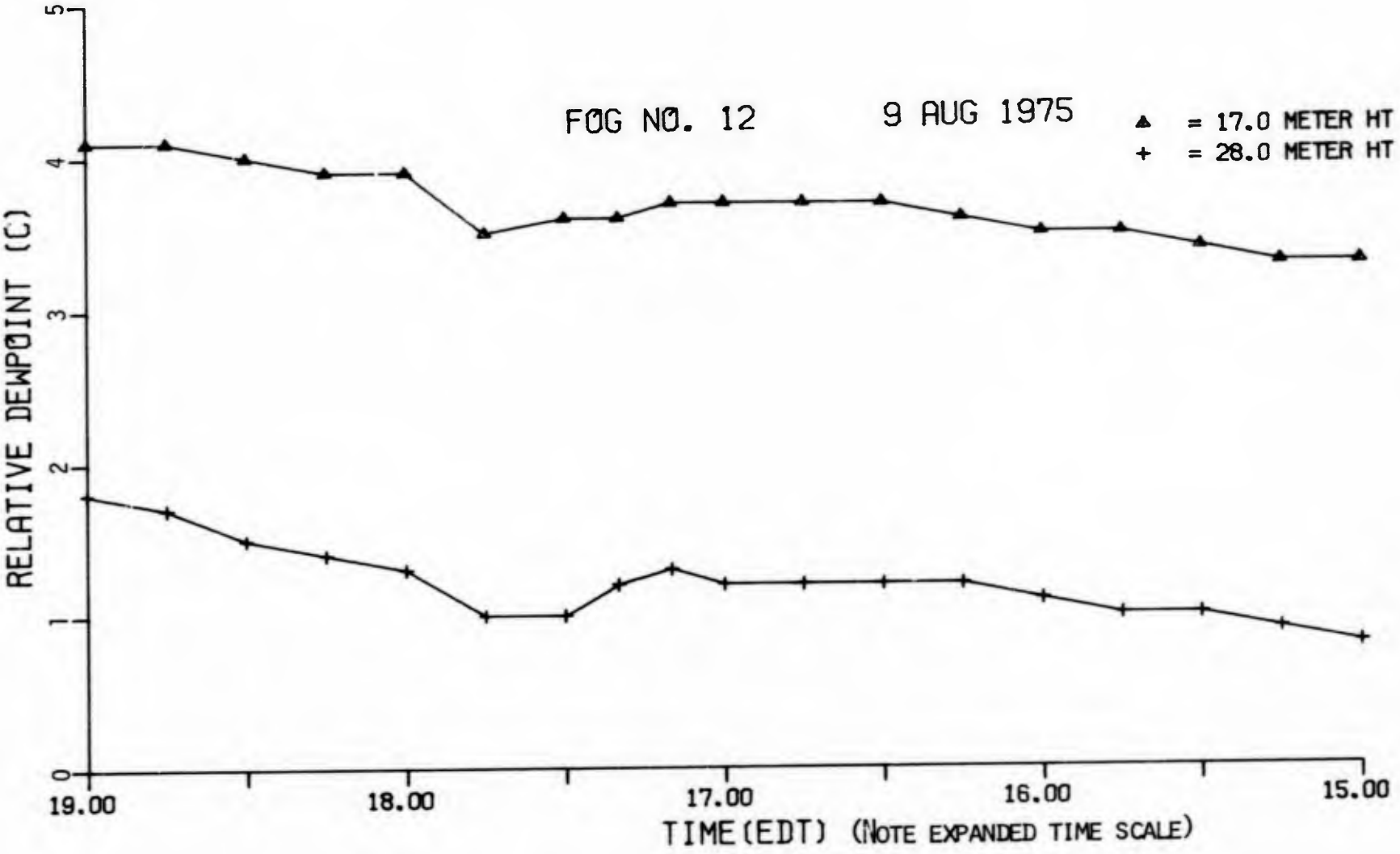

NRL CRUISE, USNS HAYES, AUGUST 1975

FIGURE A-85 RELATIVE DEW POINT vs. TIME -- FOG 12, 9 AUGUST 1975

-- CALSPAN DATA --

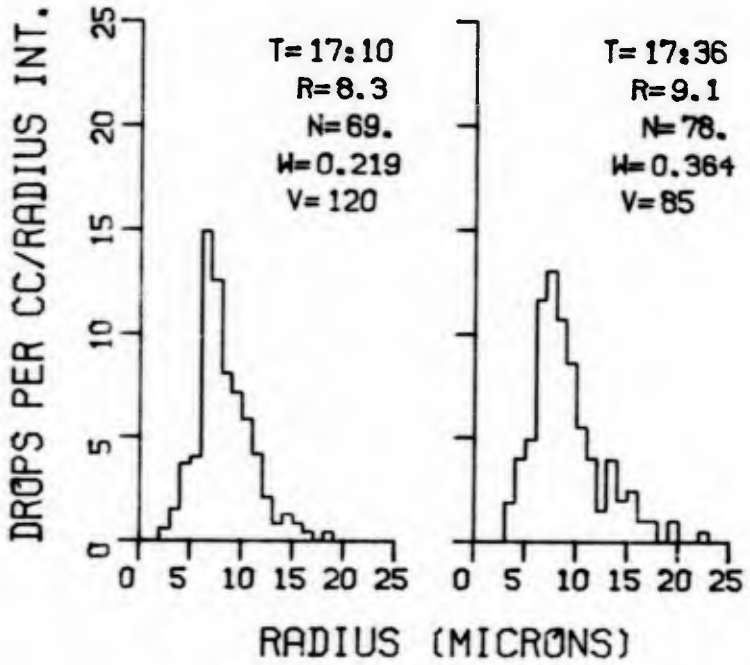

T = TIME (EDT)
R = MEAN RAD (μM)
N = CONC (CM^{-3})
W = LWC ($G\ M^{-3}$)
V = VSBY (M)

NRL CRUISE, USNS HAYES, AUGUST 1975

-- CALSPAN DATA --

FIGURE A-86 DROP SIZE DISTRIBUTIONS -- FOG 12, 9 AUGUST 1975

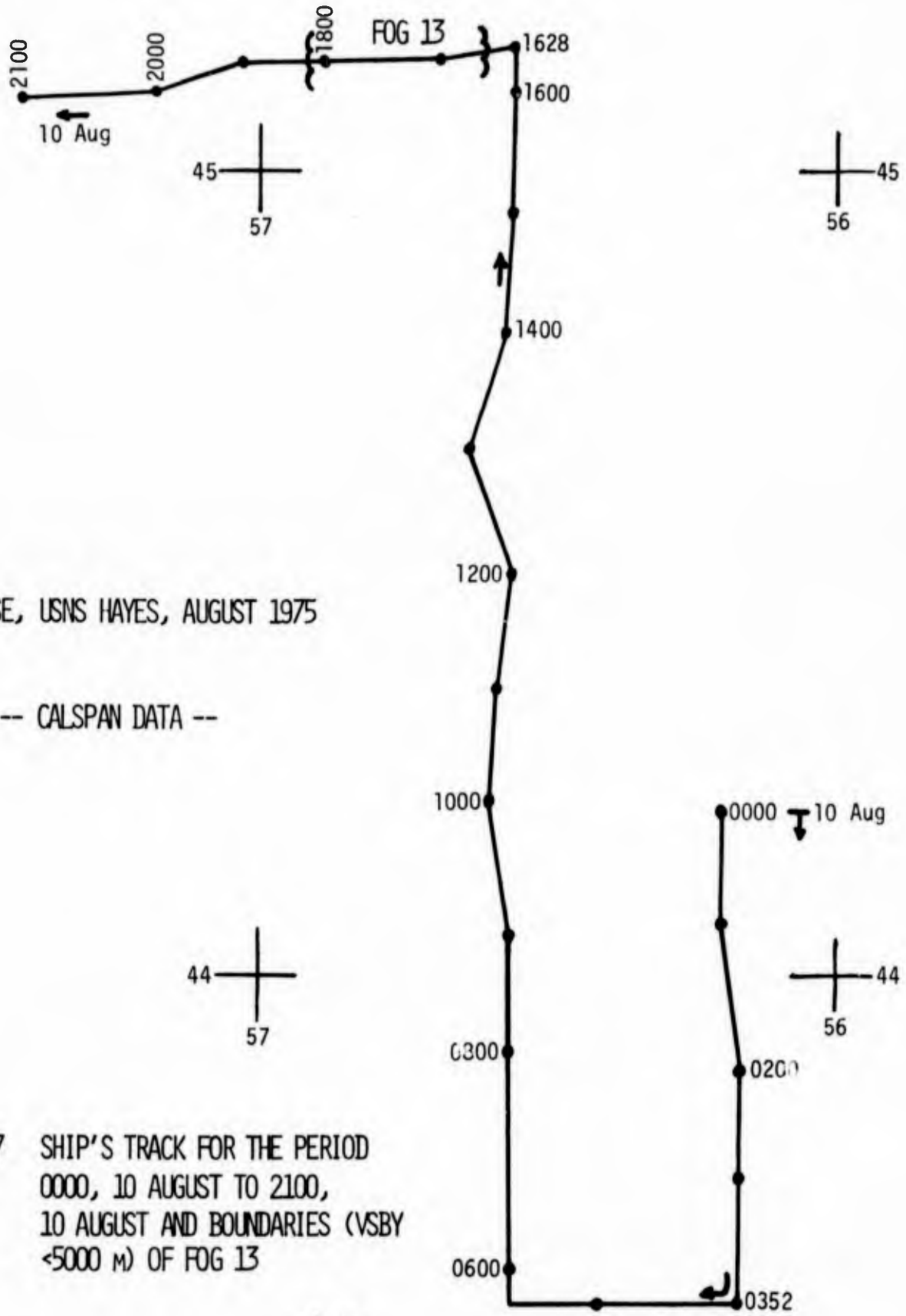

FIGURE A-87 SHIP'S TRACK FOR THE PERIOD 0000, 10 AUGUST TO 2100, 10 AUGUST AND BOUNDARIES (VSBY <5000 M) OF FOG 13

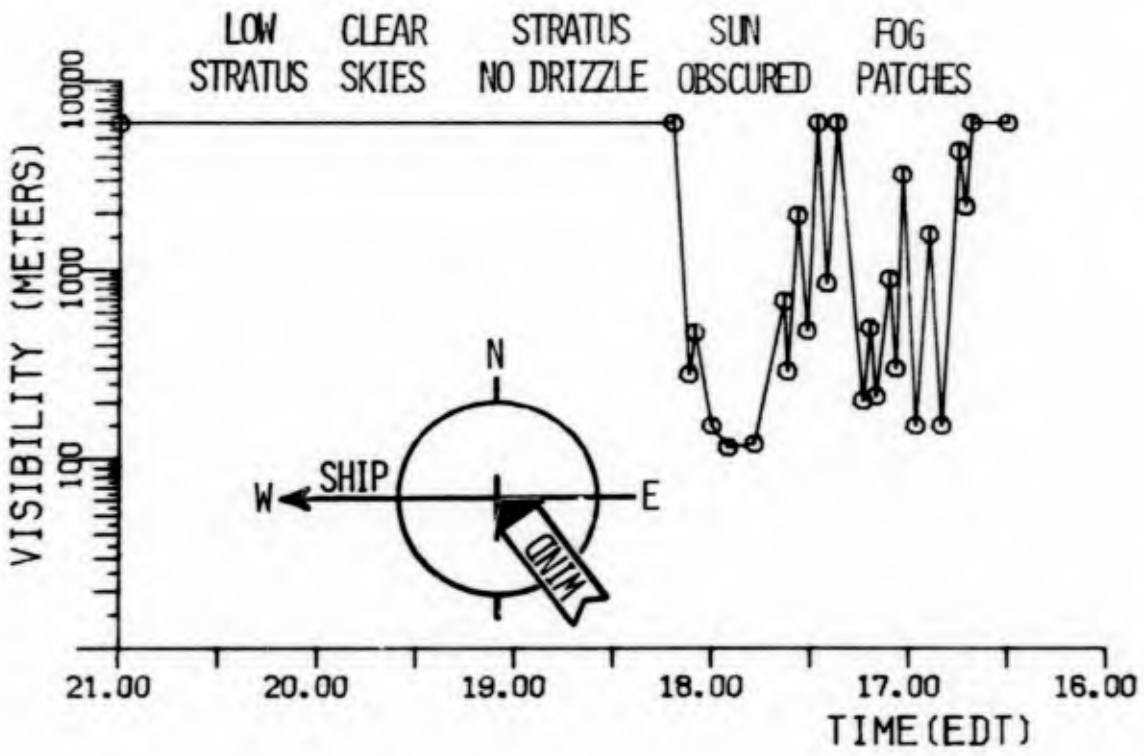

NRL CRUISE, USNS HAYES, AUGUST 1975

-- CALSPAN DATA --

FIGURE A-88 VISIBILITY vs. TIME -- FOG 13, 10 AUGUST 1975

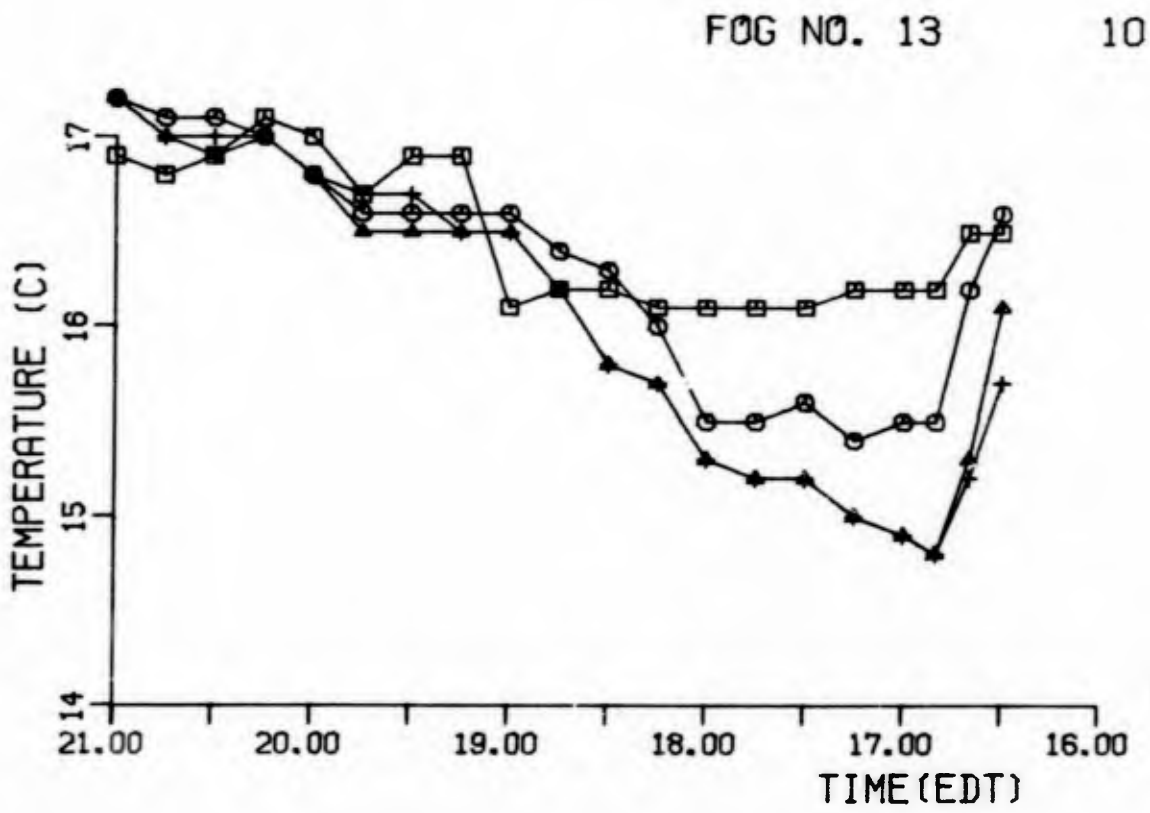

FIGURE A-89 AIR AND SEA SURFACE TEMPERATURE vs. TIME -- FOG 13, 10 AUGUST 1975

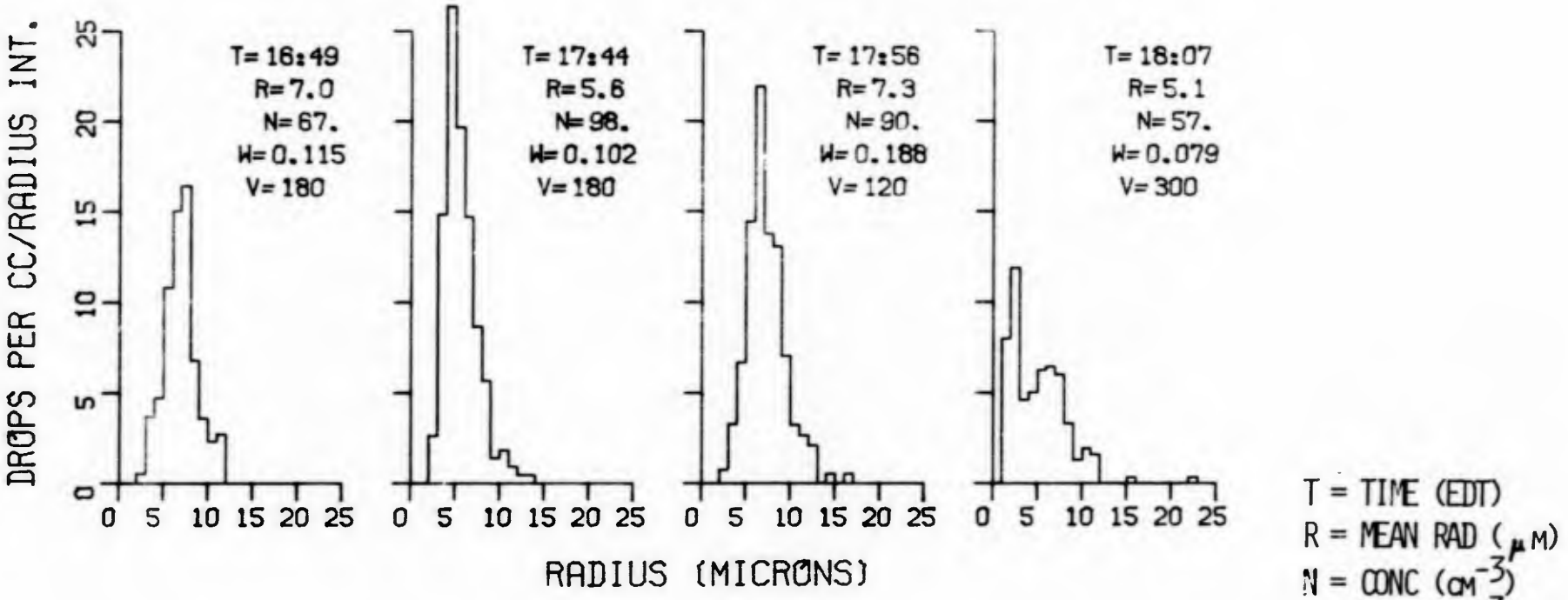

NRL CRUISE, USNS HAYES, AUGUST 1975

FIGURE A-90 DROP SIZE DISTRIBUTIONS --
FOG 13, 10 AUGUST 1975

-- CALSPAN DATA --

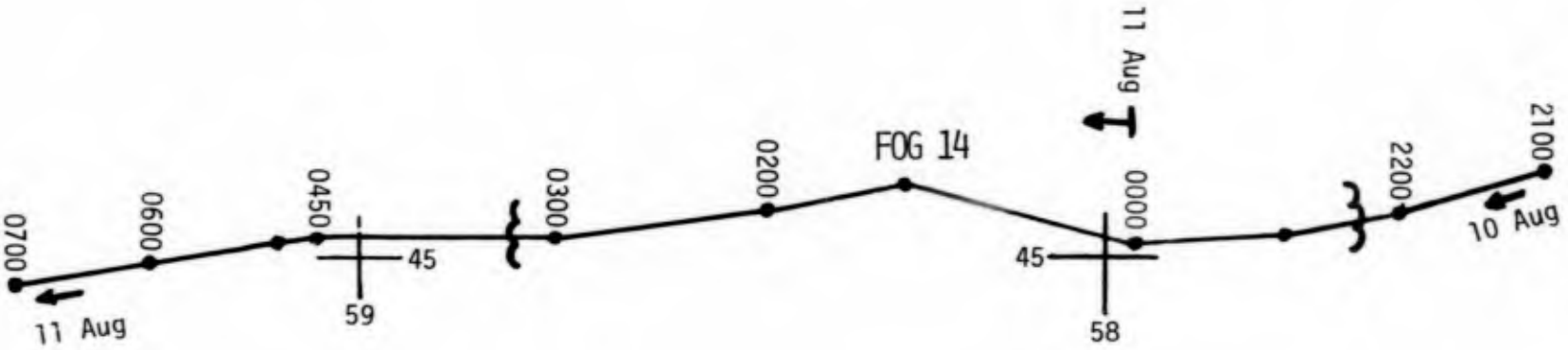

FIGURE A-91 SHIP'S TRACK FOR THE PERIOD 2100, 10 AUGUST TO 0700, 11 AUGUST AND BOUNDARIES (VSBY <5000 M) OF FOG 14

NRL CRUISE, USNS HAYES, AUGUST 1975

-- CALSPAN DATA --

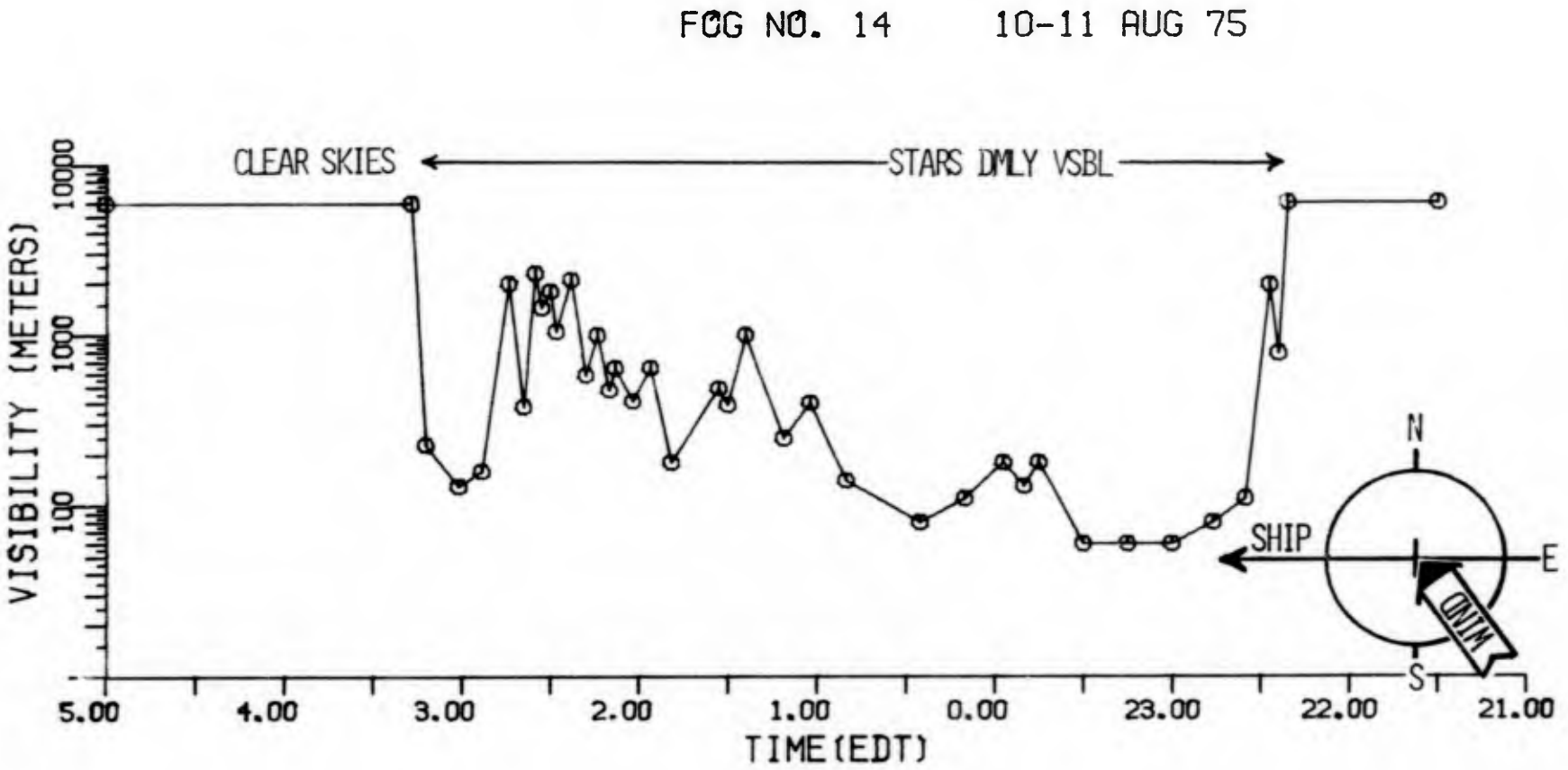

NRL CRUISE, USNS HAYES, AUGUST 1975

FIGURE A-92 VISIBILITY vs. TIME --
FOG 14, 10-11 AUGUST 1975

-- CALSPAN DATA --

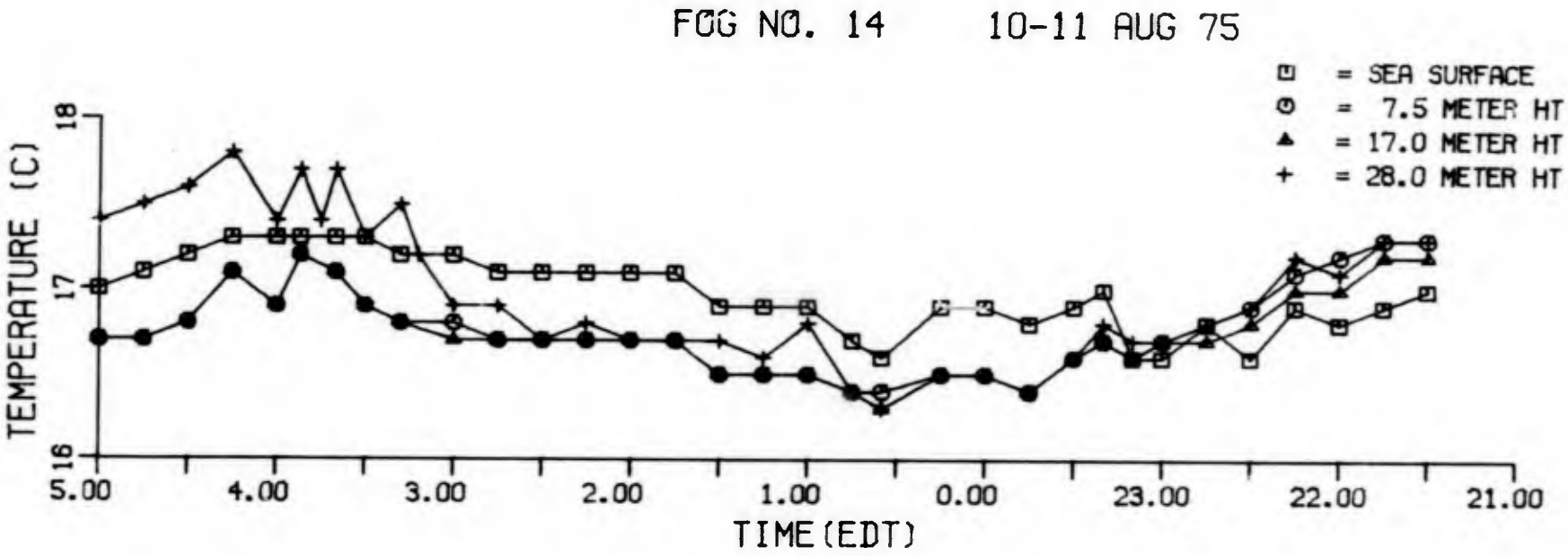

NRL CRUISE, USNS HAYES, AUGUST 1975

FIGURE A-93 AIR AND SEA SURFACE TEMPERATURE vs. TIME -- FOG 14, 10-11 AUGUST 1975

-- CALSPAN DATA --

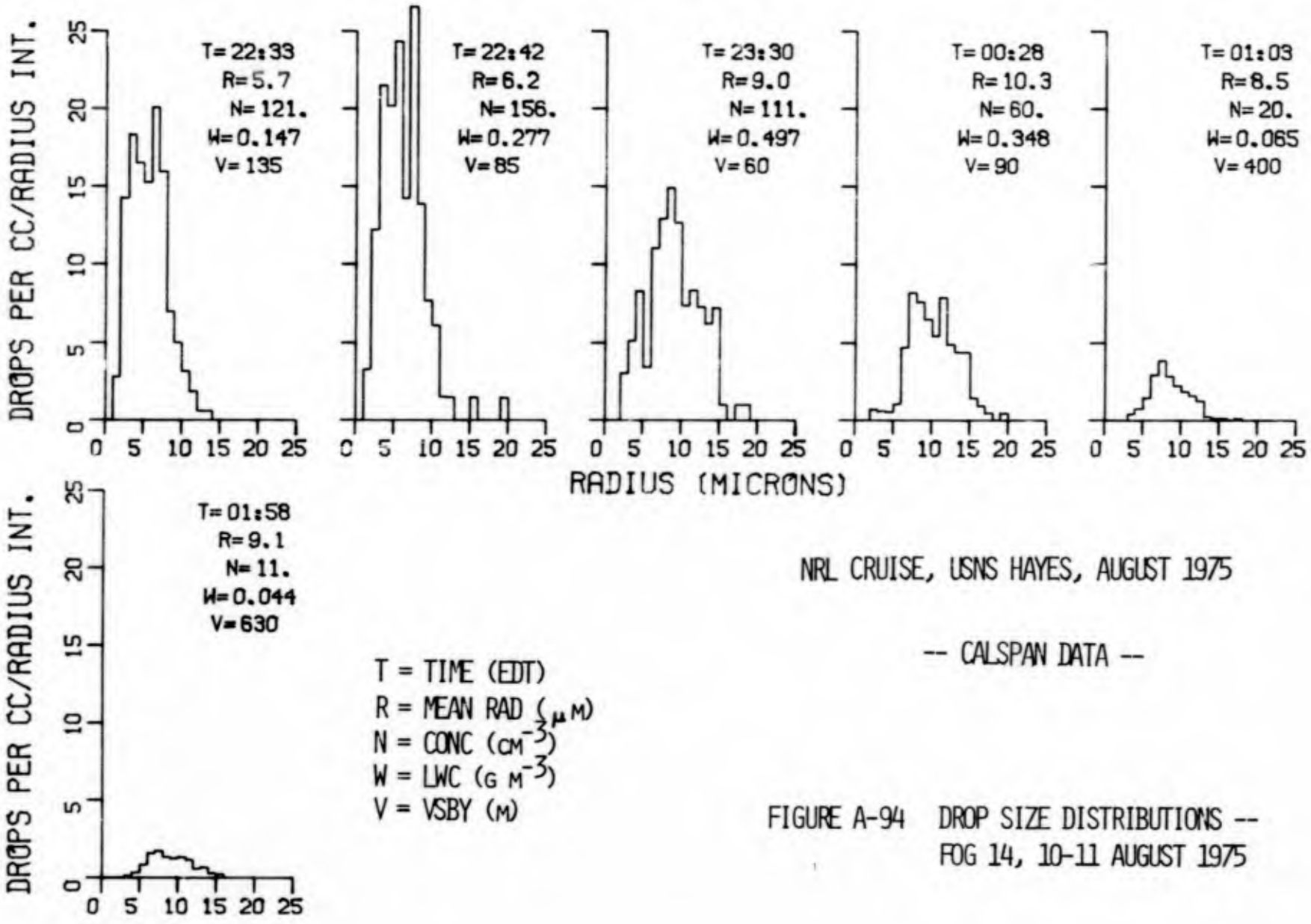

T = TIME (EDT)
R = MEAN RAD (μM)
N = CONC (cm^{-3})
W = LWC ($g\ m^{-3}$)
V = VSBY (M)

NRL CRUISE, USNS HAYES, AUGUST 1975

-- CALSPAN DATA --

FIGURE A-94 DROP SIZE DISTRIBUTIONS -- FOG 14, 10-11 AUGUST 1975

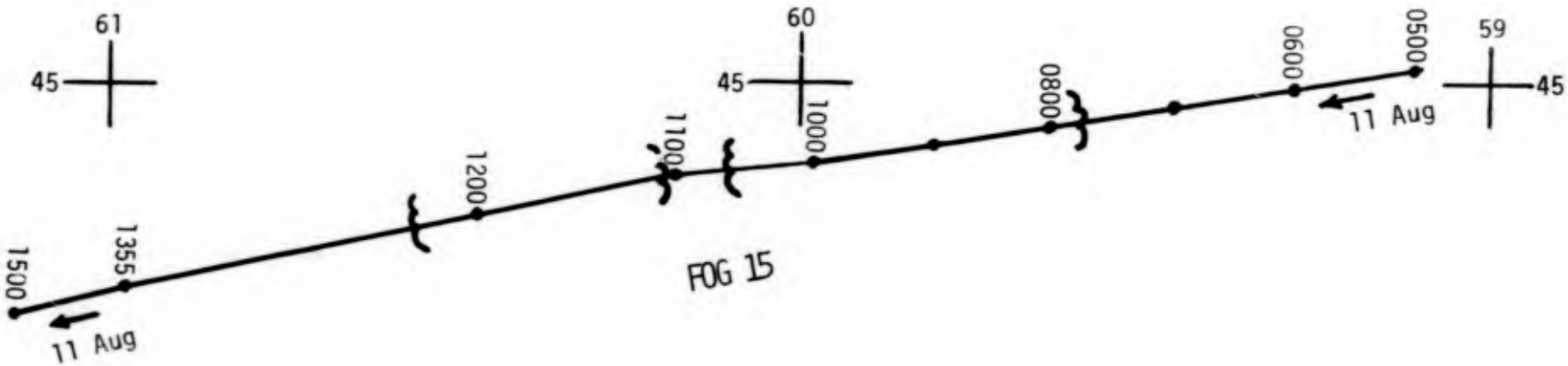

NRL CRUISE, USNS HAYES, AUGUST 1975

FIGURE A-95 SHIP'S TRACK FOR THE PERIOD 0500, 11 AUGUST TO 1500, 11 AUGUST AND BOUNDARIES (VSBY <5000 M) OF FOG 15

-- CALSPAN DATA --

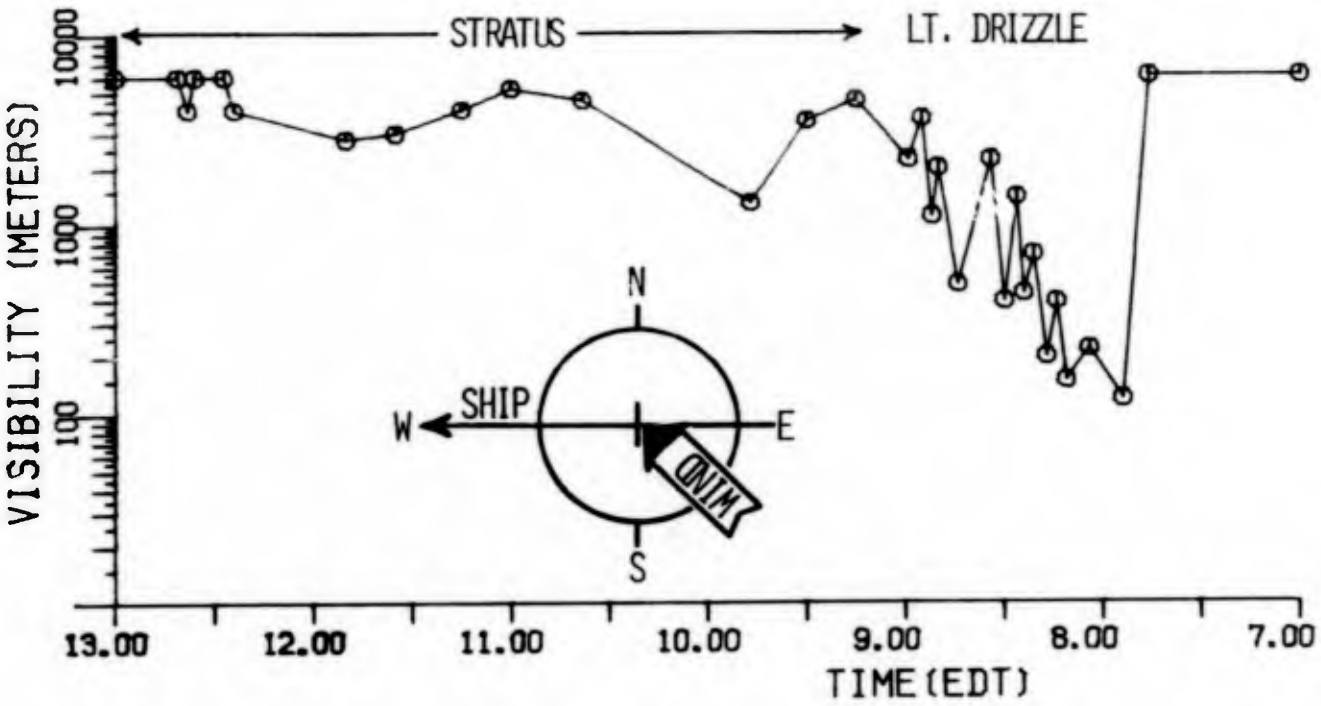

NRL CRUISE, USNS HAYES, AUGUST 1975

FIGURE A-96 VISIBILITY vs. TIME --
FOG 15, 11 AUGUST 1975

-- CALSPAN DATA --

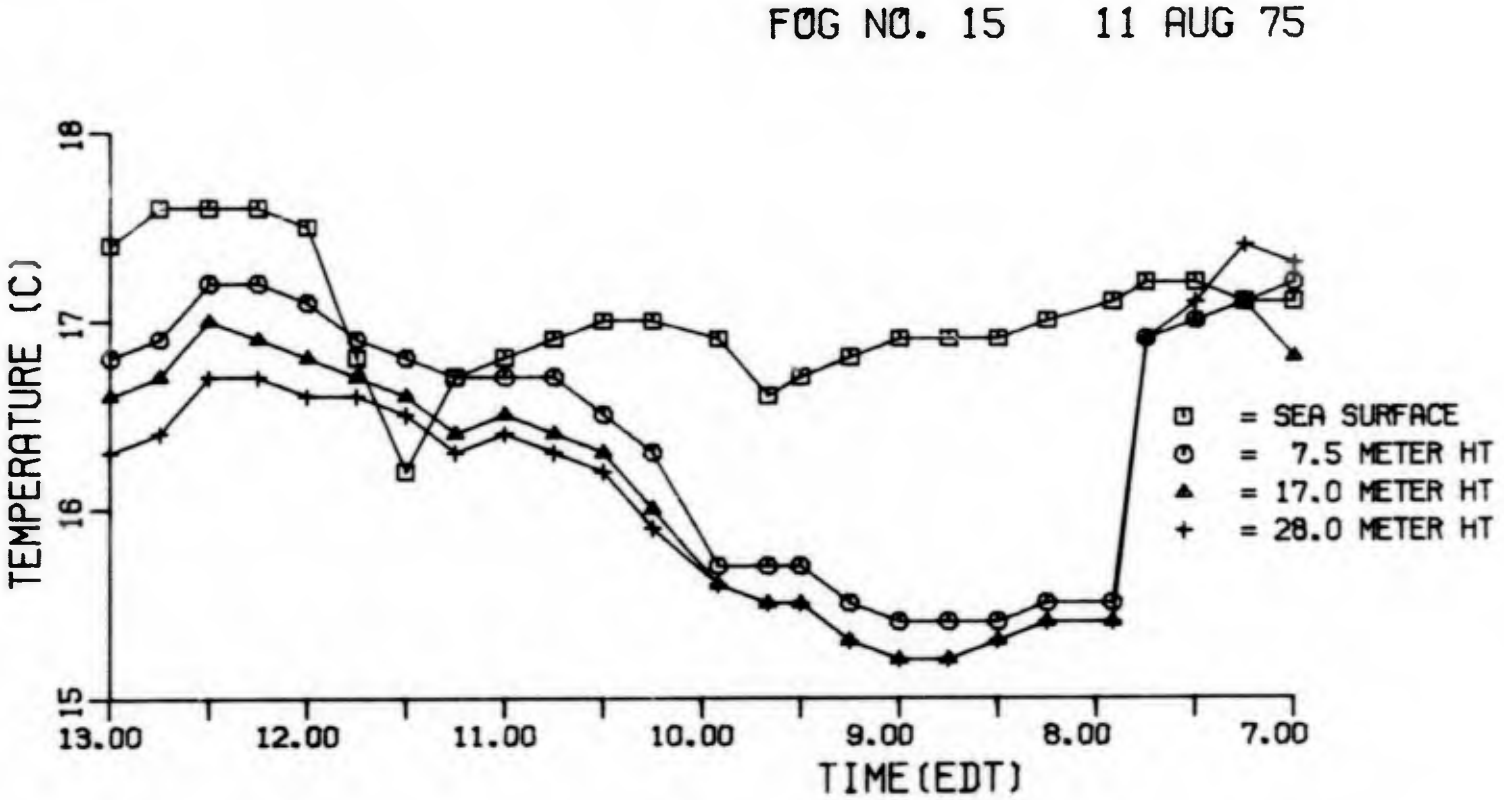

NRL CRUISE, USNS HAYES, AUGUST 1975

-- CALSPAN DATA --

FIGURE A-97 AIR AND SEA SURFACE TEMPERATURE vs. TIME -- FOG 15, 11 AUGUST 1975